Development and In-vitro Evaluation of a Potentially Implantable Fibre-optic Glucose Sensor Probe

Glyn James Matthew Hadley

A thesis submitted in partial fulfilment of the requirements of Bournemouth University for the degree of Doctor of Philosophy

June 2002

Bournemouth University

Abstract

Type I diabetics need regular injections of insulin to survive. Insulin allows the cells of the body to extract glucose from the blood supply to use as fuel. Without insulin the cells turn to other backup fuel sources, this can cause side effects that are quickly fatal or gradual wasting of the bodies tissues. The use of insulin, however, is not danger free, as an incorrect dosage can quickly lead to the reduction of glucose circulating in the blood to drop to a dangerously low level. Without glucose circulating in the blood supply the brain quickly runs out of fuel causing coma and death.

Because of this, a means to constantly monitor blood glucose levels has been sought for the last two decades. With such a device, diabetics could judge the correct amount of insulin to inject and be warned of low blood glucose levels. However, to date no reliable portable system has been produced. Recent developments in fibre optic biosensor technology, suggested a possible route to achieves this goal. The work in this thesis presents the development and testing of such a sensor.

The sensor presented in this thesis is based around a commercial fibre optic blood gas sensor, the Paratrend 7. The oxygen-sensing element of this device was modified into a glucose sensor using polymer membranes incorporating the enzymes glucose oxidase and catalase. The research was aimed at building a glucose sensor that could be developed into a working blood glucose sensor in the minimum amount of time if the research proved successful. For this reason the Paratrend 7 sensor system was chosen to provide a clinically tested sensor core around which the glucose sensor could be built.

The initial experiment, which used a Paratrend 7 sensor coated in polyHEMA and glucose oxidase, produced a sensor of diameter of ≈700μm with a range of 0 to 4mM/l of glucose and a 90% response time of <100 seconds in a solution with a 15% oxygen tension. The sensor design was then developed to incorporate the

enzyme catalase to protect the glucose oxidase and an outer diffusion limiting polyHEMA membrane This produced a sensor with a range of 0 to 6 mM/l and a response time of <100 seconds. The method of coating the sensors was then improved, through a series of stages, until an optomised dip coating technique was developed. This technique produced sensors with ranges (in 7.5KPa oxygen tension solutions) between 0 to 3mM/l and 0 to 10mM/l, response times of <100 seconds in some cases and with diameters of ≈300μm. By using a partial polyurethane outer coat the range of the sensors was increased form 0 to 4mM/l up to 0 to 24mM/l, in one case, with 90% response times in the 100 to 500 second range. The sensors were then sterilised using gamma radiation and their performance before and after sterilisation examined. The gamma sterilisation was found to cause a reduction in the range of the sensors, for example 0 to 24 mM/l down to 0 to 14mM/l in one case. The affect of 24 hour operation in a 5mM/l solution of glucose and storage, for up to three months, was then investigated. Both processes were found to reduce the operational range of the sensors, 0 to 20 reduced to 0 to 15 mM/l, in one case, for 24 hour operation and form 0 to 15mM/l reduced to 0 to 11mM/l in one case for a storage time of three months.

The use of the enzymes glucose oxidase and catalase together in a fibre optic sensor has not been previously reported in the literature as far as can be ascertained. The comparison of sensor performance before and after gamma sterilisation also appears to be unique as does the gamma sterilisation of a fibre optic glucose sensor.

Table of contents

Table of figures

List of tables

Acknowledgements

I would like to thank the following people for their support throughout the course of this research.

Professor Denzil Claremont for his inexhaustible patience, support and guidance.
The staff of Diametrics Medical Ltd for their support and assistance.
All of the staff at Bournemouth University who helped me to complete this thesis.

My parents, sister and brother and Catherine Davies for all their support without which I never would have finished.

I would also like to thank.

Simon Crowle
Thomas Teng
Peter Barker
Paul Nicholson
Austen Rainer
Colin Kirsopp
Jaqui Holmes

Declaration

This thesis contains the original work of the author except where otherwise indicated.

Abbreviations

GOD	Glucose oxidase
CAT	Catalase
HEMA	PolyHEMA
PBS	Phosphate buffered saline
PO2	Paratrend 7 oxygen sensor
P7	Paratrend 7
mM/l	Millimoles per litre
nm	Nanometers
EH	Enzyme-HEMA
KPa	Kilopascals
T90	Time to reach 90% of the total signal
μm	micrometers

1 Introduction

Diabetes Mellitus

Diabetes mellitus is a disease that prevents the cellular uptake of glucose. There are two categories of diabetes, type I and type II. Type I diabetes is the most severe but also the least common of the two diseases, accounting for only 20% of cases of diabetes (approximately 0.25% of the population of the UK). This research work is only concerned with the treatment of type I diabetes for which blood glucose monitoring and appropriate insulin dosages are essential for survival of the patient. Type II is usually controlled with simple dietary measures and limited medication, blood glucose monitoring is often not required. Type I diabetes tends to affect the young with the most common age of incidence at 12 years (Green, Sjolie et al. 1997). Type II diabetes usually occurs in older people around the age of 60 (Jones and Gill 1997).

A glucose sensor would be of little or no use to type II diabetics, for type I diabetics however, it would be of great use possibly preventing coma or even death. Its role would be to detect hypoglycaemia, potentially fatal side effect of the insulin treatment that type I diabetics need to stay alive. Type II diabetes will not therefore be discussed further in this thesis, and instead this work will focus on type I diabetes alone.

1.1 Etiology of diabetes

Type I diabetes is caused when the body loses the ability to produce the hormone insulin. Insulin is used to regulate the amount of glucose in the blood by stimulating cellular uptake of glucose by cells and suppressing production of glucose by the liver (Kruszynska 1997). The amount of insulin produced is

carefully managed by the body to maintain the blood glucose level at a constant healthy level. Insulin is normally produced in β-cells, which are structures in the pancreas within the islets of Langerhans. In type I diabetes, the β-cells have been destroyed, one hypothesis is that this is due to an autoimmune disease. In this case, the body's own immune system mistakenly attacks the β-cells. As the β-cells are progressively destroyed, the amount of insulin produced reduces until no insulin production is possible. The symptoms of diabetes are tiredness, thirst, a large increase in the amount of urine passed (polyuria) and weight loss (Jones and Gill 1997). Type I diabetes has been shown to be due to a combination of genetic predisposition and the environmental conditions, such as exposure to certain viruses (Jones and Gill 1997).

The diagnosis of diabetes is based on a technique known as an oral glucose tolerance test (OGTT). This involves a patient fasting for between 8 to 14 hours, after which a blood glucose test is taken. They are then given a 75g oral glucose load. A test of the patient's blood two hours after this is taken and compared with the fasting glucose value. If the results of the blood tests are within the ranges shown in table 1. then the patient has a reduced ability to control their blood glucose level and is most likely diabetic (WHO, 1999).

	Whole blood	Whole capillary blood	Plasma of venous blood
Fasting value (mM/l)	> = 6.1	> = 6.1	> = 7.0
Post glucose load (mM/l)	> = 10.0	> = 11.1	> = 11.1

Table 1. Blood glucose values used for the diagnosis of diabetes

1.2 Insulin therapy of type I diabetes

The only treatment for type I diabetes is insulin therapy in the form of daily injections, without this treatment type I diabetics would die as their cells would be unable to absorb glucose to use as fuel. With insulin injections the symptoms of type I diabetes can be removed as blood glucose levels return to a quasi-normal level and the fuel supply is returned to the cells (Banting and Best 1922). However, insulin injections cannot replace the glucose control system of a healthy individual, which constantly measures the amount of glucose in the blood and releases an appropriate amount of insulin. This control system can handle the constant changes in supply and demand of glucose in the body and keep the glucose concentrations to within a very narrow range of between 4 to 6 mM/l (Kruszynska 1997; Pickup 1997).

With insulin therapy, the correct amount of insulin to be injected can be difficult to judge. This is because the absorption and uptake of insulin can be affected by a number of physiological factors. In addition, the blood glucose measurement techniques currently available only give a single measurement and can be painful and inconvenient to use. This means that patients have a poor idea of the level of blood glucose they have, and therefore, the amount of insulin to inject (Linde 1997; Amiel 1998). A means of quickly and constantly measuring blood glucose levels would allow the patient to administer the correct amount of insulin and keep the blood glucose levels to within a normal range.

1.2.1. Current methods of Blood glucose measurement

Diabetics currently measure their blood glucose levels using small, portable devices that measure the glucose concentration in a small drop of blood taken from a finger or in urine samples. However, due to the pain and/or inconvenience

of these techniques these measurements are only taken a few times a day. This gives a poor representation of the constantly changing blood glucose levels

Even with insulin injections and the use of glucose meters, a diabetic patient on insulin therapy will experience plasma glucose concentrations of from 1 to 15mM/l and above compared to 4 to 6 mM/l of a healthy individual. As will be discussed later, these excursions outside of the normal glucose range will cause damage to the small blood vessels of the body. These lead to chronic and often fatal complications of diabetes (Kruszynska 1997; Pickup 1997).

1.2.2. The long and short-term complications of insulin treated diabetes

Diabetes treated with insulin has two main dangers associated with it; these are hypoglycaemia and the long-term complications caused by hyperglycaemia. Hypoglycaemia (blood glucose concentrations of below 3mM/l) is a short-term risk of insulin therapy. It is caused by a number of factors such as an overdose of insulin, insufficient glucose uptake by the cells of the body and disease (Williams and Pickup 1997).

1.2.3. Insulin induced hypoglycaemia

Hypoglycaemia first affects the brain; this is because unlike other tissues, which have alternative fuel sources, the brain depends almost exclusively on blood glucose as its fuel (Kruszynska 1997). As glucose levels drop below 2.8mM/l, cognitive function is impaired as the neurons of the brain have insufficient fuel to function correctly, once below 1mM/l, coma and possibly death occur. Hypoglycaemia affects from 25 to 30% of insulin dependent diabetics every year and causes two to four percent of all deaths in insulin treated diabetics (Krentz and Nattrass 1997).

1.2.4. The long-term complications of insulin treated diabetes due to hyperglycaemia

As insulin therapy gives only limited control of glycaemic (glucose) levels, blood glucose concentrations are often above normal. The constantly high level of glucose (hyperglycaemia) leads to damage to the microvascular system of the body. This damage accumulates over a number of years and leads to a number of pathological conditions. Forty or fifty percent of type I diabetics will develop a range of conditions, which include retinopathy, nephropathy and neuropathy. The larger blood vessels can also be affected leading to atheroma. Long-term complications lead to type I diabetics having four to seven times the mortality rate of non-diabetics (Jones and Gill 1997).

1.2.5. The Diabetes control and complication trial (DCCT) and intensive insulin therapy of diabetes

Intensive insulin therapy involves much stricter control of blood glucose levels than is achieved in normal insulin therapy. This is done by an increase in the number of blood glucose tests and insulin injections compared with normal insulin therapy regimes (Amiel 1998; Pickup 1998). It has been demonstrated (in the DCCT, 1993), that intensive insulin therapy reduces the occurrence of the long term complications of type I diabetes.

1.2.6. The DCCT and the reduced risk of long-term diabetic complications

The DCCT trial involved a study of insulin treated type I diabetics following a regime of 'intensive insulin therapy', which involved increased blood glucose tests and insulin injections compared to normal insulin treatment. The goal was to keep their blood glucose levels to within a more normal range compared to standard insulin therapy. It was found that, compared to normal insulin regimes, intensive insulin therapy reduced diabetic retinopathy by 35 to 70%, kidney complications were reduced by between 39% and 54% and other complications were significantly reduced. However, the incidence of severe hypoglycaemia increased by a factor of between two and three (DCCT 1993). Therefore, although providing a large improvement in the long-term outlook of diabetes, the associated risks in the short-tem are also increased. This increase in hypoglycaemia was probably due to the normal glucose range and the hypoglycaemic range being very close together. This made it very easy for patients to accidentally administer too much insulin and lower their blood glucose levels into the hypoglycaemic range.

1.2.7. Purpose of the research

The objective of this research was to develop a sensor capable of continuously and reliably monitoring blood glucose levels to improve the management of type I diabetes. Its development could help reduce or prevent both the long-term complications and hypoglycaemic episodes of insulin treated type I diabetes.

To safeguard against hypoglycaemia, the blood glucose concentration would need to be measured constantly and an alarm given if glucose levels approached hypoglycaemia. Constant monitoring of glucose levels would also allow the correct dosage of insulin to be calculated and administered. Unfortunately, at date of print, there exists no method of constantly measuring glycaemic levels reliably

using a portable device. It is for these reasons that a means has been sought for approximately twenty years to continuously measure blood glucose concentrations.

1.3 Glucose sensor performance requirements

There are several performance requirements to be considered, these are outlined in table 2.

Measurement range	0 to 25mM/l (Claremont 1987)
90% response time	<240 seconds (Fernquist-Forbes, Linde et al. 1988; Schmidtke, Freeland et al. 1998).
Resolution	1 mM/l
Measurement error	No error in a single measurement greater than ±0.3 mM/l below a blood glucose concentration of 2.8 mM/l or 10% of any other single measurement (Claremont 1987).
Specificity	Other chemical species must have no affect on the sensor (Claremont 1987).
Size (of the sensing element)	Less than a 25 gauge, needle (≈0.5 mm) if invasive (Claremont 1987).
Operational life span	24 hours minimum (Claremont 1987).
Calibration	Ideally calibrated only once during use or calibrated at production (Claremont 1987).
Sterilisation	Must withstand irradiation or chemical sterilisation to be of use.
Shelf life	In the order of three months.
Cost.	Cheap (Claremont 1987).
Operation	Simple (Claremont 1987).

Table 2. The sensor performance requirements

1.3.1. Glucose concentration measurement range

The glucose concentration measurement range of the sensor will need to cover the healthy physiological region, (3.7 to 6.7mM/l), the hypoglycaemic region (0 to 2.8mM/l) and the hyperglycaemic region (6.7 to 50mM/l) as shown in figure 1. Although for hyperglycaemia, measurements of up to 25mM/l have been proposed as a sufficient upper limit for a practical glucose sensor. The proposed sensor will therefore need to operate over a glucose concentration range of at least 0 to 25 mM/l (Claremont 1987; DCCT 1991; Frier 1997; Pickup 1997).

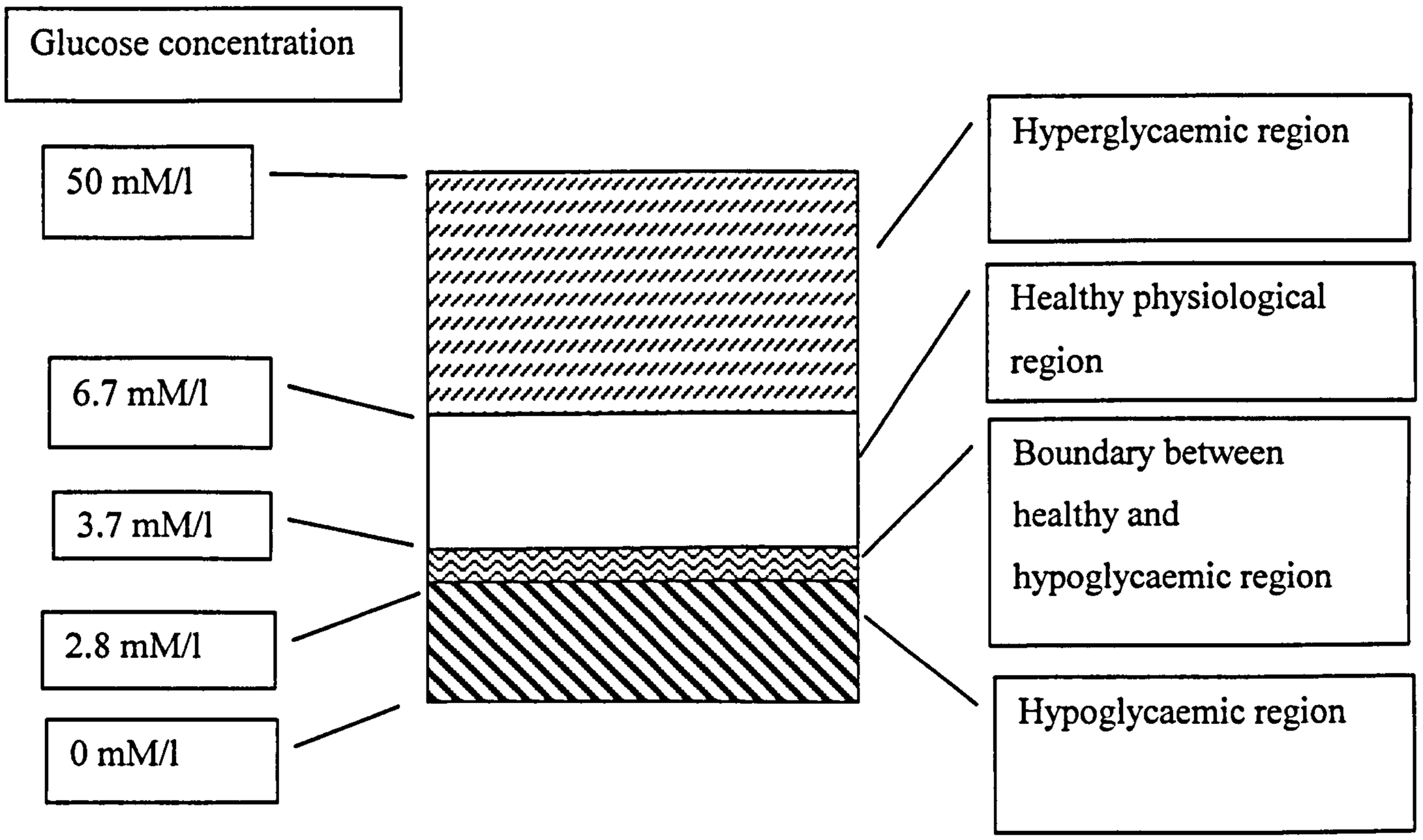

Figure 1. Physiological glucose concentration ranges

1.3.2. The 90% response time of the sensor

The 90% response time of the sensor, to glucose concentration changes, should be sufficiently short to handle the fastest glucose concentration change possible in-vivo. These will most likely occur, and are potentially most dangerous, following an injection of insulin. The most rapid plasma glucose concentration drop induced by an insulin injection in a healthy human subject reported in the reviewed literature was measured at 2.5 mM/l in 30 minutes, approximately 12 min/mM/l decrease (Fernquist-Forbes, Linde et al. 1988). In a study using rats, however, an insulin induced glucose concentration decrease was measured at 4.5 min/mM/l in subcutaneous tissue and 5.6 min/mM/l in the blood stream (Schmidtke, Freeland et al. 1998). Assuming, that the same rate of glucose decrease could occur in humans and that this is the fastest possible glucose concentration change, then the sensor will have to possess a 90% response time of less than 240 seconds. With this response time the sensor will be able to respond the fastest glucose decrease that will be encountered in-vivo.

1.3.3. Resolution, measurement error and drift

The values of signal resolution and measurement error that can be tolerated are dictated by the size of the boundary between the normal and hypoglycaemic glucose concentration regions. This is because an error in a blood glucose measurement that led to a hypoglycaemic blood glucose concentration falsely being classified as being in the normal or hyperglycaemic region could prove fatal. Therefore, the sensor must be able to reliably distinguish between hypoglycaemia and other regions.

To achieve this reliability, the sensor will ideally have a resolution (smallest detectable difference in the glucose measurement) of 1 mM/l. This will allow the sensor to distinguish the lowest normal physiological glucose concentration (3.7 mM/l) from the upper hypoglycaemic limit (2.8 mM/l). As well as resolution, the measurement error will affect the reliability of the sensor. Above 2.8 mM/l, no single measurement should have an error of greater than 10% of the true value being measured. Incorporating this error with the resolution limit gives a possible error in the lower normal glucose concentration of 3.7 ± 1.0 mM/l, so the true value could be 4.7 mM/l or 2.7 mM/l, just inside the hypoglycaemic region. For concentrations below 2.8 mM/l measurement errors are academic to an extent as it may be sufficient to indicate that the patient is experiencing hypoglycaemia. However, if measurements are to be taken in the hypoglycaemic region an error of ±0.3 mM/l should be aimed for.

As the sensor will be taking continuous measurements, it may be possible to take an average of measurement over a period. If, for example, a measurement was taken every second then the values could be averaged over say a minute. However, the safety of such an averaged blood glucose value is dependent on the frequency of measurements and the maximum possible rate that blood glucose concentrations can decrease from normal to hypoglycaemic concentrations (Claremont 1987; DCCT 1991; Frier 1997; Pickup 1997). In addition, a trend of

measurements could be monitored and steps taken to adjust glucose levels when potentially dangerous trends were detected, i.e. glucose levels decreasing while in the lower half of the normal glucose range.

1.3.4. The specificity of the sensor to glucose

The sensor signal must be specific to glucose and therefore immune from the effects of other analytes in the blood. The most obvious chemicals that may interfere with the sensors are other sugars. In blood, besides glucose, the other sugars that are present are pentose (≈0.05mM/l, L-Xylulose (≈0.01mM/l) and galactose (≈0.09mM/l), fortunately their concentration is small compared to that of glucose (≈6 mM/l) (Diem and Lenter 1975). Other analytes in the blood and even conditions such as ambient light or temperature may also have an effect on the sensor, although this will depend on the detection scheme being used and is discussed in Chapter 2.

1.3.5. Sensing element size

The sensor should, ideally, have a diameter of no greater than a 25-gauge needle, a diameter of roughly 0.5 mm. This would allow the sensor to be implanted into subcutaneous tissue with the minimum amount of pain. In addition, the response of the body's tissue to an implant is possibly related, at least in part, to the size of the wound it inflicts on insertion. The safety of the sensor may also be affected by its dimensions, as the greater the wound size the greater the chance of infection gaining access from the outside world. These considerations will be expanded in Chapter 3 (Claremont 1987).

1.3.6. Operational life span

The operational life span of the sensor should be between 12 and 24 hours. This would allow the sensor to operate overnight to monitor nocturnal glucose levels and warn of nocturnal hypoglycaemia. In addition, an entire 24-hour monitoring period could be covered with the use of only one or two sensors. This would avoid the patient having to insert several sensors per day, which would be painful and inconvenient. It may be possible to create a sensor with a longer operational lifetime. However, infection may become an issue with longer implantation times, creating problems with safety and operation.

1.3.7. Calibration of the sensor

Ideally, the sensor would be calibrated once, over its full operational range, before implantation and would then operate accurately for the duration of its use. However, in practice, the sensor will most likely require an in vivo re-calibration shortly after implantation. This calibration would probably be a one-point measurement, against a gold standard blood glucose assay, to deal with baseline changes in the signal caused by effects of implantation. A one-point calibration would be the most practical, as cycling a patient through the complete pathological blood glucose range would not be practical. In addition, the sensor may require re-calibrating at set intervals during its operation to deal with signal drift. These in vivo calibrations would have the advantage that any effects of the tissue response to the presence of the sensor and the sensor signal drift would be, at least partially, compensated for.

1.3.8. Sterilisation of the sensor

Obviously for the safety of the patient, any implanted sensor would need to be sterilised before implantation. As well as improved safety, sterilisation may also reduce errors in the sensor signal that would be caused by the tissues' reaction to any pathogens on the sensors surface, as will be explored in Chapter 2. The sterilisation process may also have an effect on the sensors performance characteristics, such as its measurement range or shelf life. Allowances for these changes will have to be made for in the design of a practical sensor. The sensor developed here is later shown to survive sterilisation using gamma radiation with some changes in performance (Woedtke, Julich et al. 2002).

1.3.9. The shelf life of the sensor

The sensor will have to be stable when stored between being produced and use. A shelf life of at least two to three months would most likely satisfy this requirement. Ideally, the sensor should be able to be stored at room temperature, although if chemical or biological components are used in the sensing element, refrigeration or other special storage conditions may be required.

2 Methods and principles of glucose measurement

A range of different techniques has been applied to the problem of continuous blood glucose measurement. These range from non-invasive infrared spectroscopy approaches to invasive needle style electrochemistry (Heinemann 2000; McNichols and Cote 2000). A discussion of these techniques is presented in this chapter. Special attention is paid to the enzyme based electrochemical glucose sensors as their enzyme layer technology is employed in the fibre optic sensor design presented in this thesis.

2.1 Electrochemical glucose sensors

Glucose in blood can be detected directly using a pair of electrodes held at an appropriate electrical potential. The electric potential causes a chemical reaction to occur between the glucose and the surface of the electrode. This chemical reaction in turn produces a flow of electric current through the electrodes. This current can then be measured and is proportional to the concentration of glucose. However, the large electric potentials needed to achieve this lead to interference from other chemicals in the blood, which also react with the surface of the electrode masking the glucose dependent signal (Lemke and Lustermann 1991).

To solve this problem, electrochemical glucose sensors detect glucose indirectly through the products of another chemical reaction that involve glucose. These products can be detected using much lower electrical potentials than is needed to directly measure glucose. These types of sensors, therefore, are relatively interference free (Lemke and Lustermann 1991). However, interference from other substances in the blood is still a problem.

These sensors are usually needle type sensors, which can be inserted through the skin into the subcutaneous area or into a blood vessel (Claremont, Sambrook et al. 1986). The electrode is often platinum, silver, or carbon with a reference electrode (needed to complete the electrical circuit) made of steel, silver or silver chloride. Instead of needle style sensors, some sensors are miniaturised and totally implanted along with all the

necessary electronics and a power supply to provide a radio link with the outside (Gilligan, Schults et al. 1994; Updike, Shults et al. 2000).

The majority of electrochemical glucose sensors use the enzyme glucose oxidase (GOD), which promotes a reaction between glucose and oxygen to produce gluconic acid and hydrogen peroxide (H_2O_2), as shown in Equation 1 (Fisher, Rebrin et al. 1994). Measurements of the oxygen or hydrogen peroxide (both of which can be detected with low electrical potentials) are then used to calculate the concentration of glucose present.

Equation 1. $$\text{glucose} + \text{oxygen} \xrightarrow{\text{glucose oxidase}} \text{gluconic acid} + H_2O_2 + 7\text{kcal}$$

(Bourdillon, Bourgeois et al. 1980; Fisher, Rebrin et al. 1994) .

2.1.1. Oxygen based electrochemical glucose sensors

In oxygen based sensors, the enzyme is coated onto the electrode usually mixed into a polymer matrix such as Poly(2-hydroxyethyl methacrylate) (HEMA). This forms an enzyme HEMA (EH) membrane. The glucose and oxygen diffuse into the membrane and react through the catalytic action of the GOD, the waste products of the reaction then diffuse out of the membrane as shown in figure 2. The reaction in the enzyme layer is shown in Equation 1, and at the electrode is shown in Equation 2.

Equation 2. $O_2 + 4H^+ + 4e^- \rightarrow 2H_2O$

(Hall 1990)

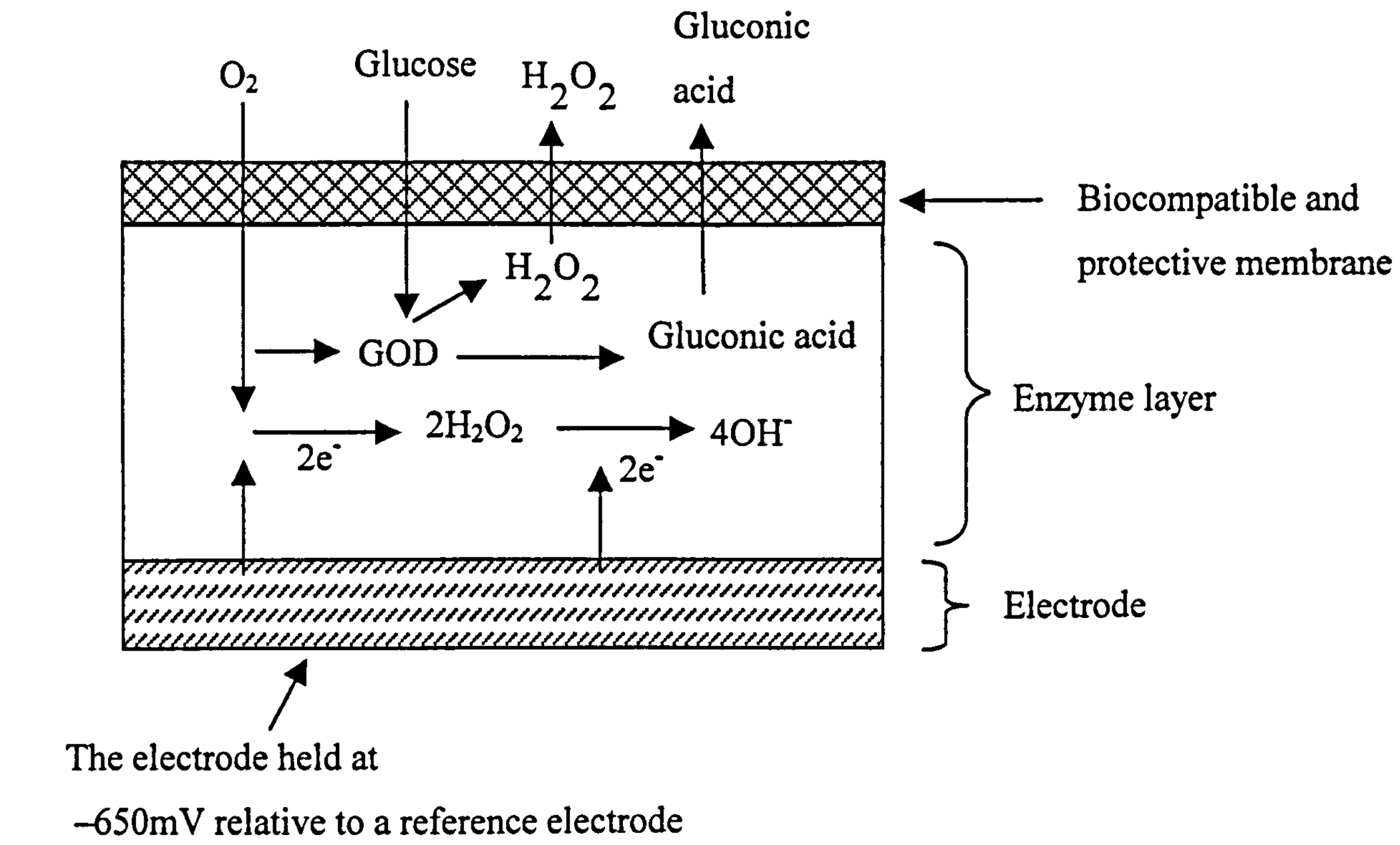

Figure 2. The chemical reaction in the enzyme membrane

If the EH layer is constructed with the appropriate diffusion characteristics, with low permeability, as will be discussed in chapter 3, the glucose concentration alone will control the rate at which oxygen is consumed. So, the glucose concentration can be calculated by measuring the rate of oxygen consumption, which is calculated from the decrease in the oxygen tension measured at the electrode.

As the electrode consumes oxygen during the measurement, problems can arise from the oxygen in the sensors environment being exhausted by the sensor. This is dealt with by an appropriate choice of membrane diffusion characteristics, with lower permeability to glucose than oxygen, see chapter 3, or by modulating the potential of the electrode, which involves switching the potential on and off several times a second (between 50 and 100Hz). This prevents the area immediately adjacent to the electrode becoming depleted of oxygen (Hall 1990).

Electrochemical oxygen sensors, although far more interference free than their glucose counterparts are subject to interference from other constituents in the blood and are also vulnerable to interference from some anaesthetic gasses such as halothane and nitrous oxide (Hall 1990).

2.1.2. The stoichiometric limitation problem of oxygen based electrochemical glucose sensors

Oxygen based electrochemical sensors, and all sensors which use GOD to detect glucose, suffer from the problem of the low concentration of oxygen compared to glucose in body tissue. The relative concentration of oxygen and glucose in tissue is roughly 0.2mM/l to 5.5mM/l respectively (Gough, Leypoldt et al. 1982). The oxygen concentration can also vary in different parts of the body (Zhang and Wilson 1993). This tends to limit the range of the glucose sensor, as there is not enough oxygen to fuel the oxidation of glucose at higher glucose concentrations.

Differentially permeable membranes allow oxygen to diffuse freely into the EH membrane while reducing the flux of glucose. This increases the range of the sensor, as less oxygen is required to fuel the enzyme reaction, and reduces the effect of the stoichiometric limitation. Appropriate choices of membrane permeability can also be used to produce a sensor with a linear response to glucose (Wilson and Turner 1992).

Another strategy to overcome the stoichiometric oxygen limitation was a radially-symmetrical sensor proposed by Gough, Lucisano et al. 1985. The radially-symmetric sensor design is shown in figure 3. With this design, glucose can diffuse into the front of the sensor but not the sides due to the hydrophobic gas permeable layer. Oxygen, however, can diffuse through all sides of the sensor. It was found that aspect ratios (face to side area) of 1/3 gave optimal performance. A second oxygen sensor was used along side the glucose sensor as a reference. This allowed a differential oxygen measurement to be taken between the two sensors that cancelled out the effects of ambient oxygen fluctuation.

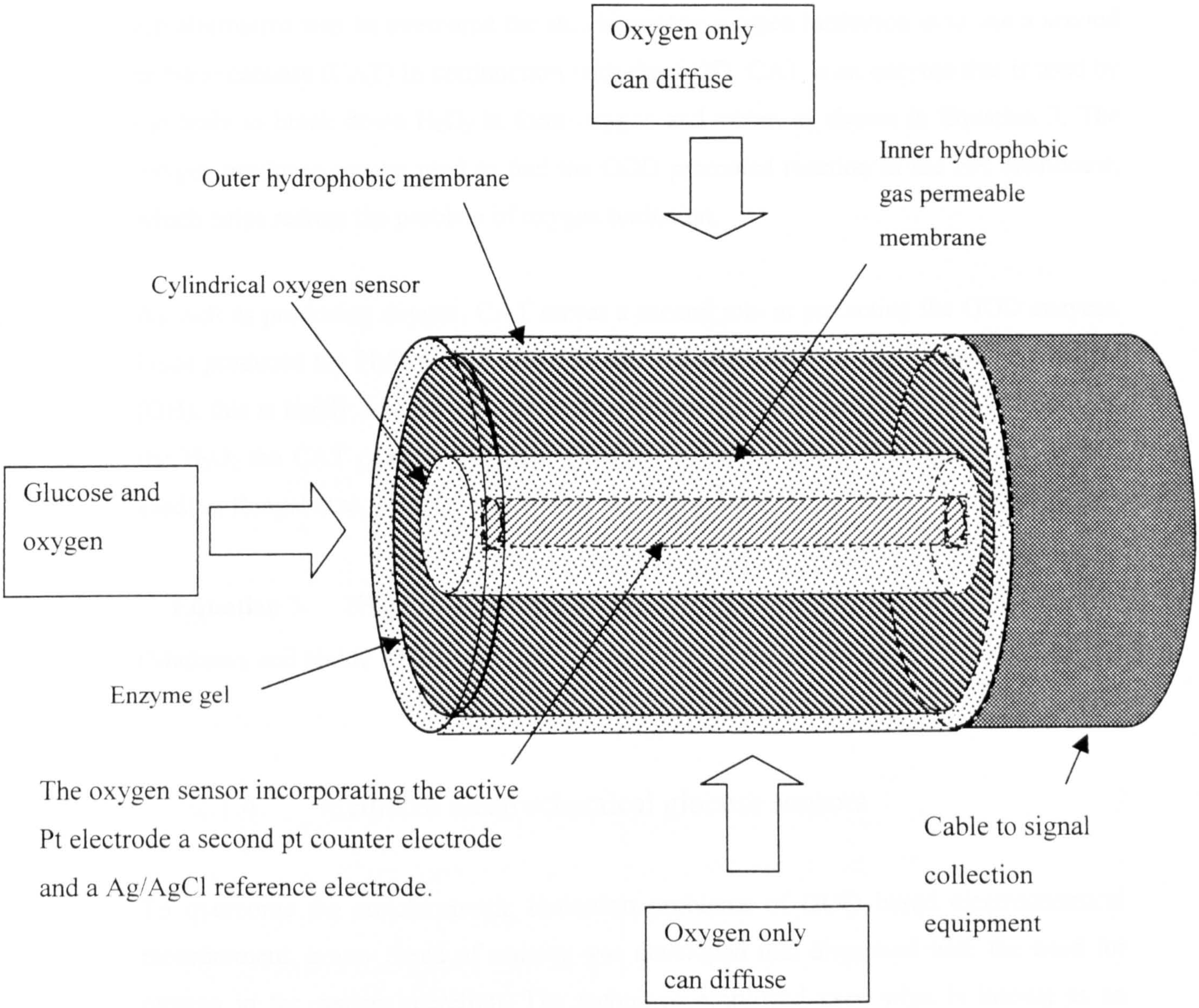

Figure 3. The radially- symmetric glucose sensor design

This sensor had a range of 0 to 500mg/dl (0 to 27.7mM/l). However, its 90% response time was 8 to 12 minutes when implanted into the femoral veins of rabbits and dogs. The sensor operated well despite 25% increases in the ambient oxygen tension. However, there was a ten-minute lag between blood glucose concentration changes and

the sensor response (Gough, Lucisano et al. 1985; Gough, Armour et al. 1986). The range of this sensor is more than sufficient for blood glucose measurement; however, its slow response time in vivo is too slow to be used as a hypoglycaemic alarm.

2.1.3. Recycling of oxygen using the enzyme catalase

An alternative way to overcome the stoichiometric oxygen limitation is to use a second enzyme catalase (CAT) in conjunction with the GOD. CAT is an enzyme that is used by the body to break down H_2O_2 to form oxygen and water, as shown in Equation 3. The oxygen produced can be used to fuel the GOD promoted reaction in the EH membrane, which helps redress the problem of oxygen limitation.

As well as producing oxygen, CAT serves a second role in protecting the GOD enzyme. Once produced the H_2O_2 breaks down in solution with water to form a hydroxyl radical (OH), this is highly reactive and can destroy or damage GOD and CAT. So, by removing the H_2O_2 the CAT protects the GOD (Tse and Gough 1987; Wilson and Turner 1992; Lledias, Rangel et al. 1998).

Equation 3. $$2H_2O_2 \xrightarrow{CAT} 2H_2O + O_2$$

(Mathews and Holde 1990).

2.1.4. Mediated electrochemical glucose sensors

To overcome the stoichiometric limitation problems of GOD based electrochemical measurement, a new breed of sensors was developed that dispensed with the need for oxygen in the sensor operation. The technique employed used what is known as an 'oxygen mediator'. The role of oxygen in the oxidation of glucose is to remove two electrons from the GOD enzyme. The enzyme then uses its depleted electronic state to break the glucose down into gluconolactone, which then dissolves to become gluconic acid. The oxygen can be replaced by an appropriate chemical (oxygen mediator), which will shuttle electrons from the enzyme to an electrode as shown in figure 4. where ferrocene is used as the oxygen mediator.

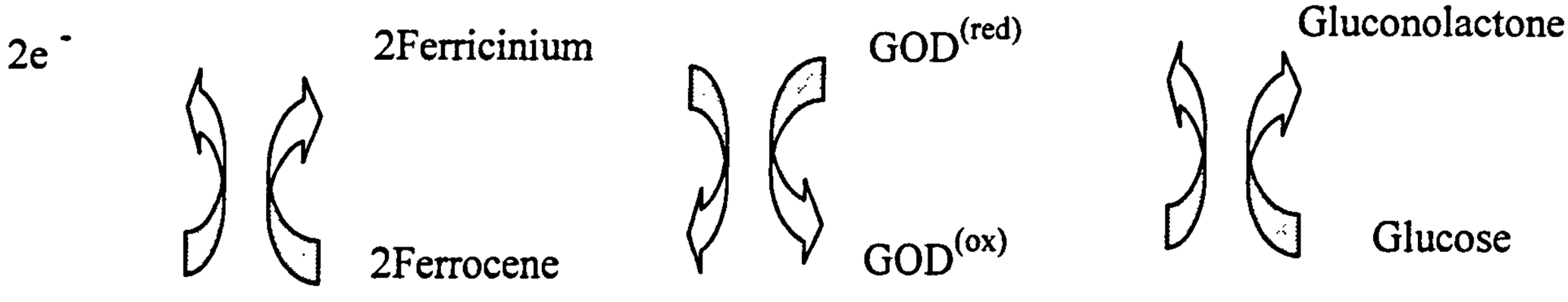

$GOD^{(red)}$ glucose oxidised reduced form [added e^-]

$GOD^{(ox)}$ oxidised form [removed e^-]

(Pickup, Shaw et al. 1989)

Figure 4. Electron mediation

The use of a mediator has another advantage in that the electrode can be held at much lower potentials than in other sensor designs, which removes some of the interference problems caused by other analytes (Pickup, Shaw et al. 1989).

2.1.5. Hydrogen peroxide based electrochemical glucose sensors

As well as the consumption of oxygen, the production of hydrogen peroxide can also be used to measure glucose concentrations. The H_2O_2 is produced as GOD promotes the breakdown of glucose, as shown in Equation 1. Hydrogen peroxide is detected by using an electrode, which is kept at approximately 700mV relative to a reference electrode, as shown in figure 5 and Equation 4. The amount of hydrogen peroxide present is calculated from the current flowing through the electrodes.

Equation 4. $$H_2O_2 \xrightarrow{+700mV} O_2 + 2H^+ + 2e^-$$

(Shichri, Yamasaki et al. 1982)

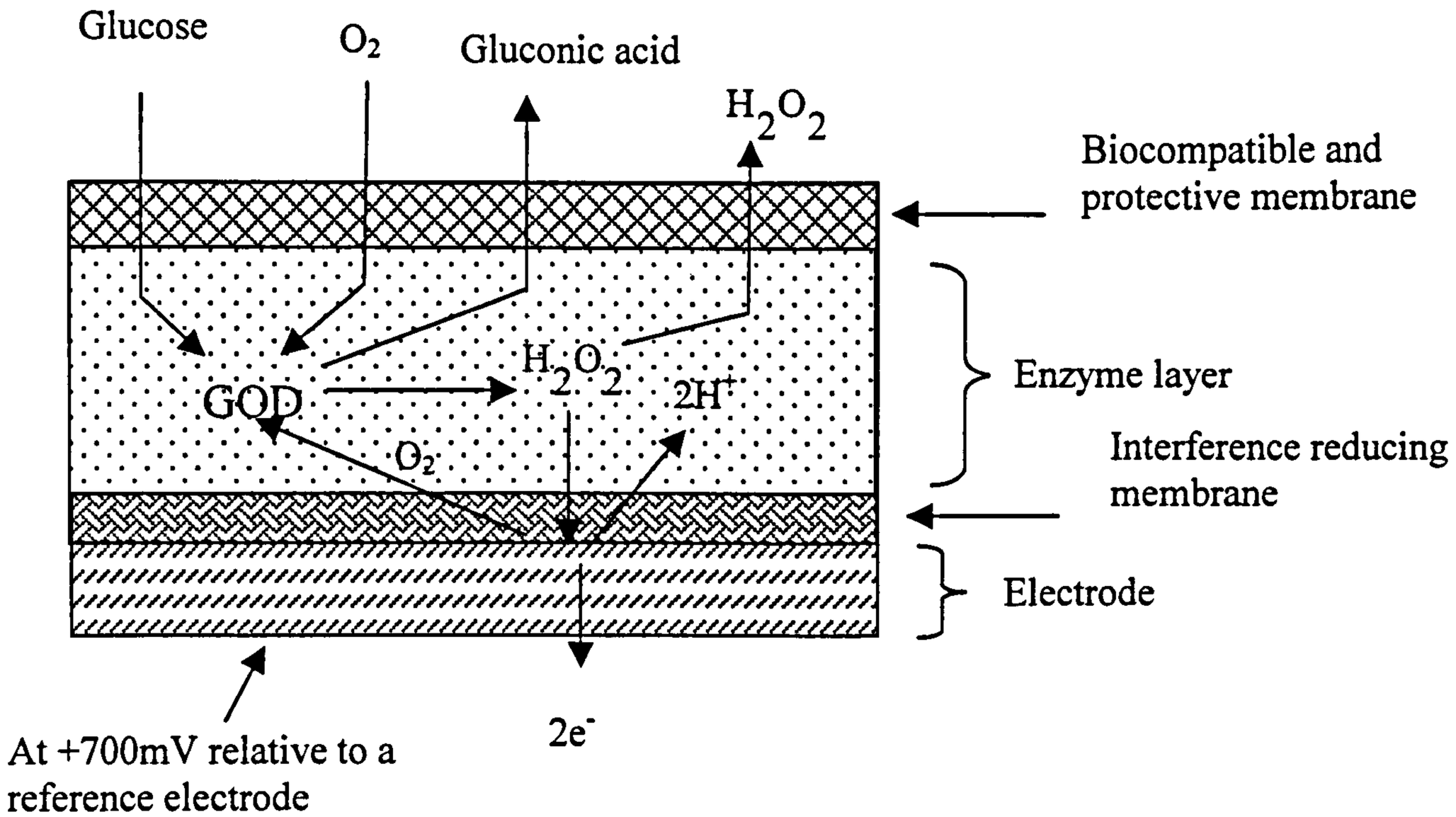

(Wilson, Zhang et al. 1992; Fisher, Rebrin et al. 1994)

Figure 5. The basic design of $\mathbf{H_2O_2}$ based glucose sensors

Because of the size of the polarisation voltage needed to measure H_2O_2, 700mV, the process can be influenced by other analytes in the blood, such as ascorbate, paracetamol, and urate (Kusano 1989; Shaw, Claremont et al. 1991; Fisher, Rebrin et al. 1994). The problem of interference is dealt with by coating the electrodes in membranes such as cellulose, nafion, and poly(m-phenylenediamine) amongst others, which prevent interfering species from reaching the electrode surface (Kusano 1989; Moussey, Harrison et al. 1993; Ward, Jansen et al. 2002; Yang, Chung et al. 2002). However, interference can still be a problem that reduces the reliability of hydrogen peroxide electrochemical sensors.

2.2 Glucose measured from exudates

Sweat is a slow process and only occurs under certain conditions, which makes it unsuitable for glucose measurement (Guilbault and Palleschi 1995; Kost, Mitragotri et

al. 2000). However, there are a number of ways to promote the passage of subcutaneous fluid to the surface of the skin, including suction, iontophoresis and ultrasound techniques.

2.2.1. Suction effusive fluid glucose measurements

The application of a negative air pressure to the surface of the skin causes a subcutaneous fluid or suction effusive fluid (SEF) to be drawn out. The glucose concentration in this fluid is then measured using electrochemical techniques. When applied to healthy subjects blood glucose concentrations were successfully measured. However, there was a delay of 10 to 20 minutes between the glucose concentrations of the SEF when compared to serum glucose, the SEF values were also 19 to 33% of the serum values. There was also some damage caused to the skin by this technique (Kayashima, Arai et al. 1991). A similar study on type II diabetics demonstrated similar correlations between SEF and serum values (0.92) but with roughly a 15-minute delay between serum and SEF values (Kikuchi, Kayashima et al. 1996). The delay in changes between the SEF and serum values makes the sensor too slow to be used as a hypoglycaemic alarm. The damage caused to the skin of the patient would also mean that the sensor would not be practical for use with diabetics due to their reduced ability to heal (Jones and Gill 1997).

2.2.2. Iontophoresis promoted exudates glucose measurements

Iontophoresis, sometimes referred to as reverse iontophoresis in this application, is a technique where an electric current is passed through the skin and subcutaneous tissue between two electrodes. Although glucose carries no charge, it is caught up from the fluid flow of charged analytes in the subcutaneous fluid, that flow through the skin to the electrodes. The glucose concentration of the fluid that arrives at the electrodes is then measured again using electrochemical technology. As with suction techniques, there was some skin damage detected. This approach allows measurement of the glucose concentration over a period of at least five minutes rather than at a particular point (Rao, Guy et al. 1995; Tamada, Bohannon et al. 1995). Although, due to its slow response time, (20 minutes), this would not provide a hypoglycaemic alarm or method for insulin dose adjustment, it has been turned into a commercial device called the Glucowatch produced by Signus Inc. The Glucowatch has been employed to deliver a means of monitoring blood glucose concentration trends in diabetics over a 12-hour period but not to adjust insulin dosage (Garg, Potts et al. 1999). As with suction effusive fluids, the slow response and skin damage mean that this would not be suitable as a hypoglycaemic alarm or to adjust insulin dosage.

2.2.3. Exudate glucose measurements through ultrasonic techniques

Ultrasound has also been used to promote the transport of glucose across the skin barrier (Kost, Mitragotri et al. 2000). Short duration ultrasonic pulses were applied to the skin, followed by the application of negative air pressure. It was found that short applications of ultrasound in two-minute bursts would increase the glucose flux across skin by a factor of 570, compared to unassisted flux with only suction. The increased glucose flux remained for 15 hours after each burst and then decreased to normal after 24 hours. No skin damage caused by the ultrasound was reported, but the suction apparatus did leave a transient imprint on the skin. There was a 30-minute lag-time between glucose levels measured and the corresponding core blood glucose levels. However, once this delay was accounted for, the measured glucose approached the core glucose levels with only one clinically dangerous error out of 53 in vivo measurements on type I diabetics (Kost, Mitragotri et al. 2000). Again, due to the lag-time, this technique is too slow to be used

to adjust insulin dosage or detect hypoglycaemia. The issue of long term effects of breaking down the skin's diffusion resistance to fluids, with regard to infection and damage, would have to be evaluated.

2.2.4. Microdialysis glucose sensors

These techniques use a small bore double lumen needle covered in a dialysis membrane, which is inserted into subcutaneous tissue. Fluid is circulated inside the membrane and glucose diffuses into the fluid from the tissue serum surrounding the probe, figure 6. The glucose gathered is then measured and this is used to calculate the blood glucose level.

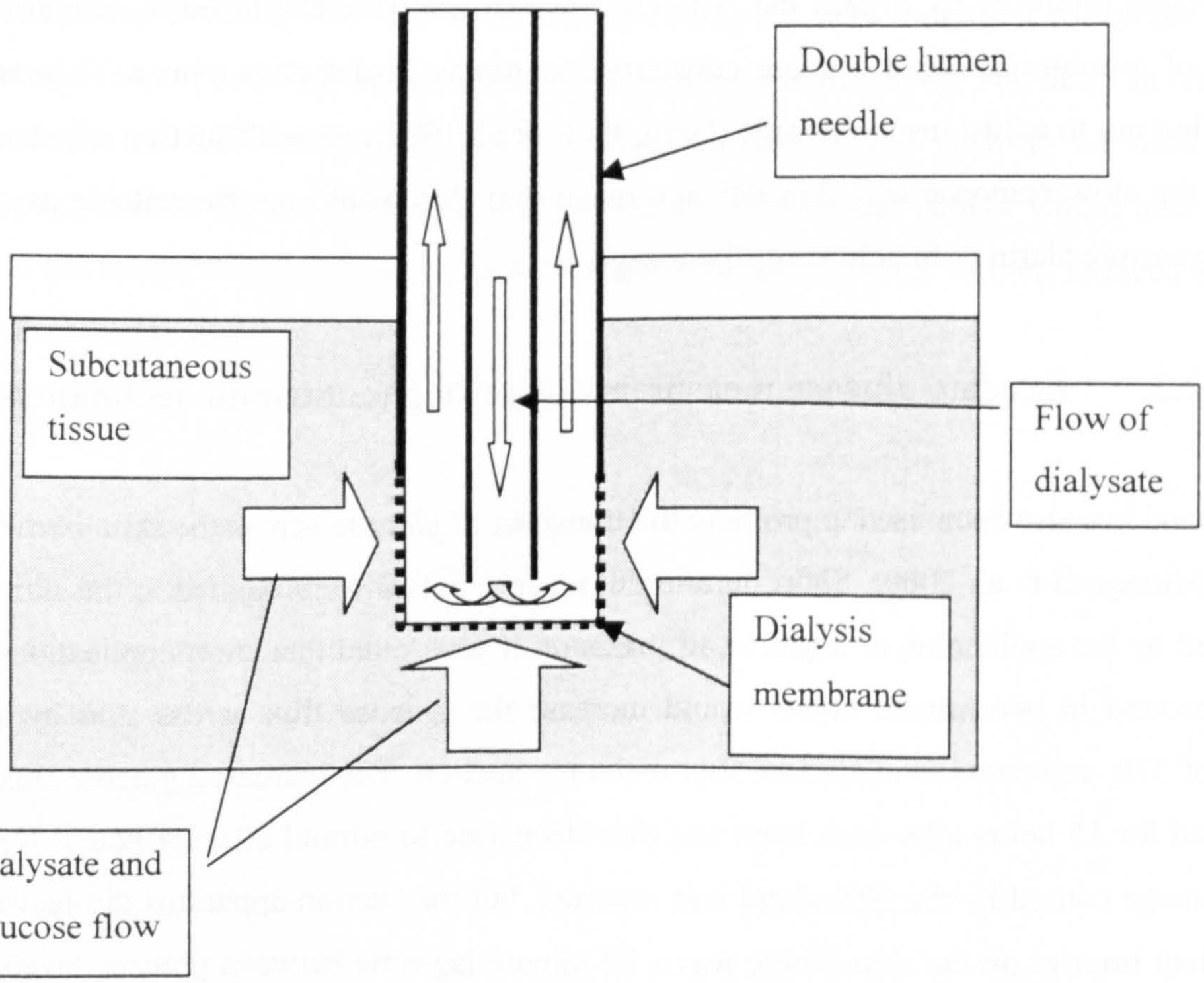

Figure 6. Design of the microdialysis probes

The basic design of the microdialysis probe is shown in figure 6 (Sternberg, Meyerhoff et al. 1995). Once collected, the glucose concentration in the dialysate is measured by a variety of methods. These include a GOD method (Bolinder, Ungerstedt et al. 1992), a GOD/peroxidase test and an amperometric glucose sensor (Sternberg, Meyerhoff et al. 1995; Rhemrev-Boom, Tiessen et al. 2002), Fourier transform infrared spectroscopy (FT-IR spectroscopy) (Bittner, Heise et al. 1997) and a hydrogen peroxide glucose sensor (Hashiguchi, Sakakida et al. 1994). The response time of microdialysis is slow as the dialysate can take several minutes to equilibrate with the surrounding tissue.

2.3 Fibre-optic glucose sensors

These sensors generally use optical fibres that have glucose sensitive chemistry along with a fluorescent dye immobilised at the tip. The fluorescence emission of the dyes is affected indirectly by the presence of glucose. A number of techniques using fibre-optics have been developed and, as this research is into the development of a fibre-optic sensor, these approaches are described here in detail.

Optical fibres transmit light using the principle of total internal reflection, briefly this involves light being reflected from the interface of two optical materials of different refractive indexes. The basic design of a fibre is shown in figure 7. below, the core of the optical fibre is made from a material with a higher refractive index than the cladding material, any light launched down the fibre within a certain range of angles range (known as the numerical aperture) will be reflected from the boundary of the core and cladding and travel down the fibre. There are two main types of optical fibre, multimode and single-mode fibres. Multimode fibres, like the type shown in figure 7, have a core that is large enough to allow several different paths (modes) to propagate down the fibre. Single mode fibres have a core that will allow only a single path to be taken by light travelling down its length. The majority of biosensor fibre-optic systems use multimode fibres. Depending on the materials used in their construction optical fibres can carry light from visible (0.4μm) up to the mid infrared wavelengths (20μm) (Ashworth and Narayanaswamy 1989; Kellener, Gobel et al. 1995; Kolimbiris 2000)

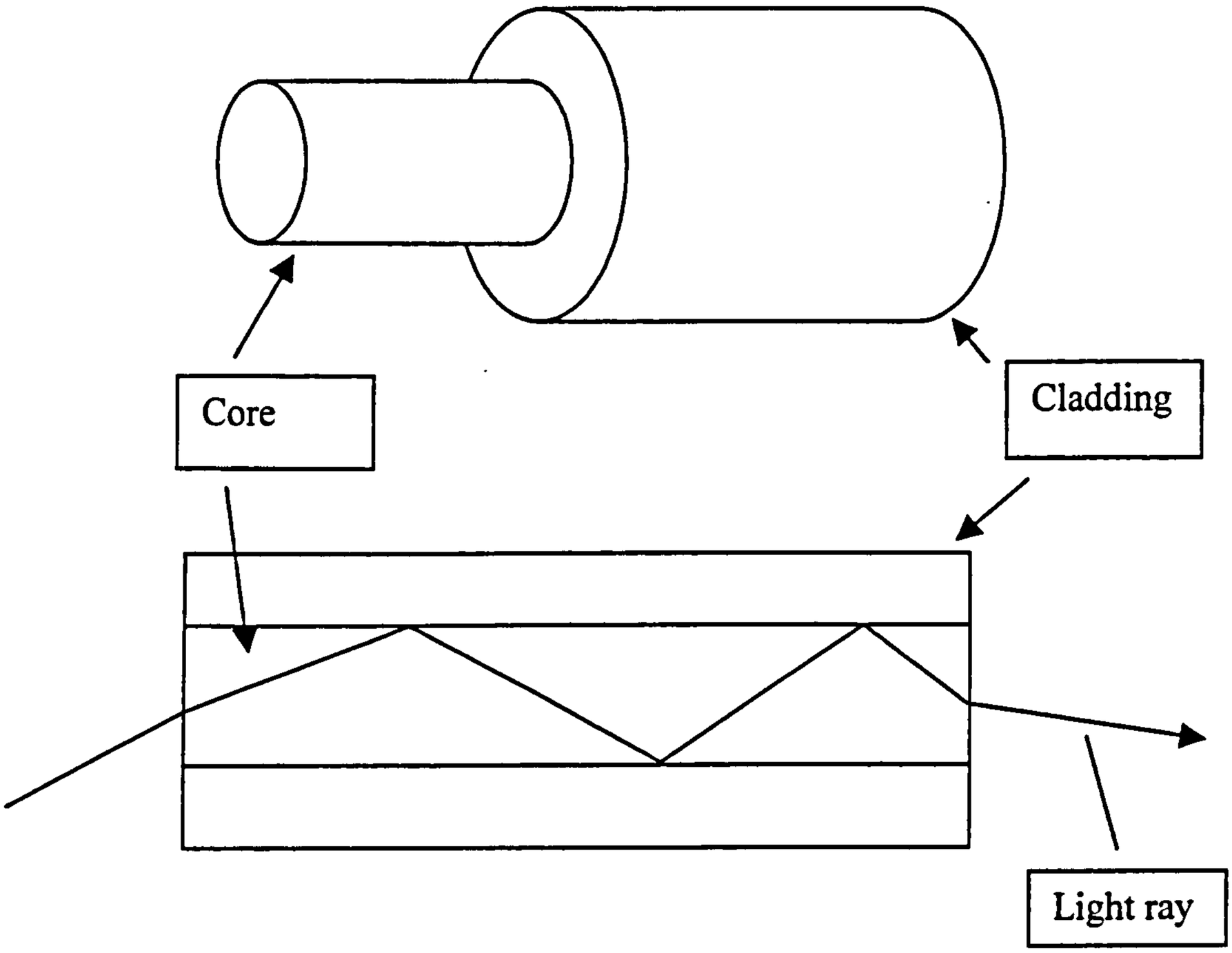

Figure 7. A multimode optical fibre

When used in sensing applications, optical fibres are used to transmit light to and/or from the target material of interest. Optical fibres can be used to simply collect light from an illuminated sample, which is then examined using spectroscopic techniques. Alternatively the cladding can be removed from a section of the fibre and this section placed in contact with a chemical sample. Light travelling through the core interacts with material in contact with the surface of the fibre by means of an evanescent wave the spectrum of the resulting light emerging at the end of the fibre then contains information about the material in contact with the fibre. In many applications, as will be discussed later in this chapter, optically active chemical species are immobilised onto the tip of a fibre. The optical fibre is then used to illuminate the immobilised chemical materials and collect any emission light produced through photochemical processes. These chemicals interact with the target species of interest and their optical emission is altered as will be described in chapter 4 (Ashworth and Narayanaswamy 1989).

There are several factors that can affect the optical signals carried by optical fibres, some of the main process are discussed here. The fibre its self will cause signal

attenuation that is wavelength dependent in its magnitude. Bending of the optical fibre will cause a loss in optical signal as a result of changes in the boundary between the core and cladding. To compensate for these changes, as well as the measurement optical signal a reference optical signal is often used. This reference signal is of a wavelength that is not affected by the sensing chemistry, by monitoring its intensity, any changes in the transmission characteristics of the system can be compensated for. Light from the outside environment can also cause interference in the signal this is compensated for by either shielding the measurement system form light or modulating the illumination light and then removing none modulated signal components from the returning light (Ashworth and Narayanaswamy 1989).

2.3.1. Fibre-optic glucose affinity sensors

A glucose affinity sensor was designed and built by Schultz, Mansouri et al. 1982; Mansouri and Schultz 1984. The sensor used the process of reversible binding of glucose to the lectin concanavalin A, (ConA). The glucose competes for binding to the ConA with another sugar, dextran, which is labelled with a fluorescent dye, fluorescein (FITC), to form FITC-dextran. The concentration of the FITC-dextran can be measured using fluorescence intensity measurements (discussed in Chapter 4). The ConA was immobilised onto the inner side of a section of dialysis tubing, see figure 8. This tubing was sealed at one end, with the other end fixed to an optical fibre to form an enclosed cavity. The sensor assembly was small enough to be inserted through a 23-gauge needle.

The FITC-dextran cannot pass out of the dialysis tubing due to its size (molecular weight of 70, 000 atomic mass units), however, glucose can freely move between the outside solution and the interior of the tube. Because of this freedom of movement, the concentration of glucose inside the dialysis cavity will be equal to that in the bulk solution. Any glucose inside the dialysis cavity will displace the FITC-dextran from the ConA on the walls of the dialysis tubing. The amount of FITC-dextran in free solution (inside the dialysis cavity) will be proportional to the amount of glucose present in the outside solution.

During in vitro tests, the sensor proved to have a range of zero to 8mg/ml (44mM/l) and a random error of ± 0.13 mg/ml (0.7mM/l). Its 90% response time was, however, around five minutes to step changes in glucose concentration of between 1 and 6mM/l, although it was suggested by the authors that it might be possible to reduce this by a different choice of dialysis tubing. The sensor was found to be sensitive to temperature fluctuations and pH, although in a healthy body both of these only vary by a limited amount. The sensor was unaffected by oxygen fluctuations and plasma constituents but due to its slow response time, the sensor is not suitable for use as a hypoglycaemic alarm.

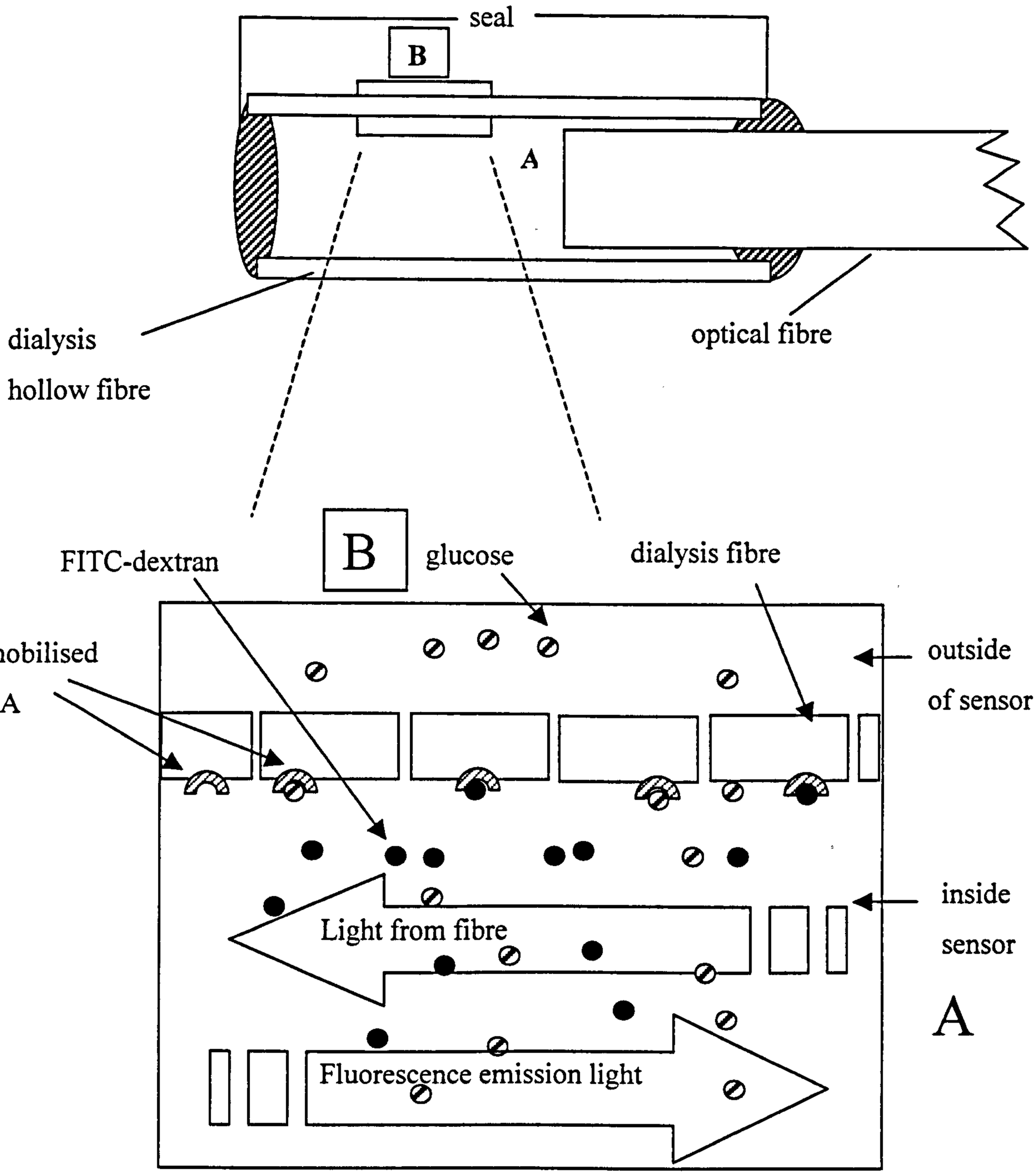

Figure 8. A glucose affinity sensor described by Schultz, Mansouri et al. 1982; Mansouri and Schultz 1984.

Some years later, (Meadows and Schultz 1993) created a modified version of the above sensor. The immobilised ConA was replaced with free-floating tetramethylrhodamine isothiocyanate labelled Concanavalin A (TRITC-ConA). When the TRITC-ConA binds to FITC-dextran, it quenches (prevents fluorescence emission) the FITC-dextrans fluorescent emission. As before, the FITC-dextran competes with glucose for the TRITC-ConA. Therefore, the amount of fluorescence quenching is proportional to the concentration of glucose. Like the FITC-dextran, the TRITC-ConA is too large to escape from the dialysis membrane. The TRITC-ConA also has a fluorescent emission wavelength of its own. This was used as an optical reference signal to measure any changes in the optical parameters of the system. However, the design exhibited baseline drift and a loss of dynamic range, which made it unusable in the space of only two hours. Until this problem is resolved, the sensor is of no use as a blood glucose sensor.

2.3.2. Oxygen based fibre-optic glucose sensors

A glucose sensor with an oxygen optrode (optical glucose sensor) was made by Schaffar and Wolfbeis 1990. The oxygen sensor was created by immobilising a fluorescent dye in silicone onto the tip of a fibre-optic cable of 8mm in diameter. The dye was quenched in proportion to the presence of oxygen. GOD was then immobilised on top of the oxygen sensor and glucose measured via the oxygen reduction during the oxidation of glucose, in the same way as the electrochemical GOD based sensors. The range of the best sensors was 0.04 - 2mM/l but this was extended to 5mM/l with the use of a dialysis membrane, with a response time of one minute. By using a 500µl dialysis encased fluid filled cell placed around the sensor, the range was further increased to 1-200 mM with a response time of three to five minutes. The size of this sensor would be too large to be practical, although its range and response time (with the dialysis membrane) is more than sufficient for the needs of a glucose sensor. The size of the sensor will have to be reduced for it to be a practical sensor. In addition, as this sensor uses the same GOD technology as the electrochemical oxygen based sensors, it will encounter the same range and stoichiometric problems.

In a very similar sensor design to the above, oxygen consumption was also used to measure glucose by Moreno-Bondi, Wolfbies et al. 1990. The sensor consisted of GOD

immobilised onto a layer of carbon, below this was a layer of silicone containing an oxygen sensitive fluorescence dye. An optical fibre bundle was then used to illuminate the sensor and collect the emission light. The sensor had a range of 0.06-1mM glucose in air-saturated solutions, with a response time of six minutes. Although having a high sensitivity, the sensor would be of no use as a practical sensor for diabetes due to its limited range. In addition, the subcutaneous tissue or blood stream would have a lower free oxygen tension than air. The response time is also too slow to be useful clinically. Tests of the sensor for interference from the other sugars; saccharose, fructose, lactose and galactose at 100mM showed no signal changes. The sensors had a lifetime of 12 months when stored at 4°C. The fabrication reproducibility was very good with different sensors having almost identical calibration curves.

Another fluorescent oxygen sensor coated in GOD was used to measure glucose concentrations by Li and Walt 1995; Healey, Li et al. 1997. The oxygen sensitive dye and the GOD were immobilised onto the tip of an optical fibre bundle, using a photo-polymerisation technique. This technique allowed very small sensing sites, around 50 micrometers in diameter, to be deposited on the surface of the fibre. The sensing areas were fabricated with a double layered polymer cone as shown in figure 9. To compensate for oxygen variations, other sensing areas were fabricated on the sensing end of the fibre that measured only the oxygen concentration in the environment of the sensor. This allowed a differential measurement to be taken between the oxygen reference and the glucose sensing sites that would remove the effect of background oxygen variations.

The small size of the sensing sites allowed several sites to be fabricated on the end of the imaging fibre bundle. The fibre-optic bundle comprised of three to six thousand individual fibres. The individual sensing sites were imaged by a charge-coupled device (CCD) camera attached to the other end of the fibre bundle. Each site could be given a different thickness of EH, allowing different sites to cover different ranges of glucose concentration. Tests of this system demonstrated an accuracy of 0.6mM over the range 0-2mM glucose over a range of oxygen tensions (down to ≈10KPa), with a response time of 9-28s, and the probe was found to operate for two days in an in-vitro environment

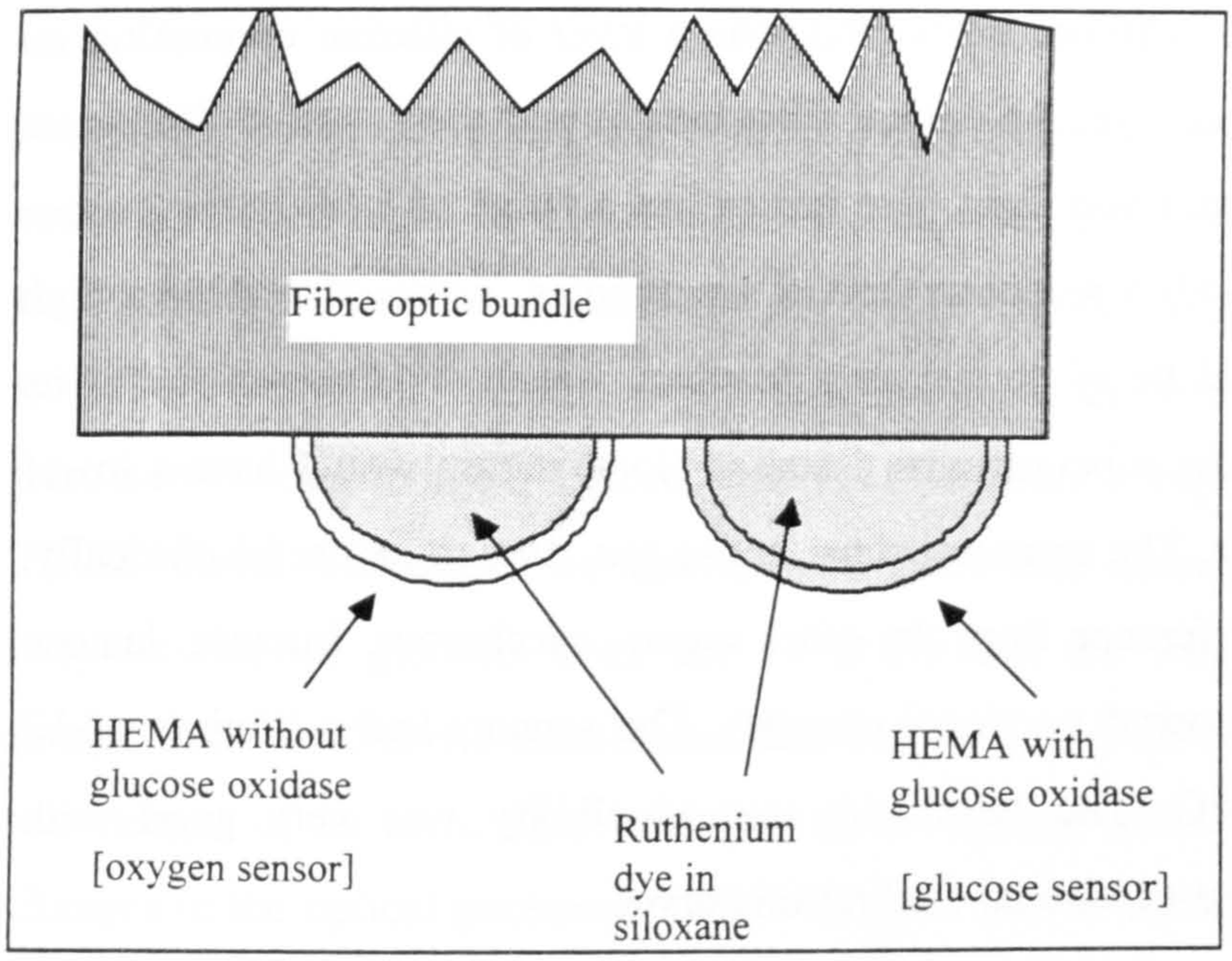

Figure 9. The design of the multiple sensing site fibre optic glucose sensor.

A highly sensitive fibre optic glucose sensor of only ten micrometers in diameter was constructed by Rosenzweig and Kopelman 1996. Again, the sensor operated by measuring the oxygen consumption as glucose was oxidised by GOD using fluorescence quenching of an oxygen sensitive fluorescent dye. The miniaturisation of the sensor was achieved by heating the tip of a 100μm diameter optical fibre with a laser beam and pulling the tip into a fine point. A mixture of dye and GOD in an acrylimide support was then coated onto the tip of the optical fibre using a photopolymerisation technique. Using this construction method sensors were fabricated with sensing areas only a few microns across. This miniaturised sensor gave very fast response times, 95% response from a 1 to 5mM steps in 1.5 seconds and a recovery of two seconds. The sensor range was from 0.7 to 10 mM with high sensitivity. The only limitation of the sensor was the short lifetime of four to six days. This is short compared with larger sensors, which have been known to operate for several weeks. The reason for this reduced lifetime was thought to be due to the effective increase of enzyme activity, which is related to the surface area to volume ratio of the EH layer. With a EH layer so small, the amount of enzyme is much less than in larger sensors. This means that any enzyme deactivation or loss will affect the sensor far more rapidly than larger sensors that have more enzyme to spare.

2.3.3. Fibre-optic glucose sensors using optical absorption of GOD

A glucose sensor based on the absorption changes of GOD was constructed by Chubdova, Vrbova et al. 1996. The sensor operated by measuring the change in the optical absorption of the GOD coenzyme FAD. In the presence of glucose, the FAD is converted to $FADH_2$ and then oxidised back to FAD as shown in figure 10.

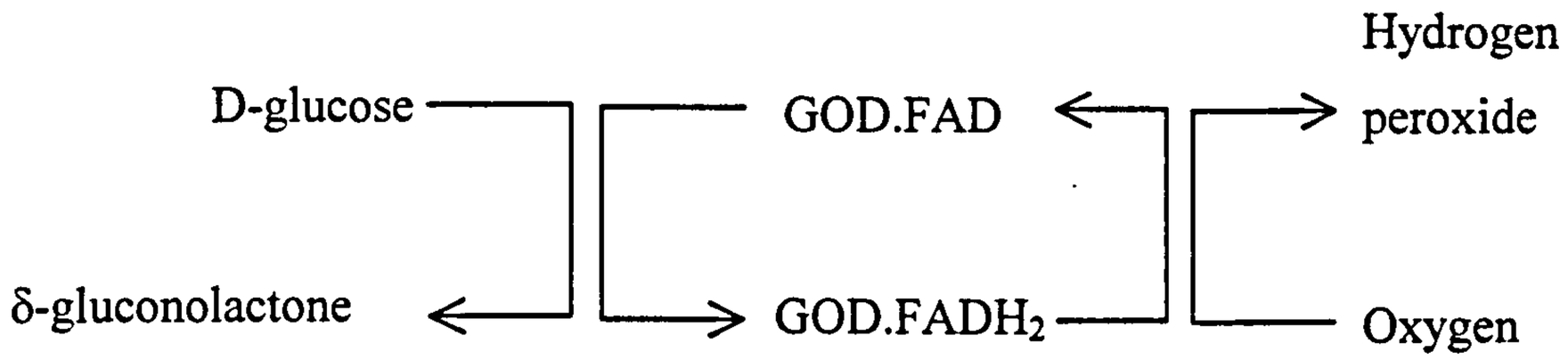

Figure 10. The GOD optcal sbsorption based glucose sensor

The GOD was covalently linked to a nylon net, which in turn was fixed to a HEMA layer. This assembly was then attached to the common end of a bifurcated optical fibre bundle. The absorption of the FAD was measured and used to calculate the concentration of glucose. Glucose concentrations could be measured in a range of 2 to 10mM in air saturated solutions, the response times of the sensor ranged from seconds to five minutes for lower concentrations; regeneration time of the sensor was two to fifteen minutes. The sensor was shown to be almost insensitive to pH changes, compared to the enzyme free solution. Maximum catalytic activity of the EH membrane was found to be at 37°C. The ambient oxygen concentration did affect the lower detection limit of the sensor. A test of the sensor in nitrogen-saturated solution, showed that the glucose detection limit had lowered to 0.45mM/l. Adding catalase to the test solution raised the lower glucose detection limit by 35%. This was thought to be due to oxygen being recycled as the catalase broke down hydrogen peroxide to produce water and oxygen. The oxygen limitation problems and the response times are outside those required for a hypoglycaemic alarm.

2.4 Non-invasive measurements

2.4.1. Near infrared spectroscopy

The most desirable method of measuring blood glucose would be a totally non-invasive technique as this would be painless and convenient. To this end, there has been a large amount of research into possible non-invasive glucose sensing using near infrared spectroscopy (NIRS). This is due to the fact that it was known that a region of the infrared spectrum, the near infra red region (NIR), can penetrate tissue deeply enough to interact with blood rich tissue. This region is often termed the therapeutic window. Values quoted in the published literature for the therapeutic window vary, as do the values of penetration depth of light in this spectral region.

Infrared spectroscopy is an established technique used for in vitro chemical analysis. It has been adapted to in vivo measurement with limited success; however, the technique has to date proved too unreliable to be used as a method for insulin adjustment.

Wavelength range				Comments	Reference
Min		Max			
(nm)	(cm^{-1})	(nm)	(cm^{-1})		
600	16667	1200	8333		(Boulnois 1985)
700	14286	1300	7692	Significant amounts of light can be transmitted through several cm of tissue in this band.	(Glaister 1988)
700	14286	1000	10000	Light is transmitted through soft and hard tissues of the head.*	(Ferrari, Wei et al. 1989)
700	14286	1300	7692	Above 1300nm, all photons are stopped past a few mm of tissue.	(Jobsis 1977)
700	14286	900	11111	Light penetrates up to several cm.	(Fantini, Franceschini-Fantini et al. 1995)
	700/14286	900	11111	Tissue is relatively transparent to NIR light.	(Faris, Thorniley et al. 1991)
714	14006	2500	4000	Light can penetrate 1mm - 1cm.	(Haaland, Robinson et al. 1992)

* Bone is a relatively low absorbing material in the NIR, (Ferrari, Wei et al. 1989),with a low and featureless absorbance spectrum in the range 650 - 900nm (15385-11111cm^{-1}) (Firbank, Hiraoka et al. 1993).

Table 3. Values quoted in the literature of the therapeutic window.

Diffuse Reflectance	Transmission
Measurements on the finger using a wavelength range from 900 - 1200nm ($11111-8333cm^{-1}$) (Jagemann, Fischbacher et al. 1995).	Through a finger using light of 800 - 1000nm ($12500-10000cm^{-1}$) (Noda, Taniguichi et al. 1994).
Measurements were carried out on the forehead and forearm at 715 ($13986cm^{-1}$) and 815nm ($12270cm^{-1}$) (Blasi, fantini et al. 1995).	Through a finger using light from 750 - 1300nm ($13333-7692cm^{-1}$) (Robinson, Eaton et al. 1992).
Carried out studies on foetal heads using wavelengths of 775nm ($12903cm^{-1}$), 805nm ($12422cm^{-1}$), 845nm ($11834cm^{-1}$) and 905nm.($11050cm^{-1}$) (Faris, Thorniley et al. 1991).	Through the forearm using laser diodes of 778nm ($12854cm^{-1}$), 813nm ($12300cm^{-1}$), 867nm ($11534cm^{-1}$) and 904nm ($11062cm^{-1}$) (Cope and Delpy 1988).
Used LED's 0f 715nm ($13986cm^{-1}$) and 850nm ($11765cm^{-1}$) on measurements of the thigh and forearm (Fantini, Franceschini-Fantini et al. 1995).	
Performed measurements of infant's head at 650 - 1000nm ($15385-10000cm^{-1}$) (Cooper, Elwell et al. 1996).	

Table 4. Examples of diffuse reflectance and transmission experiments reported in the literature

2.4.2. Data analysis of NIR spectra

The spectral signature of glucose in the NIR region, which the therapeutic window occupies, is very weak and not well defined. In addition, the spectral features of other blood analytes, such as water and haemoglobin, dwarf the spectrum of glucose making concentration measurements problematic. Because of this, highly sensitive data analysis techniques have to be used to calculate the glucose concentration. Commonly used multivariate techniques are partial least squares (PLS) and principle component regression (PCR) (Heise, Marbach et al. 1992; Bhandare, Mendelson et al. 1993; Bhandare, Mendleson et al. 1994; Heise and Marbach 1994; Martens and Naes 1994; Jagemann, Fischbacher et al. 1995). Artificial neural nets (ANN), (Patterson 1996), have also been used to create calibration models for glucose spectra with some success by Jagemann, Fischbacher et al. 1995 . They have also been combined with PLS to produce a hybrid calibration model by Bhandare, Mendelson et al. 1993. Despite some success in measuring glucose using NIRS, the weakness of the spectral signature of glucose and the interference from other analytes in the blood makes this method too unreliable.

2.4.3. Photoacoustic glucose sensors

Photoacoustic spectroscopy (PAS) works by selectively exposing a small volume of the liquid to a pulse of focused light; this causes localised heating followed by expansion produced. This thermal expansion of the liquid creates an acoustic wave, which travels out from the point of illumination. The profile of this acoustic wave is related to the geometry and energy of the incident light beam and to the concentration of component chemicals in the illuminated region. It is possible to calculate the concentration of component chemicals in the solution from acoustic signal measurements (Skoog and Leary 1992; Christison and MacKenzie 1993; MacKenzie, Christison et al. 1993). An advantage of PAS over normal spectroscopy is that it is less susceptible to scattering effects, which interfere with the standard spectroscopy techniques (MacKenzie, Christison et al. 1993). This may also offer greater sensitivity than NIRS for the weak concentrations such as glucose in blood (Quan, Cristison et al. 1993). This improvement

in sensitivity is because all the available energy of the light pulse, including the scattered portion, is still involved in the creation of the acoustic wave. In traditional NIR spectroscopy a large proportion of the incident light is lost due to scattering (MacKenzie, Christison et al. 1993). PAS has been used in a few investigations into non-invasive glucose measurement (Pan, Qui et al. 1988; Christison and MacKenzie 1993; Quan, Cristison et al. 1993). The research into this technique is limited and the improvement in reliability over NIRS techniques has not been demonstrated at this time.

2.5 Miscellaneous techniques

2.5.1. Optical polarimetry based glucose measurement

A number of groups have described the development and evaluation of non-invasive optical polarimetry systems to monitor in vivo glucose concentration of the eye (Rabinovitch, March et al. 1982) looked at the possibility of measuring optical rotation in the eye due to the effects of glucose. The apparatus used was capable of resolving $2x10^{-4}$ degrees of rotation, which allowed the detection of glucose down to 0.02% concentration. March, Rabinovitch et al. 1982 also carried out an investigation using optical rotation to measure glucose concentrations in samples of animal aqueous humour. The results showed a limited relationship between the glucose levels and the optical rotation. Cote, Fox et al. 1992 performed in vitro studies with solutions of glucose from zero to 1000mg/dl (0-55.5mmol/l). They found a correlation coefficient of 0.997 between polarisation and glucose concentration. More recent studies have also suggested that the delay between blood glucose concentrations and glucose concentration of the aqueous humor is only in the region of five minutes (Cameron, Baba et al. 2001). This technique, like PAS glucose sensing, has not been researched in depth and requires more work to investigate whether its performance is suitable for treating hypoglycaemia.

2.5.2. Raman spectroscopic glucose measurement

Raman spectroscopy was used in a preliminary investigation on glucose sensing in vitro samples of aqueous solutions of glucose. Raman spectroscopy uses the wavelength shift in light scattered from the target molecule. The samples of water containing lactic acid and urea were illuminated with a laser (514.5 nm) and the Raman scattered light at 90° was then collected. The results showed a correlation coefficient between predicted and known concentrations for glucose of 0.9952 over a range of glucose concentrations of 0 to 555 mM/l. Good correlations were also found with lactic acid and urea (Jenkins and White 1981; Geotz, Cote et al. 1995/7). However, the wavelengths used in this technique will probably not penetrate the skin deeply enough to allow measurement of blood rich tissue.

2.5.3. Modulated laser glucose measurement techniques

Spanner and Niebner 1996 used three NIR semiconductor lasers each of a different wavelength to measure glucose concentrations in aqueous solutions. The measurement system combined the laser diodes with a novel modulation technique. The absorption of each laser beam was then measured and combined to provide a value of the glucose concentration. This system was used to measure a series of glucose solutions from 0 to 55.5 mM/l (0-1000 mg/dl). A correlation was found between the measured glucose and predicted glucose levels of 0.96. Much more research is required to demonstrate the performance of this technique before it can be considered as a viable blood glucose sensing technique.

2.5.4. Kromoscopic glucose measurement

Sodickson and Block 1994 used a technique called Kromoscopic analysis to measure glucose concentrations in aqueous solutions. Kromoscopic analysis is based on the human colour vision system. Human colour perception can classify the colour of an object in real time and without independent measurement of the illuminating spectrum. In theory, Kromoscopic analysis could offer the same capabilities. The technique worked by using an array of NIR detectors each with a different spectral performance

profile. The combination of the response of each of these sensors to the spectra of light that has passed through tissue, hypothetically, could be used to calculate the glucose concentration. Kromoscopic analysis can also separate pulsate and non-pulsate components of the optical signal. This may allow the optical contribution of arterial blood in the signal to be isolated from the rest of the tissue and background by taking measurements of only the pulsate signal. In vitro experiments were carried out from 0 to 0.6 mM/l and in varying temperature 0-0.7°C, which have a large effect on optical absorption. The experiments showed that the glucose signal could be separated from the temperature variations. As with modulated lasers, this technique requires much more research to be carried out before it can be considered as a viable technique.

2.5.5. Measurement of glucose concentrations using scattering of light

As mentioned earlier, in spectroscopic techniques, scattering of light by tissue is a constant source of signal loss. However, as opposed to viewing the scattering as a barrier to glucose measurement, some investigations have sought to use this scattering process as a means to measure glucose concentrations (Kohl, Cope et al. 1994; Maier, Walker et al. 1994; Kohl, Essenpreis et al. 1995). A proportion of optical scattering in tissue is due to mismatches in the refractive indices of the extra cellular fluid (ECF) and the cellular membrane. Changes in glucose levels will in turn change the value of n_{ECF}, (where n_{ECF} is the refractive index for the ECF), whereas the value of n_{cell}, (n_{cell} is the refractive index for the cellular membrane), is assumed to be relatively constant. Changes in blood glucose levels will cause changes in the value of n_{ECF}. So any changes in the scattering of blood should be due to changes in n_{ECF}, and be related to changes in blood glucose levels. An in vivo test on one healthy subject (non-diabetic) was then carried out using a spectrometer capable of measuring the reduced scattering coefficient of tissue. A relationship was found between blood glucose levels and $n\mu_s'$ (Maier, Walker et al. 1994). Much more research is required to show the performance of this system.

2.5.6. Measurement of glucose using electrical capacitance

A glucose sensor using a capacitance sensor has been reported by Cheng, Wang et al. 2001. The sensor consisted of an electrode with an insulating polymer layer immobilised onto its surface. This polymer layer has glucose receptive sites imprinted onto it using electropolymerisation with glucose molecules as a template. Glucose can then bind to these sites changing the capacitance of the electrode polymer layer. The sensor showed a decrease in capacitance with increasing glucose concentrations over a range 0 to 40mM/l in vitro. The sensor showed little or no interference from ascorbic acid and fructose. However, signal drift was observed for operational periods of greater than 10 hours. The sensors built showed a relative standard deviation of 6% in repeatability tests at 5mM/l. As no results for decreasing glucose concentrations were given, so the reversibility of the glucose binding process has not been demonstrated.

2.6 Blood glucose measurement in subcutaneous tissue

The subcutaneous layer is made up of inhomogeneous connective tissue and blood vessels situated below the dermal and epidermal layers (Gray 2000). The interstitial fluid in the subcutaneous tissue should reflect the venous glucose concentration closely enough to be used as a measurement of core blood glucose levels (Service, O'brien et al. 1997).

Subcutaneous implantation removes the dangers posed by clots as no major blood vessels are involved; unfortunately, infection is still a risk though this may be reduced as the infection would be localised (Pickup and Williams 1997). The sensors would probably take the form of a wire style glucose sensor, which would be inserted just under the skin (Claremont, Sambrook et al. 1986; Fischer, Ertle et al. 1987; Moatti-Sirat, Capron et al. 1992; Bobbioni-Harsch, Rohner-Jeanrenaud et al. 1993).

There are some differences in the glucose values measured in subcutaneous tissue and core blood levels measured with these sensors, particularly during changing glucose concentrations (Velho, Froguel et al. 1989; Schmidt, Slutter et al. 1993; Sternberg, Meyerhoff et al. 1996; Schmidtke, Freeland et al. 1998). The response of the

subcutaneous tissue to the implantation of the sensor and to any infection, which is brought with it or gains access to the site later, will affect the performance of the sensor (Daley, Shearer et al. 1990). This is due to swelling, oedema and increased glucose uptake around the implantation site caused by trauma, infection and the tissues reaction to the sensor material. This will all affect the local glucose concentrations and diffusion rates from tissue to the sensor (Fisher, Rebrin et al. 1994). The pain of having the sensor implanted will also be present, although these problems could be removed by complete implantation of the sensor and its associated electronics and power source.

2.6.1. Completely implanted glucose sensor systems

A sensor implanted in a dog, which incorporated all necessary telemetry electronics for an electrocatalytic enzymatic sensor, operated for three to five months. However, the sensor was 7cm in diameter, much of the space was required for the battery supply; a sensor this size is impractical for human use (Updike, Shults et al. 2000). A smaller device, 26 mm in diameter and with 18 mm depth, has been developed with a battery life of one year. Glucose measurement was achieved using an amperometric sensor coated with GOD and the signal from glucose concentrations from 0 to 19.35 mM/l was linear in in-vitro tests (Beach, Kuster et al. 1999). Another completely implanted electrochemical sensor with its own on board telemetry system tested in healthy dogs allowed measurements to be taken at four minutes intervals over a three-month period. The sensors consisted of a 7 x 1 cm disc, each with bioprotective membrane to protect the active sensing site. Once implanted subcutaneously the sensors initially gave zero readings after one to five days of implantation they started producing unstable signals; between seven and fourteen days of implantation the sensors presented a stable signal that could be used for glucose measurements. The sensors were found to have long-term instability (42 days) making them unsuitable for clinical measurements. It was proposed that a monthly re-calibration would produce a viable sensor. The range of the sensors was found to be limited by tissue oxygen concentrations. Both sensors were found to have an in vitro upper limit of 33.3 mM/l but different in vivo limits of 27.8 mM/l and 17.5 mM/l of glucose. A limited time difference in the order of a few minutes between subcutaneous and serum blood glucose levels could be seen in the results. Examination of the explanted sensor showed that it had been encapsulated in an outer layer of fibrocytes and collagen and an inner layer composed of granulation tissue incorporating

many small blood vessels. However, the authors pointed out that the fibrous capsule will progressively contain less vascular tissue as time goes on, causing oxygen limitation to become an increasing factor with implant age. However, suggestions were made that growth factors or microarchitectures may be useful to promote longer-term vascularisation (Gilligan, Schults et al. 1994).

Another method of creating a totally implanted glucose sensors was investigated by Tolosa, Malak et al. 1997 who used a Concanavalin-A (Con-A) labelled with a fluorescent dye Cy5. The absorption and emission wavelengths of the dye were in the near infrared region, allowing the excitation and emission light top pass through the skin. The fluorescence lifetime of the dye would be reduced by glucose binding reversibly to the Con-A. The sensor proposed would consist of a sample of the dye labelled Con-A implanted in the subcutaneous tissue. This would then be excited using a light source outside the body and the resulting emission measured and used to calculate the concentration of glucose. Fluorescence lifetime changes were measured for glucose concentrations from 0 to 100 mM/l for increasing concentrations in vitro. However, problems were encountered with the reversibility of the binding of the Con-A and the glucose due to the attachment of the dye which resulted in problems measuring decreasing glucose concentrations (Tolosa, Malak et al. 1997).

2.7 Conclusions of glucose measurement techniques

The drawbacks of the various measurement techniques are shown in table 5 below. Non-invasive glucose measurement techniques, although potentially the most attractive approach, have many technical hurdles to overcome before they can produce a reliable measurement system. Infrared systems, including photoacoustic techniques, are handicapped by the weakness of the glucose spectral signature. The spectral signature of the many chemical species further complicates this problem. Alternatively, they rely on weak relationships with scattering coefficients or novel measurement systems, which are still in very early stages of development. Measurements of the eye require the measurement of rotational angles to an accuracy level that is at the limit of current technology. Microdialysis measurements, although more reliable, tend to be slow and there are questions over how well it represents the tissue glucose concentrations. The

electrochemical sensor designs have shown the greatest progress in producing a working sensor, however, they are dogged by interference problems. The most promising technology seems to be the fibre-optic sensor designs, especially the GOD based systems. These sensor designs can exploit the enzyme membrane technology developed for the electrochemical sensors but couple it with an interference free oxygen sensing core.

Glucose measurement technique	Comments
Electrochemical glucose sensors.	The voltages needed to detect glucose directly leads to interference form other blood constituents.
Oxygen based electrochemical glucose sensors.	Improved performance compared to electrochemical glucose sensors but still experience interference. In addition, the use of GOD leads to problems of oxygen imitation.
Radially-symmetric, catalase and mediated oxygen based electrochemical glucose sensors.	Improved ability to handle oxygen limitations but still susceptible to interference from other blood constituents.
Hydrogen peroxide glucose sensors.	Experiences interference from other blood analytes. Again susceptible to problems of oxygen limitation problems.
Glucose measurement through exudates extraction assisted by iontophoresis, ultrasound or suction	The response time of these sensors is too slow to be used as a hypoglycaemic alarm. The damage cause to the skin would also be a problem for diabetics due to their reduced ability to heal (Kayashima, Arai et al. 1991; Rao, Guy et al. 1995; Kost, Mitragotri et al. 2000).
Microdialysis sensors	The slow response of these sensors probably excludes them for use as a hypoglycaemic alarm
Fibre optic glucose sensors	Affinity sensors are too slow and show base-line signal drift. The oxygen-based sensors use the same GOD technology as the electrochemical sensors but do not suffer from problems of interference. With improvement in range and oxygen limitation immunity this type of sensor is probably the best candidate as a hypoglycaemic alarm.
NIRS, Photoacoustic sensors	The weakness of the spectral signature and interference from other blood analytes makes this technique too unreliable.
Other techniques	These techniques require much more research to demonstrate if their performance is suitable for a blood glucose sensor.
Subcutaneous sensors with sensor and telemetry equipment fully implanted.	Subcutaneous sensors will have to possess a long operational lifetime (~12 months) to be practical. The discrepancies between blood and subcutaneous values will have to be understood and controlled (Updike, Shults et al. 2000).

Table 5. Summary of blood glucose measurement methods

3 Principles of glucose oxidase based enzyme sensors

The sensor presented in this thesis uses a GOD and CAT enzyme layer surrounding a fibre-optic oxygen sensor. The details of the chemistry and physics of the operation of such enzyme layers are presented in this chapter.

3.1.1. Basic enzyme theory

Enzymes are proteins that catalyse specific chemical reactions. Some enzymes operate alone, relying only on their protein structure to operate, whilst others use cofactors, which can be either, a metal ion or an organic molecule known as a coenzyme. Most enzymes have a characteristic pH at which their activity is at a maximum (Lehnniger 1972).

3.1.2. Structure and operation of enzymes

Each type of enzyme possesses a unique structure, which will accommodate only its target chemical species, known as a substrate. This unique structure means that the enzyme will only promote one specific chemical reaction involving its target substrate. Enzymes operate by binding the target substrates to a specific region on its surface called an active site. When the substrates attach to the active site the enzyme and the substrates structure are distorted. This combined enzyme-substrate structure promotes the chemical reaction between the two target species, this is known as the 'induced fit' hypothesis. Once combined the new products of the reaction detach from the enzyme and leave it free to accept new substrate molecules (Mathews and Holde 1990).

3.1.3. The Michaelis-Menten relationship

This relationship defines the rate at which enzymes will catalyse a reaction. Considering the most basic case of an enzyme (E), which reacts with substrate (S) to form the enzyme substrate complex (ES) as shown in Equation 5. The (ES) complex then breaks down to form the free enzyme (E) and the products (P), see equation 6.

Equation 5. $$E + S \underset{k_2}{\overset{k_1}{\rightleftharpoons}} ES$$

Equation 6. $$ES \underset{k_4}{\overset{k_3}{\rightleftharpoons}} E + P$$

Key to terms used:

k_1 to k_4 are rate constants for the reactions.

E Total enzyme concentration (free and combined enzyme).

ES The concentration of enzyme substrate complex.

S Total concentration of substrate.

P Total concentration of product.

The enzyme reaction has a maximum reaction rate, V_{max}, also known as a reaction velocity, in steady state conditions this reaches a maximum value when there is enough substrate in solution to bind with all of the available enzyme (Lehnniger 1972).

The reaction rate (v) is given by the Michaelis-Menten equation shown in Equation 7. This equation assumes that there is enough substrate available in solution to combine with all of the enzyme present in solution. It is also assumed that the rate of the reverse reactions E+P→EP and ES →E + S is so small as to be neglected.

Equation 7. $v = \frac{V_{max}[S]}{K_M + [S]}$ The Michaelis-Menten equation

The Michaelis-Menten constant, K_M is equal to the substrate concentration at which the velocity is half the maximum possible value. The Michaelis-Menten constant has dimensions of moles/litre. The K_M constant is an experimentally determined value, in an ideal situation it is given by Equation 8.

Equation 8. $K_M = \frac{k_2 + k_3}{k_1}$

The value of K_M is independent of the enzyme concentration but may vary with structure of the substrate, pH and temperature. In enzymes which react with more than one substrate, each substrate has a K_M of its own (Lehnniger 1972).

3.1.4. Enzyme reactions involving more than one substrate and product

When enzymes react with two substrates and two or more products are produced there are three possible ways the reaction can proceed;

(a) Random substrate binding.

The two substrates can bind to the enzyme in any order (Mathews and Holde 1990).

(b) Ordered substrate binding

One substrate must bind to the enzyme first before the other (Mathews and Holde 1990).

(c) The ping-pong mechanism

One substrate binds to the enzyme and its product are released. Then the second substrate binds to the enzyme and its product is released. GOD is thought to follow this type of process (Mathews and Holde 1990; Wilson and Turner 1992)

3.1.5. Characteristics and operation of glucose oxidase

As described in chapter 2, glucose oxidase catalyses the oxidation of glucose to produce gluconolactone and hydrogen peroxide as shown in Equation 1 and 9.

$$\text{glucose} + \text{oxygen} \xrightarrow{\text{glucose oxidase}} \text{gluconic acid} + H_2O_2 + 7\text{kcal} \quad \textbf{Equation 1}$$

(Bourdillon,.Bourgeois et al. 1980; Fisher, Rebrin et al. 1994) .

Equation 9. $C_6H_{12}O_6 + O_2 \xrightarrow{GOD} C_6H_{10}O_6 + H_2O_2$

The glucose oxidase enzyme is a dimer composed of two identical subunits to form a globular protein of 8nm average diameter. Its molecular mass lies between $151x10^3$ and $186x10^3$ Daltons. GOD has a coenzyme of two flavin adenine dinucleotide (FAD) molecules. Its catalytic activity fails at pH values below two and greater than eight. Temperatures above 40°C denature the enzyme and the activity of the enzyme is inhibited by heavy metals such as mercury, lead and silver and a handful of other chemicals (Wilson and Turner 1992).

The overall relation promoted by GOD is believed to operate as follows, the GOD first combines with glucose to form:-

Equation 10. $E_{ox} + G \xrightarrow{K_1} E_{red} + \beta - d\text{-gluconolactone}$

Where E_{red} is the reduced form of the enzyme E_{ox} is the oxidised form of the enzyme and $\beta - d$-gluconolactone is $C_6H_{10}O_6$, which combines with water to form gluconic acid.

The reduced enzyme then reacts with oxygen to form a hydrogen peroxide enzyme complex. This complex then breaks down.

Equation 11. $E_{red} + O_2 \xrightarrow{K_2} E_{ox}H_2O_2 \xrightarrow{K_3} E_{ox} + H_2O_2$

Therefore, the enzyme has three kinetic constants associated with each step of the reaction (k_1, k_2 and k_3).

GOD has two Michaelis-Menton constants one for glucose at infinite oxygen and another for oxygen at infinite glucose concentration.

The Michalis-Menten constant for glucose at infinite oxygen (K_G) is given by:-

Equation 12. $K_G = \frac{K_3}{K_1}$

The Michalis-Menten constant for oxygen at infinite glucose (K_O) is given by:-

Equation 13. $K_O = \frac{K_3}{K_2}$

The reaction rate (v) (in free solution) is given by:-

Equation 14. $$v = \frac{V_{max} C_O C_G}{C_G C_O + K_G C_O + K_O C_G}$$

Where Vmax is the maximum rate of the reaction, C_G is the concentration of glucose and C_O is the concentration of oxygen
(Leypoldt 1981)

For the free enzyme the overall Michaelis-Menton constant for GOD has been found to be between 5.9 and 6.2 mM/l at atmospheric oxygen tensions. When covalently bound this rises to 8.8 and 10 mM/l in atmospheric oxygen (Arica and Hasirici 1993)

3.1.6. Characteristics and operation of catalase

Catalase uses iron as its coenzyme and has a Michaelis-Menton constant of 25 mM and an optimal pH of 7.6. The reaction promoted by catalase is shown in equation below in Equation 15.

Equation 15. $2H_2O_2 \xrightarrow{CAT} 2H_2O + O_2$

(Mathews and Holde 1990).

Combining the enzymes GOD and CAT in a membrane leads to the following overall reactions as shown in Equation 17. First, the GOD promotes the breakdown of glucose using oxygen and producing gluconolactone and H_2O_2. The

CAT then breaks down the H_2O_2 to produce oxygen that can be used for oxidation of further glucose molecules. The overall reaction is shown in Equations 16 and 17 and the final reaction is shown in Equation 18.

Equation 16. $C_6H_{12}O_6 + O_2 \xrightarrow{GOD} C_6H_{10}O_6 + H_2O_2$

(Wilson and Turner 1992)

Equation 17. $2C_6H_{12}O_6 + O_2 + 2O \xrightarrow{GOD+CAT} 2C_6H_{10}O_6 + 2H_2O_2$

$2O + 2H_2O$

Which can be written: -

Equation 18. $\text{glucose} + \frac{1}{2}O_2 \xrightarrow{GOD+CAT} \text{gluconic acid}$

(Tse and Gough 1987)

In steady state situations one oxygen molecule can be used to oxidise two glucose molecules, this will reduce the oxygen requirements of the sensor. Not all of the H_2O_2 will be available for recycling as a proportion will diffuse out of the membrane or break down to hydroxyl radicals before it can be broken down by the CAT. Experimentally, the addition of CAT to a GOD based sensor was found to reduce the lower oxygen limit of the sensor by 35% (Tse and Gough 1987; Chubdova, Vrbova et al. 1996)

3.2 Polymer matrices used to encapsulate enzymes

The enzyme membranes have two roles, first they must provide a structure to hold the GOD and CAT in proximity to the sensor. Secondly, they alter the

performance of the sensors by various physical interactions with the enzymes, substrates and products.

The first of these physical effects is a diffusion barrier to glucose and oxygen, hydrogen peroxide and gluconolactone. These diffusion effects are known as internal mass transport resistance. Other than diffusion resistances, the physical processes of substrate partitioning and boundary layer effects will also affect the reaction kinetics described in more detail below.

There are a variety of materials that have been used as an enzyme support. Amongst these are bovine serum albumin (Johnson, Mastrototaro et al. 1992; Moussey, Harrison et al. 1993; Yang, Atanasov et al. 1997), cellulose (Yang, Atanasov et al. 1997), HEMA (Shaw, Claremont et al. 1991).

3.2.1. Mass transport resistances

Mass transport resistances are the resistance to flow that substrates and products will experience as they diffuse in and out of the membrane. Glucose and oxygen will suffer mass transport resistances when diffusing in and out of the membrane. The rate at which H_2O_2 and gluconic acid diffused out of the membrane will also be reduced (Leypoldt 1981; Cussler 1988; Yang, Atanasov et al. 1997).

3.2.2. Substrate partitioning

Substrate partitioning may also affect the reaction rate; this is a process where a membrane can hold a greater or smaller concentration of a substrate than would be found in free solution. This phenomenon is caused by the polymer chains having an overall charge, which repels like charged substrates and attracts oppositely charged ones. An example of this is the use of cellulose acetate to reduce the interference effect of ascorbate and urate on hydrogen peroxide electrode sensors.

The urate and ascorbate are negatively charged and were repelled by the negatively charged nafion membrane (Yang, Atanasov et al. 1997).

3.2.3. Inherent and apparent reaction rates

The effects of the membrane lead to a modification of the rates of reaction of the GOD and CAT immobilised in the membrane. Two modified versions of reaction rate are used to represent these effects, these are the inherent and the apparent (or effective) reaction rate. The inherent reaction rate is the reaction rate when substrate partitioning is present but not mass transport resistance. Apparent reaction rate is the reaction rate when substrate partitioning and mass transport resistances are present (Leypoldt 1981).

3.2.4. Boundary layer effects

As well as the mass transport effects of the membrane there are diffusion effects caused by the boundary layer between the liquid and the membrane, this is known as external transport resistance. Interestingly, stirring of the solution will not remove boundary layer effects (Leypoldt 1981).

3.2.5. Immobilisation and cross-linking of enzymes

When GOD and CAT are dissolved with the polymer HEMA in an ethanol water mixture and then allowed to dry, the polymer chains will entrap the enzymes in a mesh structure or matrix (Shaw, Claremont et al. 1991). To reduce the chances of the enzymes being washed out of the membrane or 'leached' into the solution and to impart improved stability and performance on the enzyme, it has often been chemically immobilised. The immobilisation is achieved by creating chemical bonds from the enzyme to the polymer lattice or creates bonds between the enzyme molecules. Several chemicals have been used for this, including glutaraldehyde (Claremont, Sambrook et al. 1986; Armour, Lucisano et al. 1990;

Cronenberg, Groen et al. 1991; Zhang and Wilson 1993), urea and formaldehyde (Entcheva and Yotova 1994). GOD has also been immobilised using electrochemical deposition (Troupe, Drummond et al. 1998).

3.2.6. Effects of immobilisation on enzyme performance

Immobilisation can change the Michaelis-Menten constant of the enzymes. This is due to steric and conformational changes in the enzymes when it chemically interacts with the polymer matrix. In the absence of inherent and apparent kinetic effects, this alteration of reaction kinetics is known as the intrinsic kinetic parameter. It will often be different from the enzyme kinetics in free solution, this effect is combined with the effects of the mass transport resistances and substrate partition caused by the polymer support itself. Immobilisation has been found to decrease or increase the K_M value of GOD compared to free solution (Arica and Hasirici 1993). There may be alterations to the enzymes sensitivity to temperature and pH stability and irradiation. For example, increased thermal stability of GOD of up to 70°C for 1 hour when immobilised onto glass beads with little or no loss of activity was reported by Wilson and Turner 1992; Woedtke, Julich et al. 2002.

3.2.7. The use of polyurethane as a differential diffusion barrier

Several groups have used polyurethane as a differentially permeable barrier to improve the range and linearity of oxygen based glucose sensors and to redress the stoichiometric problem. In practice, these membranes are created by dip coating the sensors in weak solutions of the polymer. This creates a cover over only parts of the EH membrane surface; polyurethane was applied to glucose sensors in this way by Shichri, Yamasaki et al. 1982; Claremont, Sambrook et al. 1986; Shaw, Claremont et al. 1991. Instead of using an outer layer, some groups have immobilised the GOD into polyurethane. In this case, although the polyurethane is hydrophobic, fissures and discontinuities in the membrane allow glucose to enter the membrane to a limited extent (Gilligan, Schults et al. 1994).

3.2.8. The effect of membrane dimensions and composition on sensor performance

The range, linearity and response time of GOD based glucose sensors are controlled most simply by the dimensions and composition of the enzyme membrane in which they are coated. Enzyme membranes can operate in two modes, reaction control and diffusion control.

3.2.9. Reaction controlled mode

In reaction control, the mass transport resistances are negligible and the reaction rate is determined by the kinetics of the immobilised enzyme. In this situation, the response of the sensor is non-linear and the response time is concentration dependent. The sensor response characteristics are also vulnerable to pH changes and enzyme deactivation or loss.

3.2.10. Diffusion controlled mode

In diffusion controlled mode, pH and enzyme deactivation or loss have little effect on the response of the sensor. The response is quasi linear and response time is independent of concentration. The sensitivity of the sensor is determined by the membrane permeability. To produce a diffusion controlled system the membrane must be loaded with a high concentration of enzyme and possess a low permeability (Gough, Leypoldt et al. 1982). The diffusion constants of the membrane and therefore the response of the sensor are controlled by the dimensions, materials used as the polymer support and the immobilisation strategy of the enzyme. If a sufficient amount of enzyme is deactivated or lost the sensor will revert to a reaction controlled mode.

3.3 Mathematical models of enzyme based sensors

As a tool to aid enzyme based sensor design, several mathematical models of immobilised enzyme systems have been created (Schulmeister and Pfeiffer 1993). Steady state and transient responses have been modelled and confirmed experimentally. They have also been used to predict sensor responses with some success (Leypoldt and Gough 1984; Olsson, Lundback et al. 1986; Tse and Gough 1987; Lemke 1988; Neykov and Georgiev 1998; Rinken and Tenno 2001). These models tend to be large and require rigorous mathematical approaches to their solution (Leypoldt 1981; Scchulmeister 1990). Because of their complexity and the length of time to produce a working model, as well as the difficulty of producing an enzyme membrane to exact dimensions and composition experimentally to match a model, no mathematical models were created to aid the design of the glucose sensor in this investigation.

4 The theory of luminescence based glucose sensing

The glucose sensor design proposed in this thesis uses a fluorescence oxygen sensor as a core coated in GOD enzyme. The oxygen concentrations are measured using the interaction of oxygen with a fluorescent dye. Briefly, the dye absorbs light at one wavelength and then emits light of a slightly longer wavelength. The presence of oxygen reduces the amount of light emitted by the dye, through complex electromagnetic mechanisms. The process consumes no oxygen so, in this respect, can be thought of as an ideal sensor.

To understand the fluorescence sensing technique used in this sensor it will be necessary to review the fundamentals of luminescence theory of which fluorescence is a subset.

4.1 General luminescence theory and oxygen measurement

Fluorescence is a form of luminescence, a group of photochemical processes that also includes phosphorescence and chemoluminescence. Fluorescence and phosphorescence form a sub-group of luminescence called photoluminescence.

Chemoluminescence involves the emission of light from an electronically excited chemical created through a chemical reaction. In fluorescence and phosphorescence, the electronic orbits of the chemical (species) are excited by the absorption of one or more photons. These excited species then seek to return to an electronically relaxed state, as they are compelled to do by the laws of physics. They achieve this by releasing their excess energy in the form of a photon.

The fluorescence process takes a few nanoseconds to complete; in contrast, the phosphorescence mechanism can endure for seconds. In both fluorescence and phosphorescence, the light that is emitted at the end of the process is usually of a

longer wavelength than the absorbed light. This effect is known as a 'Stokes shift'. Rarely, the emitted and absorbed wavelengths are the same, this is known as 'resonance fluorescence' (Skoog and Leary 1992).

4.1.1. Electronic excitation by photon absorption

When a species absorbs a photon with a wavelength within the visible or ultra violet spectrum, the photon interacts with a specific part of the molecule known as the chromophore. The choromophore becomes electronically excited and an electron in its structure gains energy and moves from a lower energy state to a higher one.

4.1.2. Electronic spin

Electron spin is a quantum mechanical process analogous to an intrinsic angular momentum that can take one of two possible different directions, up or down, with respect to a specified axis (French and Taylor 1991). In any electronic orbit, there can be a maximum of two electrons following the same orbit and these must be of opposite spin as stated by the Pauli exclusion principle. This effect is known as spin pairing, even if the electrons move to different orbits they can remain paired. If this happens it creates what is known as a singlet state. Even though the two electrons are separated if one changes spin the other will change to the opposite value. After separation, the electrons can lose their spin coupling to create what is called a triplet state and both are free to orientate themselves to either up or down spin.

The difference between fluorescence and phosphorescence is that spins are changed in phosphorescence but not in fluorescence. This is the cause of the difference in the relative lifetimes of fluorescence and phosphorescence events (10^{-5} to 10^{-8}s) to (10^{-4} to seconds) respectively. The probability of a singlet to triplet or triplet to singlet event is much smaller than a singlet to singlet event. The

more likely the event, the more quickly it occurs on average (Gewehr 1991; Skoog and Leary 1992).

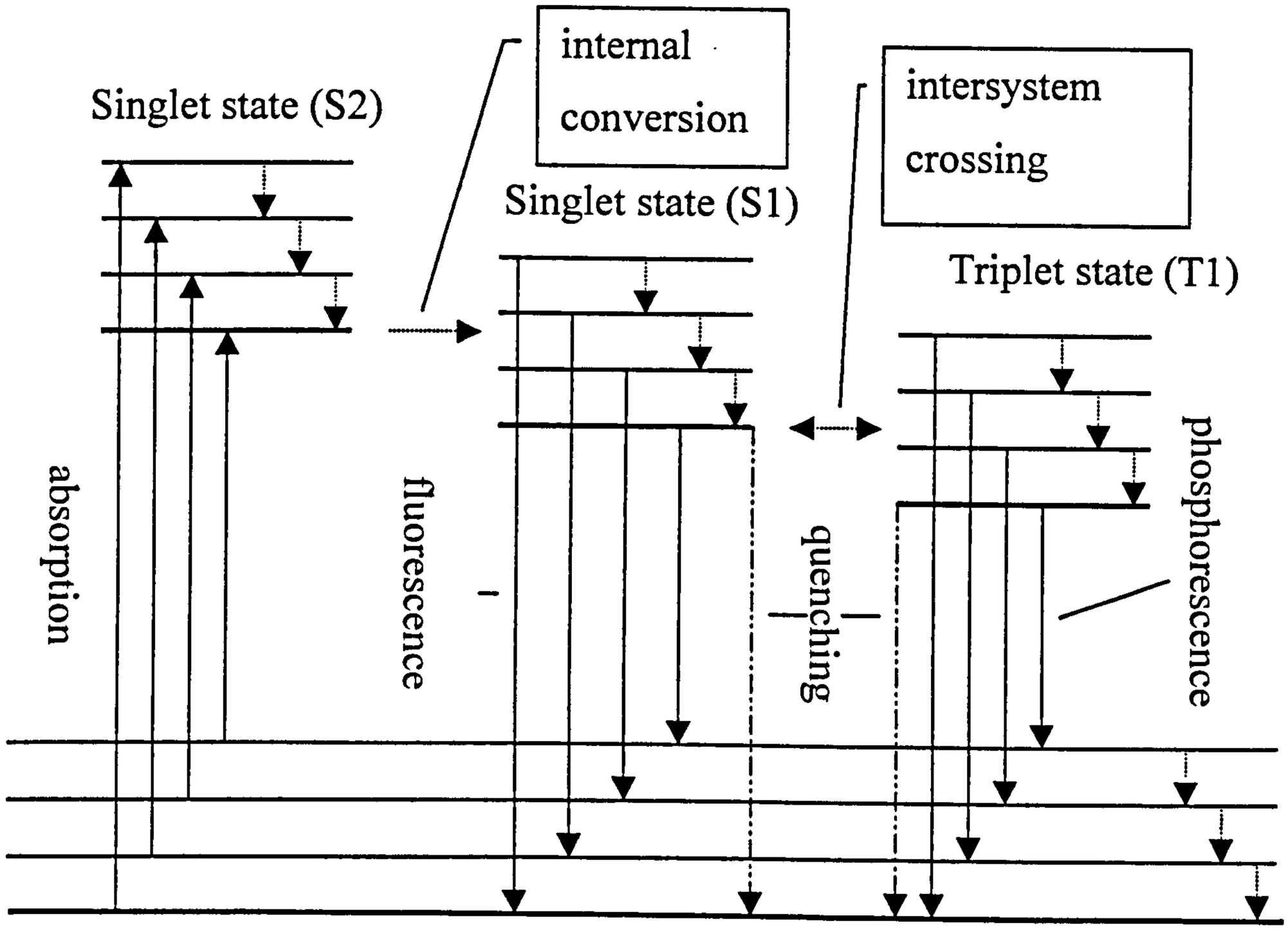

A Jabloński diagram of the molecular energy states of molecules (Gewehr 1991; Turo 1991; Lakowickz 1999).

Figure 11. The energy states of excited molecules and their paths to lower energy states

4.1.3. De-excitation of electronic energy levels

Once a species is electronically excited, it has three possible paths to a lower energy state. These are a route either through changes in vibrations of the structure of the molecule, the release of a photon or a combination of vibration and photon release. The release of a photon will only happen if the vibration route has a low probability of occurring. As can be seen from figure 11, following the absorption of a photon the electron can and usually does move to lower energy levels by vibrational relaxation. Even if a photon is emitted, it is usually from a lower energy level than the one the molecule was initially excited to. As the energy being released is now less than the amount absorbed, the photon emitted possesses less energy and therefore a longer wavelength. This causes the 'Stokes shift' of the wavelength of the emitted photon to a longer wavelength than the absorbed photon.

4.1.4. Internal conversion

One path by which an electron can move to a lower energy level without releasing a photon is internal conversion. It is a complex process, which involves electrons jumping to a nearby lower energy level and internal conversion can also cause predissociation. In this process an excited electron moves from a higher electronic state to the upper vibrational level of a lower electronic state. The energy imparted to this vibrational level is enough to rip the bond apart, breaking the molecule in two. This has a tendency to occur in large molecules, which tend to contain weak bonds between some atoms.

Another process that can cause destruction of bonds is 'dissociation'; in this process the electron of the chromophore section of the molecule absorbs so much energy from the arriving photons that the bond attaching the chromophore to the rest of the molecule ruptures. There is no intersystem crossing involved in

dissociation, the molecule is simply broken apart by the energy of the absorbed photons (Skoog and Leary 1992).

4.1.5. Intersystem crossing

Intersystem crossing is the process where an electron changes spin and moves from a singlet to triplet state or triplet to singlet state. It is found more commonly in molecules with large atoms or atomic groups such as Cl, Br, I, NO_2 and CHO (the internal heavy atom effect). In these molecules spin orbit coupling, a process where the orbit of an electron causes a magnetic torque on its spin, increases the likelihood of a spin change (Gewehr 1991; Turo 1991; Skoog and Leary 1992).

4.1.6. De-excitation by photon emission

Fluorescence and phosphorescence are the two processes that allow molecules to move to less energetic states by emission of a photon. As mentioned earlier, fluorescence involves the release of a photon to allow a molecule to move from a singlet state to a ground state with no change in spin. Phosphorescence occurs when a photon is released from a triplet state to allow the molecule to drop to the ground state following a change in electron spin (Gewehr 1991; Turo 1991; Skoog and Leary 1992).

4.1.7. Quantum yield of fluorescence

The fluorescent quantum yield can be defined as the ratio of the number of photons emitted by a sample to the number of photons absorbed (Gewehr 1991).

In fluorescence the excited singlet state has three options available to reach a ground state shown in figure 11. These routes are internal conversion, intersystem crossing (singlet to triplet) and fluorescence with corresponding rate constants, k_{ic},

k_{is}^{ST} and k_f respectively. The total rate of deactivation of the lowest excited singlet state (S1) denoted J_t^S is given in Equations 19 and 20.

Equation 19. $J_t^S = \frac{d[S_1]}{dt}$

Equation 20. $J_t^S = -\left(k_f + k_{ic} + k_{is}^{ST}\right)[S_1]$

where $[S_1]$ is the concentration of molecules in the S_1 state.

Fluorescence quantum yield (ϕ_f)

The rate of fluorescence quantum yield can be expressed as $J_f = -k_f[S_1]$ and the rate of absorption is J_a. In the steady state situation $J_a = J_t^S$ which from the above definition of quantum yield gives Equation 21.

Equation 21. $\Phi_f = \frac{k_f}{k_f + k_{ic} + k_{is}^{ST}}$

Phosphorescence quantum yield (ϕ_p)

The total rate of deactivation of the lowest triplet state, (T1 in figure11) is given by Equations 22 and 23.

Equation 22. $J_t^T = \frac{d[T_1]}{dt}$

Equation 23. $J_t^T = -(k_p + k_{is}^{TS})[T_1]$

k_p is the rate constant of phosphorescence, k_{is}^{TS} is the rate constant for intersystem crossing from the triplet to singlet state and the concentration of the molecules in the T_1 triplet state is $[T_1]$.

Phosphorescence quantum yield is the composite of two other quantities. These are the fraction of molecules in the T_1 state that emit a photon (a quantity known as the phosphorescence quantum efficiency θ_p) and the fraction of molecules in the T_1 state that cross over to the S1 state by intersystem crossing (known as the triplet quantum yield Φ_T) as shown in Equation 24.

Equation 24. $\Phi = \theta_p \bullet \Phi_T$

Using these definitions of θ_p and Φ_T and the definition of quantum yield we get the quantum yield of phosphorescence given in Equation 25.

Equation 25. $$\Phi_p = \frac{k_p k_{is}^{ST}}{\left(k_p + k_{is}^{TS}\right)\left(k_f + k_{ic} + k_{is}^{ST}\right)}$$

(Gewehr 1991)

4.1.8. Quenching of fluorescence and phosphorescence

Quenching is a process where the presence of another molecule causes the excited molecule to move from an excited singlet or triplet state to a ground state without the release of a photon. Quenching is sometimes divided into two categories, dynamic or diffusional quenching and static quenching. Dynamic quenching involves an interaction between the fluorophore (fluorescing molecule) and quenching species while the fluorophore is in an excited state. Static quenching involves the fluorophore and the quenching species forming a complex while the

fluorophore is in a ground state (Sharma and Sculman 1999). There are two types of quenching mechanisms, photochemical and photophysical.

Photochemical quenching involves a chemical reaction between the excited molecule and another molecule in the solvent or the solvent itself.

Photophysical quenching does not involve chemical reactions but relies on a number of other mechanisms. Photophysical processes are divided into two groups. The first group is self quenching where the excited molecule is quenched by molecules of its own type. The second group is impurity quenching which involves a different species of molecule. Impurity quenching is further subdivided into electron transfer, external heavy atom effect and energy transfer (Gewehr 1991; Turo 1991).

4.1.9. Electron transfer

Electron transfer involves two atoms approaching each other closely enough for their electron clouds to overlap and electron exchange to take place between the excited molecule and the quenching molecule. This allows the excited molecule to transfer its excess energy to the quenching molecule via the exchanged electron (Turo 1991).

4.1.10. The external heavy atom effect

The external heavy atom effect operates in the same manner as its internal counter-part, mentioned earlier in section 4.1.5, by promoting changes of electron spin causing movement between singlet to triple states. This reduces fluorescence or phosphorescence by allowing the excited molecule to de-excite via a different route as shown in figure 11.

4.1.11. Energy transfer

Energy transfer involves the transfer of electronic energy from the excited molecule to the quenching molecule through either the process of Coulombic interaction or the radiative 'trivial' mechanism.

The process of Coulombic interaction involves electrostatic coupling of the excited and quenching molecules. The motion of the excited electron around the molecular framework of the excited molecule causes its electrostatic field to oscillate. This oscillating electrostatic field then causes electrostatic forces to be exerted on the electronic structure of any nearby molecule. If the electronic structure of the nearby molecule has an appropriate configuration, a resonance condition can be set up between the two molecules. This allows energy to be transferred between the molecules and leads to the fluorophore being quenched.

The trivial mechanism involves the excited molecule releasing a photon but this photon is absorbed by the quenching molecule. This absorption can only take place if the absorbing molecule has the appropriate electronic structure (Turo 1991).

4.1.12. The Stern-Volmer equation of quenching

The Stern-Volmer (S-V) equation relates the quantum yield of phosphorescence or fluorescence to the rate of dynamic quenching and the quencher concentration (Rasimas, Berglund et al. 1996). The presence of the quenching species gives an excited luminescent molecule a new route of deactivation. For the case of fluorescence, the rate of deactivation of the *S1* state, Equation 20, now becomes Equation 26.

Equation 26. $$J_t^{S,Q} = -\left(k_f + k_{ic} + k_{is}^{ST} + k_Q[Q]\right)[S_1]$$

Where k_Q is the quenching constant and $[Q]$ is the concentration of the quenching species. The quantum yield of fluorescence in the presence of the quencher is shown in Equation 27.

Equation 27. $$\Phi_f^Q = \frac{k_f}{k_f + k_{ic} + k_{is}^{ST} + k_Q[Q]}$$

The situation for phosphorescence follows in a similar manner with the rate of T_1 deactivation being given by Equation 28.

Equation 28. $$J_t^{T,Q} = -(k_p + k_{is}^{TS} + k_Q[Q])[T_1]$$

Assuming that quenching only affects the triplet state the phosphorescence quantum yield derived from Equation 24 becomes Equation 29.

Equation 29. $$\Phi_p = \frac{k_p k_{is}^{ST}}{(k_p + k_{is}^{TS} + k_Q[Q])(k_f + k_{ic} + k_{is}^{ST})}$$

The above equations have assumed that the quenching constant for both phosphorescence and fluorescence is the same, this may not always be the case and different terms would have to be incorporated into the above equations (Gewehr 1991). The S-V equations can be derived by dividing the quantum yield without quenching by the quantum yield with quenching. For fluorescence, equation 21 is divided by Equation 27 to give Equation 30.

Equation 30. $$\frac{\Phi_f}{\Phi_f^Q} = \frac{k_f + k_{ic} + k_{is}^{ST} + k_Q[Q]}{k_f + k_{ic} + k_{is}^{ST}}$$

The lifetime of a singlet state is given by:

Equation 31. $$\tau_S = \frac{1}{k_f + k_{ic} + k_{is}^{ST}}$$

Substituting 31 into 30 yields equation 32.

Equation 32. $$\frac{\Phi_f}{\Phi_f^Q} = 1 + k_Q \tau_S [Q]$$

Equation 33. $$\frac{\Phi_f}{\Phi_f^Q} = 1 + K_Q [Q]$$

This is the S-V equation for fluorescence quenching.

For phosphorescence equation 30 is rewritten as equation 34.

Equation 34. $$\frac{\Phi_p}{\Phi_p^Q} = \frac{k_p + k_{is}^{TS} + k_Q [Q]}{k_p + k_{is}^{TS}}$$

The lifetime of the triplet state is given by equation 35:

Equation 35. $$\tau_T = \frac{1}{k_p + k_{is}^{TS}}$$

Substituting equation 34 into 35 gives equation 36.

Equation 36. $$\frac{\Phi_p}{\Phi_p^Q} = 1 + k_Q \tau_T [Q]$$

This can be rearranged, using k_Q in place of $k_Q \tau_T$, to give equation 37.

Equation 37. $$\frac{\Phi_p}{\Phi_p^Q} = 1 + K_Q [Q]$$

S-V equation for phosphorescence quenching (Gewehr 1991).

4.1.13. Oxygen quenching

Molecular oxygen is a highly efficient quencher of luminescent species. Oxygen atoms have four electrons that are used for bonding. When in it's diatomic form, six electrons form bonds between the two atoms. Two electrons go into antibonding orbitals that counteract one of the three bonds. These two unpaired (not spin coupled) electrons in different orbitals constitute a triplet state (Gewehr 1991). This triplet-ground state of oxygen, known as $^3\Sigma$ oxygen, is composed of two individual triplet states termed $^1\Delta$ oxygen and $^1\Sigma$ oxygen. Due to this electronic structure, oxygen has very low excitation energies. This makes it a very efficient quencher of a large number of different fluorophores through energy transfer mechanisms and will quench both singlet and triplet states (Turo 1991).

A modified S-V equation is used to describe quenching by oxygen as shown in Equation 38 and 39.

Equation 38. $\frac{I_0}{I} = \frac{\tau_0}{\tau}$

Equation 39. $\frac{I_0}{I} = 1 + k_g \tau_0 [O_2]$

(Gewehr 1991)

Where I_0 , τ_0 are the intensity and lifetime at zero oxygen concentration and I , τ are the intensity and lifetime at oxygen concentration $[O_2]$. Using a modified Smoluchowski equation (used to describe diffusion-reaction processes) to describe k_g . The value of k_g is dependent on the physical constants of the system.

Equation 40. $\mathrm{kg} = 4\pi N_P (D_D + D_A) 10^3$

N is Avagadro's constant, p is a constant which is determined by the value of the radius of interaction of the oxygen and the species that is quenched and the probability of each collision. The constants D_D and D_A are the diffusion constants for diffusion of the donor (the quenched species) and the acceptor (oxygen in this case) (Gewehr 1991; Turo 1991).

4.1.14. Oxygen sensitive luminescence dyes

Oxygen can be measured using both fluorescence and phosphorescence quenching. Fluorescent measurements use ruthenium complexes (Shahriari, Ding et al. 1993; Singer, Duveneck et al. 1994; McEvoy, McDonagh et al. 1996; McNamara, Li et al. 1998). A phosphorescence quenching oxygen measurement using metalloporphyrin was reported. This measurement system used phosphorescence lifetime measurements, which have a number of advantages over fluorescence measurements. However, fluorescence intensity measurements have been a more common method of measuring oxygen due to the availability of the problem of finding a suitable phosphorescence dyes (Gewehr and Delpy 1993).

4.2 Conclusions of luminescence theory

Phosphorescence lifetime quenching has several advantages over fluorescence measurements. It is unaffected by background light level and immune to variations in the excitation light pulse intensity. However, the lack of phosphorescence dyes stability at room temperature has been a problem and has led to fluorescence intensity measurements to dominate.

5 Experimental instrumentation and materials

5.1 Introduction

In this section, all of the apparatus and materials that were used in the experimental work will be described.

5.2 The Paratrend 7 multi-parameter blood gas monitor

The glucose sensor was developed by modifying a commercial blood oxygen sensor, the Paratrend 7 (P7) intravascular blood gas monitoring system. The P7 is produced by Diametrics Medical Ltd of High Wycombe, UK. The system continuously measures the temperature, pH, carbon dioxide (CO_2) and oxygen (O_2) tensions of arterial blood. The P7 sensing element, which is inserted into an artery, consists of a 0.5 mm diameter bundle of three fibre optic sensors and a thermocouple temperature sensor. All four sensors are encased in a biocompatible microporous hollow fibre (MPHF) as shown in figure 12. Photographs of the system are shown in Appendix B.

The pH, CO_2 and O_2 measurements are made by the three fibre optic sensors and the temperature by a thermocouple. The pH and CO_2 sensors are not used in this study and so will not be described any further here. The full P7 clinical system includes gas cylinders for calibrating the sensors, a display, controls and a printer system. All of the electronics needed to take the measurements are housed in the patient data module (PDM).

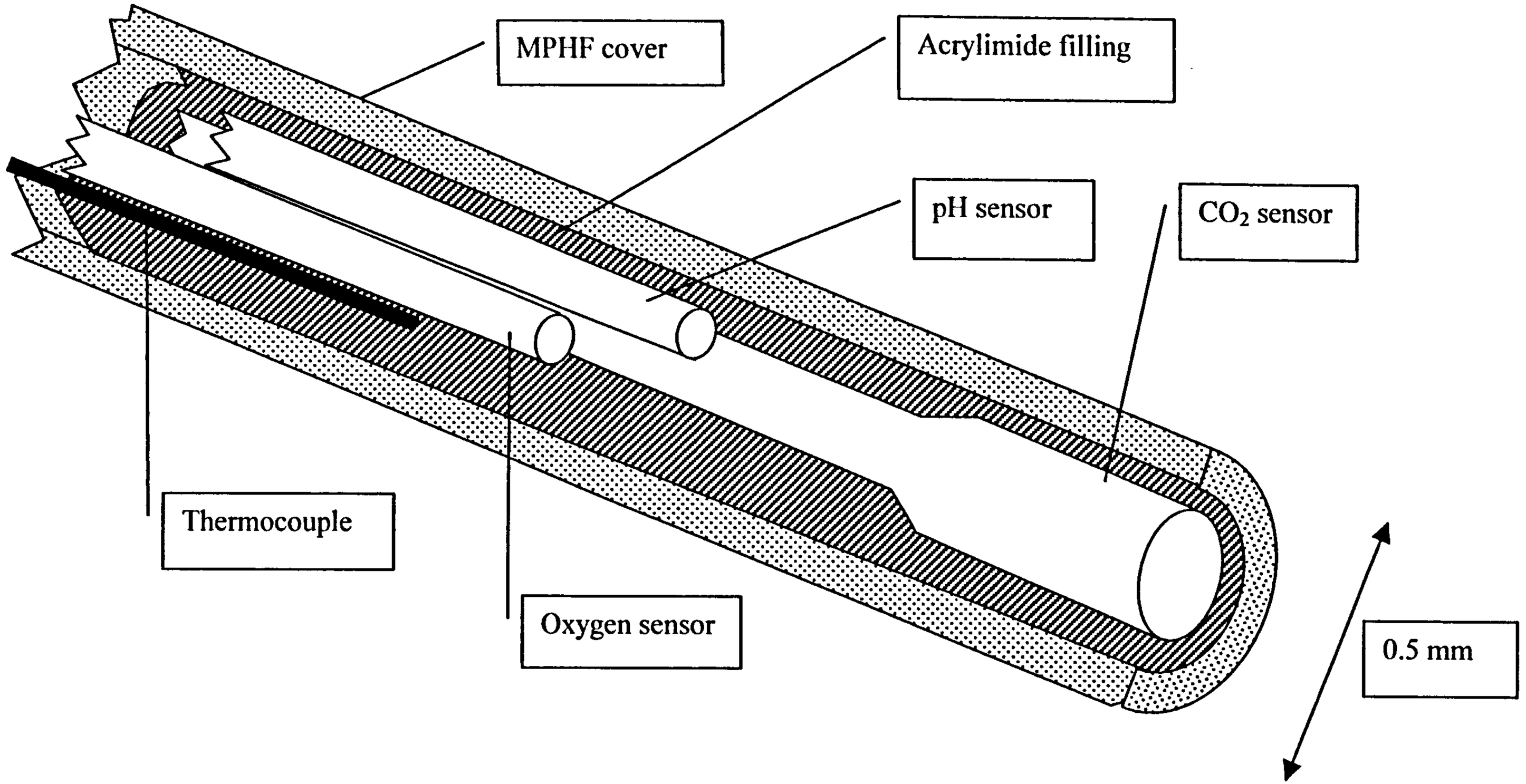

Figure 12. A diagram of the P7 sensor tip showing the three optical sensors and the thermocouple

5.2.1. The P7 oxygen (PO2) and temperature sensors

As the research will only make use of the PO2 sensor and the thermocouple these are described in detail here.

The PO2 sensor uses a fluorescence technique to measure oxygen. This involves using a fluorescent dye, ruthenium chloride (Chapter 4). When exposed to light of wavelength 470 nm (absorbance wavelength), the dye will absorb the light and then emit Stokes shifted light (emission wavelength) of 615 nm. The ruthenium dye is quenched by oxygen and therefore does not radiate the emission light. The amount of quenching and, therefore, emission intensity is proportional to the concentration of oxygen molecules in the surroundings of the dye. By measuring the intensity of the emission wavelength of the dye, the oxygen concentration can be calculated. The sensing area of the PO2 sensor is shown in figure 13.

The P7 is in clinical use in several countries. It is used in critical care situations and monitoring of neonates. The performance of the oxygen and temperature sensor in vitro and in vivo (in human clinical trials) are shown in table 6 and 7.

Sensor type	Oxygen (PO2)	Temperature
Range	20 to 500 mmHg (2.7 to 66.7 KPa).	10 to 42 °C
Accuracy	± 5% <120 mmHg (16.0 KPa) ± 10% ≥ 120 mmHg (16.0 KPa)	± 0.2 °C
Drift	< 1%/hour	None
Response time	0 % to 90 % ≤ 180 seconds @ 37 °C	As PO2
Shelf life	12 months	12 months

Table 6. The In vitro Performance of the Oxygen and Temperature Sensors in the P7

These are the results of in-vitro tests of the sensors in tonometered solutions. Sensors meet 95% confidence limits of these specifications. The sensors are sterilized by gamma radiation exposure of ≥ 25 kGy.

Bias	0.5%, 0.4 mmHg (0.005 KPa)
Precision	13.2%, 16.4 mmHg (2.186 KPa)
Range	32 – 489 mmHg (4.266 to 65.195 KPa)
Correlation coefficients	0.944

Table 7. In vivo Performance of the P7 Oxygen Sensor

Sensors were implanted into the femoral, radial or brachial arteries of 37 human subjects. The measurements taken were compared with a blood gas analyzer (BGA). The mean monitoring time was 87.5 hours with a total of 3764 hours of monitoring for all the sensors (Diametrics Medical Ltd., internal document).

There are a number of papers on the application of the Paratrend 7 in the published literature. However, there are two versions of the P7 in use at time of print, one using a fluorescence oxygen sensor and the other using an electrochemical oxygen sensor. None of the papers published state which oxygen sensing system is being used in the research so the internal Daimetrics documents will be the source of reference of the performance of the P7 sensor.

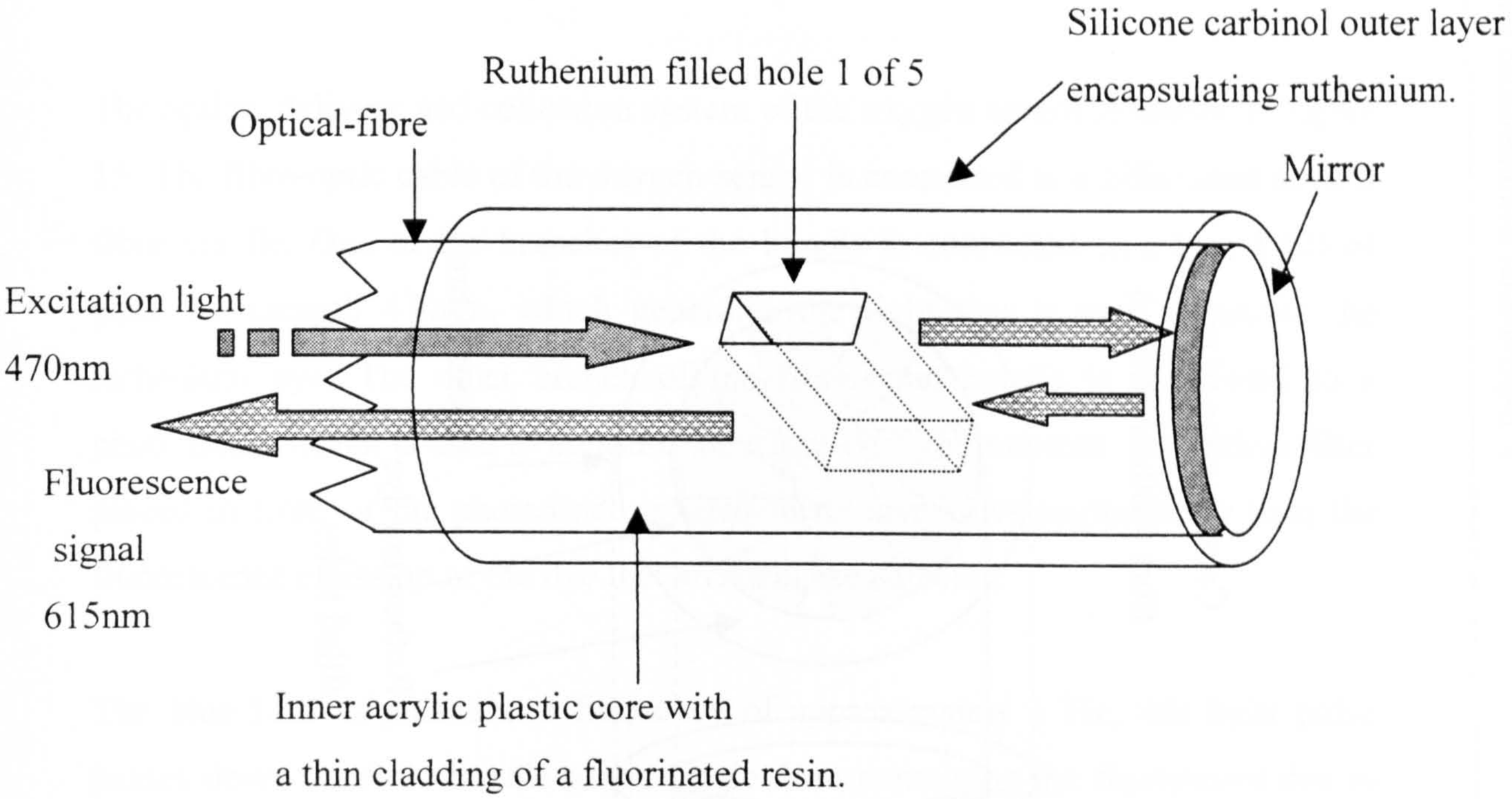

Figure 13. The design of the fibre-optic oxygen sensor

The dye filled holes in the fibre are each drilled at a different angle around the axis of the fibre. This results in the entire cross section of the fibre being covered by a ruthenium filled hole as shown in figure14.

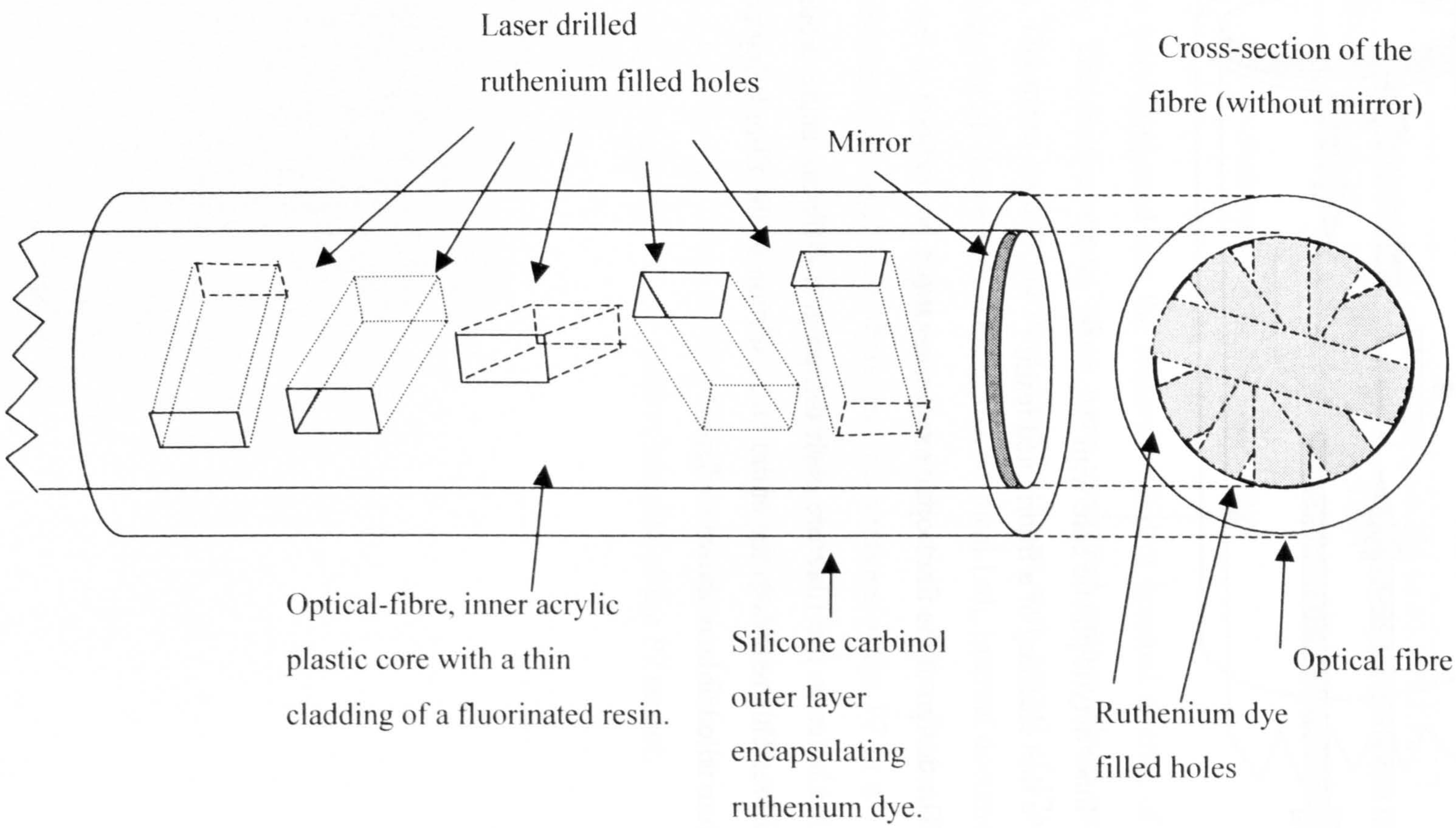

Figure 14. The arrangement of the dye filled holes in the oxygen sensors

5.3 The fibre optic light delivery and collection system of the oxygen sensor

The optical delivery and collection system of the oxygen sensor is shown in figure 15. The fibre-optic cable of the oxygen sensor is connected to a bifurcated optical fibre bundle. One of the branches of the bundle is connected to a blue LED of peak wavelength 470nm, which generates the light that is used to excite the ruthenium dye. The other branch of the fibre-optic bundle is connected to a photodiode, which is used to measure the emission light intensity. An optical filter placed in front of the photodiode is used to remove wavelengths other than the fluorescence emission of the dye that arrive at the detector.

The blue LED is pulsed at a frequency of approximately 1 Hz, this light pulse passes down the fibre bundle to the single fibre containing the fluorescent dye in holes in its tip. The light pulse then continues to the dye filled holes where a proportion of it is absorbed by the dye. The remainder of the light, which has not been absorbed, carries on to the end of the fibre where it is reflected back by a mirror on the tip of the fibre. The pulse then travels back along the fibre and is partially absorbed by the dye.

Once excited, the fluorescent dye emits light in all directions but a proportion of it travels either back down the fibre, towards the optical bundle, or in the direction of the mirror where it is reflected towards the fibre bundle. When the light reaches the fibre bundle junction, half of it travels down the branch that is connected to the photo-detector where its intensity is measured.

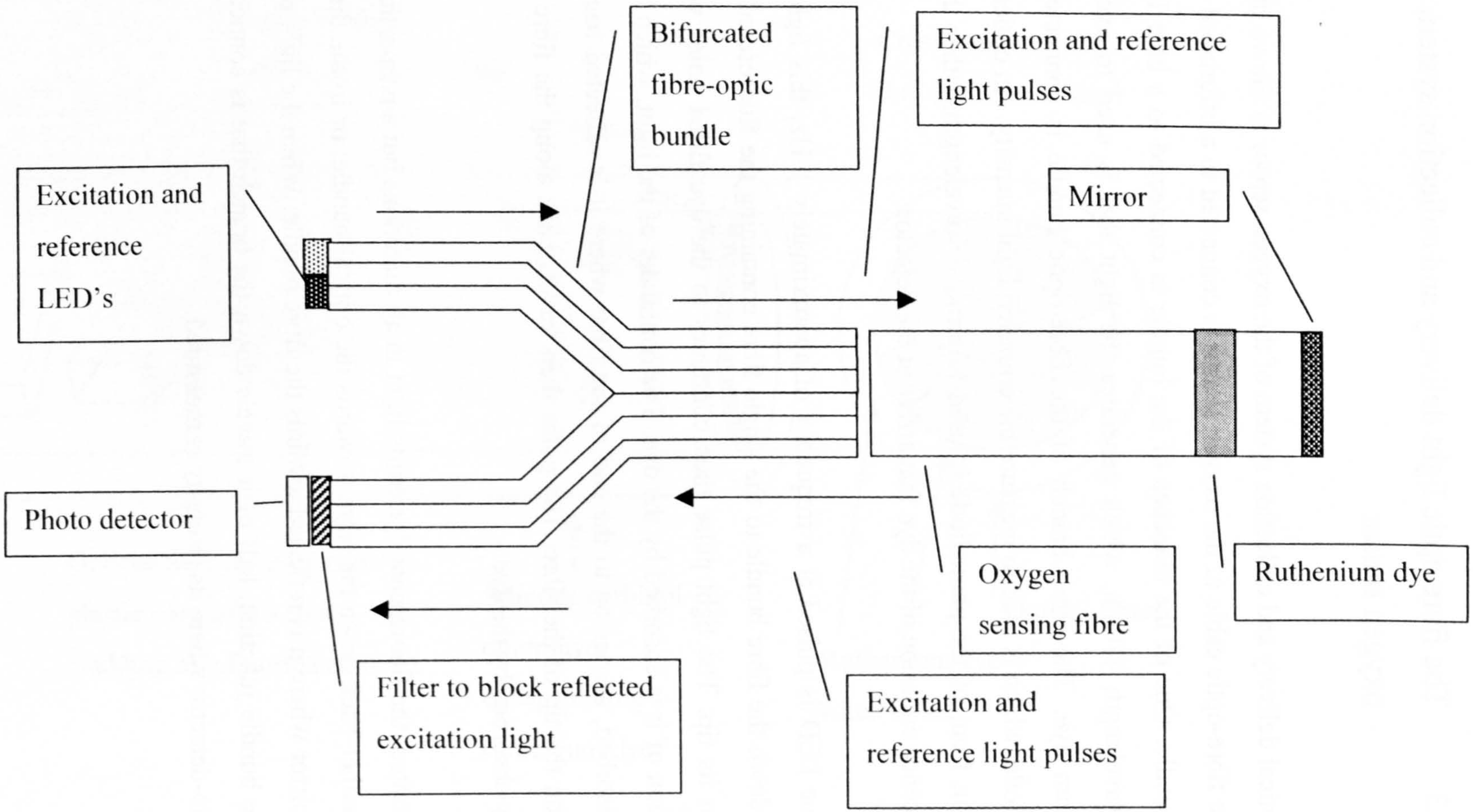

Figure 15. The optical collection system of the P7 sensor.

5.3.1. Compensation of changes in optical efficiency of the measurement system

If the sensor is moved during operation, the optical efficiency of the system (the amount of light lost as the signal passes through the fibre) will change. This will cause an unpredictable variation in the intensity of the emission and excitation light signals and therefore an error in the oxygen measurement. To compensate for this a second LED, situated next to the excitation LED, launches a reference light pulse that is sent down the fibre and follows the same path as the excitation and emission pulses.

The reference light pulse is launched in-between the fluorescence measurement signal pulses and so does not interfere with the measurement itself. The reference light pulse does not excite the fluorescent dye as its wavelength is too long. However, the intensity of the pulse will be altered by changes in the optical efficiency of the optical system. The reference light pulse passes through the optical filter, in front of the photo detector, as it has the same wavelength as the fluorescence emission signal of the dye, and is measured by the same photodiode used for the oxygen measurements. The oxygen measurement signal is then scaled to the reference signal so that optical efficiency effects are removed.

5.3.2. Application of the S-V relationship to the P7 oxygen measurements

The oxygen concentration is calculated from measuring changes in the intensity of the emission light from the fluorescent dye using the S-V relationship discussed in Chapter 4. The equations have to be modified slightly to take account of the reference pulse and any interference light, which may have entered the optical fibre from outside.

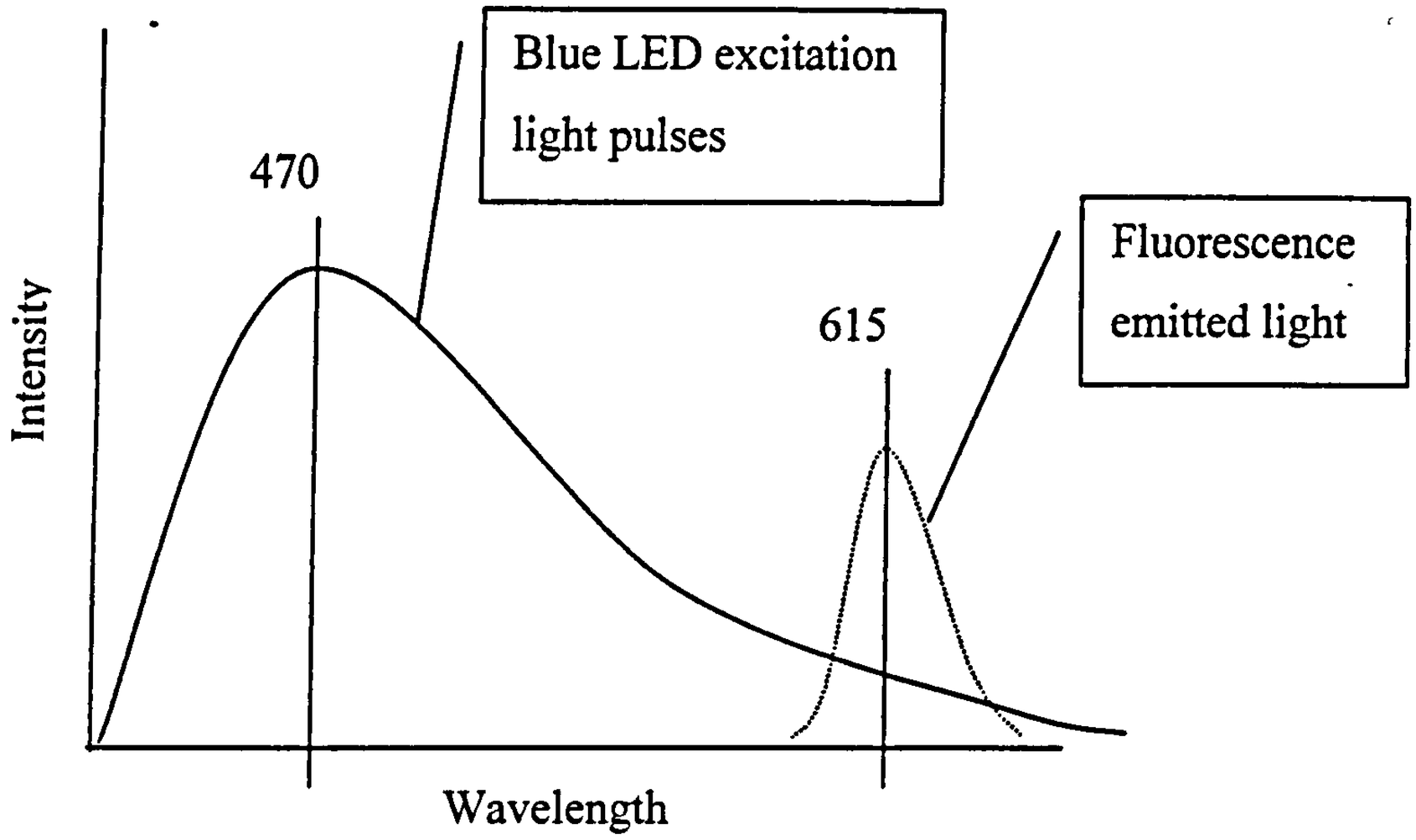

Figure 16. The spectral distribution of the LED and fluorescence signals, which are used in the sensor

From figure 16, it can be seen that the excitation LED spectra overlaps with the fluorescence emission spectra of the dye. In addition, it has been found during the sensor development at Diametrics that some of the dye immobilised in the silicone rubber does not quench in the presence of oxygen but does fluoresce. Both of these facts have to be taken into account when the S-V calculations are made. The calibration LED intensity measurements also have to be considered to improve the accuracy of the oxygen measurement.

First, the optical path calibration measurements are taken into consideration by scaling the fluorescent emission signal to the intensity of the reference signal to give the term R, referred to as the modulation, as shown in Equation 41. R is the ratio of the fluorescent signal to the reference signal.

Equation 41. $$R = \frac{\text{Fluorescent signal}}{\text{Reference signal}}$$

The overlap of the excitation and emission spectra, figure 16, and the contribution to the signal of dye that does not quench but does fluoresce are dealt with using the term C shown in Equations 42 and 43.

The fluorescent signal when no oxygen present I_0 is shown below in Equation 42. In this situation, the emission of the fluorescent dye will be at a maximum.

Equation 42. $I_0 = (R_0 - C)$

With oxygen present, the fluorescent signal decreases. As the dye is quenched to a value I shown in Equation 43.

Equation 43. $I = R - C$

Incorporating these new terms for I_0 and I into the S-V (equation 39, chapter 4) gives Equation 44.

The S-V equation derived in Chapter 4.

Equation 44. $$\frac{I_0}{I} = 1 + k_g \tau_0 [O_2]$$

This can be rearranged to Equation 45.

Equation 45. $$[O_2] = \left[\frac{I_0}{I} - 1\right] * \frac{1}{k_g \tau_0}$$

The term m can be used to replace $\frac{1}{k_g \tau_0} = m$ to give new form of the S-V relationship shown in Equation 46.

Equation 46. $[O_2]=\left[\frac{I_0}{I}-1\right]m$

Replacing the terms for I and I_0 yield s the modified S-V equation used in the P7 oxygen sensor, as shown in Equation 47.

Equation 47. $[O_2]=\left[\frac{(R_0-C)}{(R-C)}-1\right]m$

The value m is the quenching efficiency, its value equates to the resolution of the sensor over a given oxygen range.

Equation 47. has two unknown constants, C and m, as there are two unknowns, a three point calibration will therefore be needed to find these values. These are provided by the three calibration gas mixtures, which have precise O_2 concentrations covering the operational range of the sensor (Diametrics internal document).

5.3.3. Calibration cycle of the P7 oxygen sensor

The sensor is exposed to each of the three calibration gas mixtures in turn and the fluorescence intensity measurements are taken for each of the oxygen tensions in the three gas mixtures. With the three oxygen tensions and intensity measurements, the sensor is calibrated over its operational range. The calibration gas mixtures are; (a) 2% CO_2, balance N_2, (b) 5% CO_2, 15% O_2, balance N_2 and (c) 10% CO_2, 50% O_2 balance N_2. Each gas is passed through a solution containing the sensor for ten minutes to ensure that the gas tensions have reached equilibrium within the solution. The solution is heated and maintained at 37°C throughout the calibration cycle. The calibration chamber (shown in figure 17) is also the storage container for the sensing end of the sensor, protecting it from damage and keeping it sterile until use (Internal documentation, Diametrics medical Ltd).

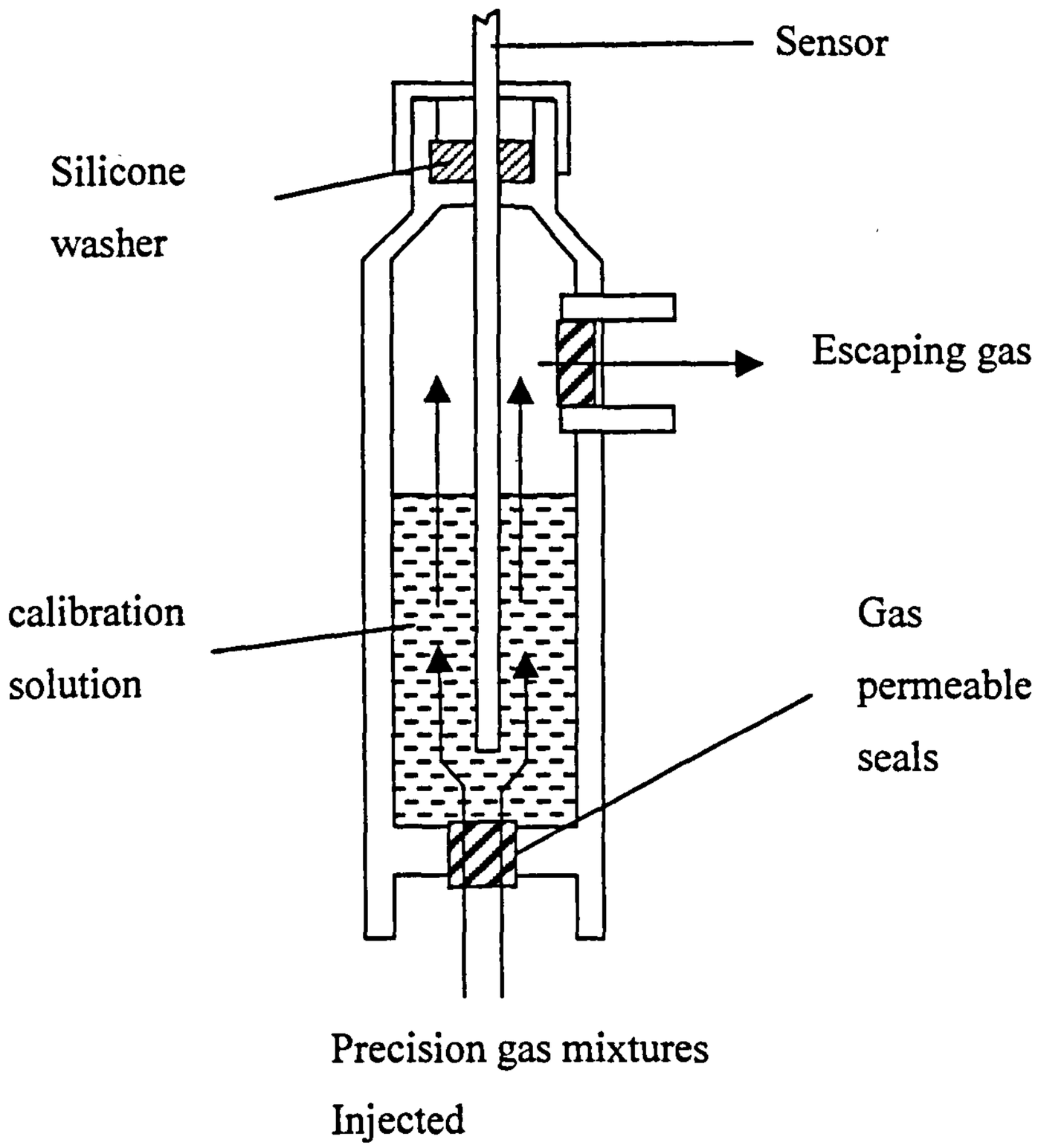

Figure 17. The P7 calibration and storage tonometer

Material	Properties	Supplier
Glucose·oxidase (GOD)	Glucose oxidase (β-D-Glucose: Oxygen 1-Oxidoreductase; EC 1.1.3.4) From Aspergillus Niger Activity form 50 to 229 unites/mg Unit definition: One unit will oxidise 1.0 micromole of β-D-Glucose to D-gluconic acid and H_2O_2 per minute at pH 5.1 at 35°C. (If reaction is saturated in oxygen, the activity may increase 50-100%) (Sigma product numbers G9010, G2133 and G7016)	Sigma Aldrich Co Ltd, Poole, Dorset, UK
Phosphate Buffered Saline (PBS)	Dissolve 1 tablet in 200 ml water to obtain a 137 mM NaCl, 2.7 mM KCl and 10 mM phosphate buffer solution, pH 7.4 at 25°C. (Sigma product number 79382)	Sigma
Catalase (CAT)	Catalase: H_2O_2 (H_2 oxidoreductase: EC 1.11.1.6) From Bovine Liver Activity: 2000 to 5000 units per mg protein One unit decomposes 1.0 μmole of H_2O_2 per min at pH 7.0 at 25°C, while the H_2O_2 concentration falls from 10.2 to 9.2 mM. (Sigma product number C9322)	Sigma
HEMA	HEMA: Poly(2-hydroxyethyl methacrylate) $[-CH_2C(CH_3)(CO_2CH_2CH_2OH)-]_n$(Sigma product number 192066 and P3183)	Sigma

Glutaraldehyde	Glutaraldehyde: Pentane-1, 5-dial $C_6H_8O_2$ (Sigma product number G7651)	Sigma
Tetrahydrofuran (THF)	C_4H_8O (Sigma product number T4303)	Sigma
Ethanol	90% v/v C_2H_5OH (Fisher code F/0400/08)	Fisher Scientific UK Ltd, Loughborough, Leicestershire, UK
Polyurethane	Estane 5714 Thermoplastic polyether based polyurethane	Goodrich chemicals, Hunslow, Middlesex, UK
Glucose	D-Glucose (Sigma code G-7528) $C_6H_{12}O_6$	Sigma
Precision gas mixtures :-	100% Nitrogen 7.5% oxygen balance nitrogen 15% oxygen balance nitrogen 50% oxygen balance nitrogen	Linde Gas Ltd Newfield Industrial estate, Stoke-on-Trent, Staffs UK

Table 8. Chemicals used in the research

5.4 Apparatus to control solution gas tensions and temperature

The sensors were tested in a purpose built test apparatus shown in figure 18 based on the design developed by Diametrics Medical Ltd. at their High Wycombe, UK, site. The apparatus allows phosphate buffered saline (PBS) to be aspirated with precision gas mixtures. The temperature of the solution was also maintained at 37°C by means of a water bath. The precision gas mixtures consisted of (a) pure nitrogen, (b) 15% oxygen balance nitrogen and (c) 50% oxygen balance nitrogen. These were adaptations of the P7 calibration gas mixtures, which also contain carbon dioxide for calibration of the pH and CO_2 sensors, that were not used in this work. The humidifiers and tonometers were filled with PBS to ensure a pH of 7. The experiments were carried out in 50 or 100ml of PBS at 37°C equilibrated at gas tensions of 15% oxygen and 85% nitrogen or 7.5% oxygen and 92.5% nitrogen that were aspirated into the tonometer at a rate of either 50 or 100cm^3/minute.

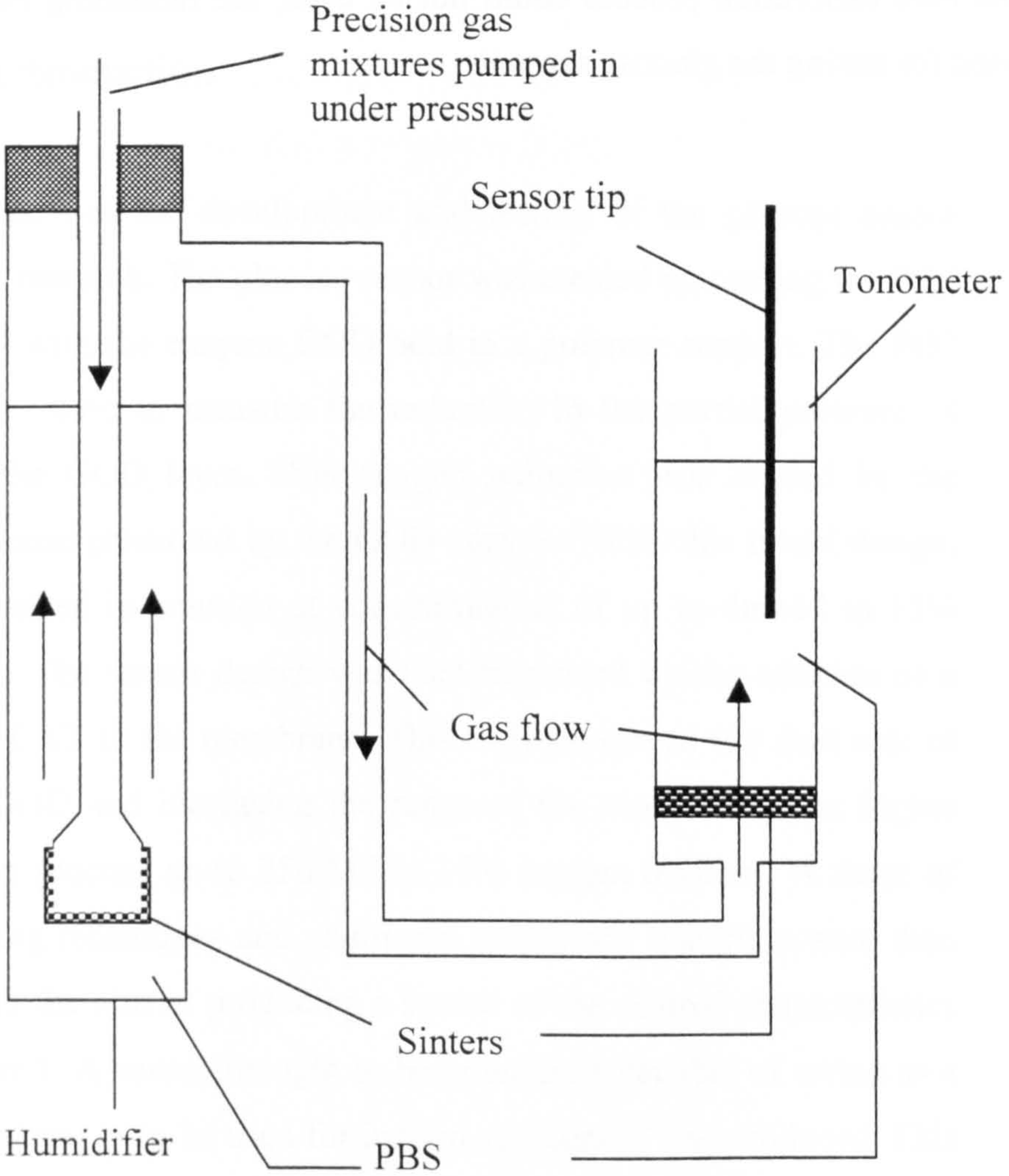

Glassware supplied by Robal Microspec, High Wycombe, UK.

Figure 18. The humidifier and sinter

As the precision gas mixtures are stored in a dry state, they are first passed through the humidifier to ensure that the gas has the correct saturated water vapour pressure (SVP). The sinter at the base of the humidifier is to ensure the gas was dispersed thoroughly throughout the liquid to increase the rate the gas dissolves into solution. The gas is then passed into the tonometer, where a second sinter ensures full aspiration of the tonometer solution. The tonometers and humidifiers are placed into a water bath maintained at 37°C. Five identical

humidifier-tonometer systems were used in the test apparatus. Three were used to calibrate the sensor, each one aspirated with one of the calibration gasses. When the auto calibration process could not be used, the remaining two systems were used for testing the glucose sensors.

6 Sensor development and testing

6.1 Introduction

This chapter describes the development and testing of the glucose sensor produced in this research. The glucose sensor was created by coating the PO2 sensor of the P7 with the enzyme GOD held in a polymer support. The PO2 sensor was then used to measure the reduction in the partial pressure of oxygen inside the GOD layer. This oxygen reduction was caused by the oxidation of glucose promoted by the GOD enzyme. With this initial design, glucose was detected in solution at concentrations of up to 4mM/l in 15% oxygen tensions. The sensor design was then improved by the addition of a second enzyme CAT to the membrane. This enzyme served the duel role of protecting the GOD and increasing the range of the sensor to cover higher concentrations of glucose up to 25mM/l in 15% oxygen tensions. A range of membrane coating techniques and additional membrane materials were then investigated with the aim of producing a sensor of the desired characteristics stated in Chapter 1. A sensor thought to be potentially capable of acting as a hypoglycaemic alarm or to be used for insulin adjustment was produced. This design of sensor was tested in physiological pH (7.4), temperature (37° C), and oxygen tensions (7.5KPa) were produced. Finally, these sensors were tested for their ability to survive storage (3 months) and sterilisation by exposure to gamma radiation. Although suffering some changes in performance, the sensor design was found to still function after both these trials.

6.2 Fabrication of the glucose sensors membranes

As discussed in Chapter 2, the diffusion reaction-characteristics of enzyme membranes control how the sensor will perform. The reaction-diffusion process is controlled by the composition and thickness of the membrane coated onto the oxygen sensor.

To produce the enzyme membranes, GOD and CAT were dissolved in distilled water or PBS solution and mixed with HEMA dissolved in ethanol. The sensors were then dipped into the mixture to coat the sensors in a thin layer of the enzyme HEMA (EH) mixture. As the sensor design improved, the composition of the mixtures was changed to improve the coating of the sensor. To improve the immobilisation of the GOD and CAT in the membranes, the enzymes were cross-linked (chemical connections formed) by dipping the coated sensors into glutaraldehyde.

6.3 Testing of the sensors performance

The sensors were tested in solutions of PBS of controlled temperature, pH and oxygen tension using the apparatus described in Chapter 5. Glucose concentrations were increased by adding appropriate volumes of 1M glucose solutions to the tonometer, using a precision pipette (Pipetteman P200 and P1000 Gilson Inc USA) the increases were made in controlled steps, usually 1mM/l. Decreases in glucose concentrations were achieved by adding appropriate volumes of PBS equilibrated at the required gas tensions and temperature.

6.4 Initial experiment on a modification of the P7 sensor to detect glucose.

This initial experiment was carried out to investigate if the principle of the sensor design was sound. The experiment simply involved dip coating a P7 sensor in an EH mixture. In theory, this should create a sensor whose oxygen reading is proportional to the concentration of glucose in the solution.

6.4.1. Sensor construction and testing

Sensor 1 was made by dip coating the P7 sensor into an EH mixture that contained 100 mg/ml of HEMA in a 75% ethanol and distilled water, figure 19. The enzyme solution consisted 70mg of GOD dissolved in distilled water. This was mixed with the above HEMA solution in a 5:1 ratio to form a homogenous suspension (Shaw, Claremont et al. 1991). The P7 sensor was left intact, although it was allowed to dry out for 30 minutes before coating that would damage the pH and CO_2 sensors.

After being dip coated in the EH layer, the sensor was allowed to dry for a further 30 minutes and then rinsed with PBS. The sensor was then placed into a tonometer containing PBS at 15 % oxygen, balance nitrogen aspirated into the tonometer at 100 cm^3/min and tested. The P7 oxygen sensor had already been calibrated in the P7 base unit before it was dip coated. Calibration following coating would have been preferable, however, once removed from its calibration tonometer, the sensor could not be replaced; hence, post coating calibration was not possible. Once a steady signal was observed from the PO2 sensor, glucose solution was added to the tonometer to raise the glucose concentration in steps of 1mM/l.

The results of the initial glucose test of sensor one are shown in figures 20 and 21, which are scans of printouts from the P7. Figure 20 shows the response of

the sensor to an increase of from 0 mM/l to 1 mM/l of glucose. Figure 21 shows the full range of the sensor, demonstrating that after the glucose concentration reaches 3mM/l the sensor no longer responds to increases in glucose concentrations.

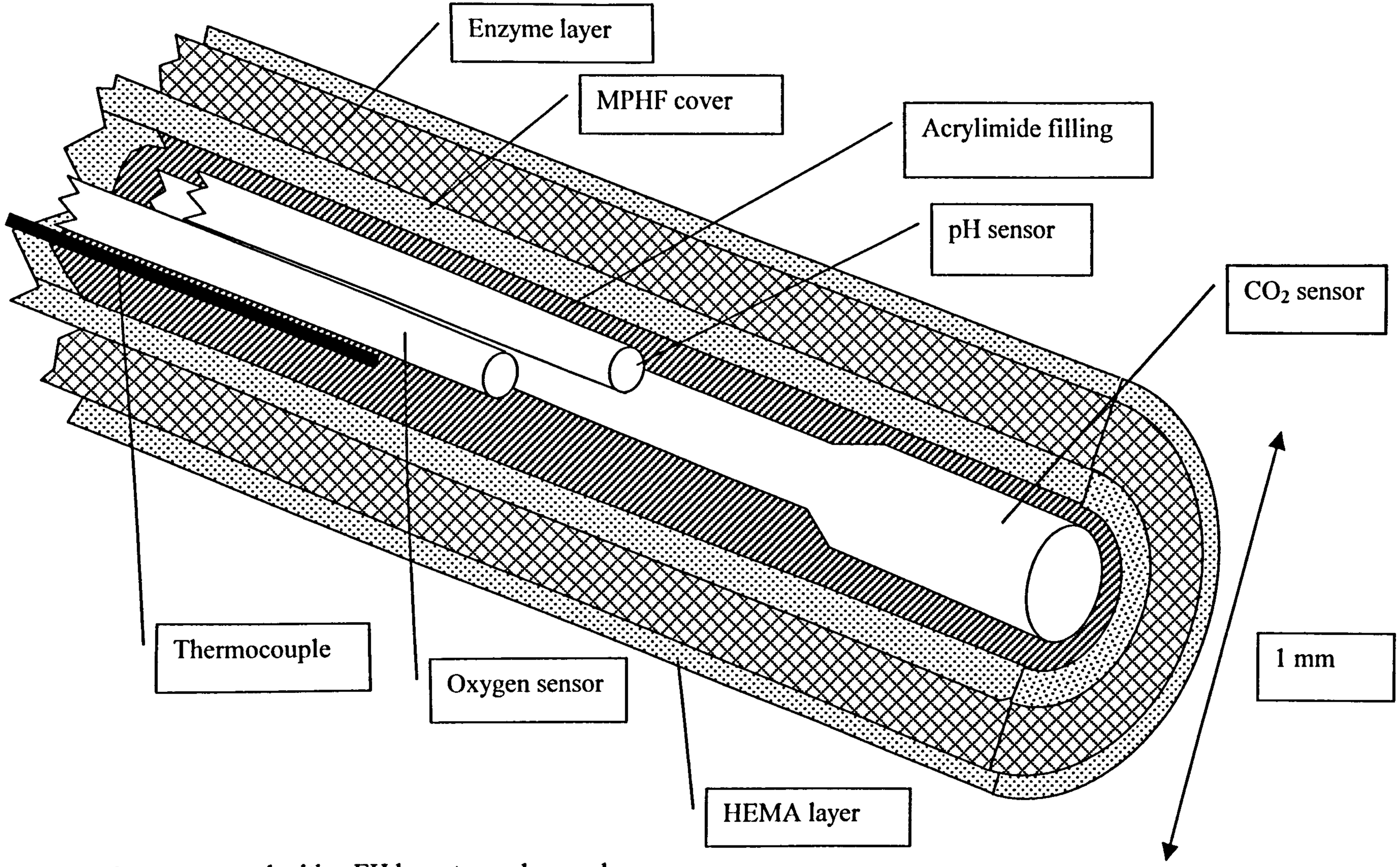

Figure 19. The P7 sensor coated with a EH layer to produce a glucose sensor

6.4.2. Results of the tests of the prototype sensor, Sensor 1

The results of the initial test, the addition of the HEMA layer and the 12-hour glucose solution test, are shown in figure 21 and Table 13.

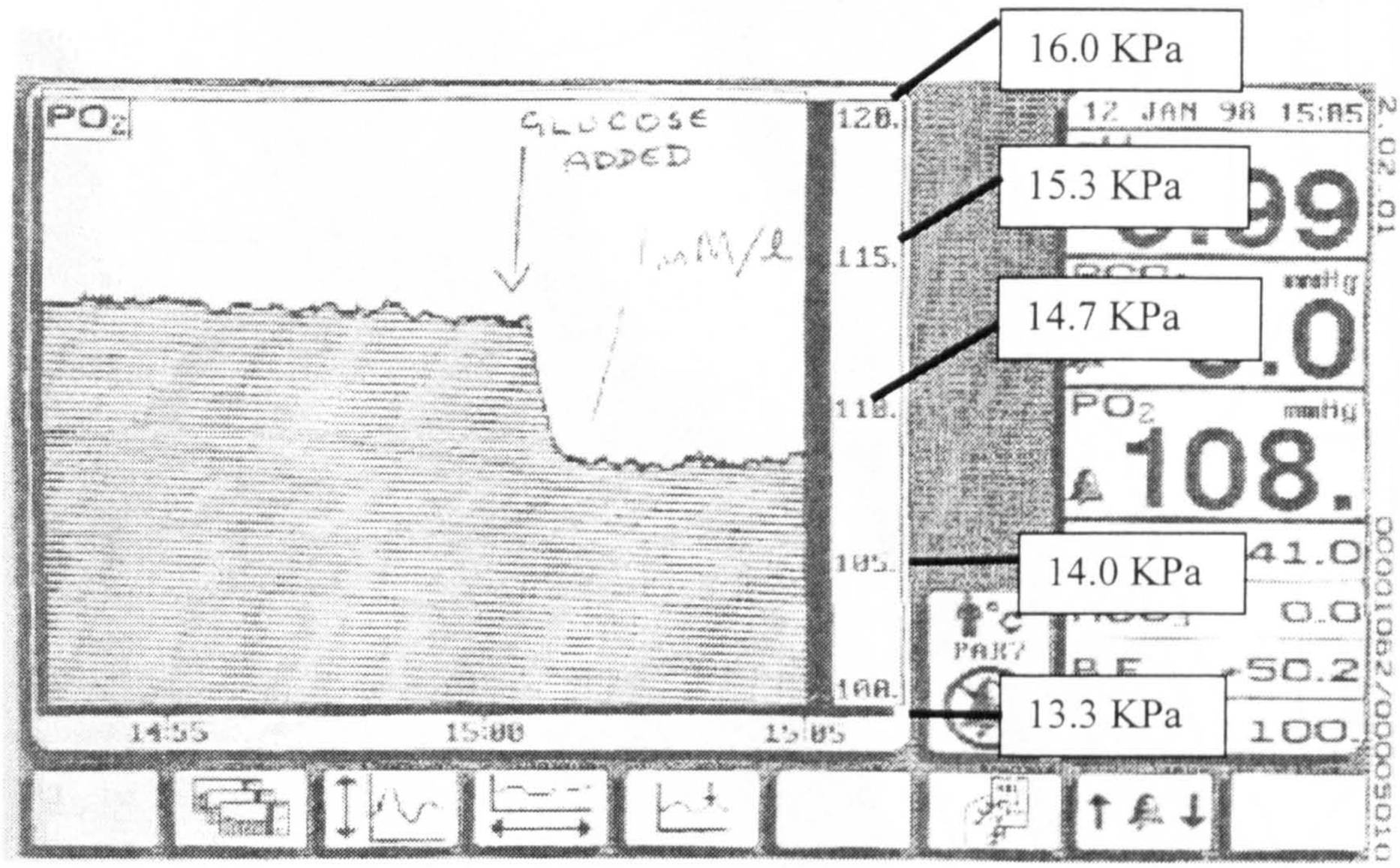

Figure 20. The P7 printout of a glucose step from 0 to 1 mM/l for sensor 1.

The temperature was intended to be 37 °C, however, the water bath available at this time had poor thermostatic control, and caused the temperature to vary from the desired value. It can be seen here that the temperature of the solution was 41°C.

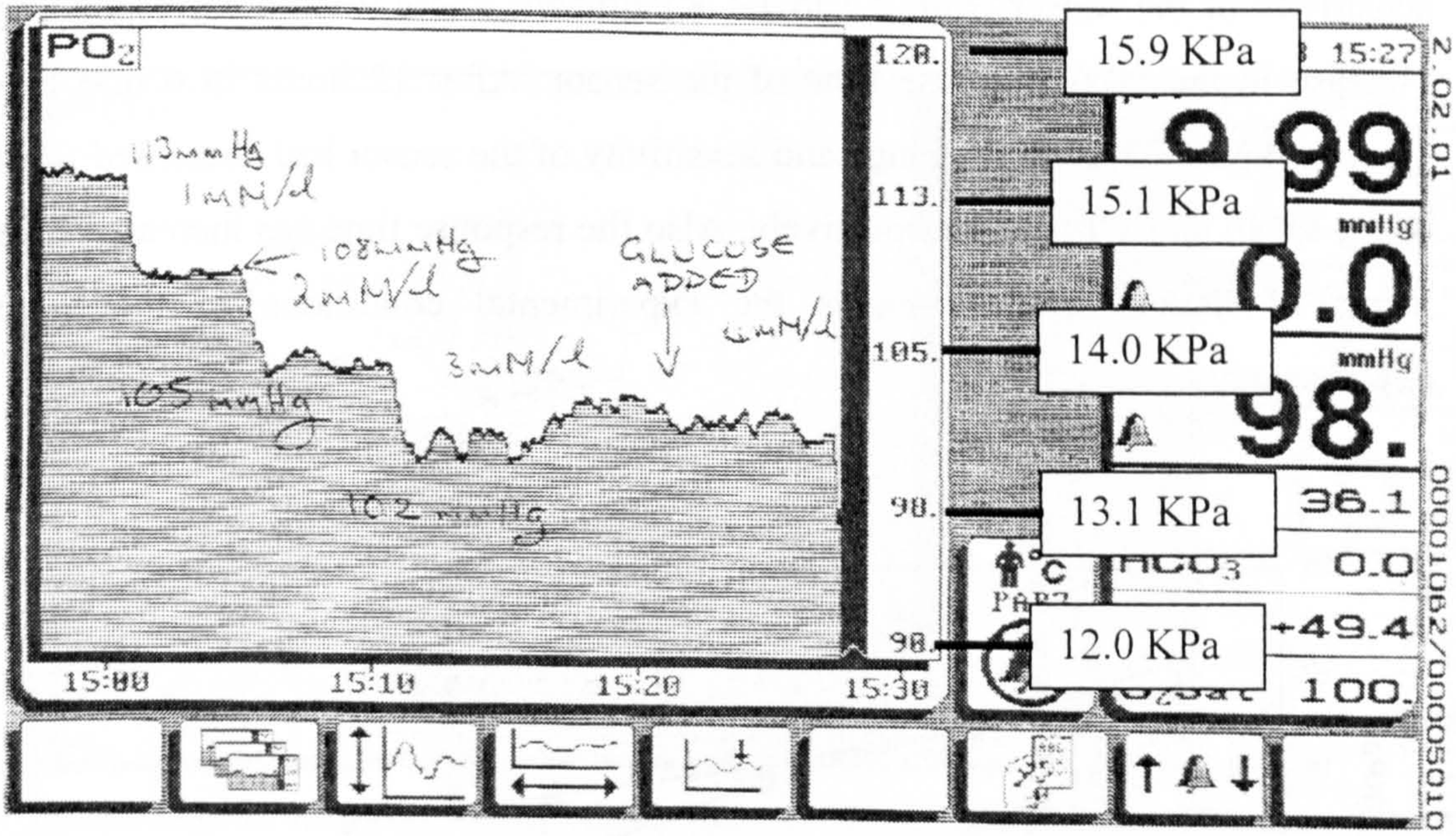

Figure 21. The P7 printout of PO2 values against time for increasing glucose concentrations before the outer HEMA coat was added.

6.4.3. Extension of the range of sensor 1 using an outer HEMA coat

Having shown that the basic design of the sensor was sound, it was decided to attempt to increase the range of the sensor using a diffusion limiting outer membrane. HEMA was readily available and so it was decided to dip coat the sensor in a layer of HEMA.

Sensor 1 was then dip coated in the HEMA solution used in its construction and re-tested, using the protocol described above. Finally, to test the longevity of the sensor, it was left in solution containing 6 mM/l overnight (approximately 12 hours). This is roughly the blood glucose concentration of a healthy individual.

From figure 22 and Table 10, it can be seen that the addition of the HEMA layer caused the range of the sensor to double from 3 to 6 mM/l. and increase in the sensitivity of the sensor from 0.7 to 1.1 KPa/mM/l. There was no corresponding increase in the 90% response time of the sensor. After 12 hours in 6 mM/l of glucose, figure 23, both the range and sensitivity of the sensor had decreased from 6 to 4 mM/l and 1.1 to 0.4 respectively. Also the response time has increased by a factor of three. Table 9 shows the experimental conditions of the three experiments.

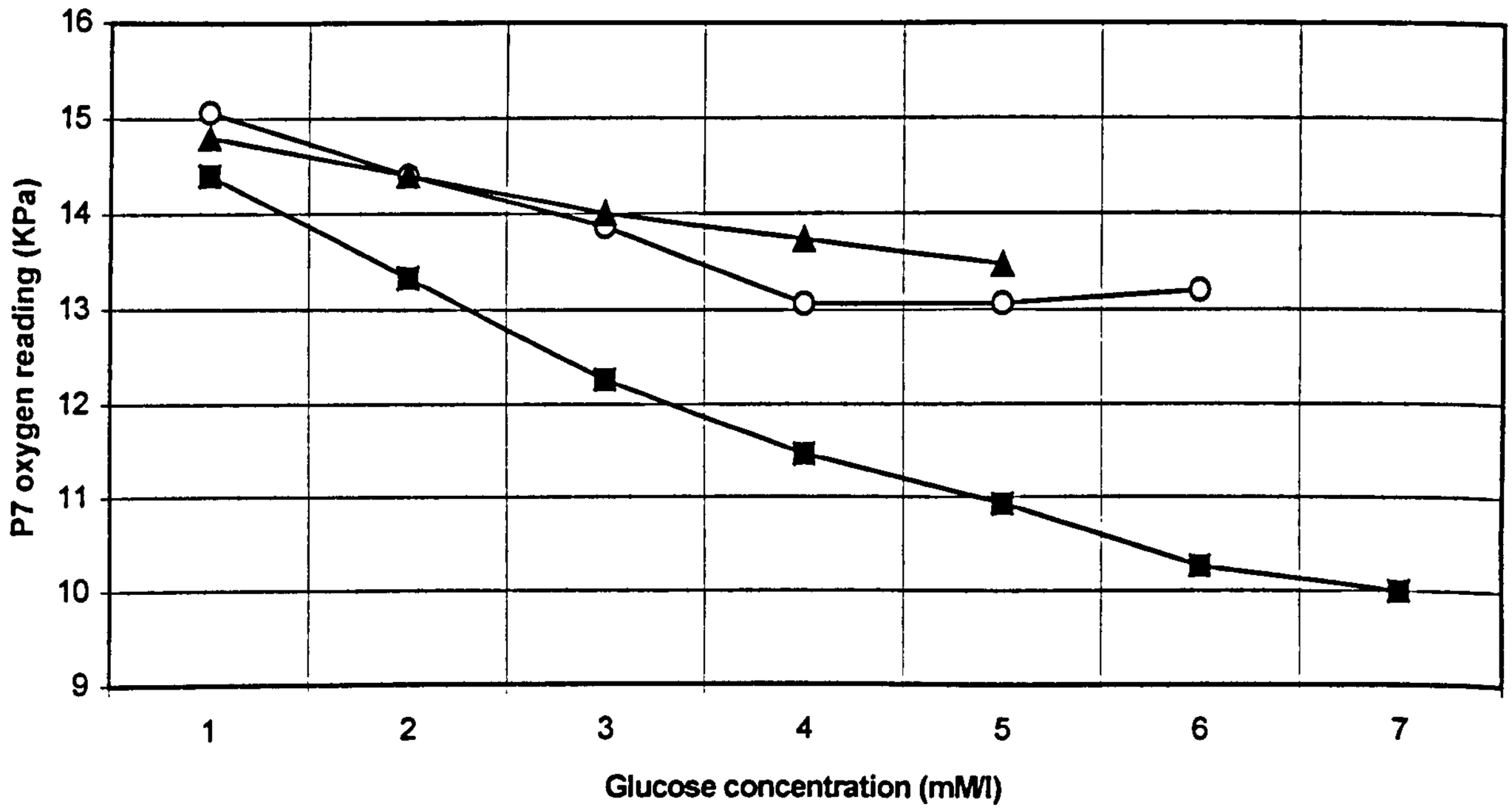

The sensor with only the EH coating —○—, after the addition of the outer HEMA coating —■— and after being left in 6mM/l of glucose PBS overnight at atmospheric gas tensions and room temperature —▲— . The temperature of the tonometer solution for the outer HEMA coat experiment was 39.9°C and for the post over night experiment was 38.9°C.

Figure 22. A plot of glucose concentration against P7 oxygen reading for Sensor 1.

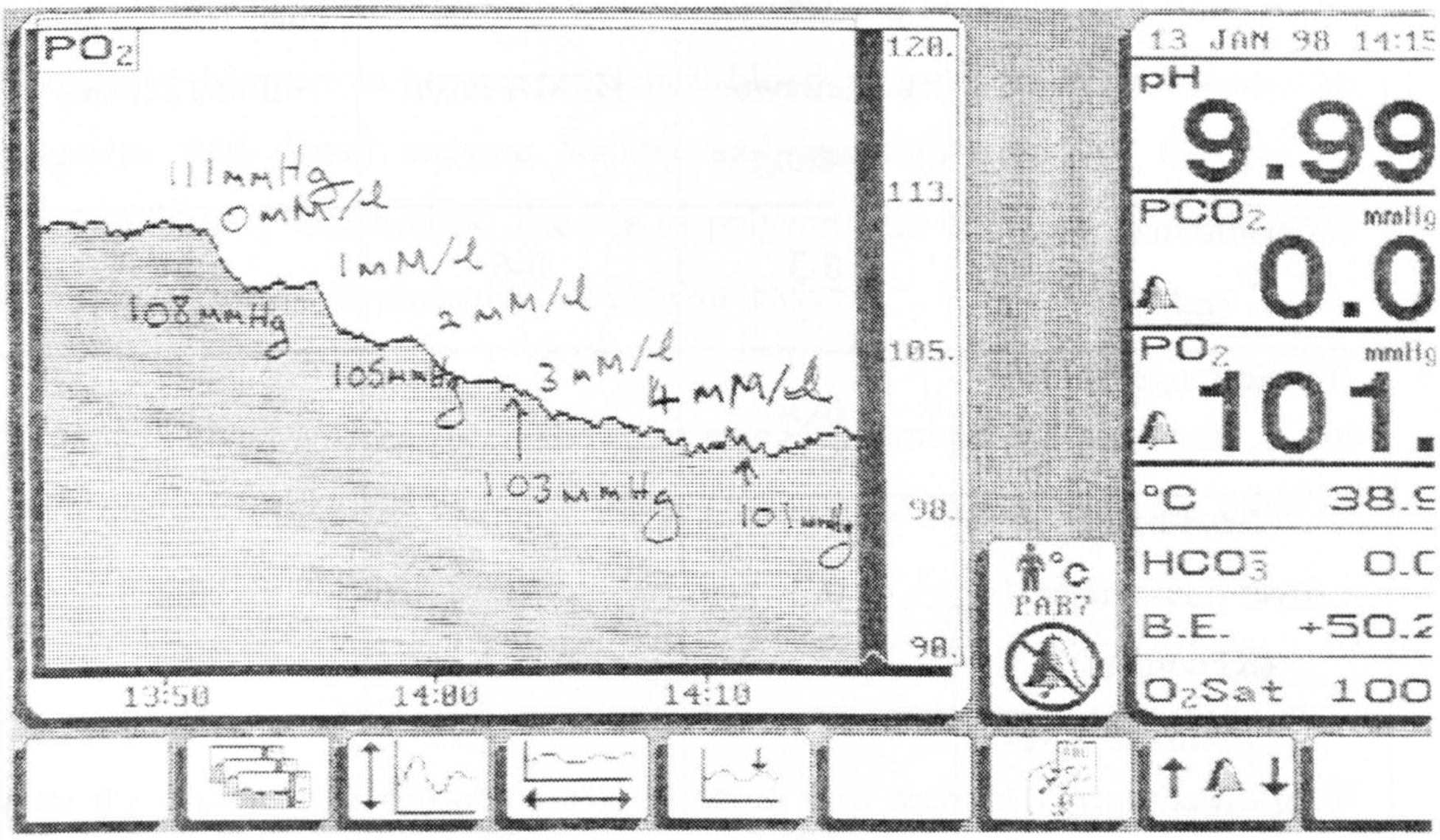

Figure 23. The response of Sensor 1 after 12 hours in glucose concentration of 6 mM/l

	Initial experiment	With outer HEMA coat	After 12 hour run
Atmospheric pressure (KPa)	100.1 [1]	100.1 [1]	99.9 [2]
Temperature (°C)	41.0	36.1	38.9
Dry PO2 tension (KPa)	15.0	15.0	14.9
SVP corrected PO2 tension (KPa)	13.8.	14.1	13.9

[1] Taken at start of initial experiment [2] Taken at end of experiment

All atmospheric pressure measurements were taken using the barometer on board the P7.

Table 9. The oxygen tensions and SVP adjusted partial pressures used in the tests of Sensor 1

	Sensor 1 with only HEMA and enzyme coating	Sensor 1 with extra outer HEMA layer	Sensor 1 with extra outer HEMA layer after 12 hours
Operational range (mM/l)	0-3	0-6	0-4
Linear range (mM/l)	0-3	0-5	0-4
Sensitivity (over linear range) (KPa/mM/l)	0.7	1.1	0.4
Approximate 90% Response time (over linear range) (seconds)	<100	<100	100 to 200

Table 10. The characteristics of Sensor 1

The response times of the sensor are only approximate values because it was impossible to know the rate at which the added glucose mixed with the PBS solution.

6.4.4. Conclusions of the initial glucose sensor tests

The prototype sensor has proved very successful; it covers the healthy and hypoglycaemic range and has response times well within those desired. The sensor does respond to the presence of glucose in solution, so the theory of the sensor design has been shown to be sound. However, even in this elevated oxygen tension of 15%, which is above those seen in subcutaneous tissue, its range is limited to 6 mM/l and its operation is significantly degraded by exposure to

glucose solutions of 6 mM/l for a 12 hours period. The increase in 90% response time of the sensor may indicate that it is now operating in reaction-controlled mode due to enzyme deactivation, as described in Chapter 3. The range of the sensor will have to be increased and the operational stability will have to be improved if this were to become a practical blood glucose sensor. This should be achievable with better enzyme loading and immobilisation and the use of diffusion limiting membranes. The use of polyurethane in particular should help the sensor to operate in physiological oxygen tensions.

The HEMA outer coat has been shown to extend the range and sensitivity of the sensor without increasing response time. This is encouraging from the point of view of using it to extend the range of the sensor.

The readings of the P7 oxygen sensor are above the SVP corrected values, even when the error of the sensor (± 5%) is taken into account the reading is still approximately 0.5KPa above the correct reading. This could be a result of damage to the sensor during construction or the experimental conditions, such as temperature or gas tension errors. As the sensor is dried out during construction, there will be some shrinkage and then re-expansion of the membrane in the sensor. This could have a detrimental effect on the oxygen sensor leading to performance characteristics outside of those expected during the oxygen sensor calibration procedure. The elevated temperature of the first experiment (41°C) is unlikely to be the source of the problem, as the oxygen reading would be lowered rather than increased. This is due to the greater value of water vapour pressure at this temperature than at 37°C, which the P7 is calibrated to operate. It is possible that the gas has not reached full saturation with water vapour during its passage through the humidifier.

Ideally the sensor design would have been improved in single steps, however, as there was only a small number of P7 sensors available for experimentation, two features were put into the next sensor.

To improve the range of the sensor, a thicker outer HEMA coat was employed in the next sensor and, to improve the operational stability, CAT was included in the EH layer. This should protect the GOD in the sensor from the action of H_2O_2, which was possibly the cause of the degradation seen in the previous sensor.

6.4.5. Construction and testing of Sensor 2

Sensor 2 used GOD and CAT in its EH layer. The CAT has two roles, first to recycle oxygen from the H_2O_2 to help redress the stoichiometric limit and secondly, protect the GOD as described in Chapter 2. Sensor 2 was also dip coated twice in HEMA to provide a diffusion limiting outer layer of twice the thickness of that used in Sensor 1. With these two features, it was expected that the range of the sensor would be greater than Sensor 1.

The EH layer consisted of 0.5ml of 2400 active units/ml of GOD[1] and 360,000 units/ml of CAT dissolved in distilled water. This was mixed with 0.5ml of HEMA solution containing 100mg/ml of HEMA dissolved in 75% ethanol water. The same HEMA solution was used for dip coating the sensor to produce the outer membrane. The experiment was extended to include a test of the sensor's response to decreasing glucose concentrations. The decreasing glucose concentrations were achieved by adding appropriate volumes of PBS to the tonometer, which had been equilibrated at the appropriate temperature and oxygen tensions.

The results of the sensor tests are shown in Figure 24, 25 and Table 12. It can be seen that the sensor reading at 0 mM/l of glucose is below the 14.0 KPa. The sensor showed a maximum response to glucose concentrations of up to 7 mM/l, only 1mM/l greater than the maximum response to glucose of Sensor 1. Also, at 7

[1] *The difference in this and the previous GOD value was due to small variations in weighing out of the GOD.*

mM/l a large amount of noise was seen in the signal from Sensor 2, this was in the order of ≈0.5KPa, 50% of the sensitivity, as can be seen in figure 25. Lowering the glucose concentration caused no change in the signal from the sensor, which remained at 4.2 KPa, the same reading as 7 mM/l of glucose, still exhibiting the noise observed at the end of increasing glucose concentrations. There was little difference in the sensitivity of Sensors 1 and 2, with sensitivities of 1.1 KPa/mM/l and 1.2 KPa/mM/l respectively. The experimental conditions are shown in Table 12. below.

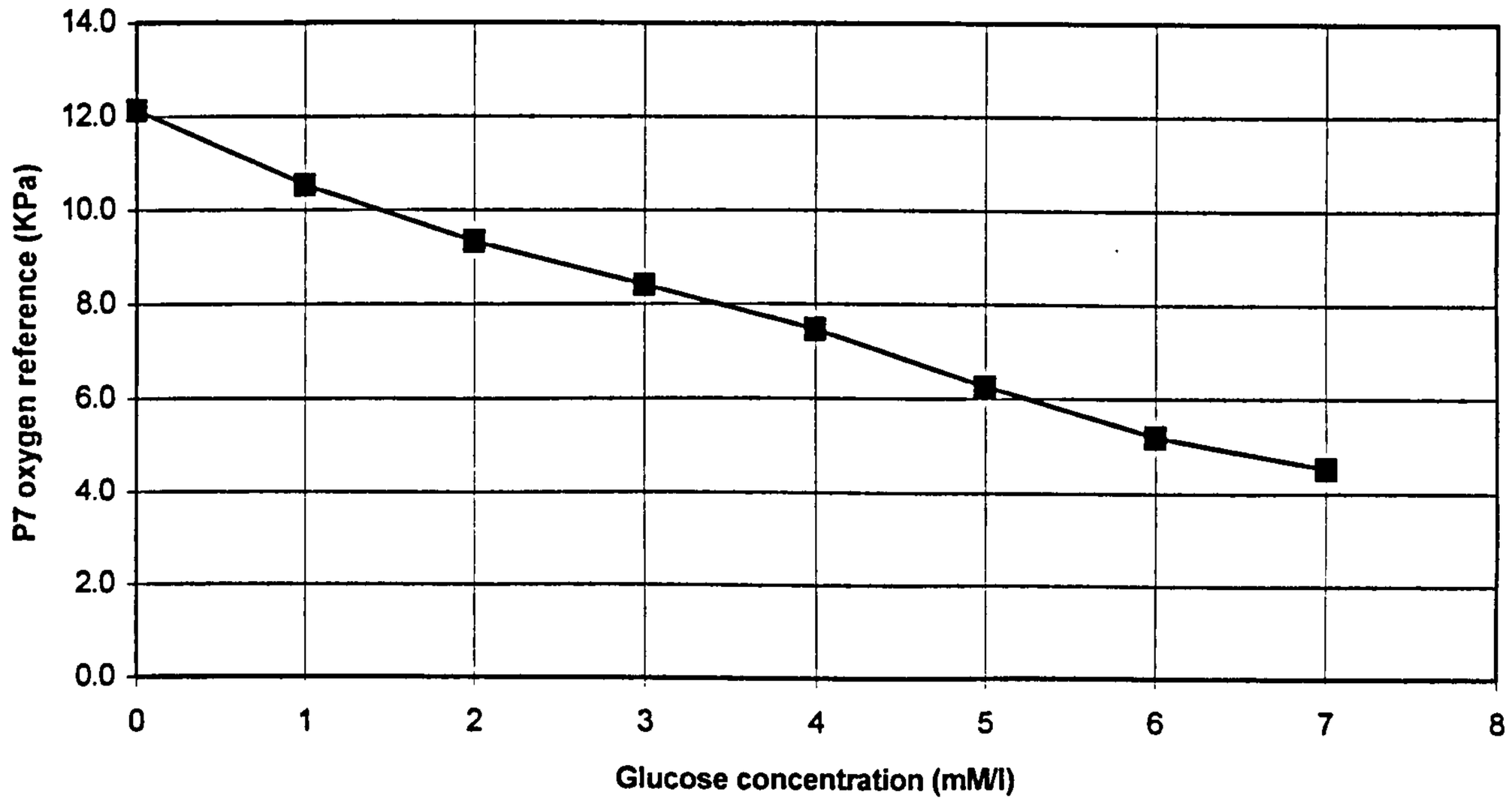

Figure 24. The performance of sensor 2. The oxygen signal from the enzyme coated P7 oxygen sensor against glucose concentration.

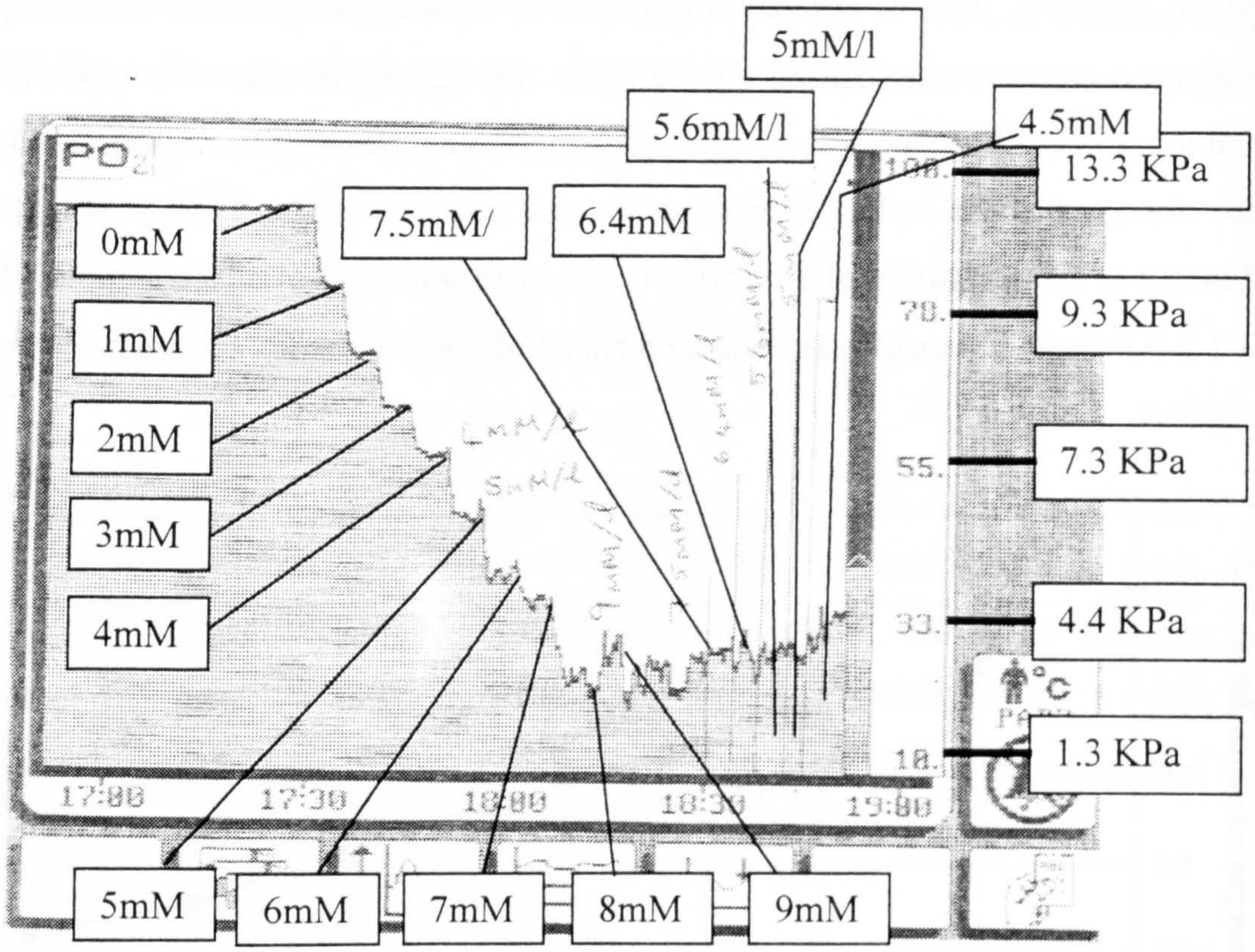

Figure 25. The response of Sensor 2 to increasing and decreasing glucose concentrations.

	Sensor 2
Operational range (mM/l)	O-7
Linear range (mM/l)	0-6
Sensitivity (over linear range) (KPa/mM/l)	1.2
Approximate 90% Response time (over linear range) (seconds)	<100

Table 11. The performance characteristics of Sensor 2

Atmospheric pressure (KPa)	99.9[2]
Temperature (°C)	37.6
Dry PO2 tension (KPa)	15.0
SVP corrected PO2 tension (KPa)	14.0

Table 12. The experimental conditions during the testing of sensor 2.

6.4.6. Conclusions of sensor 2 experiments

Sensor 2 shows little improvement on the performance of Sensor 1. The lack of response of the sensor to decreasing glucose concentrations could have been a fault with the experiment, possibly with the temperature or oxygen tension of the solution that was added to lower the glucose concentration. These may have equilibrated with the atmospheric gas tensions and temperature during the transfer of the solution between the tonometers. However, temperature is lower than the tonometer and the atmospheric oxygen tension is greater than those of the solution. As the solubility of oxygen in water increases with decreasing temperature so the lower temperature would cause increased oxygen tension in the solution. This is coupled with the atmospheric oxygen tension that the fluid is temporarily exposed to, being higher than the 15% supply, so that had the fluid absorbed oxygen from the atmosphere again an increase in oxygen tension should have been observed. Therefore, the oxygen tension of the solution would have increased instead of reduced. Because of this, these causes were discounted. The double HEMA coat did not increase the range by a large amount and, most importantly, the sensor did not respond to decreasing glucose concentrations. The

[2] *Atmospheric pressure taken using the onboard P7 barometer at the start of the experiment*

next sensor constructed was given a thinner HEMA layer to investigate if this will allow the sensor to measure decreasing glucose concentrations. Although not thought to be a factor, the transfer of the solution for dilutions will be carried out more quickly to reduce changes in temperature and oxygen tensions in transit.

6.4.7. The detection of decreasing glucose concentrations

Sensor 3 had essentially they same design as Sensor 2, except that it was only dip coated in HEMA once instead of twice as with Sensor 2. The EH solution was identical to those used in sensor 2. When a glucose concentration of 5mM/l had been reached, PBS equilibrated at 37°C and 15% oxygen 85% nitrogen gas tension was added to the tonometer to lower the glucose concentration. The flow rate of the gas mixture was reduced to 50 cm^3/min, as this reduced the gas used but still allowed full aspiration of the tonometer. This was the case for all the following experiments. The sensor was then tested after 12 hours in a solution containing 5 mM/l of glucose. 5 mM/l of glucose was chosen as opposed to 6mM/l as it was thought that 5 mM/l better reflected a normal physiological value.

6.4.8. The performance of sensor 3 to decreasing glucose concentrations

The sensor did respond to decreasing glucose concentrations, although an increased level of noise can be seen in the signal, shown in figure 26. This noise could be due to temperature and gas tensions changes in the added PBS during transfer to the test tonometer. The signal from the tests of the sensor range can be seen to be relatively noise free compared to the dilution experiment, figure 27.

After 12 hours in 5mM/l glucose concentrations, the response of the sensor had degraded significantly with a range reduction of 4 mM/l from 5 to 1 mM/l and sensitivity degradation from 1.1 to 0.4 KPa/mM/l. The 90% response time had also increased from 60 to 120 seconds. The results of all the experiments are

shown in Table 15 and figure 28. In this experiment the zero glucose, reading did match the SVP adjusted oxygen values.

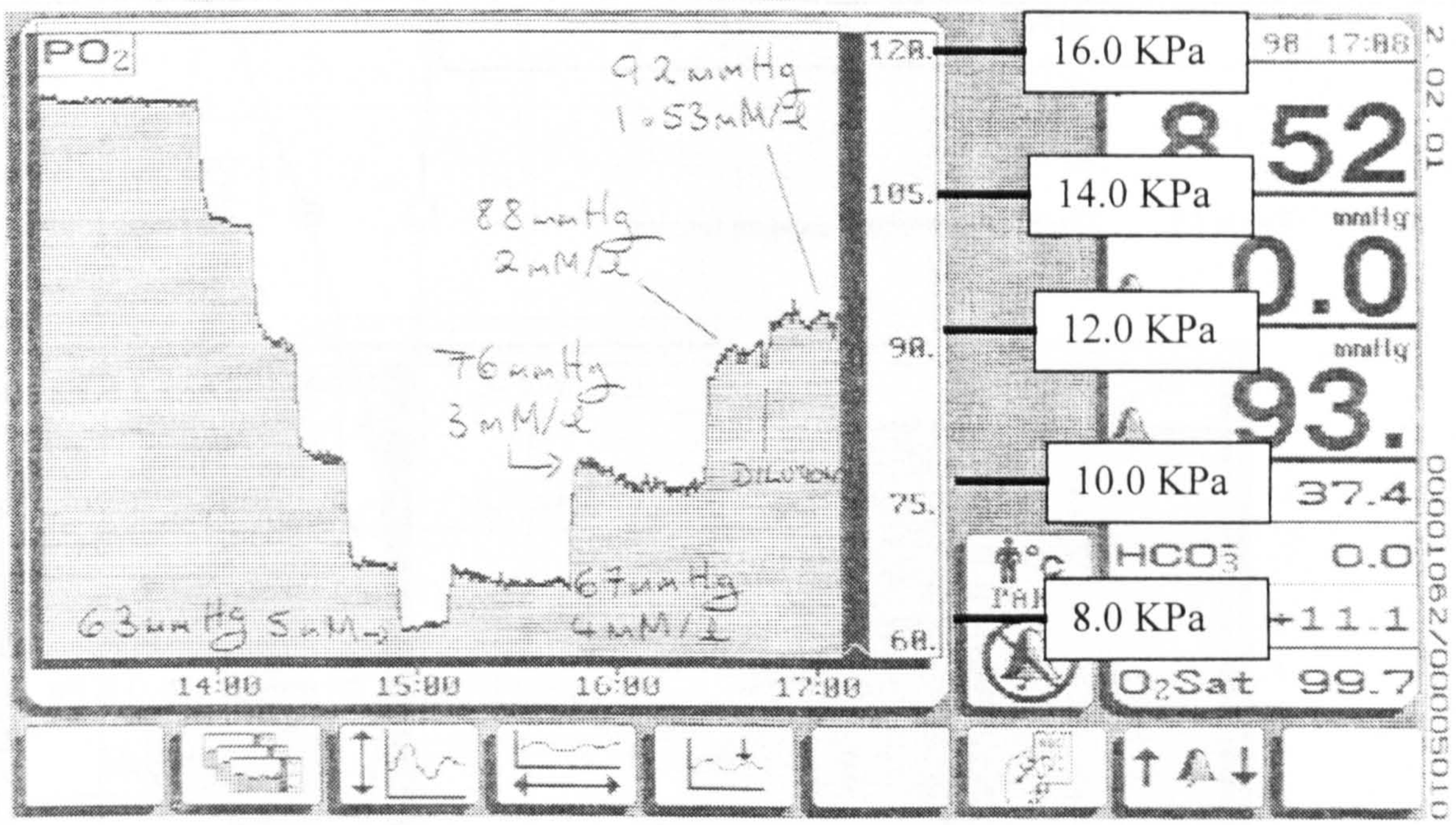

Figure 26. The response of the Sensor 3 to increasing and decreasing glucose concentrations.

Atmospheric pressure (KPa)	102.5
Temperature (°C)	37.4
Dry PO2 tension (KPa)	15.0.4
SVP corrected PO2 tension (KPa)	14.4

Table 13. The SVP corrected oxygen tension

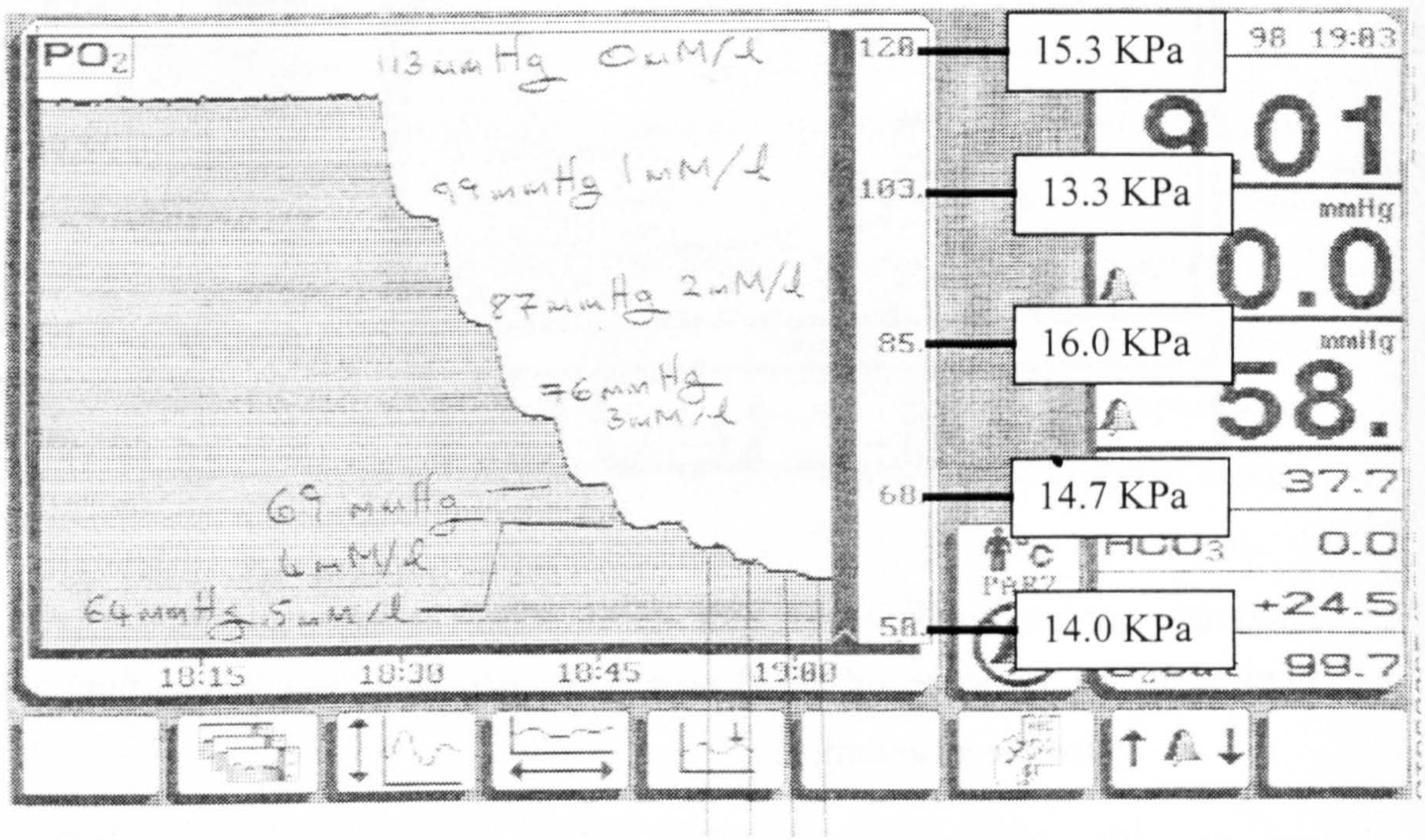

Figure 27. The test of the full range of Sensor 2

Atmospheric pressure (KPa)	102.5
Temperature (°C)	37.7
Dry PO2 tension (KPa)	15.0.4
SVP corrected PO2 tension (KPa)	14.4

Table 14. The SVP corrected oxygen tension

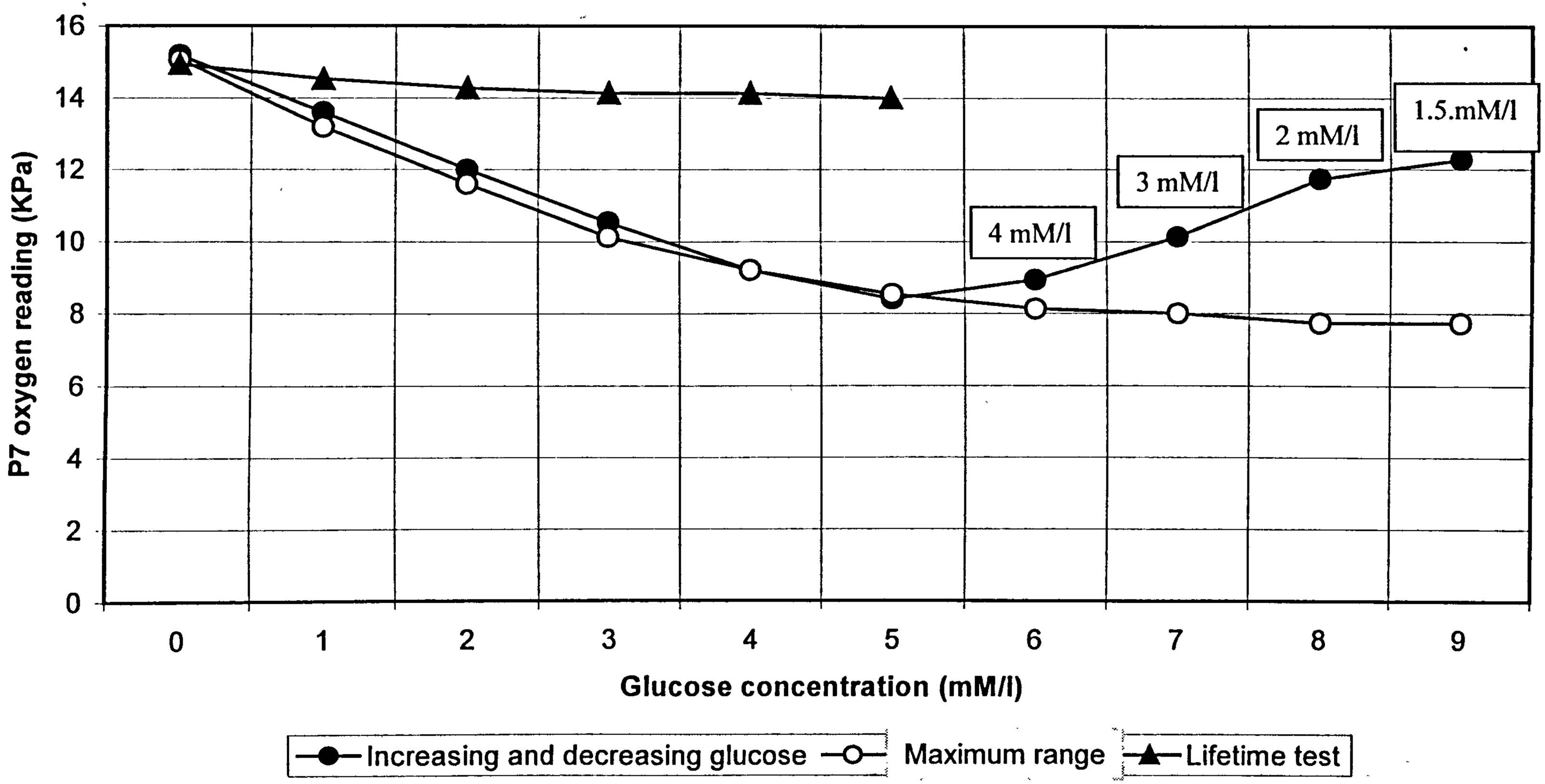

Figure 28. The response of Sensor 3 during all three experiments

	Initial test	Maximum range test	Test of sensor after 12 hours operation
Operational range (mM/l)	Only tested to 5mM/l	0-6	≈1
Linear range (mM/l)	0-5	0-4	NOT LINEAR
Sensitivity (over linear range) (KPa/mM/l)	1.1	1.1	0.3
Approximate 90% Response time (over linear range) (seconds)	<100	<100	100 to 200

Table 15. The characteristics of Sensor 3

6.4.9. Conclusions of the response of the sensor to decreasing glucose concentrations

Sensor 3 successfully measured glucose concentrations up to 9 mM/l and responded to decreasing glucose concentrations with minimum hysteresis. The 90% response time of 60 seconds is well within the desired level for the glucose sensor. However, after 12 hours in 5 mM/l, the sensors maximum range had reduced to only 1 mM/l and its 90% response time had increased to 120 seconds. The thinner HEMA layer does not seem to have reduced the range by a large amount. However, the sensor does respond to decreasing glucose concentrations, which may be a result of the thinner HEMA layer or better experimental procedure. This loss of sensor response after 12 hours is most likely due to

leaching of the enzyme out of the sensor into the tonometer solution as the CAT should protect it from the action of hydrogen peroxide. The leaching out of GOD into the tonometer solution may possibly be detected by looking for oxygen tension changes in the tonometer solution when glucose was added.

The normal test of GOD is complex and it may be deactivated quickly in free solution preventing its detection. As a second P7 unit had become available at this point, it was now possible to take measurements of the oxygen tension in the tonometer concurrently with glucose measurements and look for this effect. The matching zero glucose concentration readings may be due to the lower flow rate of the oxygen into the tonometer, allowing the gas to become fully humidified.

6.4.10. Investigation of the integrity of the EH membrane

The aim of these experiments was to look for signs of any GOD leaching into the test tonometer solution out of the EH layer. This was to be detected by virtue of the decrease in the oxygen tension of the solution, brought on by the GOD reacting with glucose. This oxygen change was detected by using a second P7 sensor to measure the oxygen tension of the test solution in the test tonometer during the experiment. The second sensor also allowed differential oxygen measurement to be taken between the glucose sensor and the oxygen sensor. This will allow any oxygen fluctuations in the tonometer solution to be accounted for, removing any error in the glucose measurement from this source. The detection of escaped GOD in solution using this method makes several assumptions. First is the assumption that the oxygen is not replaced into the tonometer solution, through aspiration, at such a rate that no change can be measured. Switching off the gas supply caused the oxygen tension to change in an unpredictable manner. As the solution equilibrated with atmospheric oxygen tensions, this means that GOD induced changes would be masked. Second, it is assumed that enough GOD has leached into the solution to change the oxygen tension by a measurable amount. Third, if GOD is leaching into the solution then it is logical to assume

that CAT is also entering the solution through the same mechanism. The CAT will reduce the effect of GOD by recycling oxygen from the H_2O_2, perhaps reducing the effect below a level that could be detected.

Sensor 4 was constructed using identical materials and methods as Sensor 3. The sensor and a second P7 sensor were then put in a tonometer and tested under the same condition as Sensor 3.

6.4.11. The results of the membrane integrity experiment

The response of the glucose sensor and the reference oxygen sensor to the initial increase of the tonometer glucose concentration from 0 to 1 mM/l was identical as can be seen in figure 29. This indicated that GOD had leached into the solution and was causing a drop in the oxygen tension of the solution when glucose was added. Following this experiment, the glucose sensor was rinsed thoroughly in PBS to remove any free enzymes which may have been on the surface. The sensor was then re-tested with fresh tonometer solution. In the second test the oxygen sensor showed no change when the glucose concentration was increased. However, the glucose sensor did show a response that is shown in figure 30.

Due to time constraints on the availability of the equipment, the sensor was only taken up to 4 mM/l so no maximum range was found, the performance of the sensor, after rinsing, is shown in table 16 and the experimental conditions are shown in table 17.

	Test after rinsing with PBS
Operational range (mM/l)	Only taken to 4
Linear range (mM/l)	4
Sensitivity (over linear range) (KPa/mM/l)	1.1
90% Response time (over linear range) (seconds)	<100

Table 16. The characteristics of Sensor 4 after washing with PBS

Atmospheric pressure (KPa)	99.6
Temperature (°C)	37.7
Dry PO2 tension (KPa)	14.9
SVP corrected PO2 tension (KPa)	14.0

Table 17. The SVP values for the sensor 4 experiment

The reference oxygen sensor.

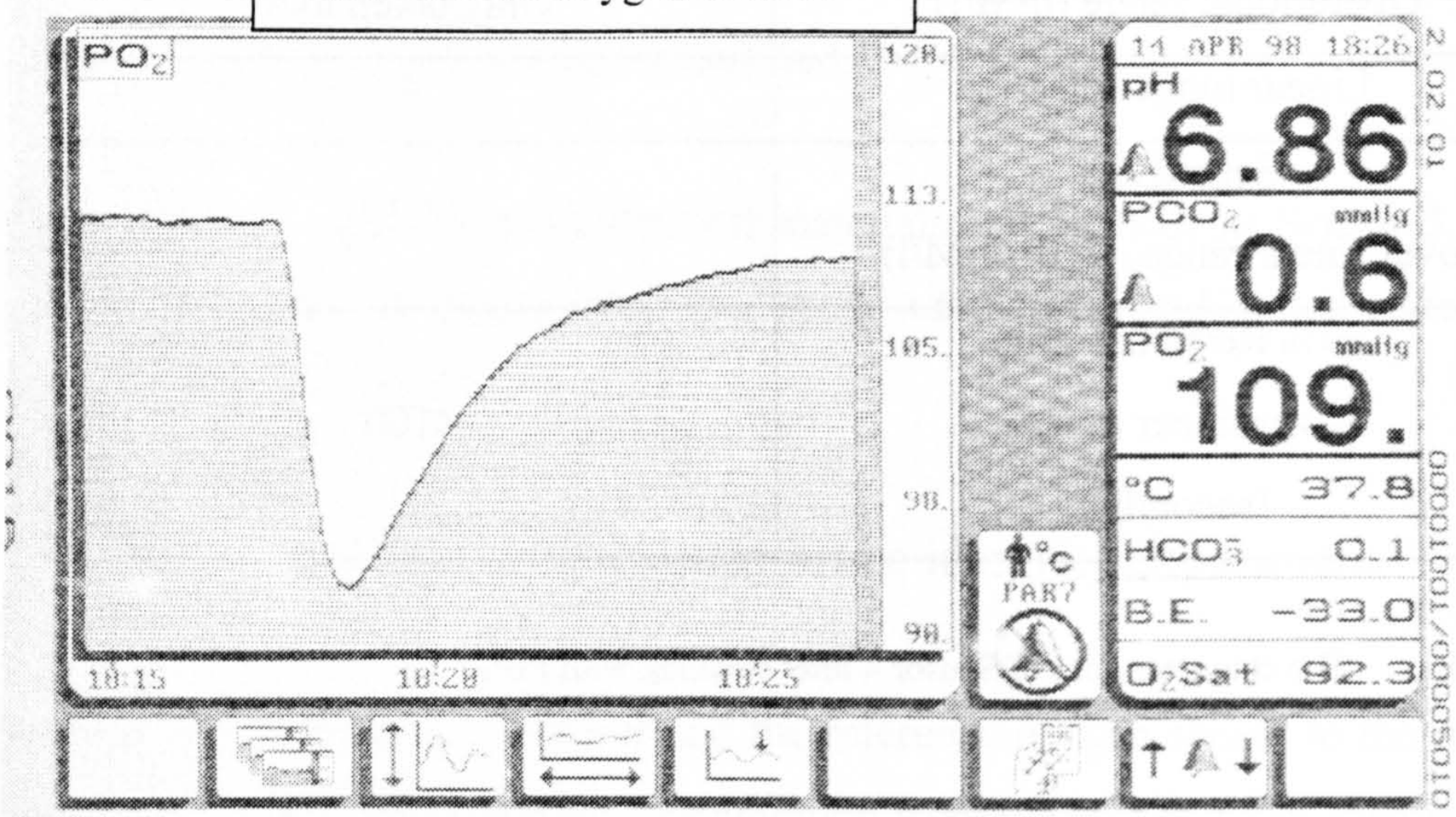

The glucose sensor

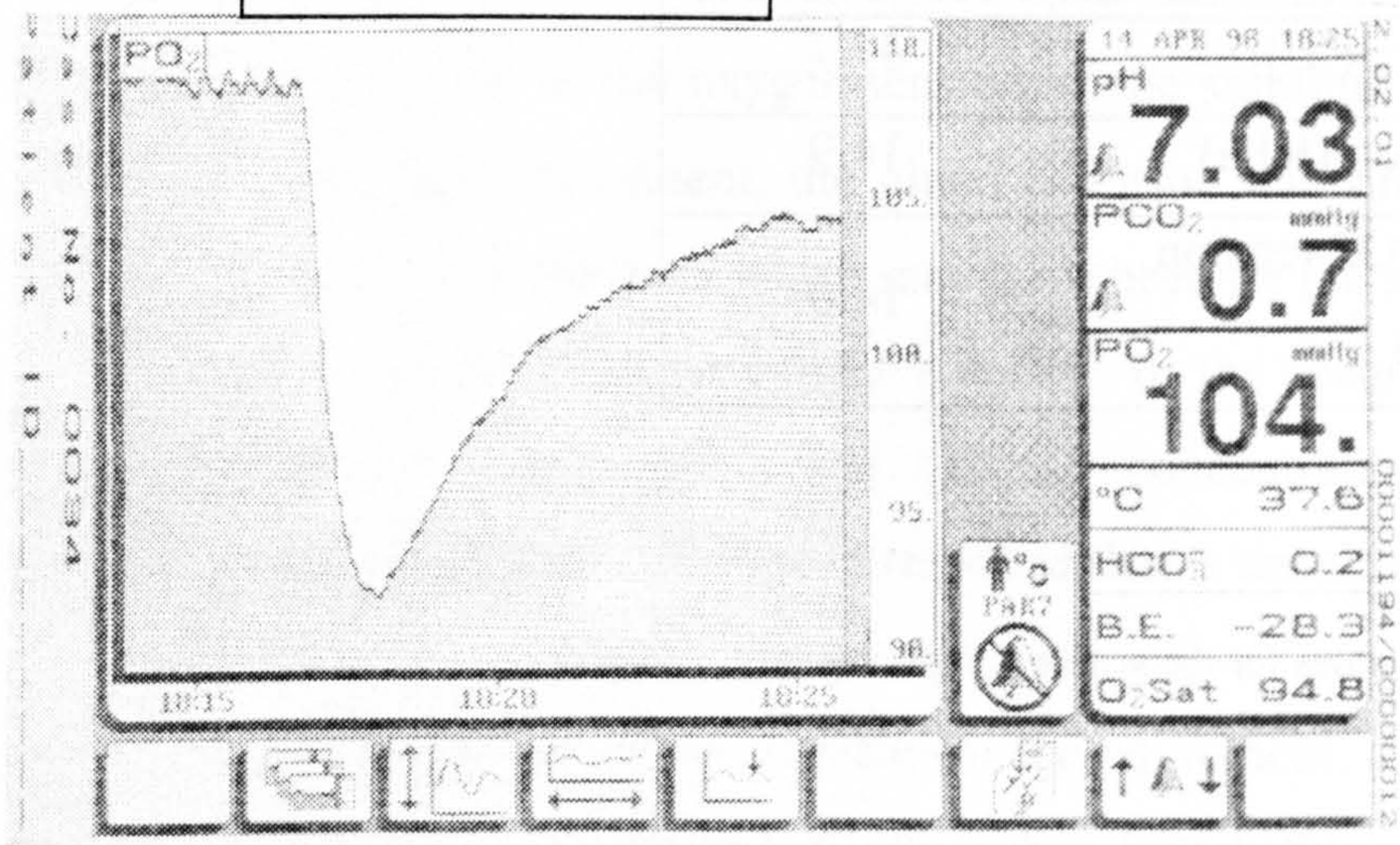

Figure 29. The response of the glucose Sensor 4 and the reference oxygen sensor

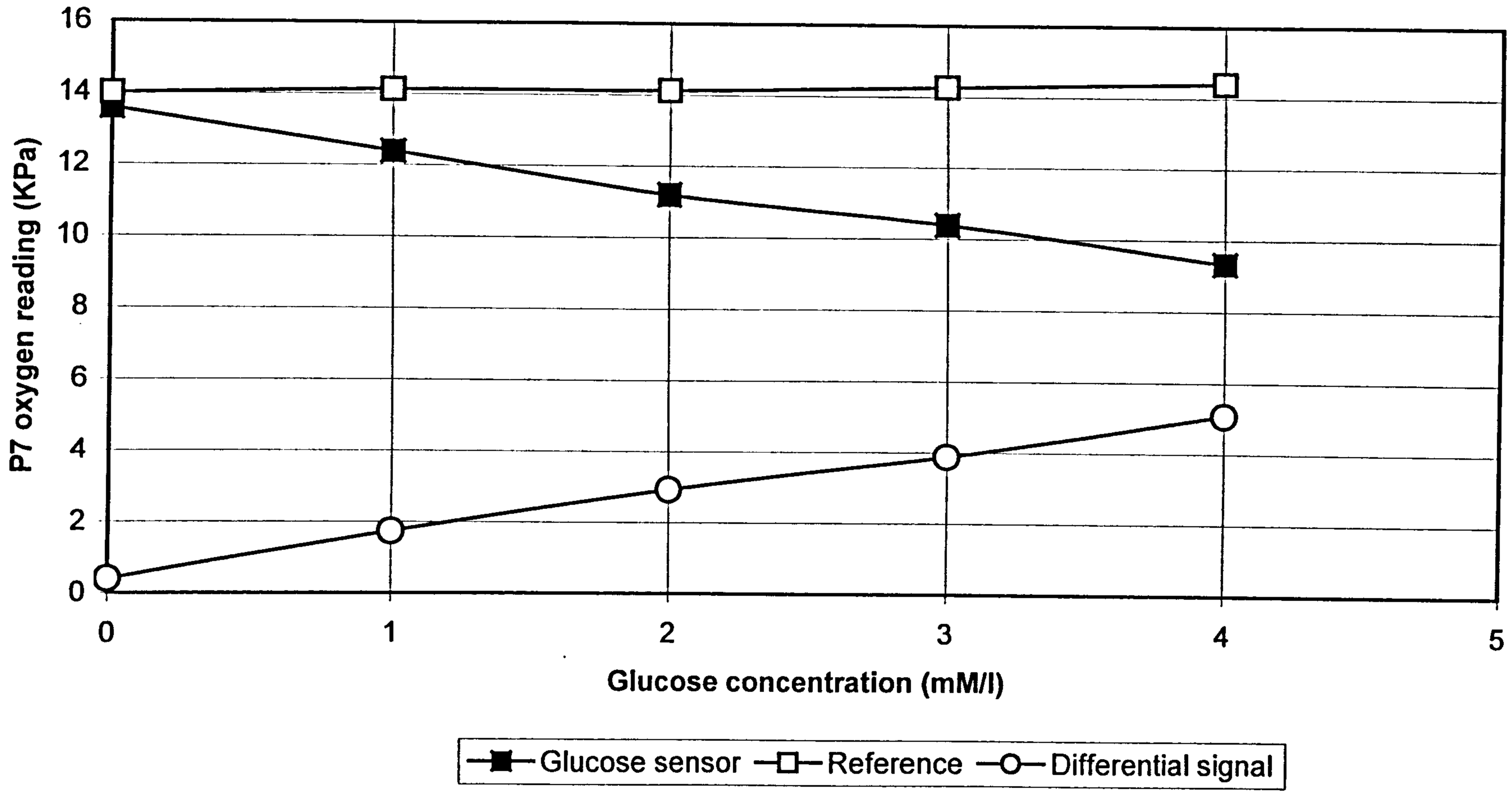

Figure 30. The response of the glucose sensor after rinsing with PBS with the reference oxygen sensor

6.4.12. Conclusions of the membrane integrity experiment

After washing, the sensor with PBS, the reference oxygen sensor showed no detectable GOD activity. This suggests that the GOD, which had entered the solution in the first test of Sensor 4, had not leached out of the sensor but instead had washed off the surface of the sensor. The washing of the sensor with PBS removed this loose GOD. Therefore, more thorough rinsing of the sensor than used previously should prevent this error occurring.

6.5 A differential oxygen measurement glucose sensor of reduced size

As the sensor measures glucose through the depletion in oxygen, background oxygen fluctuations could introduce an error in the measurement, see Chapter 3. To solve this problem a differential sensing system can be used. A differential measurement system takes two simultaneous measurements, one of the property being measured and a second reference measurement of the environment. By using the difference between these two values any environmental affects will be removed (Skoog and Leary 1992). This type of sensor uses a GOD coated oxygen sensor to detect glucose and a second reference oxygen sensor to measure the background oxygen tension. By calculating the differential signal between the two sensors, any background oxygen fluctuations will be cancelled out and the difference in the two signals will be exclusively due to the concentration of glucose. This will create a sensor insensitive to oxygen tension changes in the environment, provided those changes do not reach a value so low that the sensor is deprived of oxygen and can no longer function. The use of the differential oxygen signal introduces another source of error in the measurement. As there are now two oxygen sensors involved in each single measurement of glucose the uncertainties in each sensor measurement will contribute to the final uncertainty in the glucose value.

In addition to the use of reference oxygen sensor, the design was also improved by miniaturising the sensor. Having demonstrated, using Sensors 1 to 4, that the fundamental design of the glucose sensor was sound, the design was improved by coating on the EH directly onto the PO2 sensor rather than onto the surface of the whole P7 sensor bundle. This would allow the construction of a much smaller sensor that could be incorporated into an MPHF sleeve along with a second oxygen sensor.

These two improvements were now possible because a variant of the P7 sensor which possessed two oxygen sensors rather than the pH, CO_2 and O_2 sensors of the standard design that had become available. The initial sensor design involved dip coating a PO2 sensor into EH solution in the same way that the whole P7 sensors were dip coated in the previous sensors. The Diametrics production facilities had become temporarily available, allowing the PO2 sensor to be coated and then placed inside the MPHF sleeve as shown in figure 31. Previously the PO2 sensors had not been coated directly with EH. This was because cutting open the MPHF sleeve of the P7 would almost certainly result in damage to one or more of the sensors causing the P7 software to reject the sensor and stop functioning. However, with the P7 fabrication facility at our disposal it was possible to coat the PO2 sensors before they were inserted into the MPHF sleeve.

The GOD loading of these mixtures was increased from the previous experiments in an attempt to improve the longevity of the sensor, as the previous sensors had shown limited operational lifetimes. By having excess enzyme in the membrane layer, it was hoped that enzyme deactivation would take longer to affect the sensors performance. Initially, one of the oxygen sensors was dip coated in a HEMA, GOD and CAT mixture consisting of 60 mg of GOD and 60 mg of CAT dissolved in distilled water. This was mixed with 0.5ml of the HEMA solution containing 100mg/ml of HEMA dissolved in 75% ethanol balance. Once coated, the PO2 sensor was then put through the Diametrics production line used to build its standard P7 sensors. This resulted in the GOD coated sensor and an uncoated PO2 sensor being enclosed in MPHF and Acrylimide as in figure 31.

Sensor 5, was then tested in PBS equilibrated at 15% oxygen 7% CO_2 and 78% nitrogen (the standard P7 calibration gas mixture). The oxygen sensors were calibrated manually using a research and design (R&D) variant of the P7 software, which allowed the sensor to be calibrated outside the normal calibration chamber of the P7. Calibration was instead carried out in three tonometers in a water bath, each equilibrated with one of the three calibration gas mixtures and maintained at 37°C.

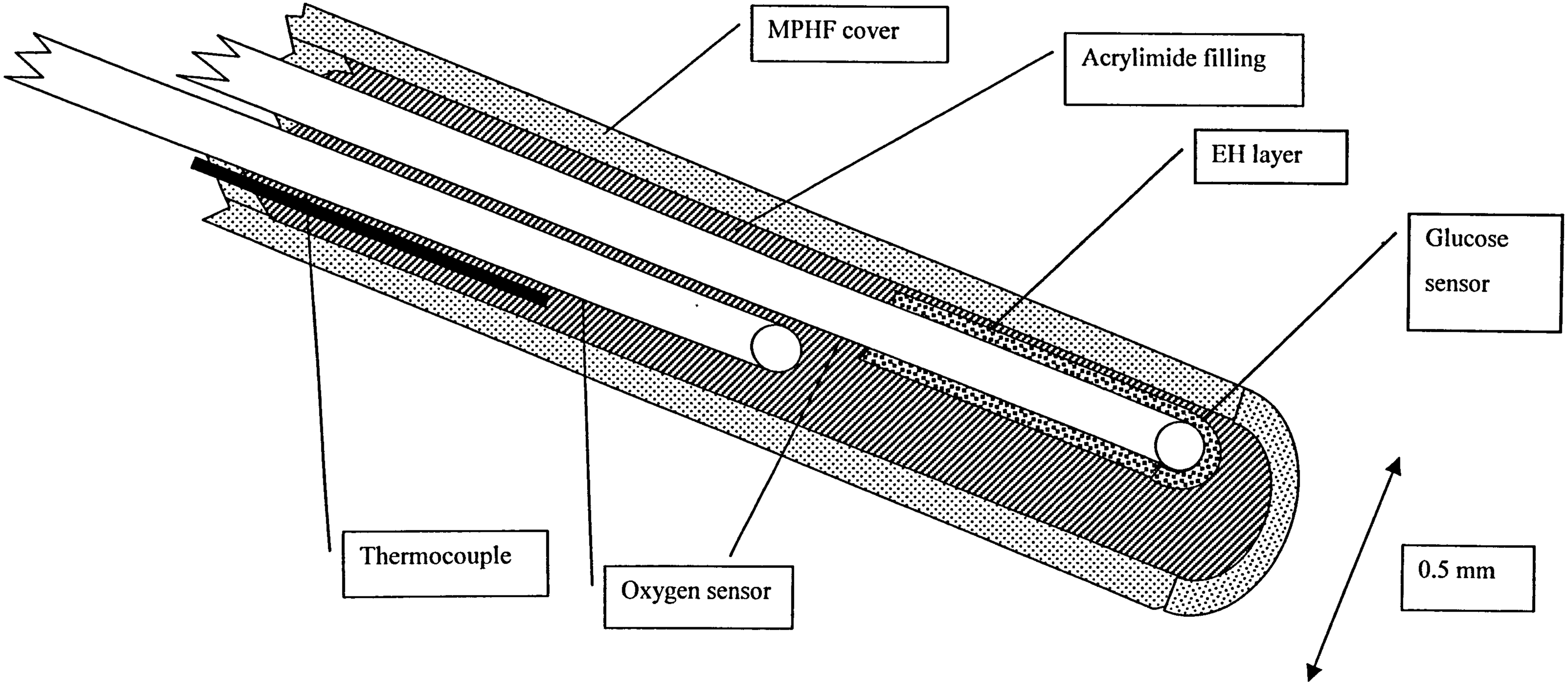

Figure 31. The duel oxygen sensor converted to detect glucose

6.5.1. Response of Sensor 5 to glucose in solution

As can be seen in figure 32, no response was seen for increases in glucose concentrations from 0 to 1mM/l. The glucose concentration was then increased up to 12 mM/l but still no response was seen from the glucose sensor.

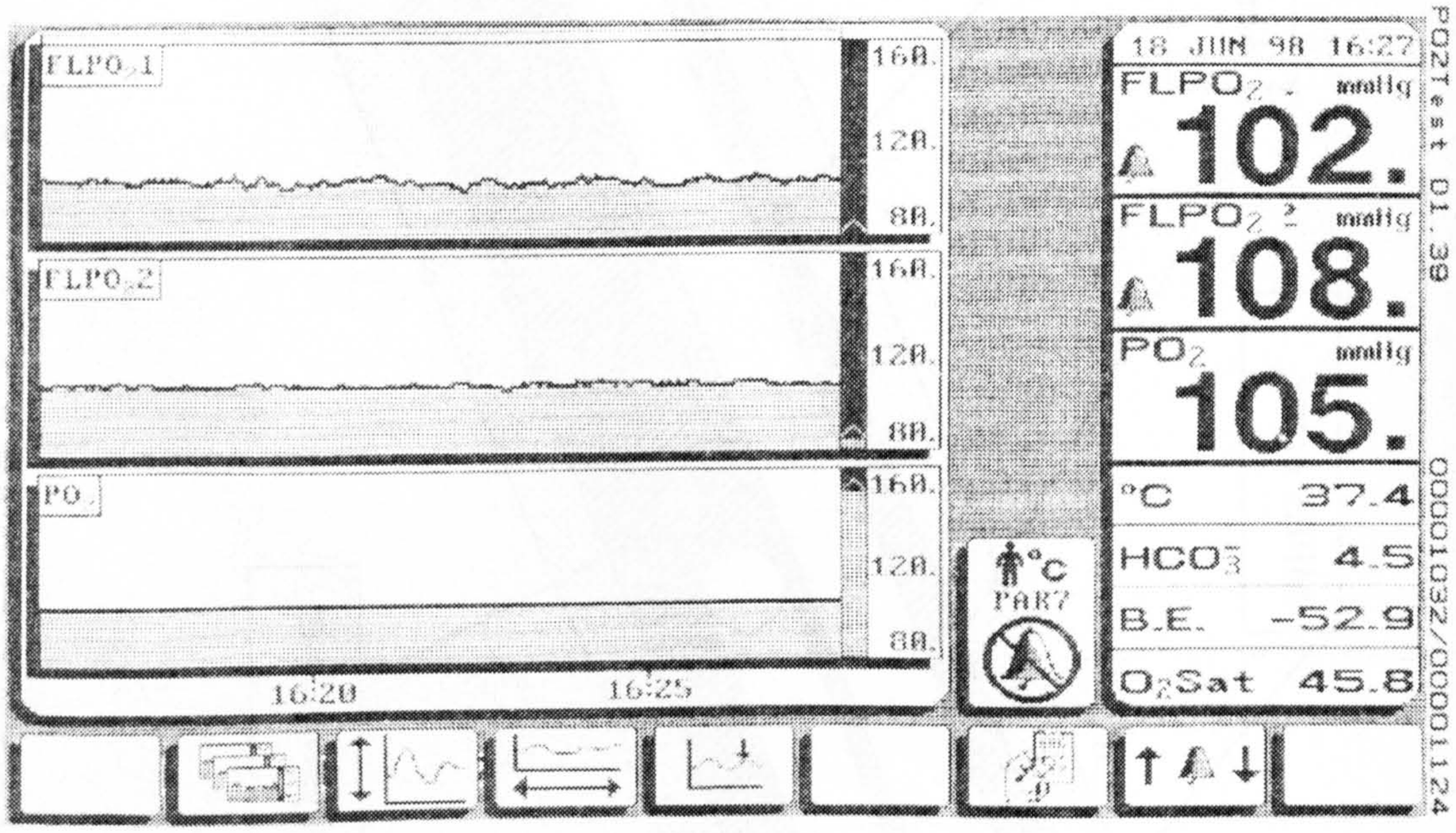

Figure 32. The first test of the duel sensor with its MPHF sleeve intact the glucose step was from 0 to1 mM/l.

6.5.2. Reasons for the failure of Sensor 5.

The failure of the sensor has several possibilities;

a) The enzymes have been destroyed by heat or chemicals used in the P7 sensor fabrication procedure.

b) The GOD had been washed away during the production process, as the sensors were rinsed to remove chemicals used in production.

c) The EH layer was so thin that oxygen could easily diffuse into the layer and replace that used up in the oxidation of the glucose.

Before points (a) and (b) could be investigated, it had to be shown that coating the PO2 sensor with EH would produce a working sensor. This was not certain, as the previous sensors had possessed EH layers covering the MPHF sleeve. Firstly, this was much larger than the PO2 sensor, 0.5 mm diameter compared to 150μm respectively, which meant that much more GOD was present in the larger sensors. Secondly, the EH readily adhered to the MPHF material, allowing uniform layers of EH to be built up. In comparison, the coating of the PO2 sensor caused irregular layers to form on the sensor when it was dip coated. Unfortunately there was insufficient time to create new sensors as the production of the sensors took 12 hours and the Diametrics fabrication facility was no longer available. It was decided that the MPHF sleeve could possibly be removed from the P7 without destroying the PO2 sensor.

Using a digital capture microscope, the MPHF sleeve and acrylamide filling of Sensor 5 were removed and the oxygen sensor was re-coated with the same EH mixture. After several attempts, a mass of HEMA and enzyme was built up on the end of the sensor over the five dye filled holes, using a 'painting technique' which involved using a piece of wire to apply the EH to the sensor, as shown in figure 33. This mass was approximately five times the diameter of the fibre and highly irregular in shape (many times the thickness of membrane deposited in the first

experiment). The sensor was then calibrated and re-tested. A second normal P7 sensor was also used as an external oxygen reference to monitor the oxygen tension of the tonometer solution.

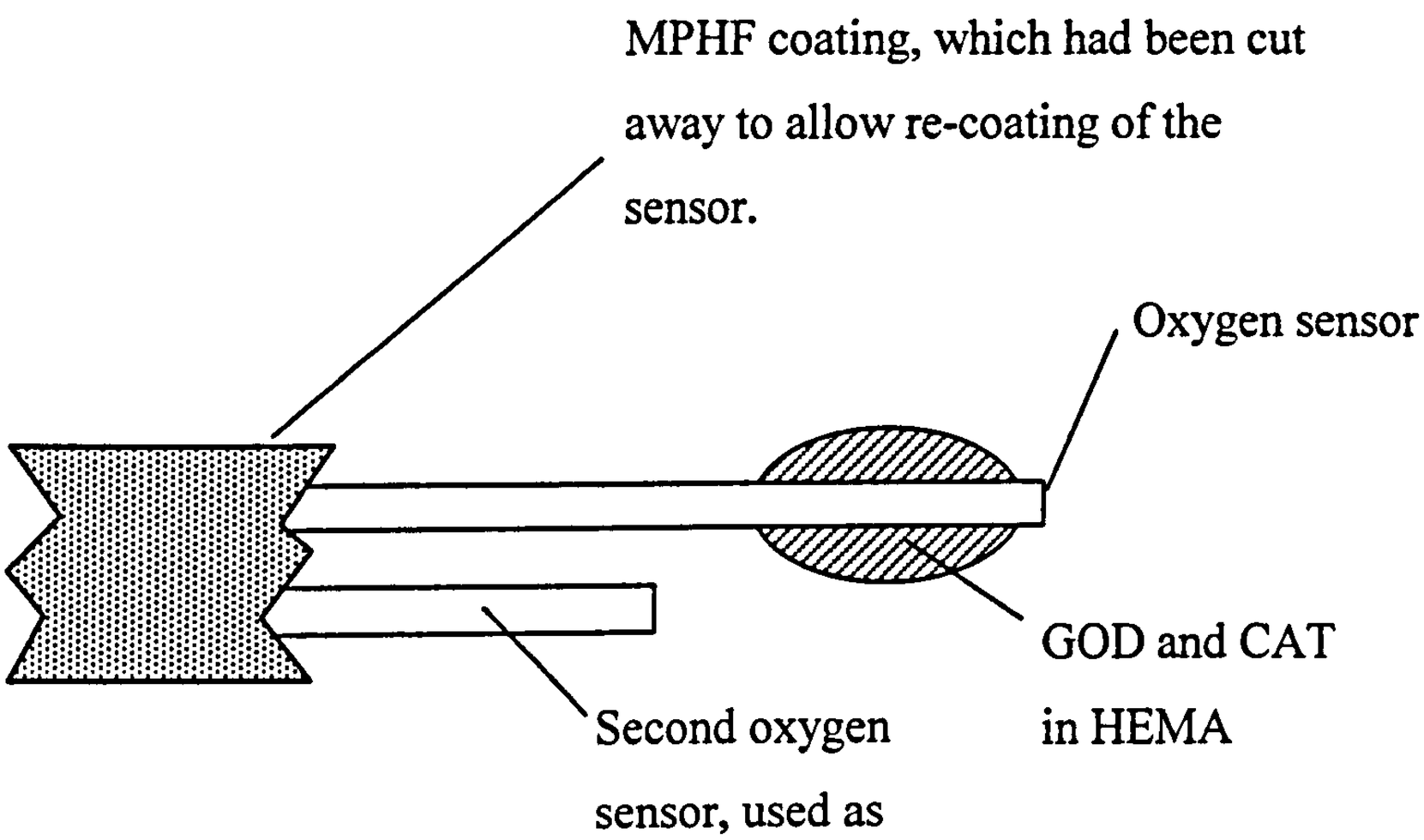

Figure 33. The sensor with the MPHF removed and the primary oxygen sensor coated with EH

6.5.3. Performance of the re-coated differential oxygen sensor

After re-coating, the sensor showed a response to glucose concentrations of up to 3 mM/l, with no cross-talk between the glucose and oxygen sensors despite the close proximity (≈10 mm), as shown in figures 34, 35 and table 18.

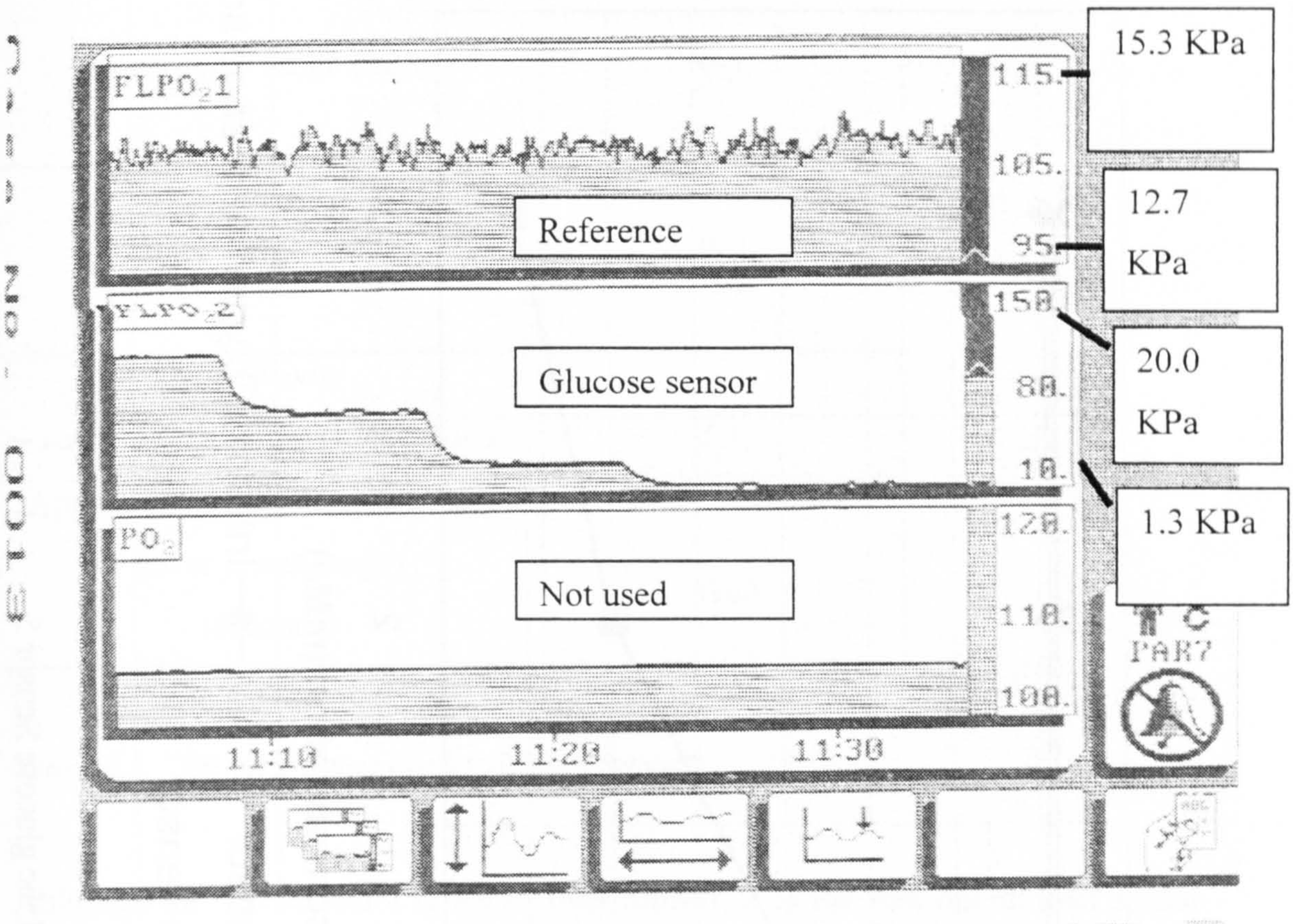

Figure 34. The response of Sensor 5 after being split open and re-coated.

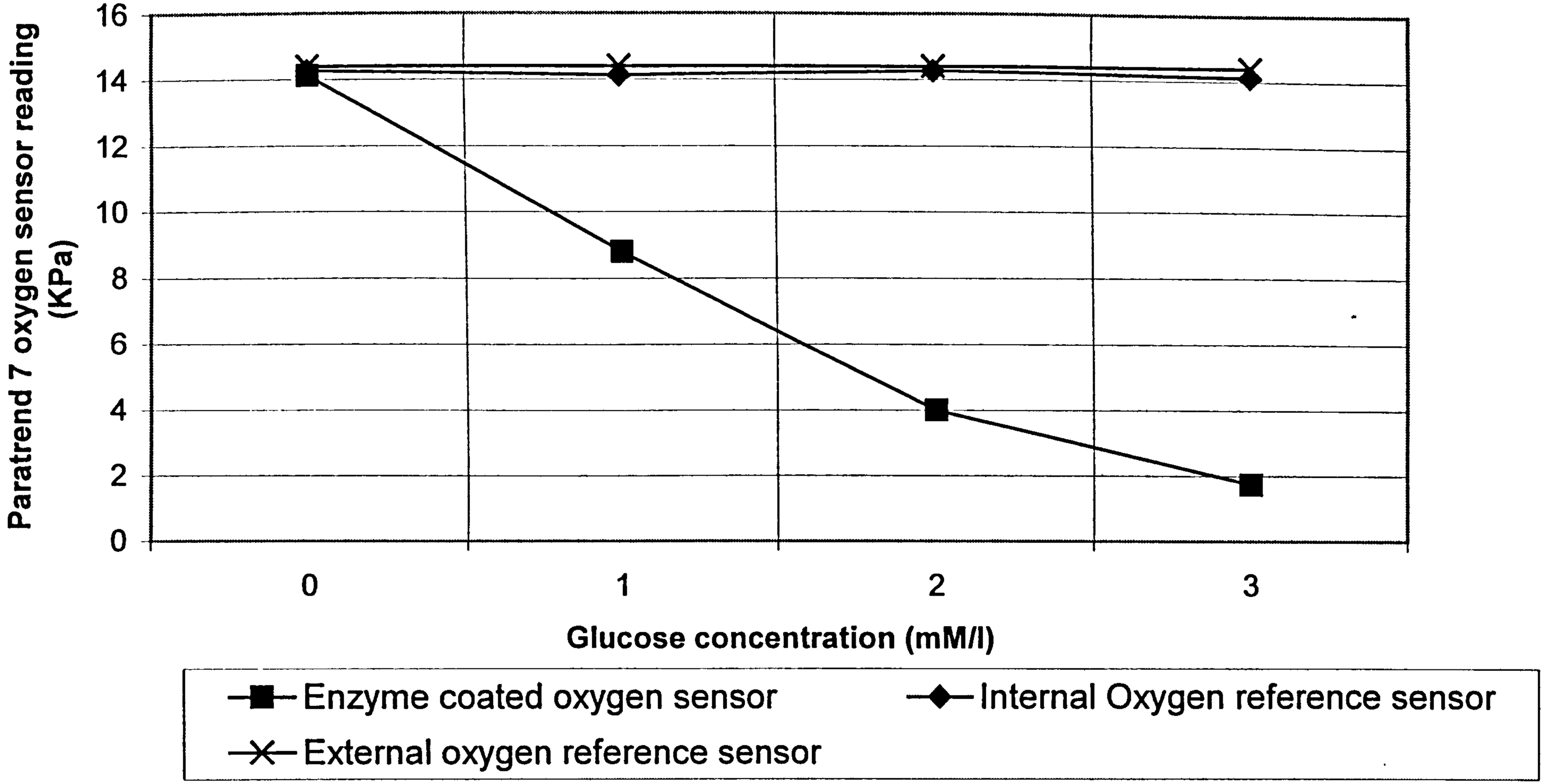

Figure 35. The response of the two oxygen reference sensors and the glucose Sensor 5

Operational range (mM/l)	0-3
Linear range (mM/l)	0-2
Sensitivity (over linear range) (KPa/mM/l)	5.1
Approximate 90% Response time (over linear range) (seconds)	<100

Table 18. The performance characteristics of Sensor 5.

Although the sensor had a range of only 3mM/l, it is the first operational sensor constructed by coating the oxygen sensing fibre directly with EH. The two oxygen sensors act as a reference, showing that the oxygen changes are localised to the sensor and are not a result of GOD leaking into the tonometer solution. To increase the range of the sensor will require outer diffusion limiting membranes or a change to the EH layer dimensions or consistency.

6.6 A P7 oxygen sensor coated with HEMA entrapped GOD and CAT in an MPHF sleeve

From the previous experiment, it was evident that the GOD, CAT and HEMA mixture did not readily adhere to the silicone carbinol coating of the oxygen sensor. Due to this problem, the dip coating technique, used in Sensors 1 to 4, was not an option for coating the PO2 sensor directly. A possible alternative was to provide a support to hold the HEMA and enzyme in place on the PO2 sensor until it had dried. A section of MPHF tubing used in the P7 construction was thought to be a good candidate, as its pore filled structure would provide a diffusion-limiting layer to reduce the glucose flux and the material is biocompatible. The construction and sensor design is shown in figures 36 and 37. As the front and rear ends of the sensor will not be covered with MPHF, the glucose will be able to diffuse freely into the sensor from the front or rear ends of the MPHF tube. Glucose should also be able to diffuse into the sensor through the MPHF tube, although the flux will be reduced as the glucose can only diffuse through the pores of the MPHF. This will make a radially-symmetric design sensor similar to that built by Gough, Lucisano et al. 1985; Gough, Armour et al. 1986 described in Chapter 2.

6.6.1. Construction and testing of Sensor 6

A P7 sensor, previously split open and the MPHF and acrilyimde filling removed, was used to construct the glucose sensor. The P7 oxygen fibre was isolated from the other three sensors and a section of MPHF tubing (pelathane 400μm outside diameter, wall thickness of 20-25μm and 20% porosity) was placed over it. The space between the MPHF and the oxygen sensing fibre was then filled by placing the fibre end into an EH mixture, see figure 36. Capillary action drew the EH mixture into the space between the MPHF and the sensor. This mixture consisted of 60 mg GOD and 60 mg of CAT dissolved in 0.5ml of distilled water. It had

been decided to increase the enzyme loading of the sensor to further ensure an excess enzyme. It was hoped that this would allow the sensor to operate in a diffusion-limited mode, even after operation for 12 hours. This solution was mixed with 0.5 ml of 100 mg/ml of HEMA in a 75% ethanol and distilled water solution. Later 1ml of 90% ethanol was added to this mixture to lower its viscosity, so that it would move into the MPHF more easily. It should be noted that some of the EH mixture coated the exterior of the sensor.

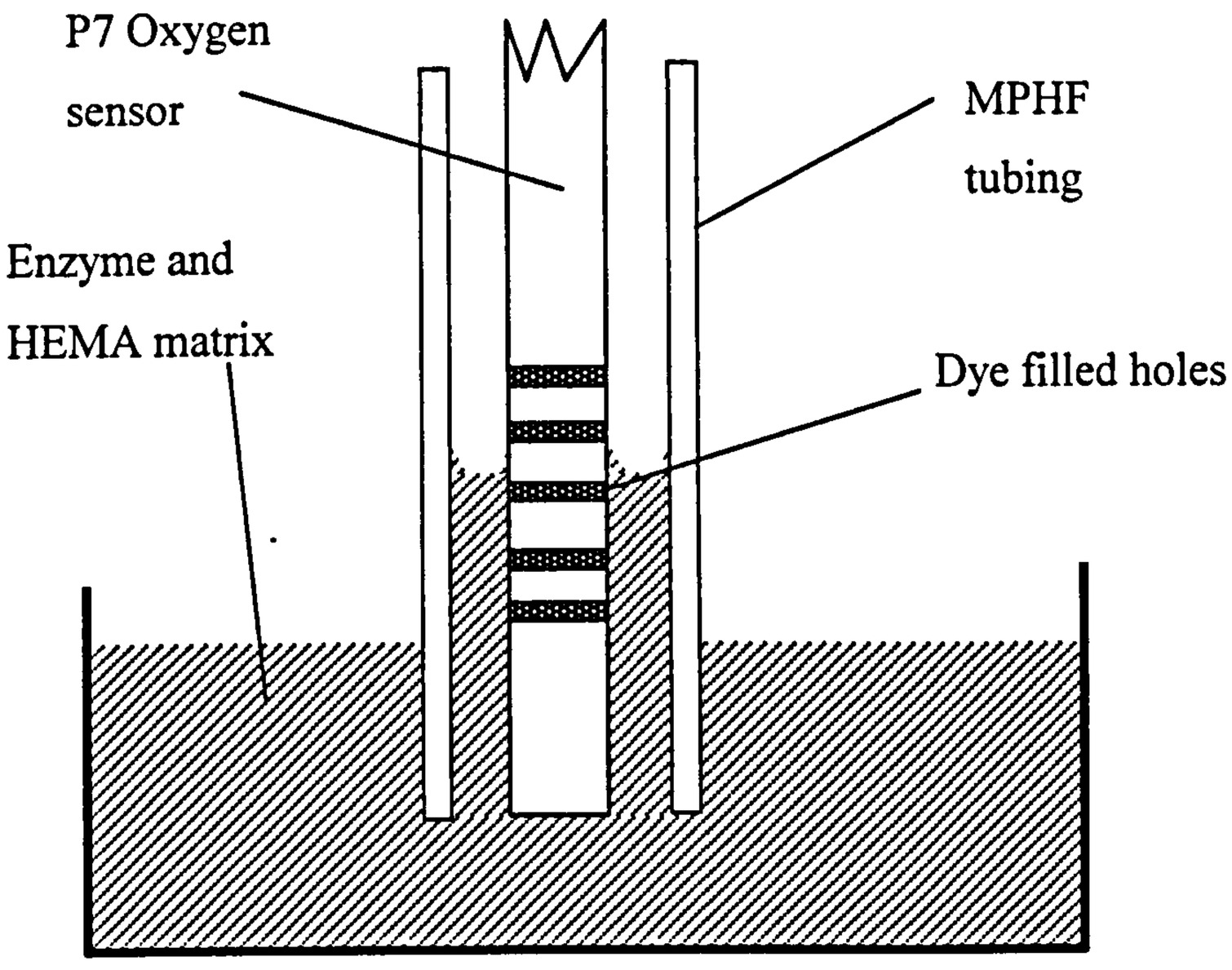

Figure 36. Construction of Sensor 6 using capillary action.

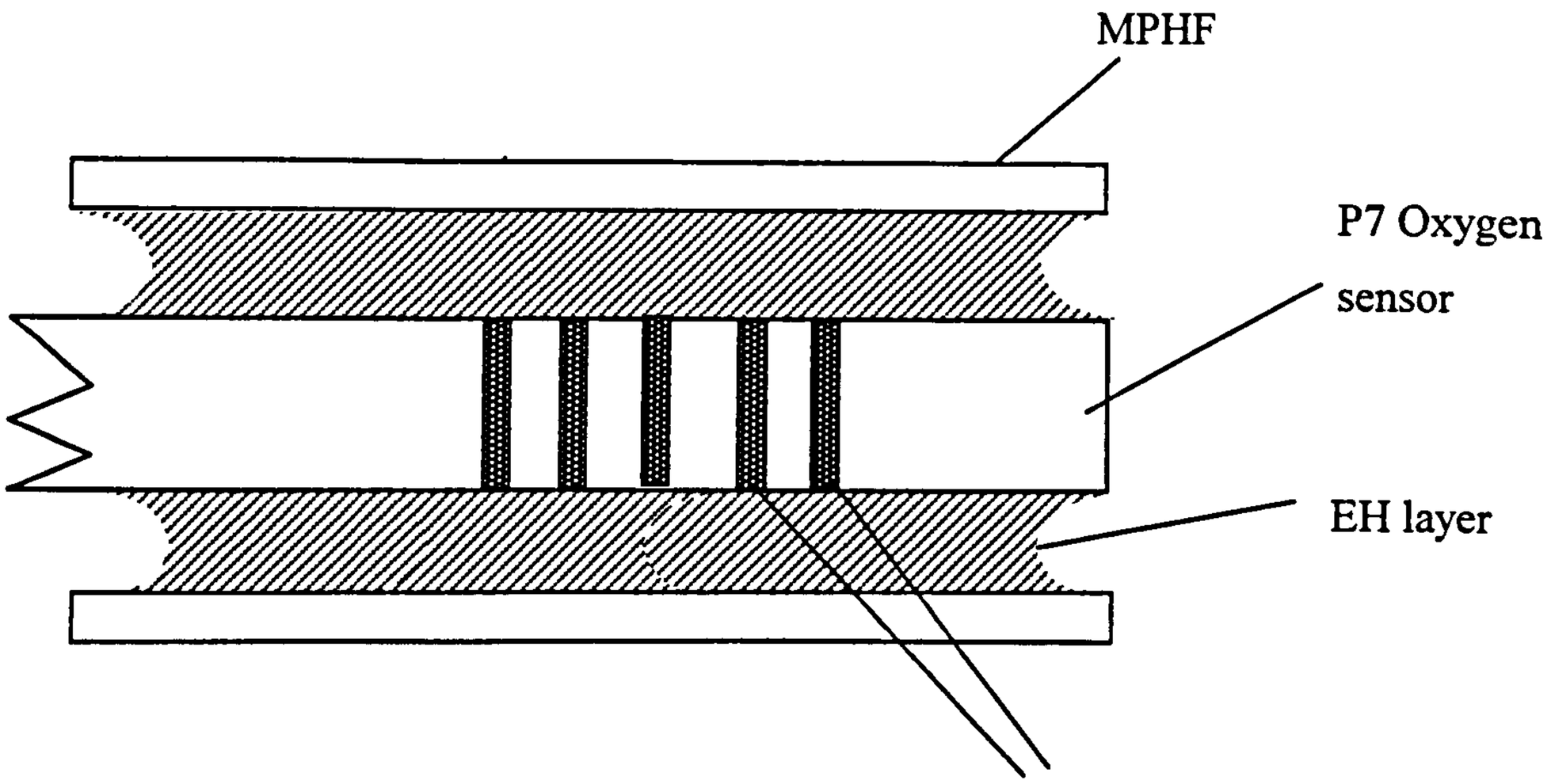

Figure 37. The design of Sensor 6; an oxygen sensor coated with an enzyme –HEMA matrix and with an outer MPHF cover.

After construction, the sensor was placed in a beaker of PBS and left for approximately one hour, after which it was thoroughly rinsed with PBS to remove any loose enzyme. The soaking procedure was to improve the removal of any loose enzyme or enzyme leaching out of the EH layer. The sensor was then manually calibrated using the R&D software now installed on the P7 system. This allowed the sensor to be calibrated using tonometers in the water bath which were aspirated with the calibration gas mixtures. This removed the need to either calibrate the sensor before enzyme coating or attempting to re-insert the sensor into the P7 calibration tonometer, a process that often caused sensors to break. By calibrating after coating the sensor, any changes caused to the performance of the oxygen sensor would be taken into account by the calibration.

6.6.2. Performance of the MPHF coated sensor

Figure 38 shows the data captured from the P7 via a serial port connection using software written for the task, which is described in Appendix A. The resolution of the data is slightly less than that displayed on the P7 plots for reasons discussed in Appendix A. This was a built feature of the P7 base unit and could not be changed. However, the ability to continuously take measurements and insert time flags when glucose was added or dilutions made was thought to outweigh this small resolution loss. Glucose was added to the tonometer to raise the concentration in steps of 2 mM/l, as it was wrongly assumed that the MPHF would create a sensor to have a large range by virtue of its diffusion characteristics. However, the full range of the sensor was reached in the first glucose step, as can be seen in figure 38. After the full range had been reached at the appropriate temperature and oxygen tensions PBS was added to the tonometer to lower the glucose concentration to 0.25 mM/l, the maximum dilution that could be achieved with this tonometer volume. The experimental conditions and performance characteristics of the sensor are shown in table 19 and 20 respectively.

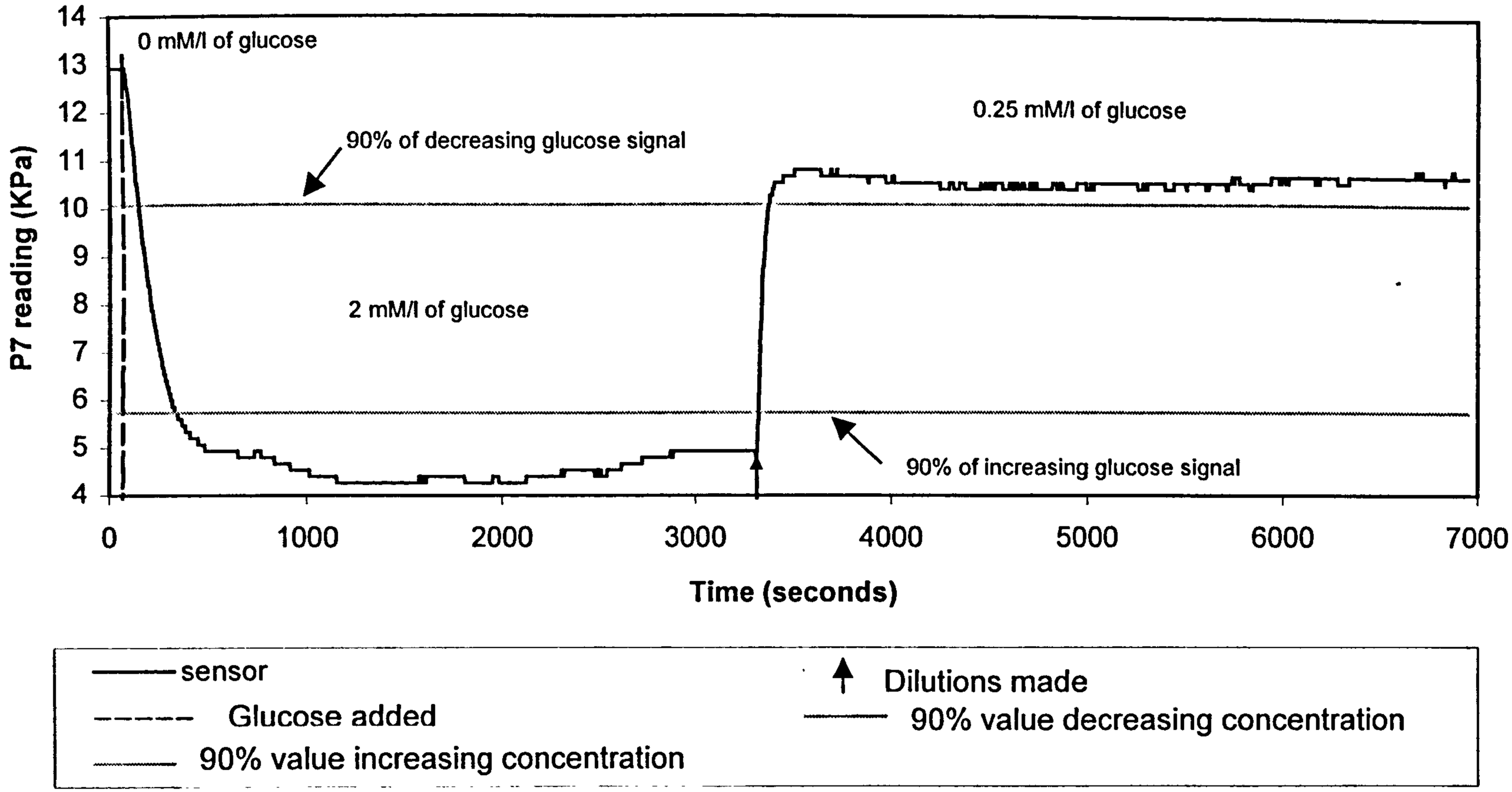

Figure 38. The data captured from the P7 during the tests of Sensor 6

Atmospheric pressure (KPa)	100.9
Temperature (°C) .	39.3
Dry PO2 tension (KPa)	15.2
SVP corrected PO2 tension (KPa)	14.0

Table 19. The SVP corrected oxygen tension and temperature of the tonometer solution used in the experiment

Operational range (mM/l)	2
Linear range (mM/l)	N/A
Sensitivity (over linear range) (KPa/mM/l)	4
90% Response time (over linear range for increasing concentration) (seconds)	100 to 200
Approximate 90% Response time (over linear range for decreasing concentration) (seconds)	<100

Table 20. The performance characteristics of sensor 6.

6.6.3. Conclusions of the MPHF sensor experiments

In figure 38, the response to both decreasing and increasing glucose changes can be seen to overshoot its final value and then return. This was thought to be due to the complex nature of the reaction-diffusion process in the EH membrane. A marked difference in the 90% response times between the increasing and decreasing concentration changes can be seen in table 20. This was attributed to the fact that when the concentration is increased only a small amount of 1M glucose solution is added to the tonometer, typically 100µl to 50ml. This then has to diffuse throughout the tonometer to affect the concentration near the sensor, which may take several seconds, even though the solution is effectively stirred by the gas perfusion. However, when a dilution is carried out the volume of PBS in the tonometer, in this case, increased form 25ml to 100ml. The extra 75ml will have a much faster effect on the sensors' environment compared to the glucose solution.

Both the increasing and decreasing response times are much shorter than the 180 seconds stated earlier for the P7 sensor. This is due to the conservative values quoted by Diametrics Medical Ltd for their sensor to avoid the possibility of making false performance claims about the sensor. Also the HEMA may have less diffusion coefficients than acrylimide. The use of the MPHF left little room for control of the EH and dimensions. If a dip coating technique could be developed to coat the PO2 sensor, this would allow smaller sensors to be made and the control of the EH thickness could be used to construct a sensor of the appropriate response parameters. The manual calibration had caused errors as can be seen in figure 38 and table 19. Both SVP and the uncorrected values are different from the oxygen reading of the sensor. However, this may be a result of calibrating PO2 sensors with no acrylimide or MPHF cover. So a new technique was still required.

With MPHF and the acrylamide removed from the sensor, the oxygen sensor would equilibrate more quickly with the calibration gasses causing a difference in the calibration compared with a standard P7 sensor. If this equilibration time is taken into the account in the calibration algorithm, this would create an error. The coating technique used in Sensor 7 left the pH, temperature and CO_2 sensors exposed and made the sensor virtually impossible to re-insert into the calibration tonometer and made them vulnerable to being damaged.

6.7 An improved method for coating the PO2 fibres in enzyme

Several methods of applying the EH coat to the oxygen sensing fibre were considered and attempted on sections of PO2 sensors cut from the previously used sensors. After trial and error, a painting technique, was developed, similar to that used to coat Sensor 5. This involved using a piece of fine copper wire to apply the EH mixture to the oxygen sensor. In this way, a thick but irregular layer of EH could be coated directly onto the oxygen sensor.

Several P7 sensors had their MPHF sleeves removed at the Diametrics facility and were provided to investigate coating the EH directly onto the PO2 sensors. One of these sensors was used to develop the enzyme coating technique. The PO2 sensor was coated with a layer of EH as shown in figure 39. This was applied to the sensor over the dye filled holes in the oxygen fibre. The enzyme mixture used contained 0.5ml of 63 mg of GOD and 63 mg of CAT dissolved in distilled water. This was mixed with 0.5ml of 100 mg/ml of HEMA in 75% ethanol solution. The layer deposited was highly irregular but did adhere to the silicone carbonyl coating of the oxygen sensor once the ethanol in the mixture had evaporated. The sensor was then soaked in PBS for around one hour and then rinsed repeatedly with PBS to remove any loose enzyme.

Once constructed the sensors were automatically calibrated in a modified P7 calibration tonometer. The neck had been widened to allow insertion of the three separate optical fibres and the thermocouple. The reason for returning to the auto calibration technique was to remove any calibration errors that could be introduced during the manual calibration as seen in the previous experiment.

The sensor was then tested for its response to glucose and its upper range found to be 8mM/l. PBS, at appropriate temperature and gas tensions, was added to the tonometer to lower the glucose concentration to 4 and then 2 mM/l.

The results are shown below in figures 40, 41 and table 22, the sensor exhibited hysteresis shown when the glucose concentrations were decreased. The maximum range of the sensor was only 8mM/l and the initial readings at zero glucose concentrations were below the SVP oxygen tension, indicating an error in the calibration despite the automatic calibration process that was used, see table 21.

A second P7 had become available for use on the research at this time; this was a variant of the P7 known as a satellite unit. The satellite system operated identically to the normal P7 except that it was unable to calibrate sensors lacking the calibration gasses and calibration chamber. This sensor was used as an oxygen reference to measure the oxygen tension of the test tonometer solution.

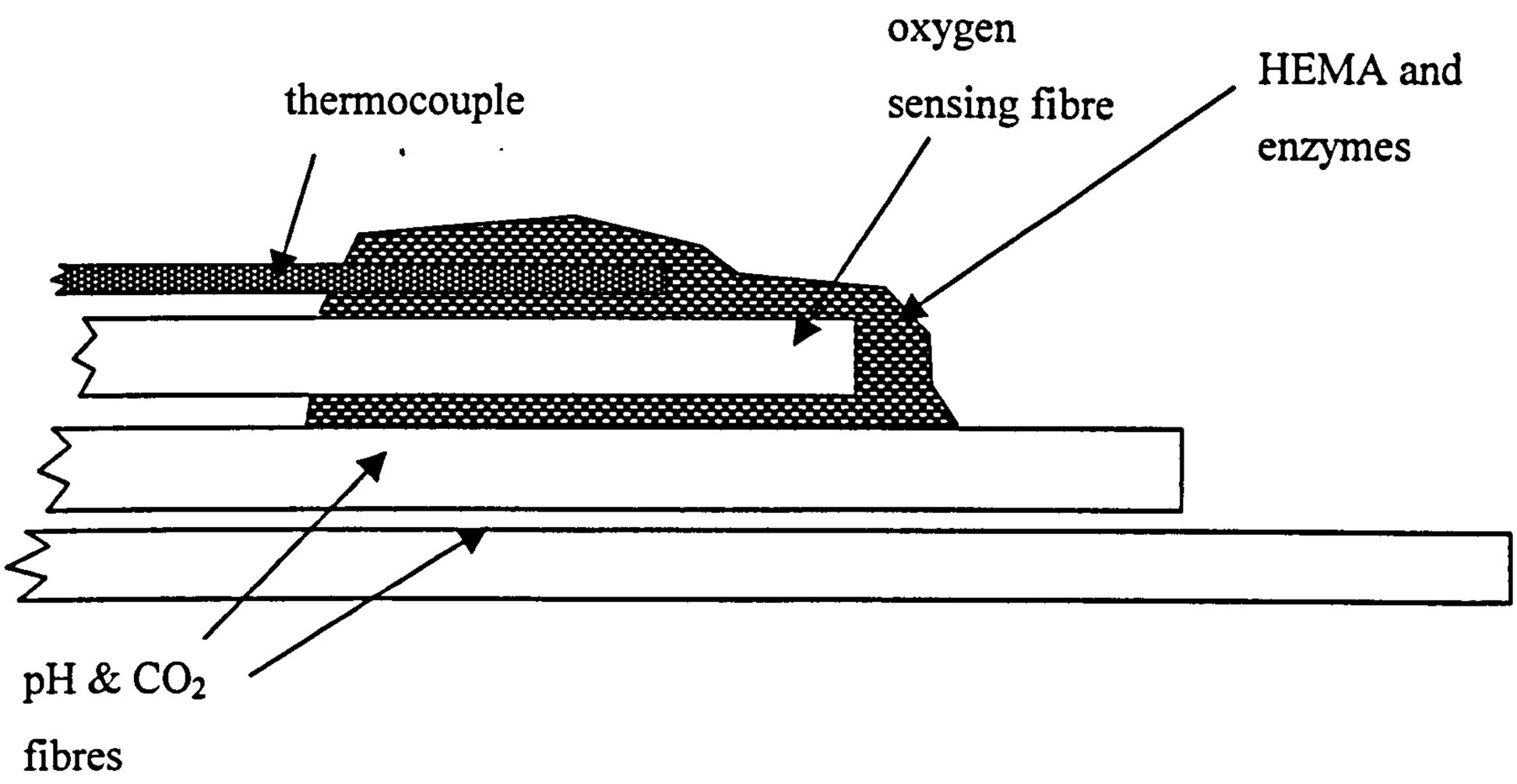

Figure 39. Sensor 7 created using the EH painting technique

Sensor 7 has a range of only 0 to 8mM/l but its sensetivity is very low only roughly (0.4 KPa/mM/l) at maximum. The 90% response times are approximately 45 seconds and this low sensetivity and short response time were probably due to the dimensions of the EH layer, which will define the response of the sensor. In this case, the EH was very thick around ten times the oxygen sensor diameter. With development of the coating technique, it may be possible to control the dimensions of the EH layer precisely enough to construct a sensor with greater range. It was noticed during the construction that the EH mixture would adhere to all four sensors due to capillary action. It was decided to use this process as a means to coat the sensors.

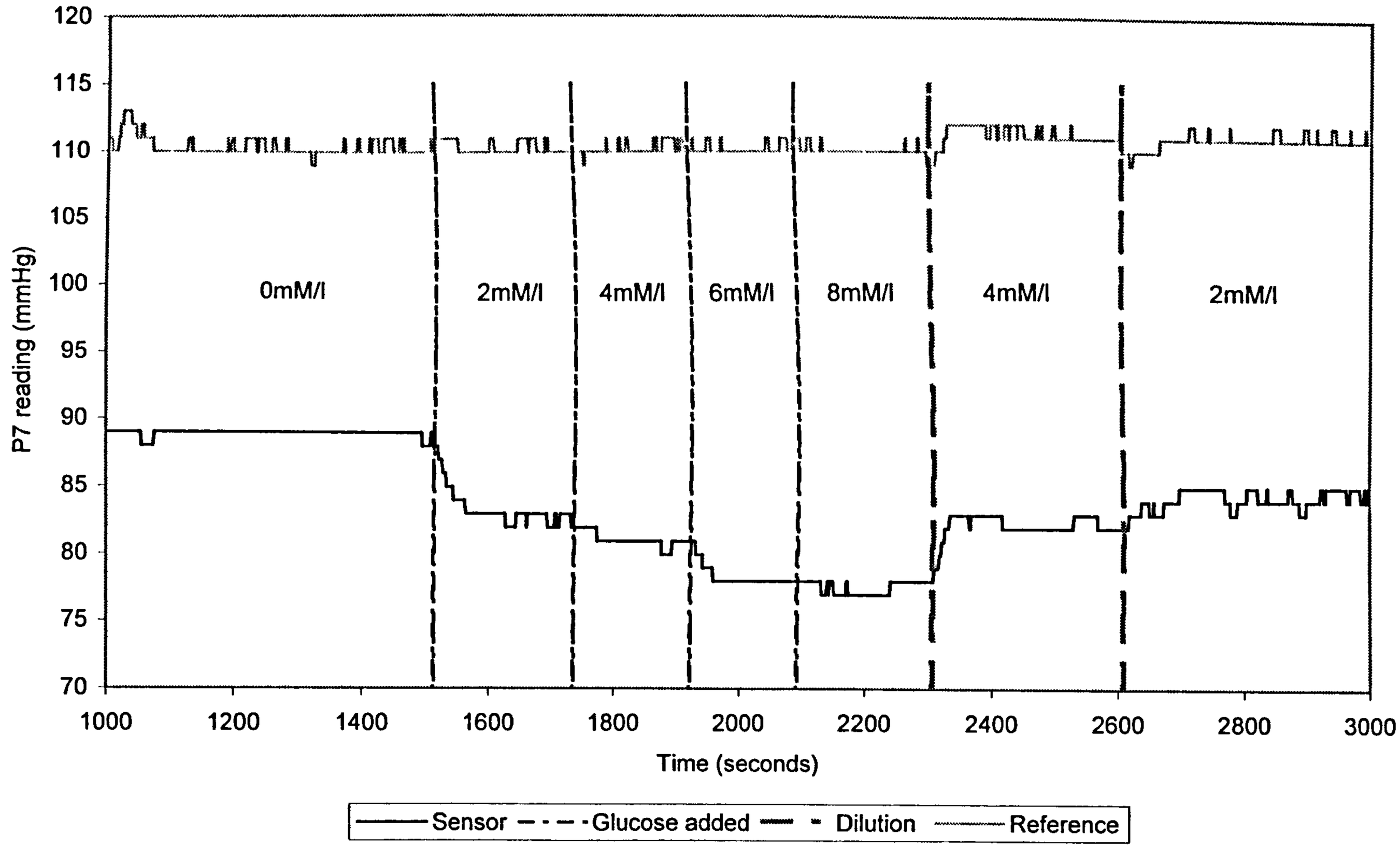

Figure 40. Graph of the performance of the Sensor 7

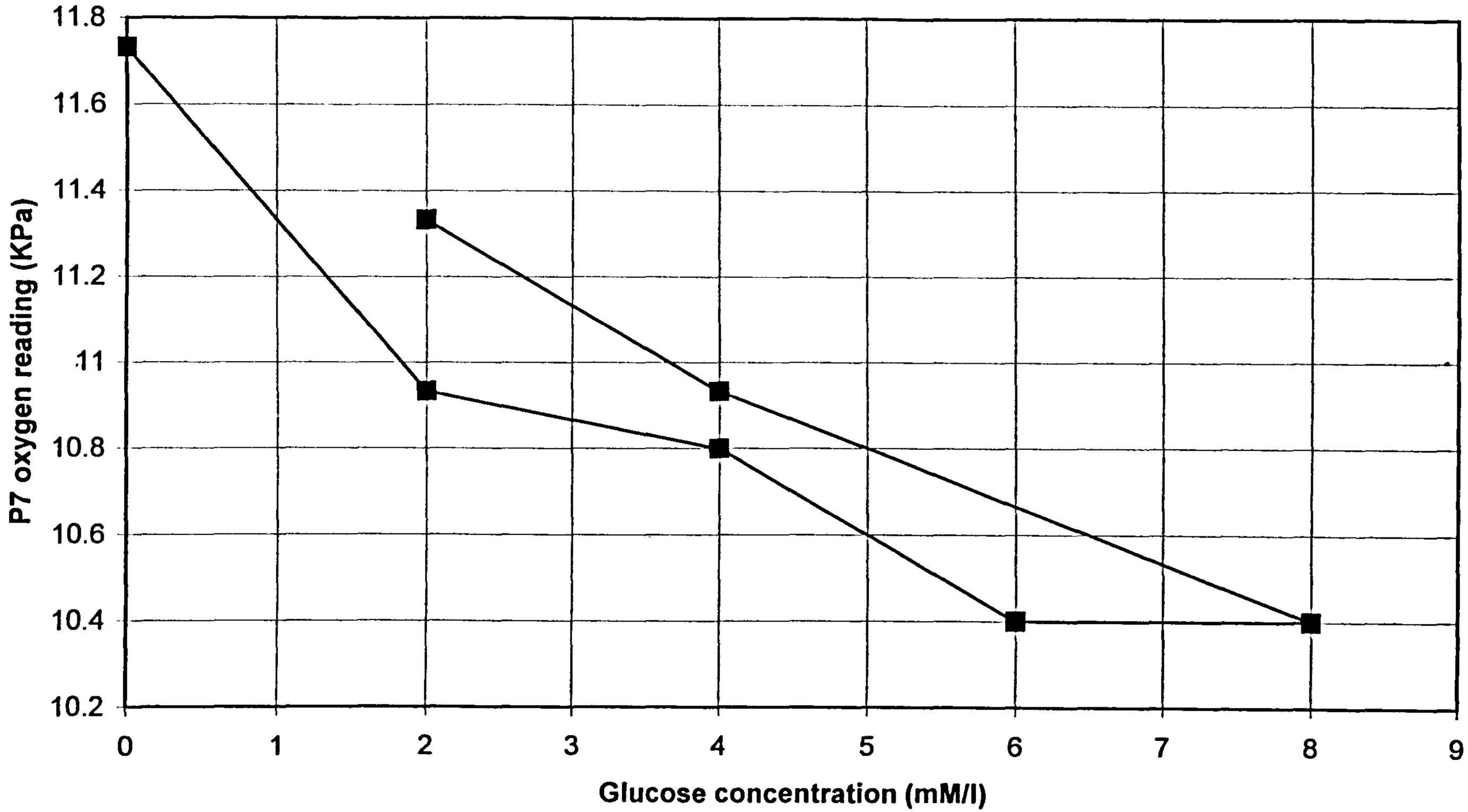

Figure 41. The response of Sensor 7 to glucose concentration changes

Atmospheric pressure (KPa)	100.3
Temperature (°C)	37.6
Dry PO2 tension (KPa)	15.0
SVP corrected PO2 tension (KPa)	14.1

Table 21. The SVP corrected oxygen tension

Operational range (mM/l)	6
Linear range (mM/l)	N/A
Sensitivity, increasing and decreasing. (KPa/mM/l)	0.05 to 0.4
Approximate 90% Response time For increasing and decreasing concentration (seconds)	<100

Table 22. The performance characteristics of Sensor 7.

6.8 PO2 oxygen fibres coated with GOD and CAT in a HEMA matrix cross linked with glutaraldehyde

The previous sensor coating technique had proved to be problematic and formed an irregular EH layer which was hard to control. In addition, it was noted that when coated the EH would flow around the other optical fibres probably by capillary action. It was decided to try an alternative design where all of the four sensors were dipped into the EH mixture. The capillary action effect would then help the EH to form a layer covering all of the sensors including the PO2 sensor, see figure 42. In this way, it was found that a regular layer of EH could be formed over the sensors. This approach had two advantages. Firstly, as the sensors were bunched together and enclosed in a layer of EH, they were far less likely to fracture during calibration or testing. Secondly, a dip-coating technique could be used with this approach, allowing much more regular controlled layers to be built up than with the painting technique used previously.

To further improve the stability of the EH layer, glutaraldehyde was used to cross-link the enzymes in the HEMA layer. It was hoped that this would give the sensors longer operational lifetimes by improving the resistance of the enzymes to damage or loss as discussed in Chapter 3.

Eight sensors (8a to 8h) were made using this new technique. P7 sensors, which had previously had their MPHF coating removed, were used in this construction. Following the removal of the MPHF coating the four internal P7 sensors were all dipped into the EH mixture, as shown in figure 42. This enzyme mixture contained 60 mg of GOD and 60 mg of CAT dissolved in 0.5 ml of PBS mixed with 0.5 ml of HEMA solution containing 100 mg/ml in 90% ethanol 10 % water.

The sensors were not stored in PBS as with previous experiments. Instead, the sensors were refrigerated, dry, overnight to avoid leaching out the enzymes into the solution. The following day. they were dipped in glutaraldehyde to cross-link the enzymes and improves the integrity of the EH layer. The sensors were then refrigerated again, dry. Dry storage was used as it was considered that this would limit chemical reactions taking place in the EH layer. It was hoped, therefore, that the sensor would not suffer degradation in storage. However, a problem with dry storage was that the HEMA layer would swell when placed in the PBS solution to be calibrated and tested. This may cause an error during testing as the dimensions of the EH layer changes over time. The sensors were stored for between 6 and 21 days before testing.

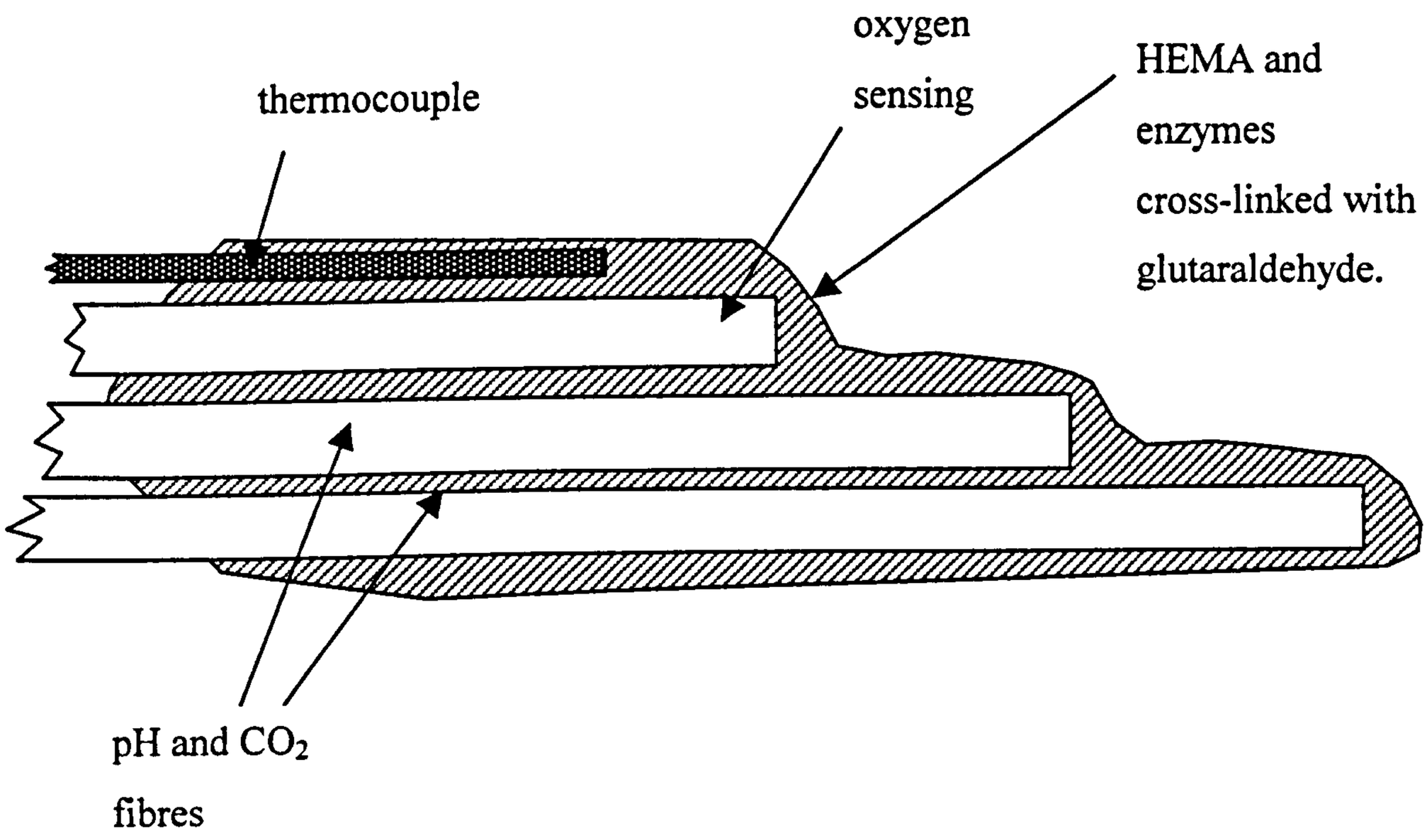

Figure 42. The layout of the enzyme based sensors 8a to 8h

The sensors were manually calibrated in the experimental tonometers, which, although possibly less reliable, reduces the amount of breakages that often occurred when sensors were inserted into the P7 calibration tonometers for automatic calibration. A standard P7 sensor was also calibrated and used as a

reference oxygen sensor in each experiment. The sensors were then tested as described previously.

6.8.1. The performance of the cross linked sensors 8a to 8h

The results of the tests sensors 8a to 8h are shown in figure 43 to table 23. After the test of sensor 8c the oxygen reference sensor failed and with no replacement available, the rest of the experiments 8d, 8e, 8f and 8g were conducted without a reference. The initial zero glucose oxygen values for all of the sensors except Sensor 8d are close or within the tolerance for a normal P7 sensor in that oxygen tension. The SVP for these sensors and from now on were not calculated, as the effect on the measurement was small, usually in the order of 0.5 KPa.

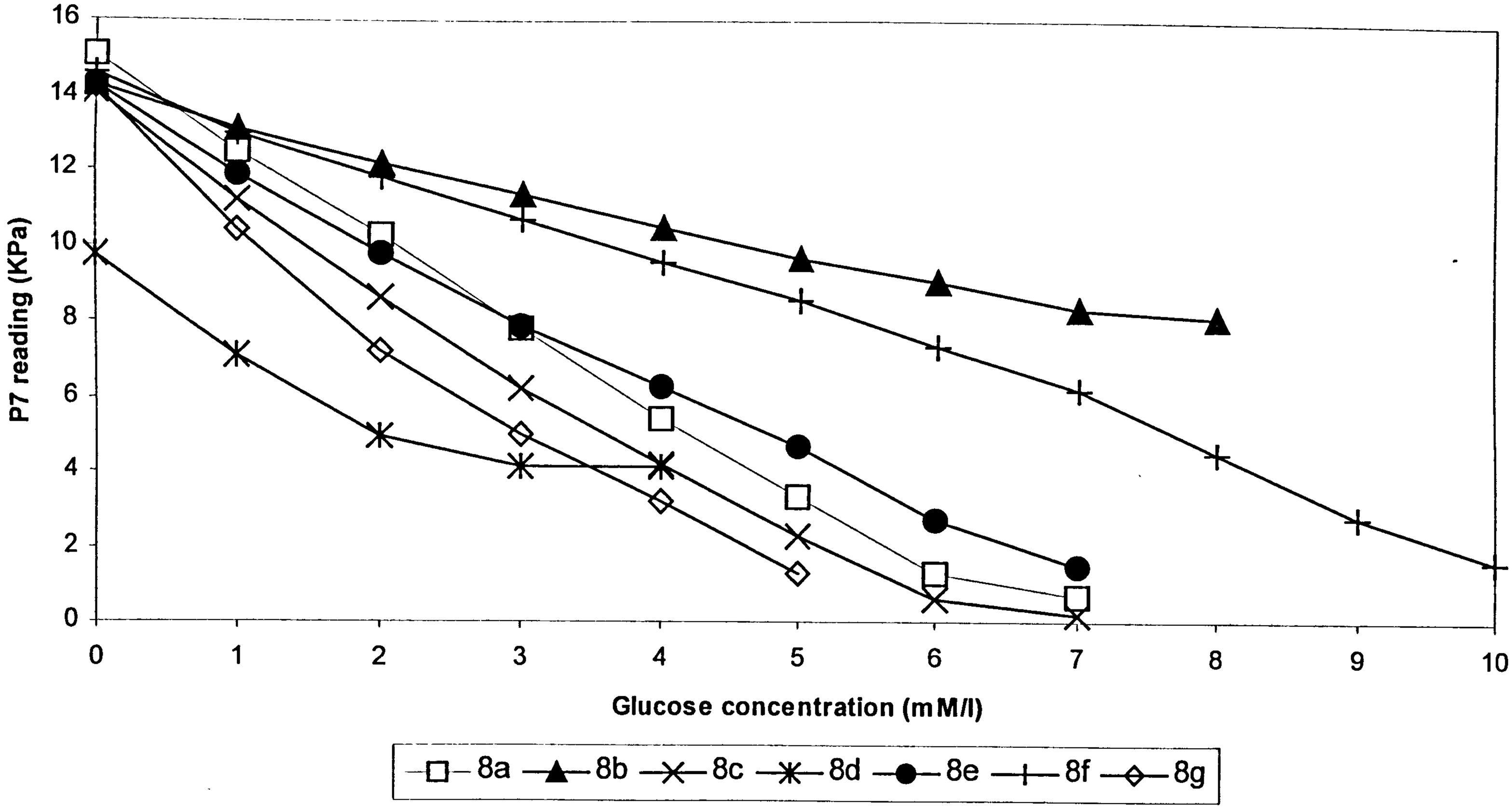

Figure 43. Plot of Oxygen tension against glucose concentration for Sensors 8a to 8g

Sensor	8a	8b	8c	8d	8e	8f	8g
Operational range (mM/l)	0 - 7	0 – 8	0 – 7	0 – 3	0 – 7	0 – 10	0 – 5
Linear range (mM/l)	0 - 6	0 - 7	0 - 6	0 - 2	0 - 7	0 - 10	0 – 5
Sensitivity (over linear range) (KPa/mM/l)	2.6	0.8	2.3	2.4	1.8	1.3	2.6
Approximate 90% Response time (over linear range) (seconds)	300 to 400	<100	300 to 400	200 to 300	100 to 200	200 to 300	100 to 200

Sensor 8h was excluded due to the large amount of noise it exhibited when tested.

Table 23. Summary of the performance characteristics of Sensors 8a to 8g

The variation in the sensor performance is most likely due to differences in the EH layer dimensions. Sensor 8d may have become either incorrectly calibrated or damaged during construction, resulting in its incorrect oxygen reading at 0 mM/l of glucose following calibration.

The variation in the sensors performance is most likely due to the differences in the EH dimensions on the sensors, which resulted from the crude coating technique used. The range of the sensors was below the 25mM/l desired. In addition, it has to be noted that although the sensors have a range of up to 10 mM/l (sensor 8f) it has to be remembered that the sensors are being tested in 15% oxygen tensions that are much higher than those that would be seen in subcutaneous tissue.

Increases in range could be achieved by increasing the EH membrane layer depth but this would probably result in a corresponding increase in response times. A better approach would be to use a partial polyurethane outer coat, as described in

Chapter 3. It was decided to use the polyurethane coating method to attempt to increase the range of these sensors.

6.9 Extension of the range of the Sensors 8a to 8e using a polyurethane outer coat

In order to attempt to increase the range of the sensors, an incomplete polyurethane outer coat was applied to Sensors 8a to 8e using a dip coating technique described by Shaw, Claremont et al. 1991. The response of the sensors to glucose was then evaluated and compared with the results of the sensors before coating with polyurethane. The performance characteristics of the sensors in different oxygen tensions were also investigated, to observe the dependence of the sensors on oxygen.

6.9.1. Method of coating of Sensors 8a to 8g in polyurethane

After the completion of the previous set of experiments the sensors were dried in air for approximately two hours. The sensors were then dip coated in a solution of 4% polyurethane (Estane 5714) dissolved in THF and left to dry for two hours. The sensors were then returned to their P7-tonometers, which had been refilled with PBS. All of the sensors were then refrigerated in PBS for a further three weeks until oxygen reference sensors became available for use.

6.9.2. Testing of the polyurethane coated sensors

To investigate the response of the sensor in different oxygen tensions the experimental apparatus was modified to allow two different oxygen tensions 7.5% and 15%, balance nitrogen. For each increase in glucose concentration, the sensors were first tested in a 15% oxygen environment, once a steady state reading had been reached the gas supply was lowered to 7.5% oxygen. The sensors were manually calibrated and once a steady state reading had been reached, the glucose

concentration was increased. When the sensor showed a steady state signal at this glucose concentration, the gas tension was increased back up to 15% oxygen. The process was then repeated until the sensor showed no changes to increasing glucose concentration, or the oxygen tension reading reached zero. A second unmodified P7 sensor was used as a reference to measure the oxygen tension of the tonometer solution.

6.9.3. The effect of the polyurethane membrane on sensor performance

Of the five sensors coated with polyurethane one, 8c, fractured. Sensor 8a exhibited cross talk between the glucose sensor and the oxygen reference, indicating that GOD had leached into the solution. Sensor 8b initially showed a response to glucose but its reading began to climb steadily with the progression of time. The reference sensor measured no corresponding oxygen tension change. The sensor was rinsed and the experiment repeated. In the second experiment, the sensor showed a very limited response to glucose with readings of 30.4 to 26.0 KPa for glucose concentrations of 0 to 52 mM/l respectively. Sensors 8d and 8e gave a usable signal, however, their oxygen tension readings did depart from the oxygen tensions in the tonometer. However, problems were encountered with the reference sensors, which also showed incorrect measurements of the oxygen tensions in the solution. This was attributed to a calibration fault but the experiment was continued without a reference due to the shortage of reference sensors.

The results of the sensor calibration tests before and after coating of the sensors are shown in figure 44. The uncoated sensors (dark triangles and squares) can be seen to have inferior range to the polyurethane coated sensors (open triangles and squares). The characteristics of the sensor calibrations are shown in table 24. A comparison of the sensors performance in the two oxygen tensions (filled squares and triangles for 15% oxygen and unfilled symbols for 7.5% oxygen) are shown in figure 45 and table 25.

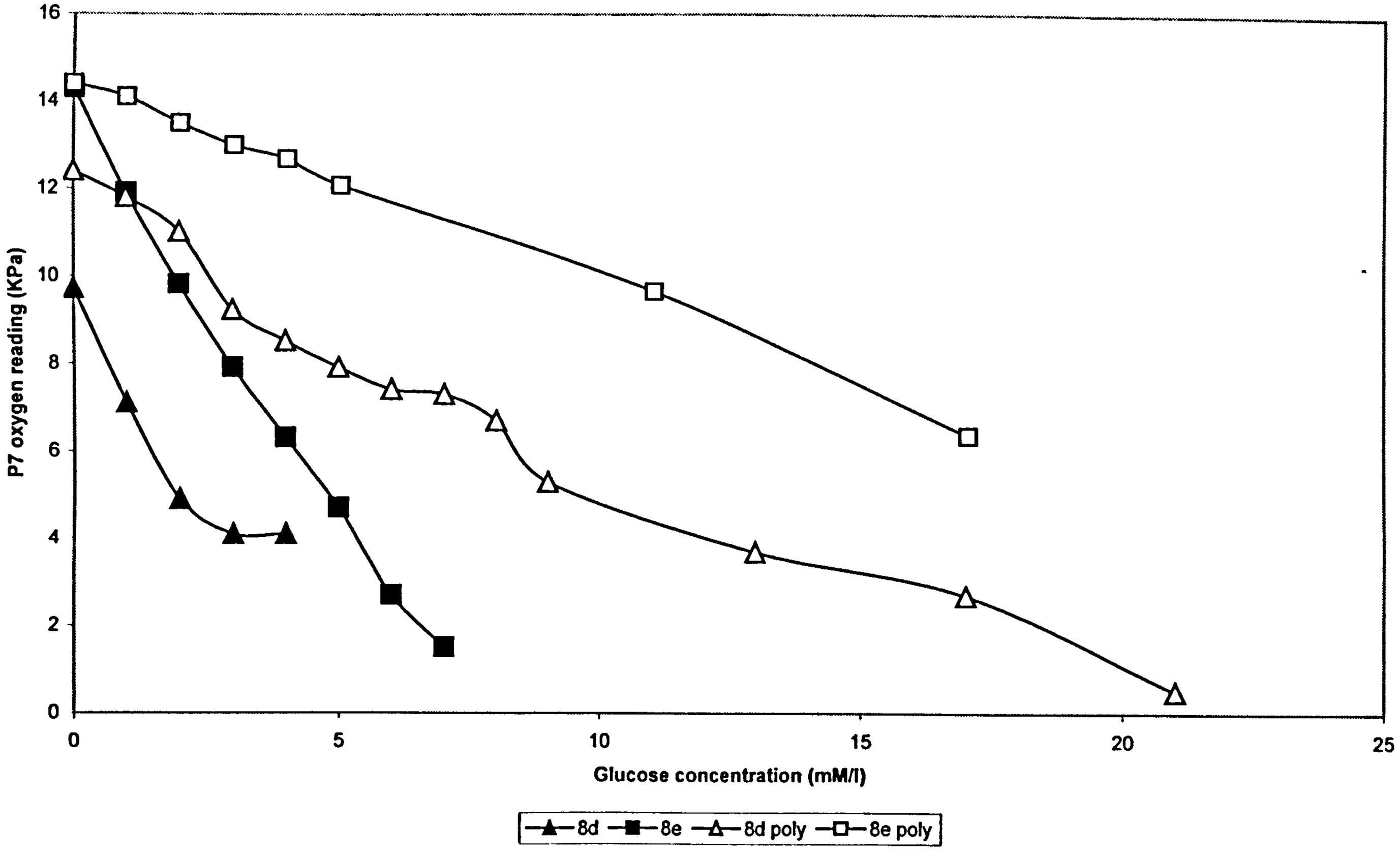

Figure 44. The performance of Sensor 8a before and after dip coating with the polyurethane solution (poly)

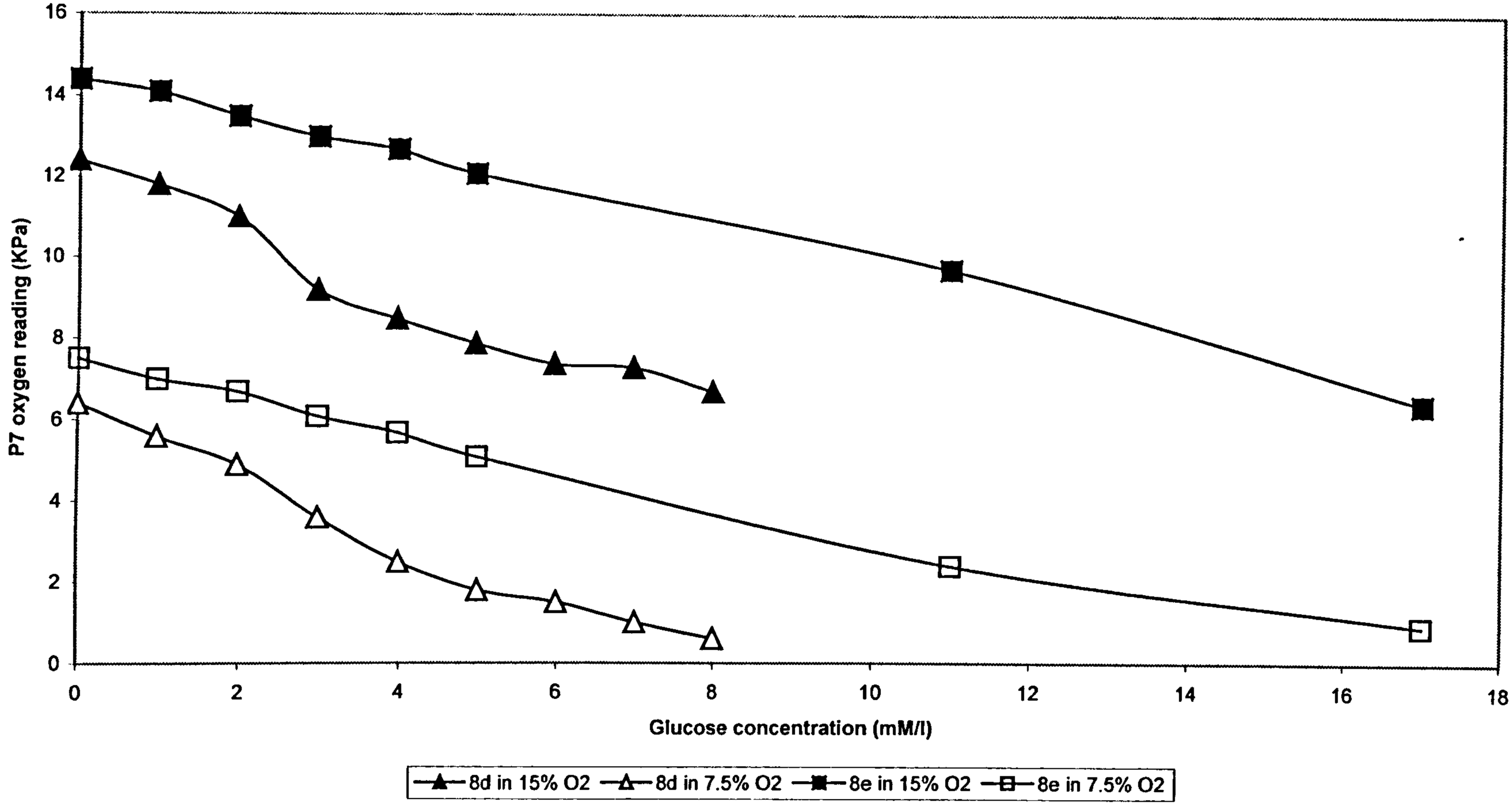

Figure 45. A comparison of the performance sensors 8d and 8e to glucose concentration changes in two different oxygen tensions

Coating	EH only		Polyurethane	
Sensor	8d	8e	8d	8e
Operational range (mM/l)	0 – 3	0 – 7	0 – 21	0 – 17
Linear range (mM/l)	0 - 2	0 – 7	0 - 21	0 – 11*
Sensitivity (over linear range) (KPa/mM/l)	2.4	1.9	0.6	0.5
Approximate 90% Response time (over linear range) (seconds)	200 to 300	100 to 200	NA due to signal noise	NA due to signal noise

Table 24. The Summary of the characteristics of Sensors 8d and 8e before and after polyurethane coating in 15% oxygen tensions

Sensor	8d	8d	8e	8e
Oxygen tension	7.5%	15%	7.5%	15%
Operational range (mM/l)	0 – 8	0 – 21	0 – 17	0 – 17
Linear range (mM/l)	0 – 8	0 - 21	0 – 17	0 – 11*
Sensitivity (over linear range) (KPa/mM/l)	NA	0.6	NA	0.5
90% Response time (over linear range) (seconds)	NA due to noise			

* Large noise seen at 17 and 23mM/lof roughly 50% of the sensitivity.

Table 25. The Summary of the characteristics of Sensors 8d and 8e after polyurethane coating in 7.5 and 15% oxygen tensions

6.9.4. Conclusions of polyurethane coated sensor experiments

Adding the polyurethane has increased the range of sensors, 8d and 8e, but it has also caused a large increase in the response times. The response of the polyurethane coated sensors in two oxygen tensions shows that the sensors are relatively oxygen independent over this range. The range differences are caused by the sensors running out of available oxygen in the 7.5 % saturated solution to carry on breaking down glucose, although there are some differences in the profiles. Sensor 8e has good performance characteristics for our purposes as its range of 0 to 17 mM/l would provide a possible practical glucose sensor

6.10 Sensors constructed by direct coating of the EH onto a P7 oxygen sensing fibre with the pH and CO_2 sensors removed.

In the previous design, Sensors 8a to 8g, all three of the P7 internal sensors were dipped into the EH mixture. To improve the sensor design it was necessary to coat the PO2 sensor alone, as this would reduce the size of the sensor and allow better control of the EH dimensions. However, previously the other sensors in the P7 could not be easily separated from the PO2 sensor. A research and design (R&D) version of the P7 software had become available and was installed on the P7, this allowed the pH and CO_2 fibres to be removed from the sensor while allowing the oxygen sensor to still operate. Previously the removal of the pH or CO_2 sensors would prevent the oxygen sensor from operating as the P7 software would detect the sensor loss and stop operating. The thermocouple was left intact as this was required for the calibration of the oxygen sensor and was a useful measurement in itself due to the dependence of oxygen solubility on water temperature.

The CO_2 and pH sensors were cut away from the P7 sensor to leave the PO2 and temperature sensor exposed. The new sensor construction is shown in figure 46. Two further sensors, 9c and 9d were also created and tested. To avoid repetition, the results from these two sensors will be reported later in sensor gamma sterilisation investigations.

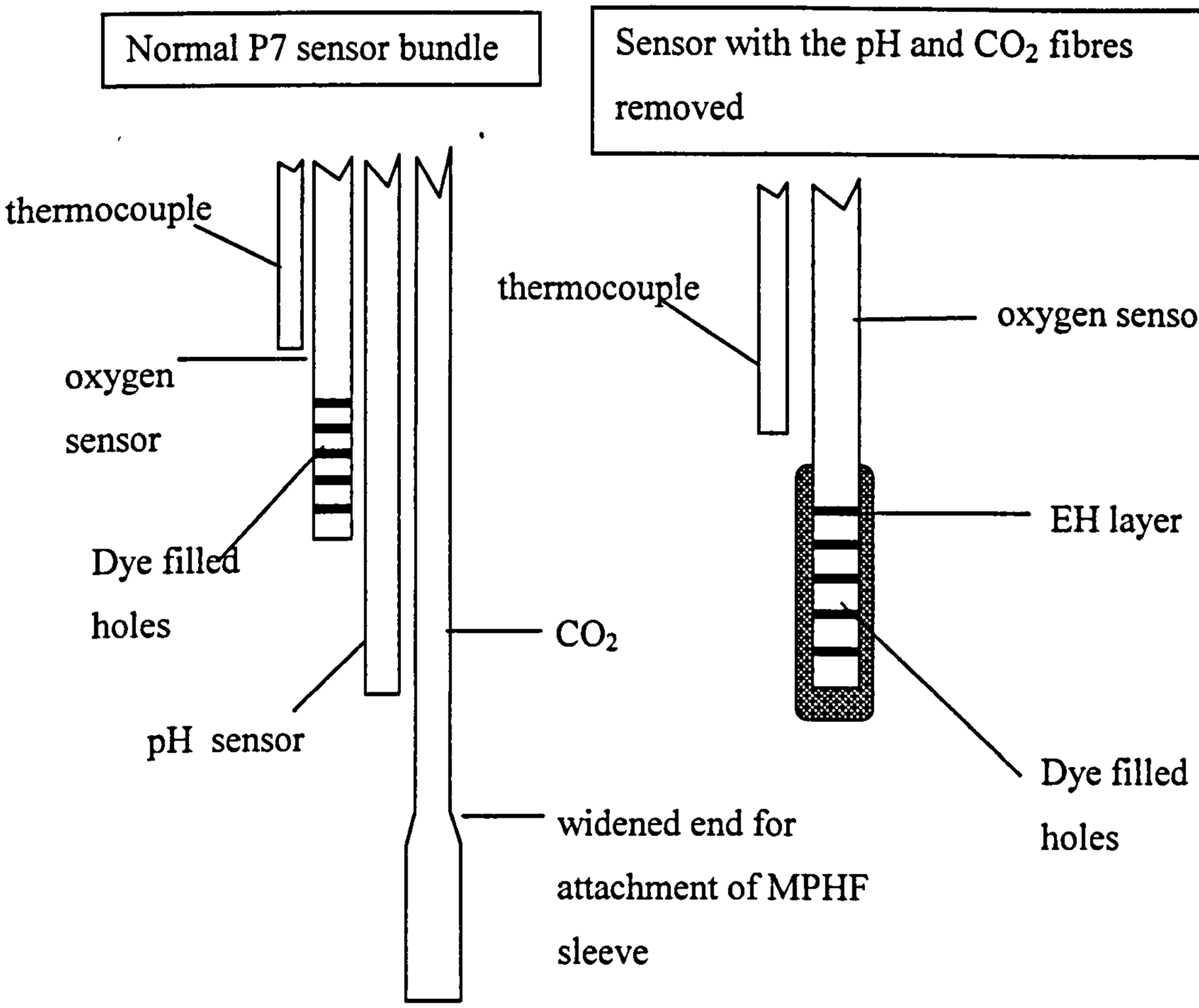

Figure 46. The Sensor design with the pH and CO_2 optical fibre sensors removed.

Sensor 9a was then dip coated into an enzyme mixture, that consisted of 30 mg of GOD and 30 mg of CAT dissolved in 0.25 ml of PBS, mixed with 0.25 ml of 0.25ml of 10 % HEMA solution, dissolved in 90 % ethanol 10 % distilled water. The EH mixture was applied to the oxygen sensors using the 'painting' technique as used in Sensor 7. To cross-link the enzymes the sensor was dipped into glutaraldehyde. As it was considered that little or no chemical reactions will take place while the GOD is in its dry form, the sensor was left dry and refrigerated overnight to minimise any degradation that the sensor would suffer as GOD was broken down. The coating technique allowed a layer of uniform thickness of EH to be deposited on the sensor.

6.10.1. Initial results of EH coating on an isolated PO2 sensor

The range of the initial sensor design was only 1mM/l with a 90% response time of 60 seconds as can be seen in figure 47. The sensor was coated in polyurethane to attempt to increase its range. However, the sensor failed to give a signal probably due to a fracture occurring during the coating process.

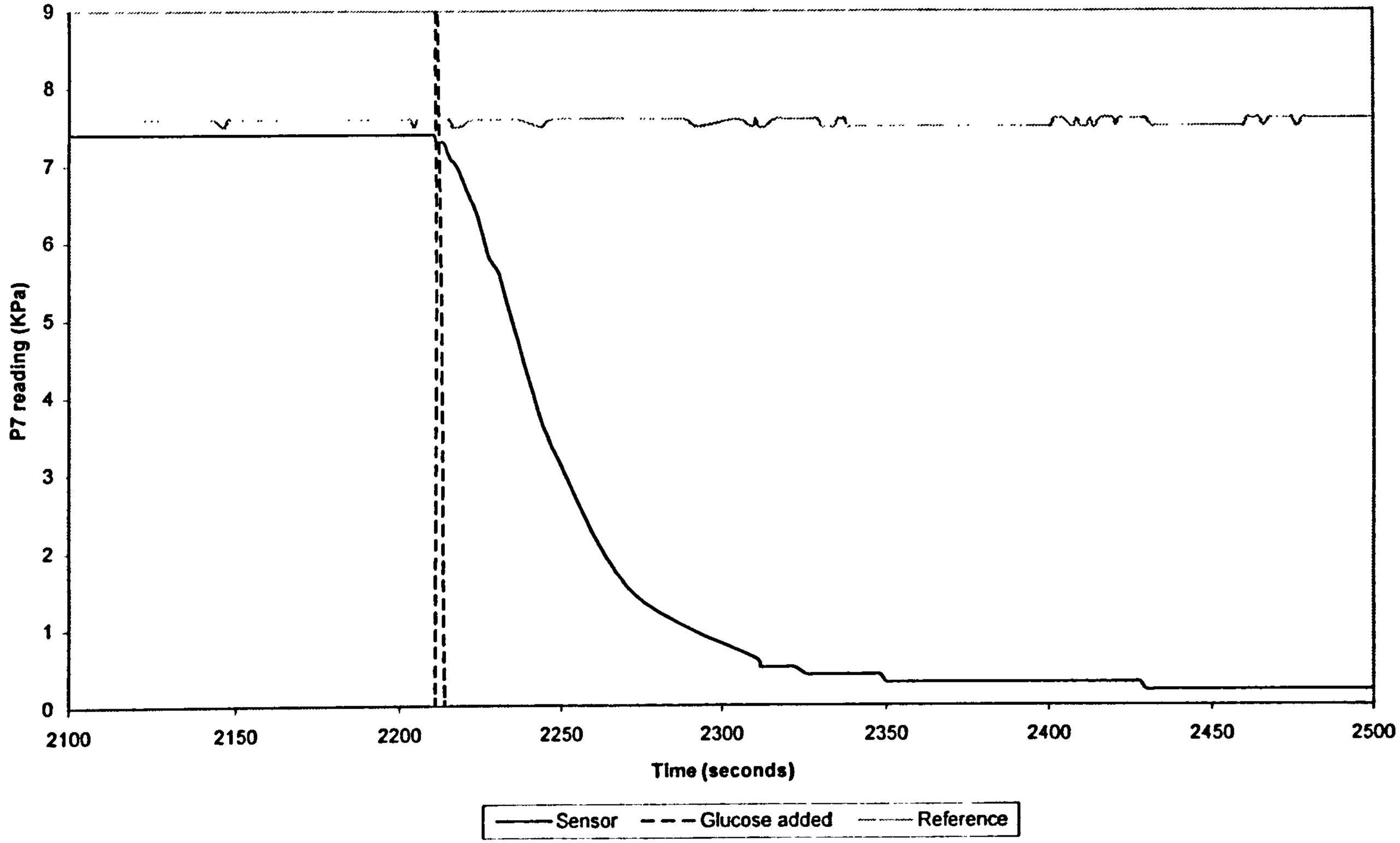

Figure 47. Sensor 9a glucose performance test

6.10.2. Conclusions EH coating on an isolated PO2 sensor

Although a much more regular thickness EH layer has been created, its thinness compared to previous designs has limited the sensors range to only 1mM/l. Although showing that an EH can be laid down on the sensor, the membrane will have to be made thicker, polyurethane or an outer HEMA coat was used to increase the range. The painting technique, although usable, made control of the membrane thickness virtually impossible. This sensor, although of no practical use, demonstrates the sensitivity of glucose sensors that can be produced using this technique. The development of a dip coating technique, similar to the one used in the first experiment, applied to the P7 sensors in experiment one to four would be the most desirable solution and this was now investigated.

6.11 An isolated PO2 sensor coated by absorption of enzymes from solution

A new approach to coating enzymes onto the HEMA sensor was investigated; this involved coating the oxygen sensor with HEMA and then absorbing enzymes into the HEMA layer from solution. Initial investigations had shown that without the GOD and CAT mixed in with the HEMA the pure HEMA solution did not adhere to the coating silicone carbinol of the oxygen sensing fibre. To lay a HEMA layer a method of improving the adhesion of the HEMA to the silicone carbinol was needed. Coating the oxygen sensing fibre with agrose before the EH was proposed as a possible approach[3] .

[3] *Suggested by staff at Salisbury District Hospital, UK*

6.11.1. Experimental protocol

The pH and CO_2 sensor were removed and the oxygen sensor was dip coated in a solution of 2% agrose. The sensor was then repeatedly dipped into the EH mixture until a round mass had built up over the five dye filled holes. The sensor was then placed in a solution containing 30 mg of GOD and 30 mg of CAT. After 30 minutes the sensor was removed and dip coated in the HEMA to add a final outer layer. The sensor was finally dipped in glutaraldehyde to cross-link the enzymes. The sensor was then refrigerated dry overnight and tested the following morning. The sensor was tested using the same method as previously described except that 7.5% oxygen balance nitrogen tensions were used to perfuse the solution. From this point on, sensors were tested in 7.5% oxygen tensions as these better reflected the oxygen tension of tissue (Zhang and Wilson 1993). A second normal P7 sensor was used as a reference. The sensor was then dried and dip coated in 4% polyurethane to increase its range and was then re-tested the following day.

6.11.2. Performance of the absorption coated sensor

The sensor had a range of 15mM/l and a 90% response time of approximately 200 seconds, as shown in figure 48 and table 26. The reference sensor showed no change in oxygen readings during the experiment confirming that no GOD was leaching into solution. This was expected as no immobilisation procedures had been used to entrap the enzyme. To further increase the range, the sensor was dip coated in 4% polyurethane immediately following the experiment. The sensor was then refrigerated, dry, overnight and tested the following day. The sensor initially showed a response to increasing glucose concentrations but after 4mM/l the oxygen reading climbed to a level above the 0mM/l concentration as shown in figure 49.

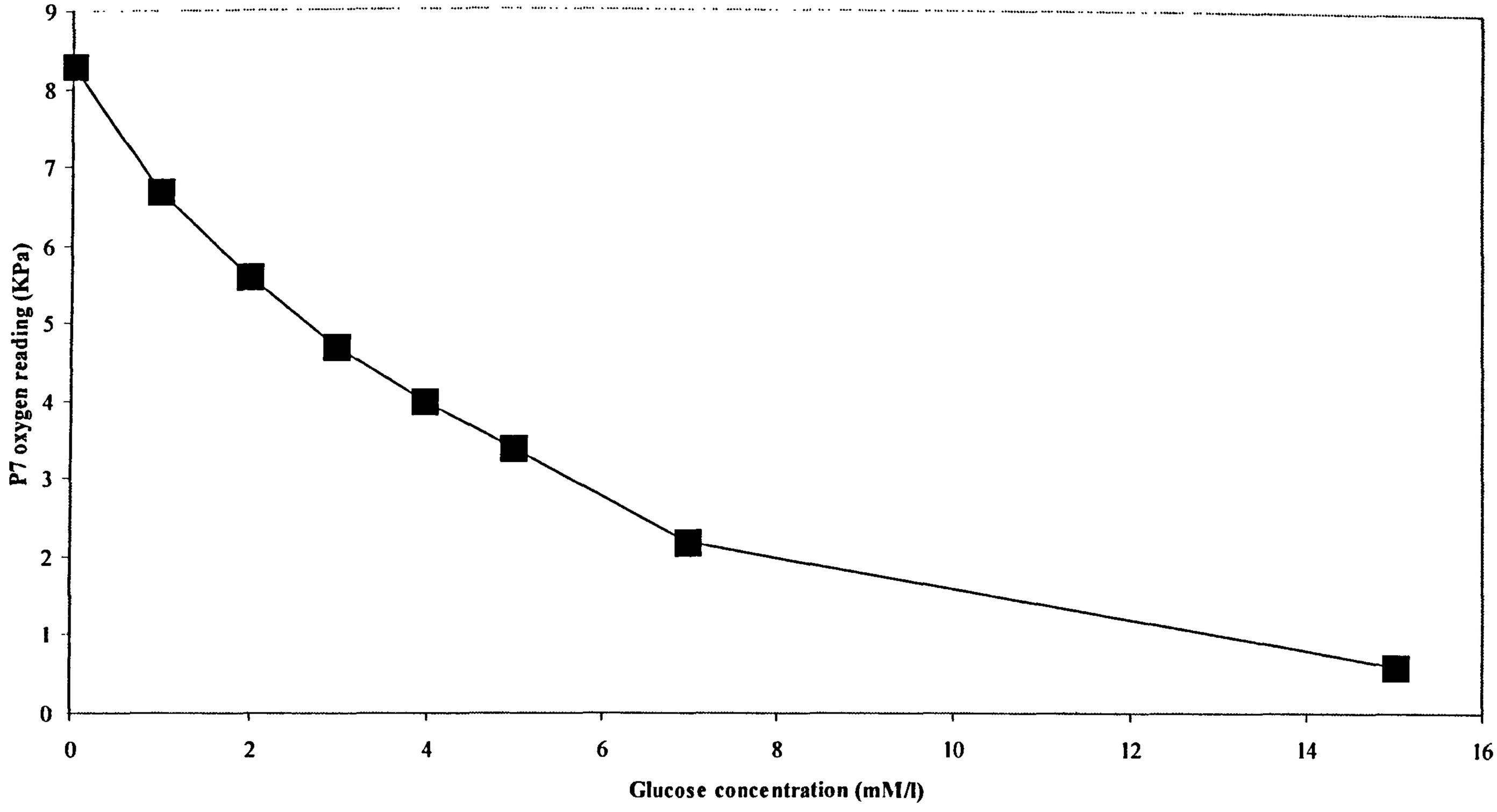

Figure 48. The performance of Sensor 9b

Operational range (mM/l)	0 – 7
Linear range (mM/l)	0 – 15
Sensitivity (over linear range) (KPa/mM/l)	NA due to low sensitivity of sensor
90% Response time (over linear range) (seconds)	NA due to low sensitivity of sensor

Table 26. The performance parameters of Sensor 9b

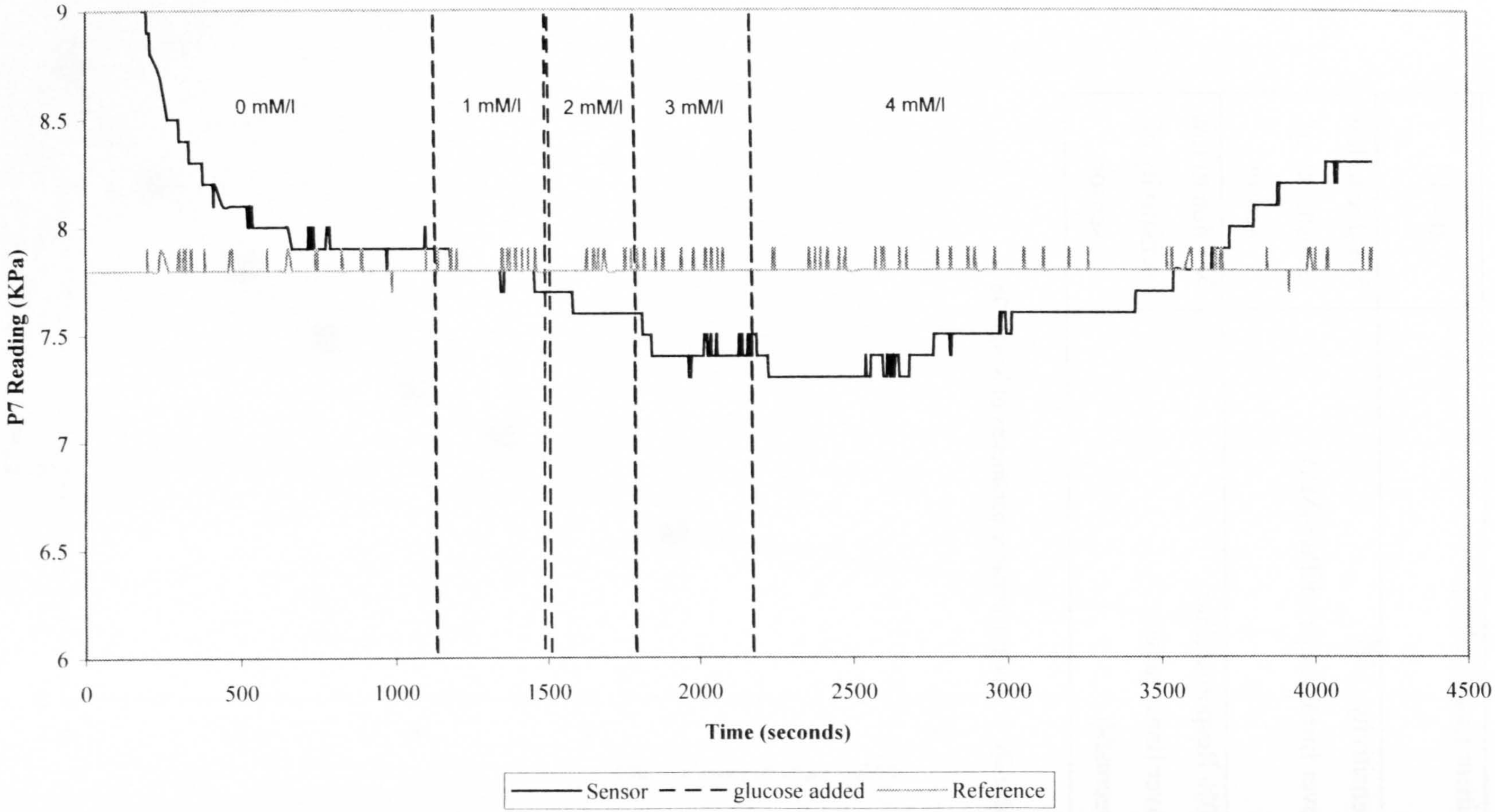

Figure 49. The performance of Sensor 9b after coating in polyurethane

The construction method has produced an operational sensor. Even without its polyurethane outer coat, the sensor had a good range (15mM/l) and response time of 159 seconds. After the addition of the polyurethane, the sensor showed a greatly reduced response to glucose concentrations. The increase in the oxygen tension registered by the sensors after 4 mM/l seems to be due to phenomena internal to the glucose sensor, as the reference sensor showed no deviation. In addition, the sensor signal reaches a level of oxygen tension higher than its starting place with no glucose present.

The only source of oxygen apart from the gas supplied to the tonometer and the atmospheric gas is from the action of catalase breaking down H_2O_2. It is possible this oxygen increase is a result of a reaction diffusion system set up inside the sensor membrane. Alternatively, a calibration fault in the P7 R&D software may have cause a drift in the sensor signals.

Putting aside the failure of the sensor after coating with polyurethane, this construction method has proved effective. However, it is essential for performance and lifetime considerations that the enzyme membrane is loaded to excess with enzymes, which cannot be guaranteed with this approach. A dip coating method, adapted to operate on the oxygen sensor would be the most useful method.

6.12 Development of a precision dip coating using a laser micrometer

In an attempt to find a technique of dip coating the PO2 sensor with EH, the viscosity of the EH mixture was varied. After some trial and error, using used PO2 sensors from previous experiments, and EH solution mixture ratios ranging from 0.25 ml enzyme mixed with 0.25 ml of HEMA solution to 0.25ml enzyme

solution to 1 ml of HEMA solution and dip coating techniques, an effective method for coating the P7 oxygen sensor was found.

The enzyme solution contained 30 mg of GOD and 30 mg of CAT dissolved in 0.75 ml of PBS. The HEMA solution consisted of 10 % HEMA solution dissolved in 90 % ethanol 10 % distilled water. The PO2 sensor was dipped once into the EH mixture and then allowed to dry in air for 20 minutes. The process was then repeated until a layer of EH of twice the sensor diameter was built up. Although this took approximately 12 hours, a uniform EH layer of controlled thickness was built up.

To examine the dimensions of the layer deposited on the sensor a laser micrometer (available for a short time) was used to take measurements.

6.12.1. Laser measurement of the diameter of EH coated glucose sensors

The diameter of the sensor was measured using the ALS13XY/100/B00 laser micrometer (Scantron, Taunton, UK). This device measures diameters to within 0.1 μm in two perpendicular axes. This allows ovalarity to be measured (the ratio of the diameter of the two axes). The laser is scanned across the fibre at 100 Hz in each axis and an average measurement displayed. The ovalarity in this case is caused by two possible sources, first the EH could be thicker on some sides than others, secondly the sensor could be held at an angle of less than 90° to the laser beams causing a gross section to be measured at an angle see figure 50.

Normally, when wires are measured by this diverse they are held in place mechanically to ensure they are positioned at 90° to the beams, however, in this case, the sensor is too fragile and small to be gripped in this way. As a result, the sensor had to be held by hand and this introduced two possible sources of error.

Firstly, shaking of the hand and secondly holding the sensor at less than 90° as shown in figure 50.

Five measurements were taken of the bare fibre over the region of the dye filled holes and the diameter and the ovalarity were then averaged. The sensor was then dip coated in the above solution until a layer of roughly twice the sensor diameter had been deposited. This was allowed to dry and the sensor was then measured again, over the same section of the fibre also taking an average of five measurements.

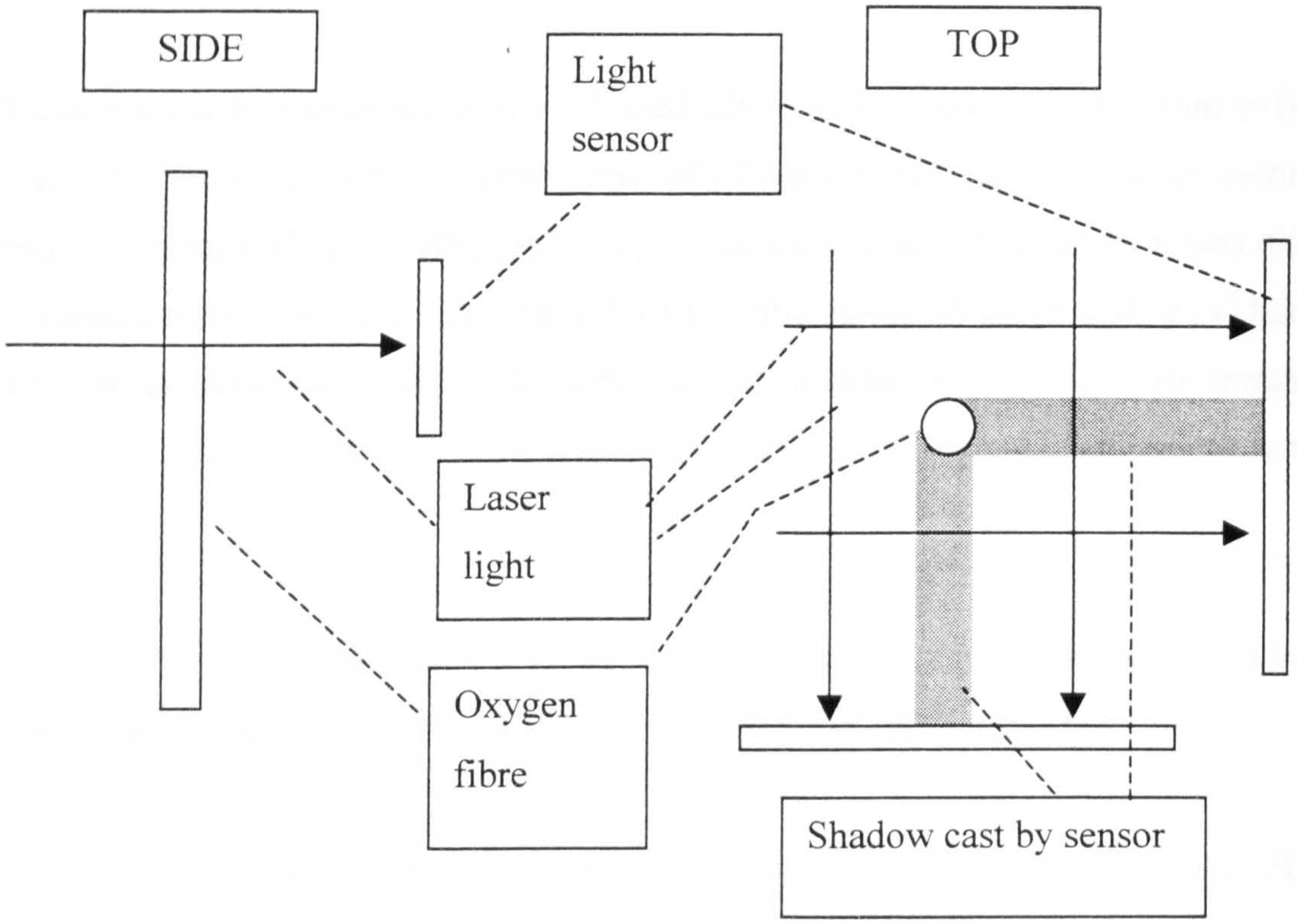

Figure 50. Measurement of the diameter of the sensor

The results of the measurement are shown in table 27; the coating technique has laid down a layer of ≈ 60 μm with an ovalarity of ≈28 μm across the diameter.

	Bare oxygen sensor	Standard deviation	Dip coated sensor	Standard deviation
Average diameter (μm)	174.4	1.0	296.0	53.8
Average ovalarity (μm)	1.3	1.1	28.0	30.0

Table 27. The diameter and ovalarity of a coated and uncoated PO2 sensor

6.12.2. Performance of the improved dip coating technique

The dip coating technique has laid down a uniform EH layer of only 60 μm thickness. The ovalarity measured in the EH layer was probably in part due to incorrect positioning of the sensor in the laser beam. Therefore, the true ovalarity of the membrane layer is probably less than 28 μm. This coating technique should allow better control over sensor performance through control of membrane dimensions.

6.13 Performance of sensors produced using the new dip coating technique

The aim was to use the new dip coating technique to coat two sensors and then measure their characteristic response to glucose. Two sensors, 9c and 9d were constructed using the dip coating method described above. The solution mixture ratio had been further improved from the previous experiment by reducing the amount of HEMA in the mixture. This allowed the EH layer to be more easily coated onto the PO2 sensor. The P7 sensors had their pH and CO_2 sensors cut away and were then dip coated as described above using a mixture of 0.25ml of PBS containing 30 mg of GOD and 30 mg of CAT, mixed with 0.5 ml of 10% HEMA dissolved in a 90% ethanol and 10% water. Once a depth of approximately half the oxygen sensor diameter (≈100 μm) had been built up, the sensors were then refrigerated, dry, overnight and then dipped into glutaraldehyde to cross-link the enzymes in the membrane. After being air-dried, the sensors were tested for their response to glucose.

After the sensors had been tested, they were dried and then dip coated in 4% polyurethane solution dissolved in tetrahydrafuran. The sensors were dried and refrigerated overnight and re-tested.

6.13.1. Performance of the sensors dip coated using the improved technique

As can be seen in figure 51, before coating with polyurethane, Sensor 9b displayed over shoot in its response to glucose concentration changes. However, after coating with polyurethane, this feature was lost and the sensor responded closely to concentration changes as shown in figure 52. Sensor 9c faithfully responded to glucose concentration changes both before and after coating with the

polyurethane. The response of both sensors before and after coating with polyurethane to glucose concentrations changes are shown in figures 53 and 55 for Sensors 9b and 9c respectively and the sensor characteristics are given in table 28.

The spike seen in figure 51 at the 4 mM/l glucose concentration was caused by a recurring fault in the P7 R&D software, which occasionally caused oxygen values below a value of 1 KPa to be falsely displayed as ten times its true value. In this case 0.3 is represented as 3.

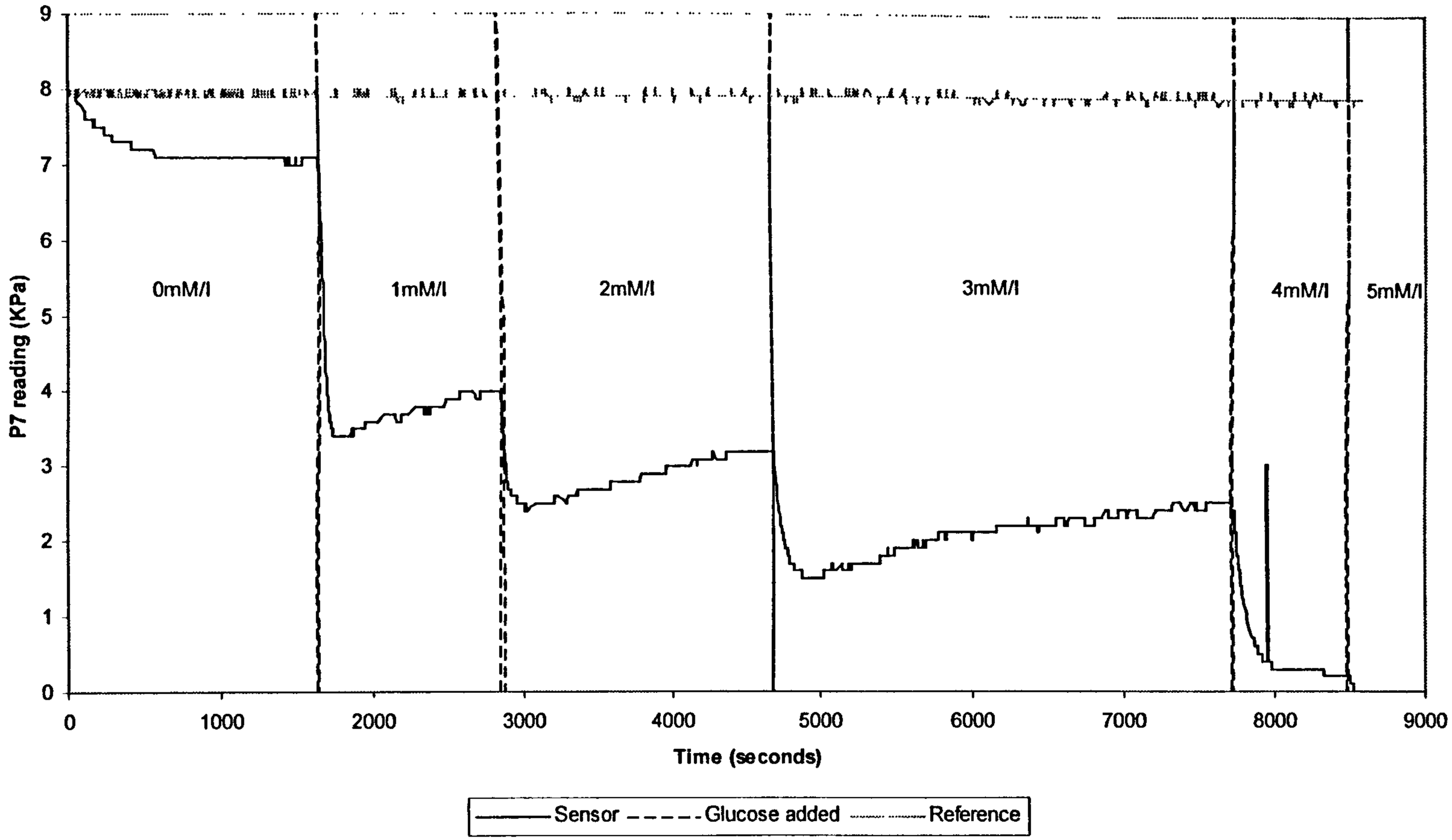

Figure 51. The performance of Sensor 9c before coating with polyurethane.

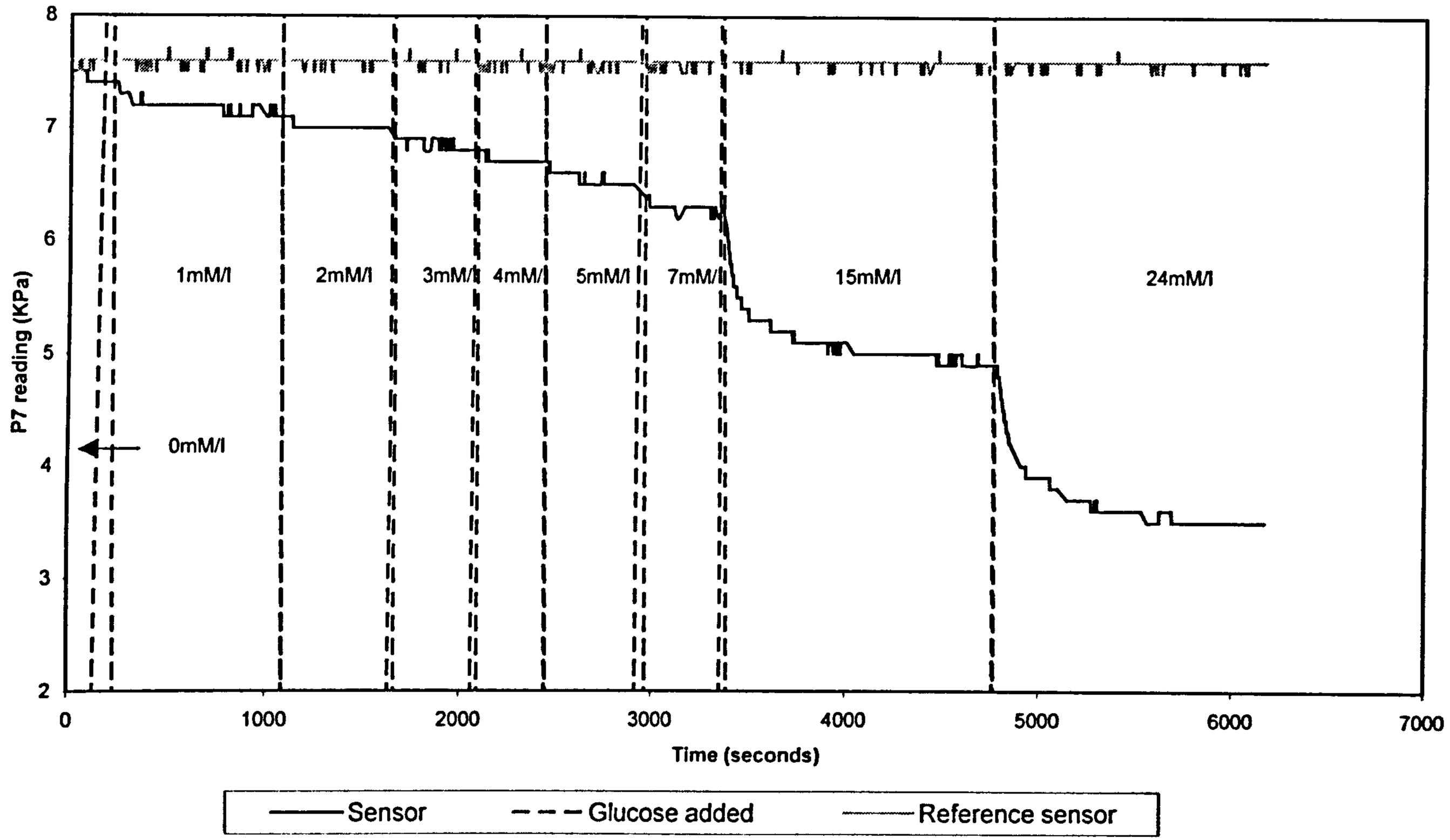

Figure 52. The performance of Sensor 9c after coating with polyurethane.

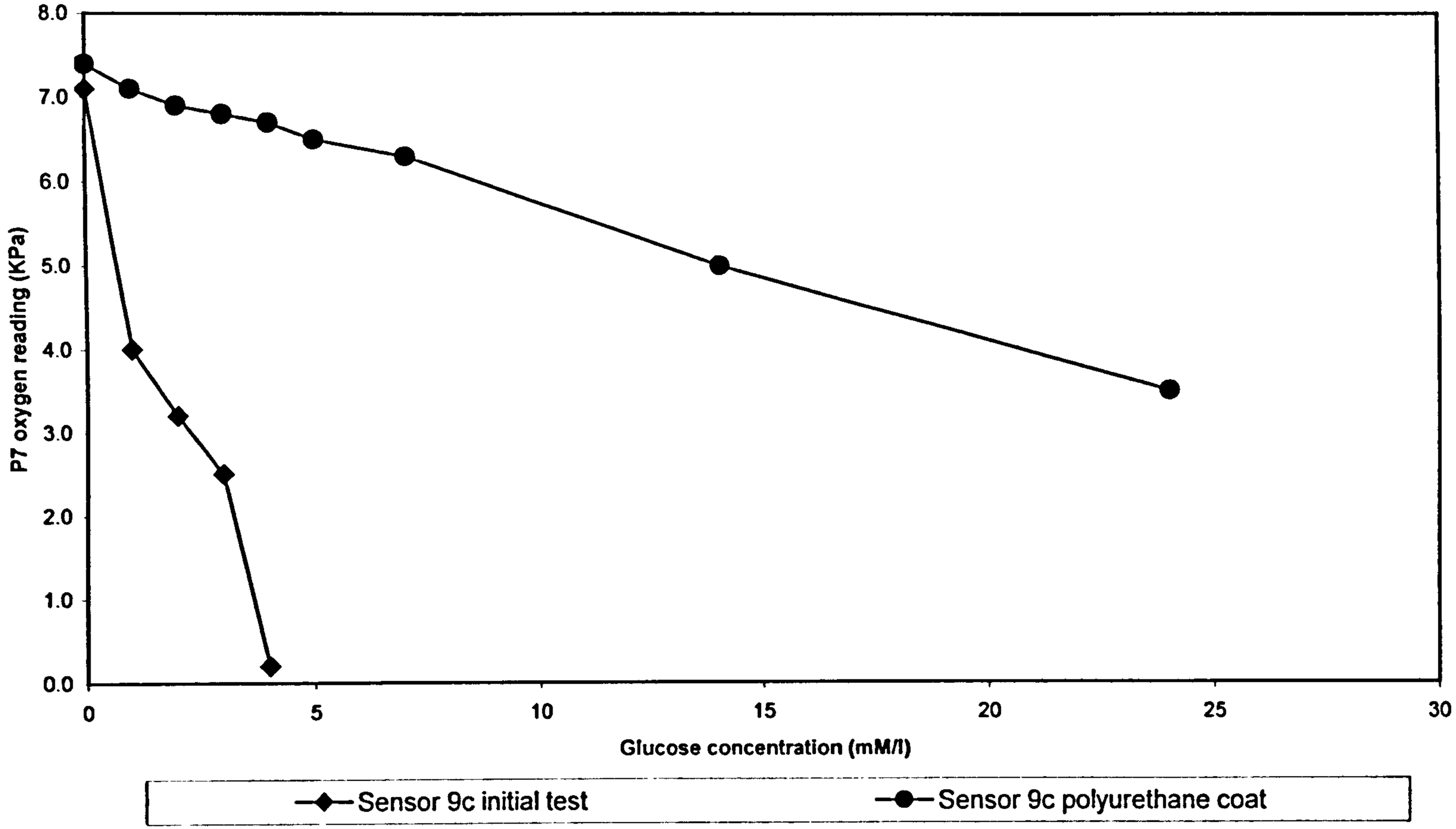

Figure 53. The response of Sensor 9c before and after polyurethane coating

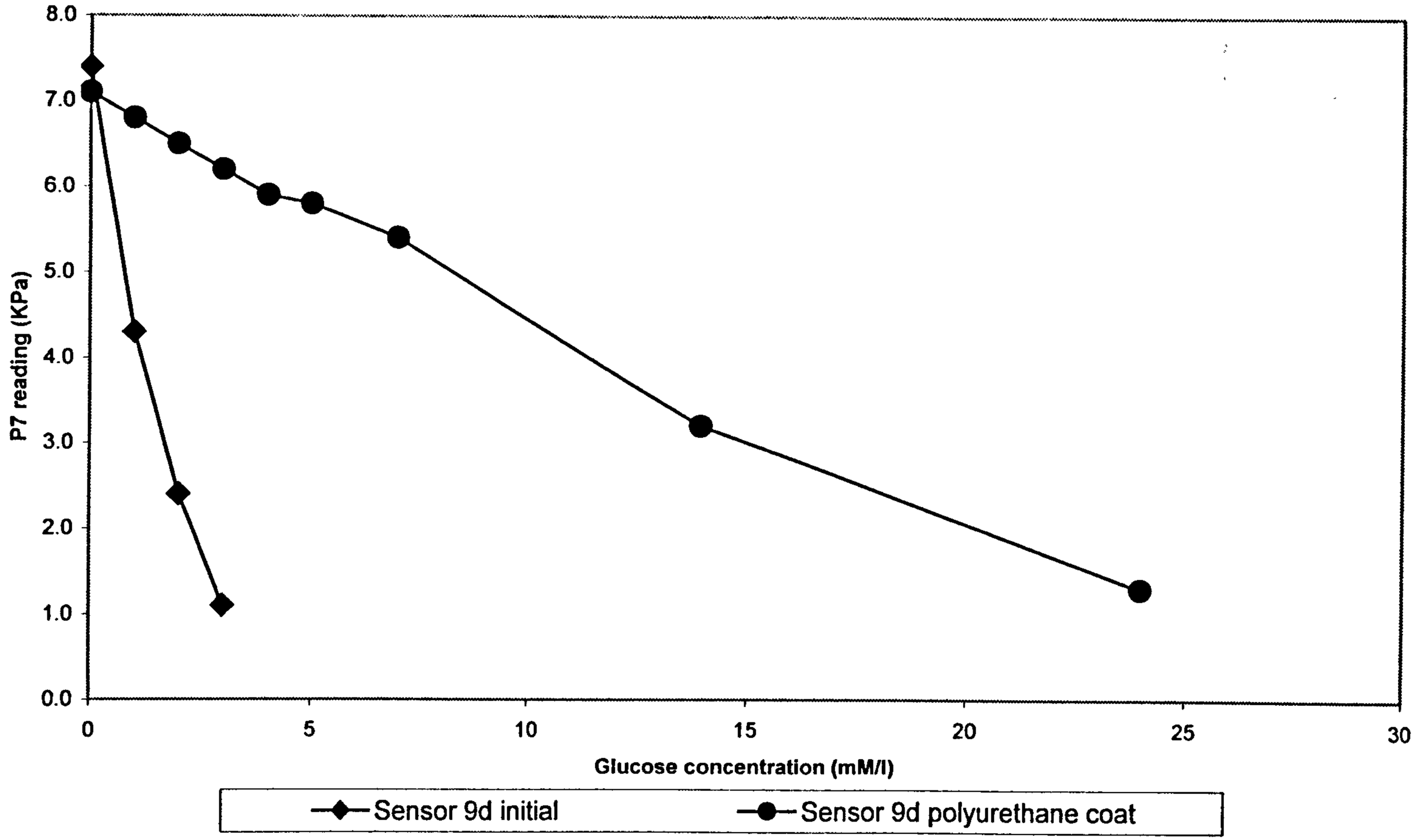

Figure 54. The response of Sensor 9d before and after polyurethane coating

Coating	EH only		Polyurethane	
Sensor	9c	9d	9c	9d
Operational range (mM/l)	0 – 4	0 – 7	0 – 24	0 – 24
Linear range (mM/l)	NA	0 – 7	0 – 15	0 – 5*
Sensitivity (over linear range) (KPa/mM/l)	NA	1.8	0.16	0.3
90% Response time (over linear range) (seconds)	NA	<100	NA	NA

* noise level approaches resolution above this concentration

NA – not applicable due to low sensitivity or the response of the sensor to step change

Table 28. The characteristics of Sensors 9b and 9c with and without polyurethane coats

The over shoot observed in the response of Sensor 9b was probably a result of the reaction-diffusion process in the membrane layer being such that the system essentially behaved as a heavily damped oscillator. In this situation, each increase in glucose concentration caused a transient drop in the oxygen tension in the membrane as oxygen was consumed faster than it could be re-supplied by oxygen from outside or from that recycled by the action of CAT. This led to the reaction in the membrane slowing down until the consumption of glucose could be matched by diffusion of oxygen from outside and from recycling of oxygen by the CAT. The sensor then settled down to a steady state value. The polyurethane coat solved this problem probably by reducing the glucose flux to below a value that

could trigger this oscillation. Sensor 9c did not show this oscillating behaviour, which was possibly due to differences in the EH membrane deposited on the two sensors, indicating that there is still some variation in EH layer formation using this technique.

The addition of the polyurethane layer increased the range of both the sensors by a large amount (between two and three times the original). The range of both sensors covers the whole hyperglycaemic range required. However, this was obviously at the expense of sensitivity.

6.14 Comparison of HEMA and polyurethane outer coatings to extend the range of the glucose sensors

After the initial EH coating there were three possible ways to extend the range of the sensor. Firstly, more EH could be added to the sensor, but this would cause the sensor to become much larger. Second, a layer of HEMA could be added to the sensor to increase the range, as with sensors 1 to 4, with a smaller increase in sensor size. Finally, polyurethane could be used as with the sensors 9c and 9d above.

The smallest possible sensor was aimed for and adding more EH was discarded as an option. This left a polyurethane coat or extra HEMA as the available options. To compare these two techniques two glucose sensors, 10a and 10b were given an EH coat and tested. One of the sensors, 10a, was then coated with HEMA and the other, 10b with the incomplete polyurethane coat, both of the sensors were then re-tested.

The enzyme mixture used contained 60 mg of GOD and 76mg of CAT dissolved in 0.5ml of PBS. This was then mixed with 1ml of HEMA solution. The HEMA solution contained 100mg/ml of HEMA in 100% ethanol. Once an EH had been

built up, the sensors were left to dry for another 20 minutes and dipped into glutaraldehyde to cross-link the enzymes. The sensors were then dried and refrigerated in PBS for 24 hours.before being tested.

It was decided to store sensors in PBS, as opposed to dry as with the previous experiments, to ensure that the EH layer had fully hydrated. If left dry the EH membrane would swell, causing changes in the sensors performance. In addition, overnight storage in PBS will allow any loose enzymes to diffuse out of the EH layer reducing the chances of contamination of the test tonometer with GOD.

After the initial tests, Sensor 10a was dried for one hour and then dipped into the HEMA solution described above. It was then dried for another hour before being dipped again. The sensor was then allowed to dry before being replaced in PBS and refrigerated. Following testing, Sensor 10b was also dried for one hour and then dip coated in 4% Estane as described earlier.

Finally, after both sensors had been recalibrated and re-tested with their new outer coats, sensor 10a was dried and dip coated in polyurethane and then re-tested.

6.14.1. The performance of the two sensors before and after HEMA and polyurethane coating

Initially both sensors had a maximum range of only 1mM/l with sensitivity of 6.6 and 6.5 KPa/mM/l and a 90% response times of the two sensors of <100 and 100-200 seconds for sensors 10a and 10b respectively, see figures 55 and 59. The results of adding the HEMA layer to Sensor 10a and the polyurethane layer on 10b are shown in figures 57 and 58. Sensor 10a failed after the dip coating with the polyurethane solution, probably through a fracture in the fibre. The responses of both sensors with all of the coatings are shown in figure 59 and table 29. The HEMA has extended the range of the sensor to 4mM/l with a 90% response time of 180 seconds and the polyurethane has given the sensor a range of 8mM/l with a 90% response time of 90 seconds.

The oxygen reference sensor shows no change, indicating that no enzyme is leaking into the tonometer and that all the oxygen tension changes are localised inside the EH layer of the glucose sensors. The error in the R&D software can be seen in figure 56, where a spike can be seen at 700 seconds. More data that are faulty can be seen in figure 58, where the error can be seen at 7000 seconds.

Although the polyurethane is clearly the better solution in this case, neither method has extended the range of the sensor to cover the upper glycemic levels seen in diabetics of around 25 mM/l. To increase the range of the sensors it was decided to try using both the extra HEMA outer layer and the polyurethane coat. To this end, Sensor 10a was dried for one hour and then dipped in the 4% polyurethane solution (Estane 5714) dissolved in THF, allowed to dry for one hour and then refrigerated in PBS.

Two days later it was calibrated for a test of its range with the new membrane, however, the sensor signal failed through fracture of the fibre.

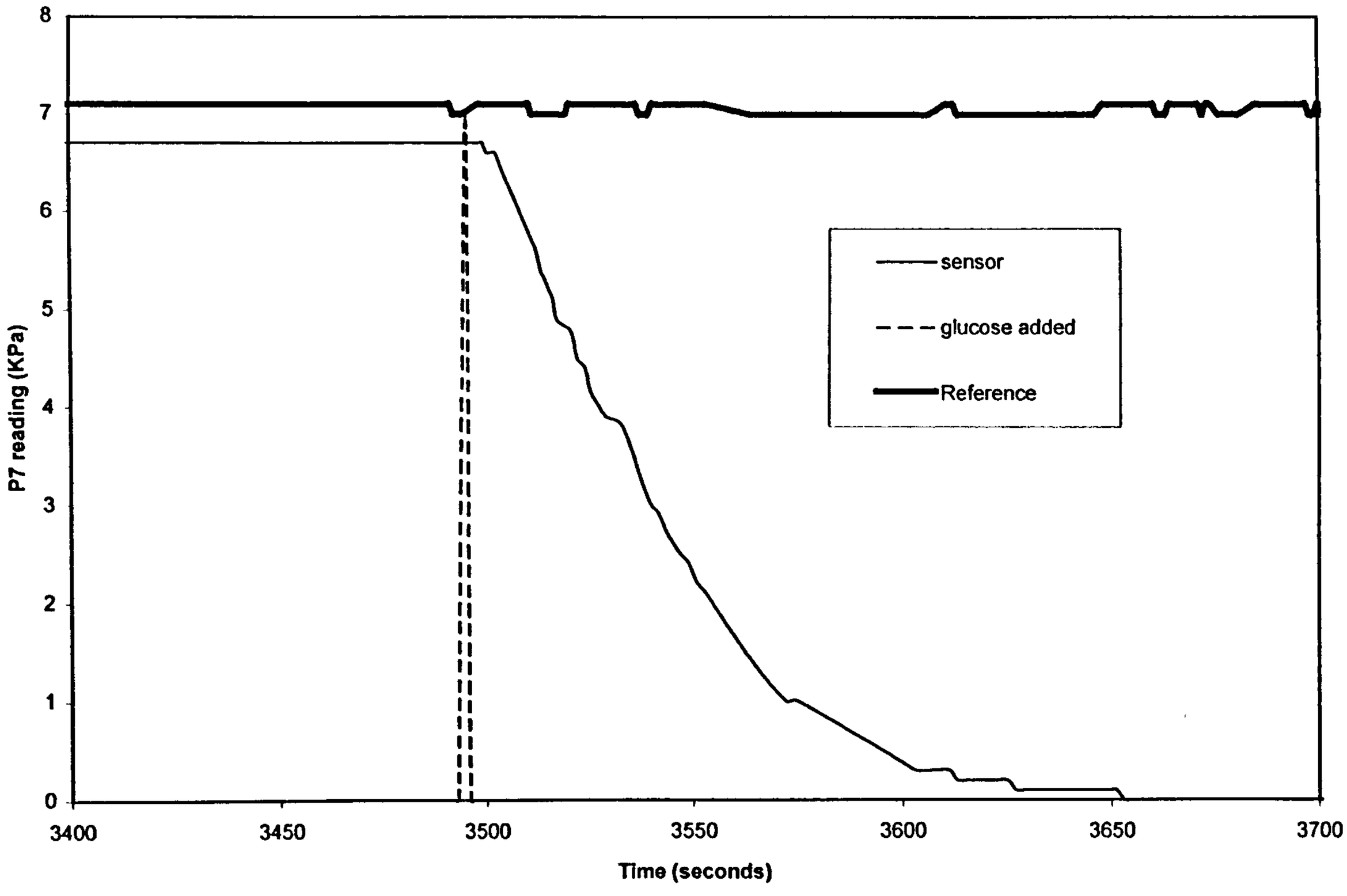

Figure 55. Sensor 10a response to a 1mM increase in glucose concentration

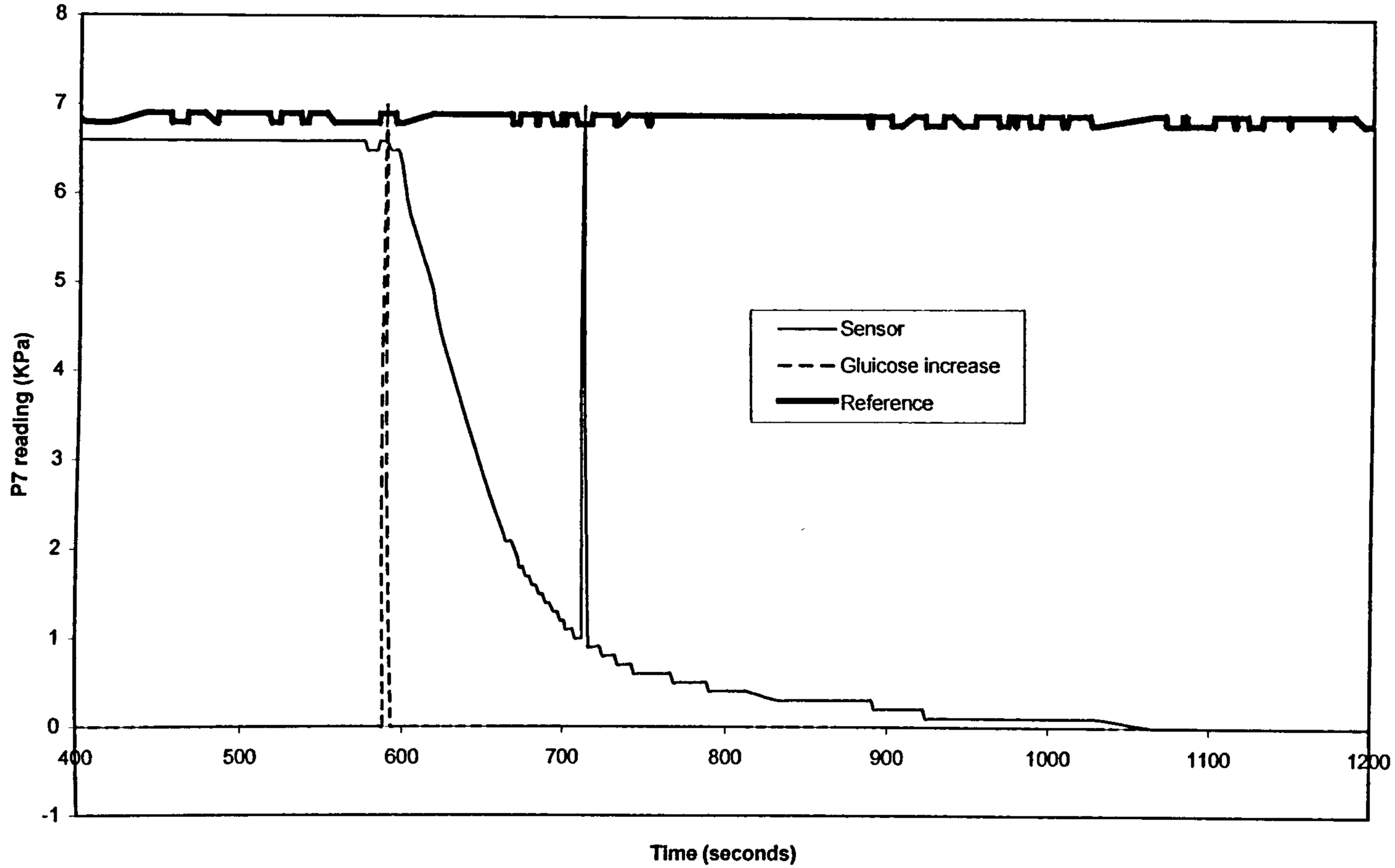

Figure 56. Sensor 10b response to a 1mM glucose step increases

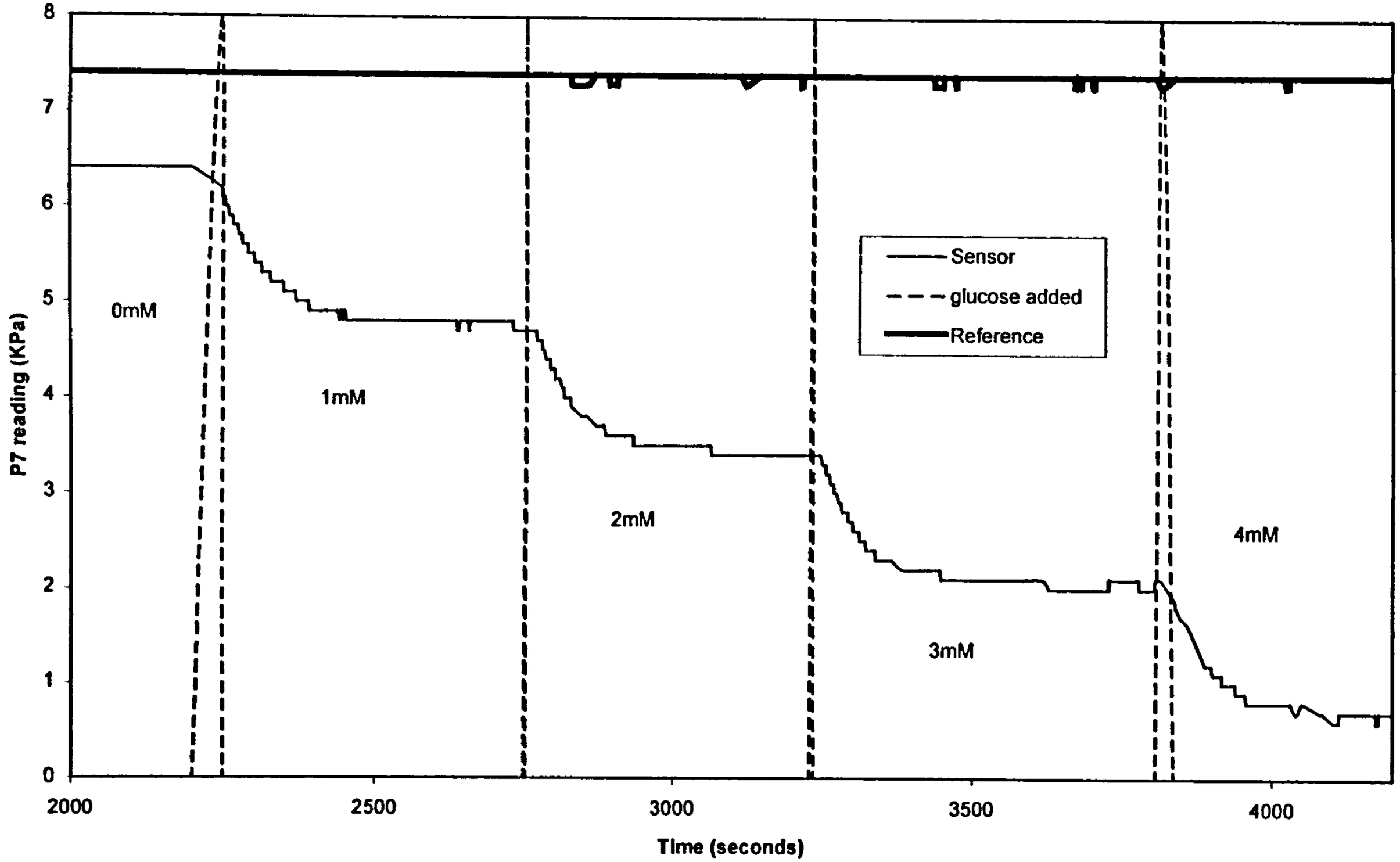

Figure 57. Sensor 10a After coating with an outer HEMA layer

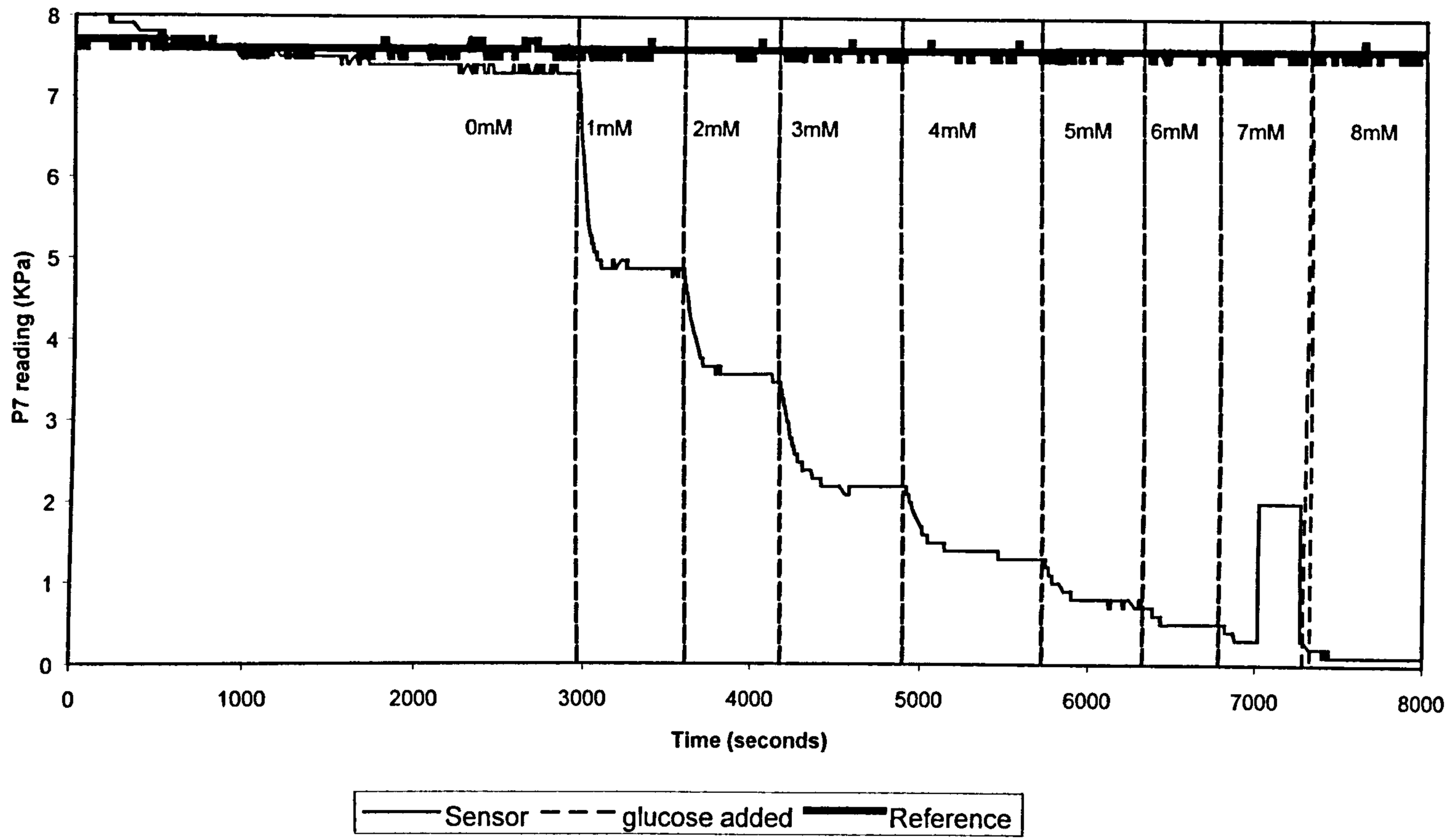

Figure 58. Sensor 10b after coating with polyurethane

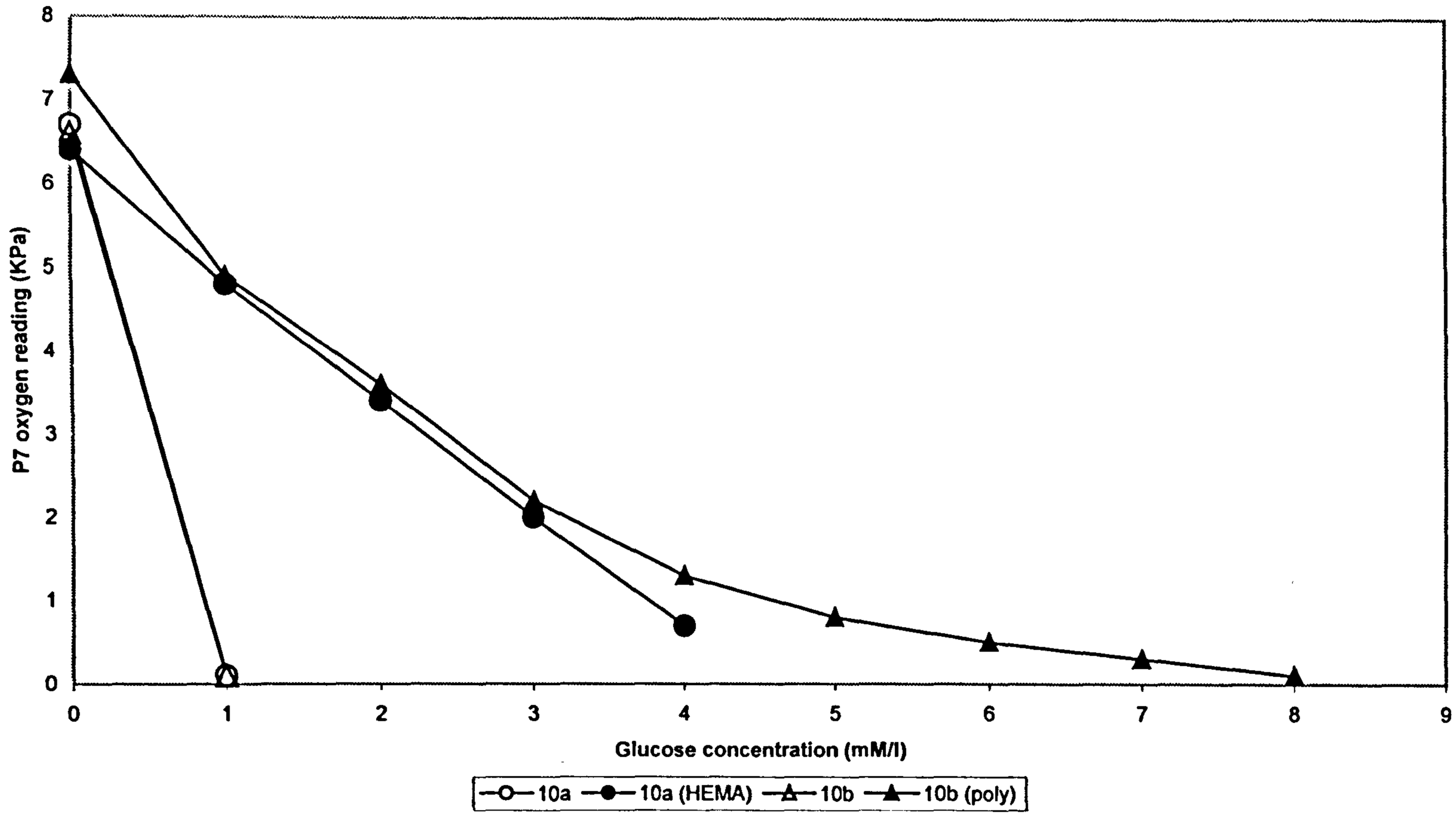

Figure 59. The results of Sensors 10a and 10b before and after the HEMA and polyurethane layers were deposited.

Coating	EH only		HEMA	Polyurethane
Sensor	10a	10b	10a	10b
Operational range (mM/l)	0-1	0-1	0-4	0-8
Linear range (mM/l)	N/A	N/A	0-4	None
Sensitivity (over linear range) (KPa/mM/l)	6.7	6.6	1.4	NA
Approximate 90% Response time (over linear range) (seconds)	100 to 200	100 to 200	100 to 200	NA

* noise level approaches resolution above this concentration

NA – not applicable due to low sensitivity or the response of the sensor to step change

Table 29. The characteristics of Sensors 10a and 10b with and without polyurethane and HEMA outer coats

With no diffusion limiting membranes, both sensors reached their maximum range at only 1mM. This was most likely due to the EH layer being extremely thin only ≈60 μm, which puts up an inadequate resistance to glucose causing all oxygen to be consumed inside the sensor faster than it can be replaced by diffusion from outside. The polyurethane coat is the better of the two solutions however the range of the polyurethane sensor is still only 8mM/l.

It may be possible to increase the range of the sensors by increasing the EH layer depth and then adding polyurethane. However, this would have the effect of increasing the size of the sensor. Also, the result of increasing the EH layer depth may not be linear, possibly causing a reduction in range, increase in response time or complex response to glucose concentration changes. As the current coating method created sensors of very similar and stable responses, it was decided to use a combination of both HEMA and polyurethane coats. This would minimise the size increase of the sensor, whilst increasing range sufficiently to cover the upper hyperglycaemic ranges.

6.15 Investigation of dip coated PO2 sensors with both HEMA and polyurethane outer coats

The variation between sensors constructed using the new dip coating technique and the effect of adding both a HEMA and polyurethane outer coat were now investigated.

Eight sensors, were made using the dip coating technique and given an outer HEMA coat. The sensors were tested and then coated in polyurethane and re-tested.

The first two of the sensors, 10c and 10d, were constructed identically to sensor 10a and tested. They were then coated in polyurethane, however due to a problem with the polyurethane, the concentration of which had increased in storage, the sensors failed to give useful data.

6.16 Extension of the range of sensors 10f to 10j using HEMA and polyurethane

Sensors 10f to 10j were constructed identically to sensor 10a, dried for one hour and dip coated in HEMA, they were then dip coated in HEMA twice more to form a triple HEMA layer. The sensors were then tested in the 7.5% oxygen tensions. Following testing, the sensors were then dried and dip coated in the new 4% polyurethane solution and then re-tested.

Sensor 10h broke during construction, and of the surviving fibre sensors, there is still a lot of variation, with two of the sensors having a range of 3mM/l and another of 6mM/l. After polyurethane coating, Sensor 10e fractured, Sensor 10g showed some contamination of the PBS by GOD, as the reference oxygen sensor showed a drop in the ambient oxygen tension of form 6.8 to 5.7 for glucose concentrations 0 and 15 mM/l respectively. Sensor 10j exhibited a very noisy signal and showed little response to glucose. After testing the sensors were dip coated in 4% polyurethane. The results of the sensors, which did not fail or showed cross talk, 10f, 10g and 10i, are shown in figures 60, 61 and table 30. A comparison of their performance before and after polyurethane coating is shown in figure 62 and table 31. The loss of so many sensors during construction is most likely a reflection of the fragile nature of the fibre-optic cables. The P7 oxygen sensing fibre is only ≈174μm in diameter (see section 6.12.1) and is consequently easily damaged by even slight mechanical stress during the dip coating technique.

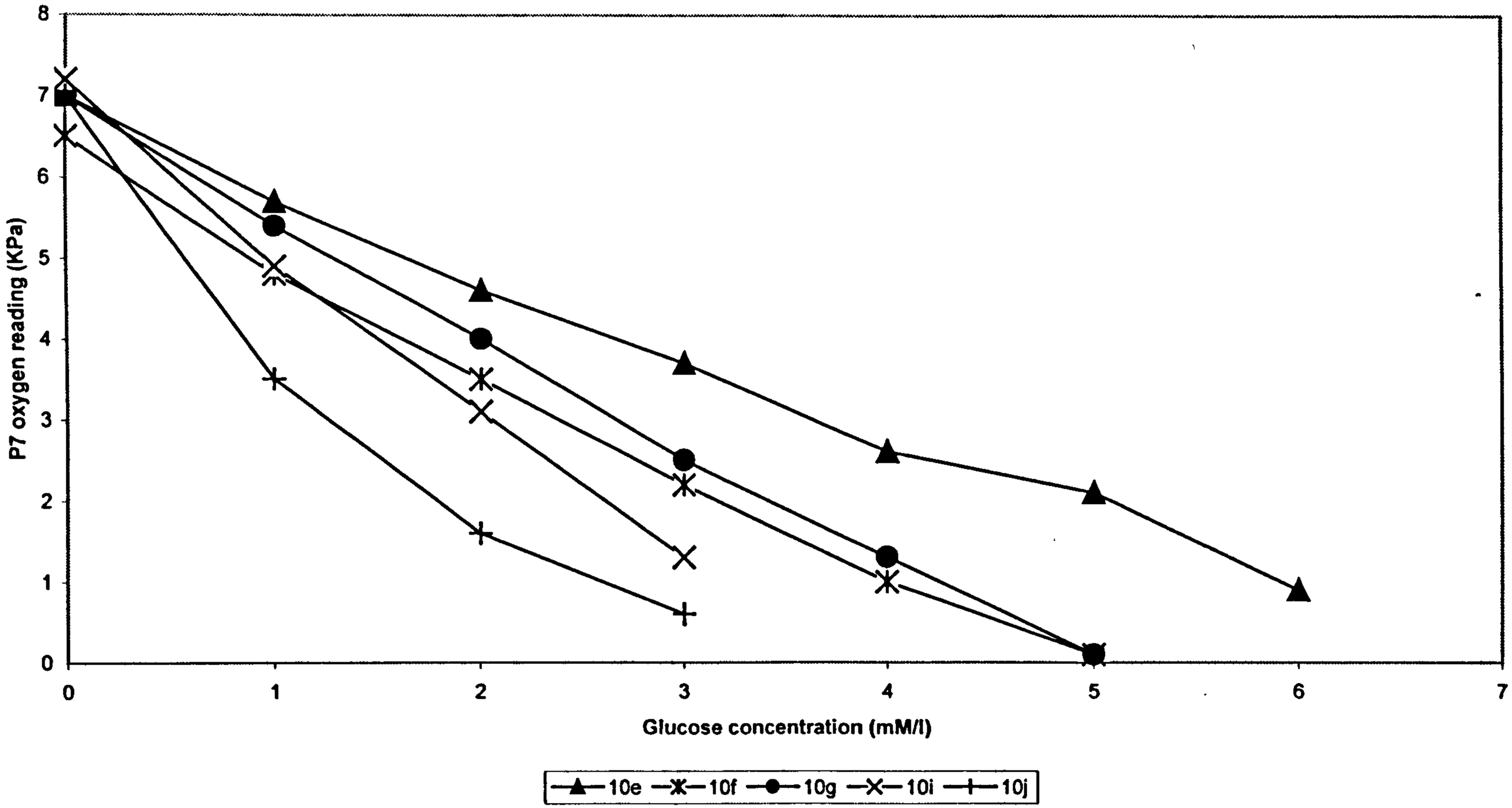

Figure 60. The response of the HEMA coated sensors 10e to 10j

Sensor	10e	10f	10g	10h	10i	10j
Operational range (mM/l)	0 to 6	0 to 5	0 to 5	Broken	0 to 3	0 to 3
Linear range (mM/l)	0 to 6	0 to 5	0 to 5	Broken	0 to 3	None
Sensitivity (over linear range) (KPa/mM/l)	1.0	1.0	1.4	Broken	2.0	None
Approximate 90% Response time (linear range) (seconds)	100 to 200	100 to 200	200 to 300	Broken	100 to 200	None

Table 30. The performance characteristics of sensors with a double HEMA coat 10e to 10j

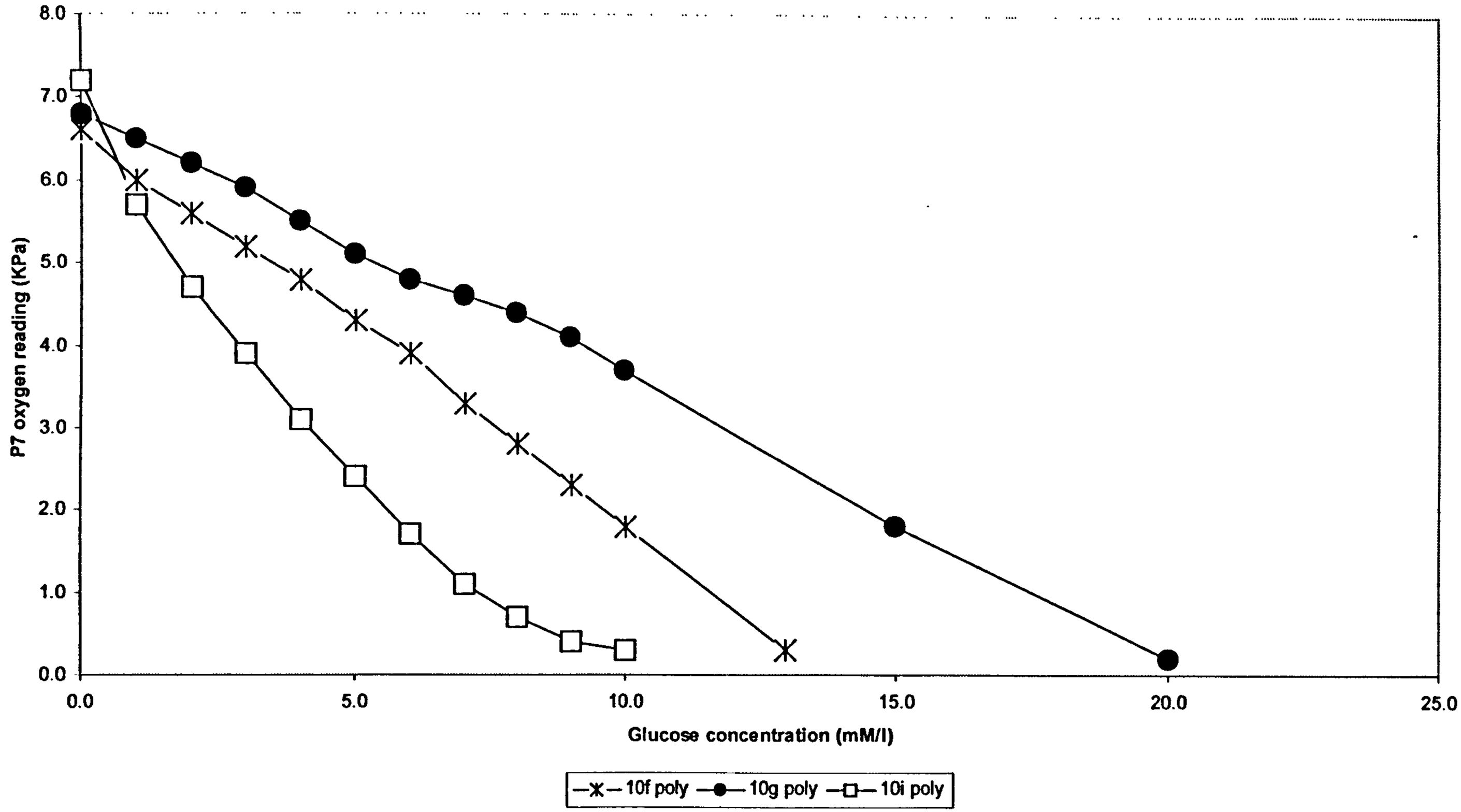

Figure 61. The performance of the sensors after coating with polyurethane

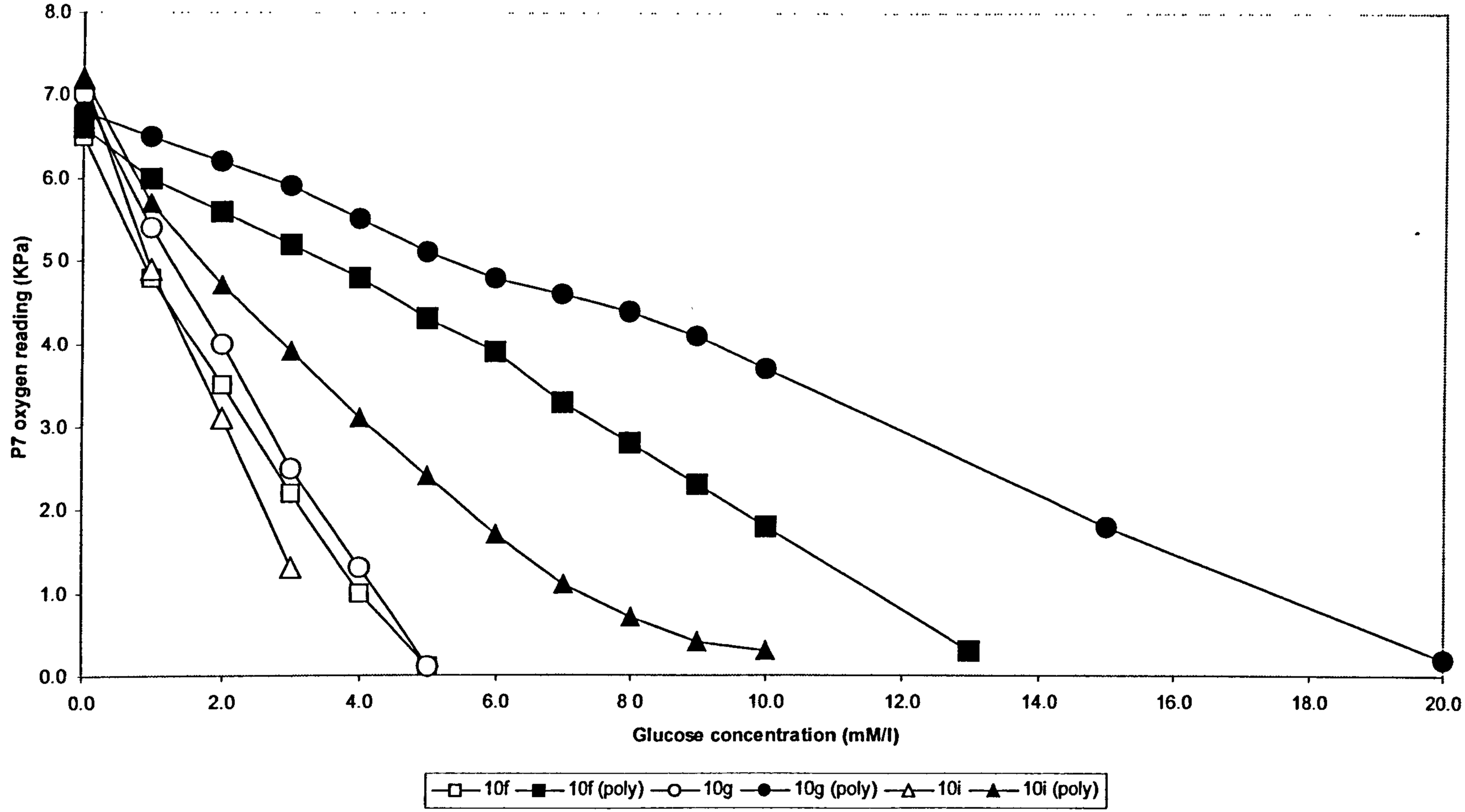

Figure 62. The sensors performance before and after polyurethane coating

Coating	HEMA	Polyurethane	HEMA	Polyurethane	HEMA	Polyurethane
Sensor	10f	10f	10g	10g	10i	10i
Operational range (mM/l)	0 to 5	0 to 13	0 to 5	0 to 20	0 to 3	0 to 10
Linear range (mM/l)	0 to 5	0 to 13	0 to 5	0 to 20	0 to 3	0 to 7
Sensitivity (over linear range) (KPa/mM/l)	1.0	0.5	1.4	0.3	2.0	1.0
Approximate 90% Response time (linear range) (seconds)	100 to 200	100 to 200	200 to 300	400 to 500	100 to 200	100 to 200

Table 31. The performance parameters of sensors 10f, 10g and 10i before and after coating with polyurethane

The dip coating technique and outer HEMA coating has produced sensors of similar range and 90% response times. The lack of correlation in response times and ranges is probably a product of the complex nature of the reaction-diffusion process occurring in the enzyme membrane layer. This complexity causes the sensors performance, range response time and linearity of the sensor to be non-linearly dependent on the membrane dimensions and composition.

The response times and sensitivity of the sensors were similar, although, there does not seem to be any correlation between range and response time. In table 31 it can be seen that for Sensor 10f, the range of the sensor doubles after polyurethane coating but the response time remains virtually unchanged. For Sensor 10i, polyurethane coating actually reduced the response time while increasing the range by a factor of three.

6.17 Gamma sterilisation of glucose sensors

Before the sensors can be implanted in vivo, they will need to be sterilised. The method of sterilisation used in the production of the P7 is exposure to gamma radiation. The sterilisation process involves exposure to 25 - 40 KGy of gamma radiation, however this also causes the optical fibre to become opaque. To redress this the sterilisation is followed by five days of heating at 55°C, by heating the fibre for this period the fibre regains its transparency.

6.18 The effect of gamma sterilisation on glucose sensors while dry

Following the completion of the previous experiments using sensors, 9b and 9c, (Section 6.13) the sensors were dried in air and posted to the Diametrics factory where they were forwarded to the gamma sterilisation facility. After 15 days, the sensors were returned from sterilisation and were re-tested. The sensors were not sterilised in PBS, as this removed the need to re-insert them into the tonometers, often leading to fractures. The response of the sensors was then compared to their response before sterilisation and with their response before coating with polyurethane.

6.18.1. The results of gamma sterilisation

The results of the tests of the sensors are shown in figures 63 and 64 for sensors 9c and 9d respectively. The characteristics of the sensors are shown in table 32. The gamma sterilisation has reduced the range of the sensors compared to the polyurethane tests.

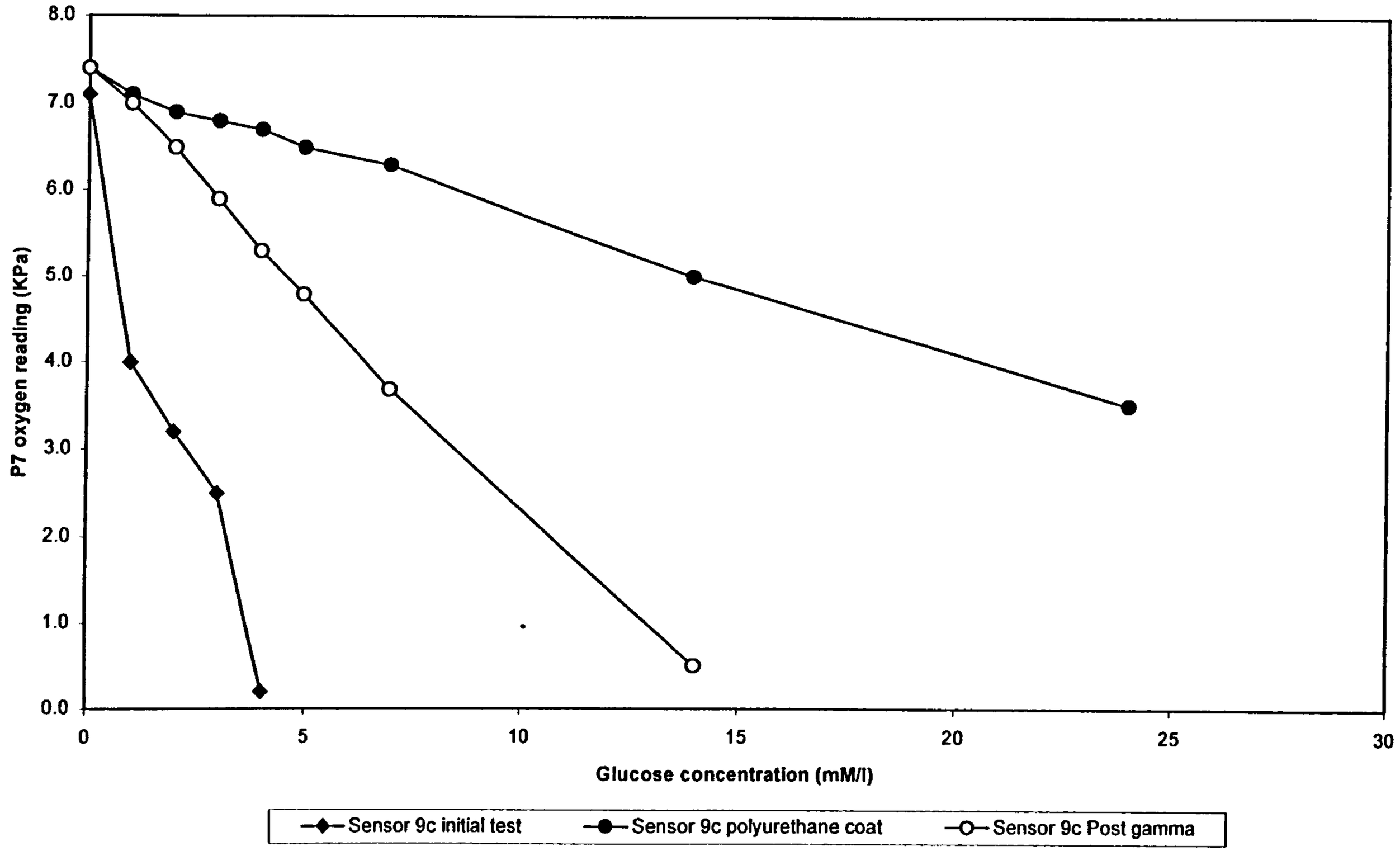

Figure 63. A plot of P7 oxygen reading against glucose concentrations for Sensor 9c for all of the experiments

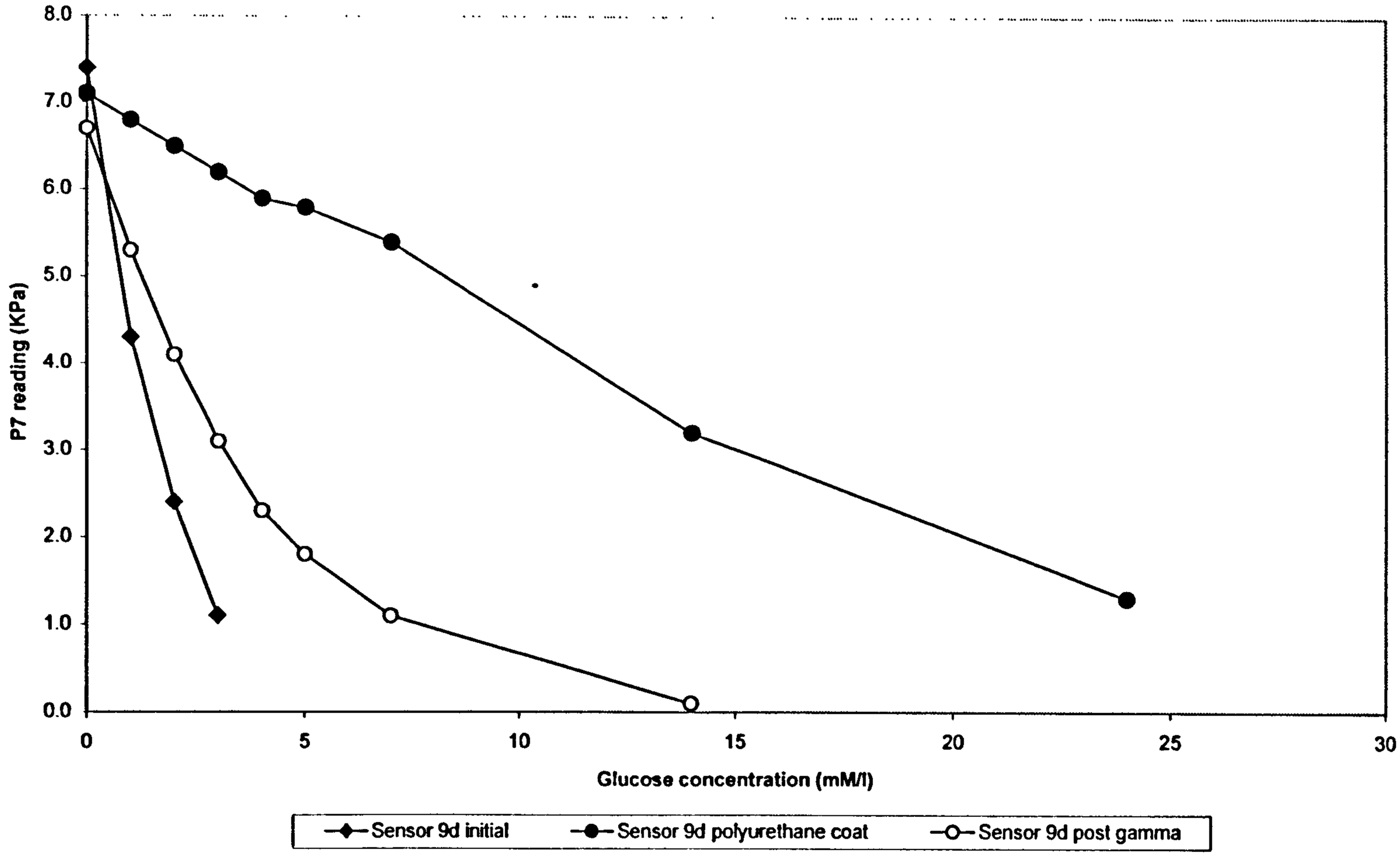

Figure 64. A plot of P7 oxygen reading against glucose concentrations for Sensor 9d all of the experiments

Coating	EH only		Polyurethane		Post gamma Sterilisation	
Sensor	9c	9d	9c	9d	9c	9d
Operational range (mM/l)	0 – 4	0 – 7	0 – 24	0 – 24*	0 – 14	0 – 14
Linear range (mM/l)	0 – 4	0 – 7	0 – 15	0 – 5*	0 – 14	0 – 4
Sensitivity (over linear range) (KPa/mM/l)	1.7	1.8	0.16	0.3	NA	NA
Approximate 90% Response time (over linear range) (seconds)	NA	<100	NA	NA	NA	NA

* noise level approaches sensitivity above this concentration.

NA – not applicable due to low sensitivity or the response of the sensor to step change.

Table 32. The response of Sensors 9b and 9c with and without polyurethane and following gamma sterilisation

The gamma sterilisation of the sensors has reduced the range of the sensor. The change in response times is less clear-cut with an increase for sensors 9c and a decrease for sensor 9d. This is most likely due to changes in the parameters of the membrane, mainly the diffusion coefficients, through chemical changes in the HEMA support, due to the complex nature of the reaction diffusion process. The polyurethane coat may also be affected, possibly increasing the area through which glucose can diffuse, hence lowering the range.

6.19 Gamma radiation sterilisation of the glucose sensors in PBS

The sensors have been shown to survive gamma sterilisation in a dry state. However, as the HEMA used in the sensor will swell when placed in PBS, this may cause changing in the sensors characteristics and introduce a measurement error. For this reason, the sensor will probably have to be in PBS so that it could be used immediately when needed.

To test the effect of gamma sterilisation in sensors in PBS six sensors were used, half were dispatched to be gamma ray sterilised in PBS. The remainder were kept refrigerated in PBS until the sterilised sensors returned and were the controls for the experiment. Six sensors 8a, 8d, 8e, 8f and 8g from the previous HEMA and polyurethane tests, (section 6.9), were used in this investigation.

Once all of the sensors had been tested, the six sensors were randomly split into two groups. Sensors 8a, 8d and 8f were returned to their calibration tonometers which had been filled with PBS and were posted to Diametrics Medical Ltd where they were forwarded to the gamma sterilisation facility. The remaining sensors, 8e and 8g, were also returned to their tonometers, which had been filled with PBS and were refrigerated until the other sensors returned from gamma sterilisation. These sensors were the control group for the experiment.

The time delay between the initial tests and the post sterilisation tests was approximately two months as the sensors had to be included in the scheduled sterilisation batch at the Diametrics facility. The seal on the P7 tonometer had to be removed to insert the sensors, as shown in figure 17.

6.19.1. The performance of the sensors following gamma irradiation in PBS

Upon the return of the sterilised sensors, all of the sensors were re-tested. When the control sensors were removed from refrigeration, it was found that sensors 8b and 8g appeared to be 'frozen' into their tonometers either from ice crystals or from salts from the PBS that had crystallised out in the neck of the tonometer. With the use of fresh PBS, the sensors were freed but both sensors failed to calibrate almost certainly due to breaks in the optical fibres caused by the crystal, or ice formations. However, sensor 8e was still operational and calibrated normally following removal from refrigeration. The results of the tests of the sensors before and after irradiation are shown in figure 65 and control in figure 66.

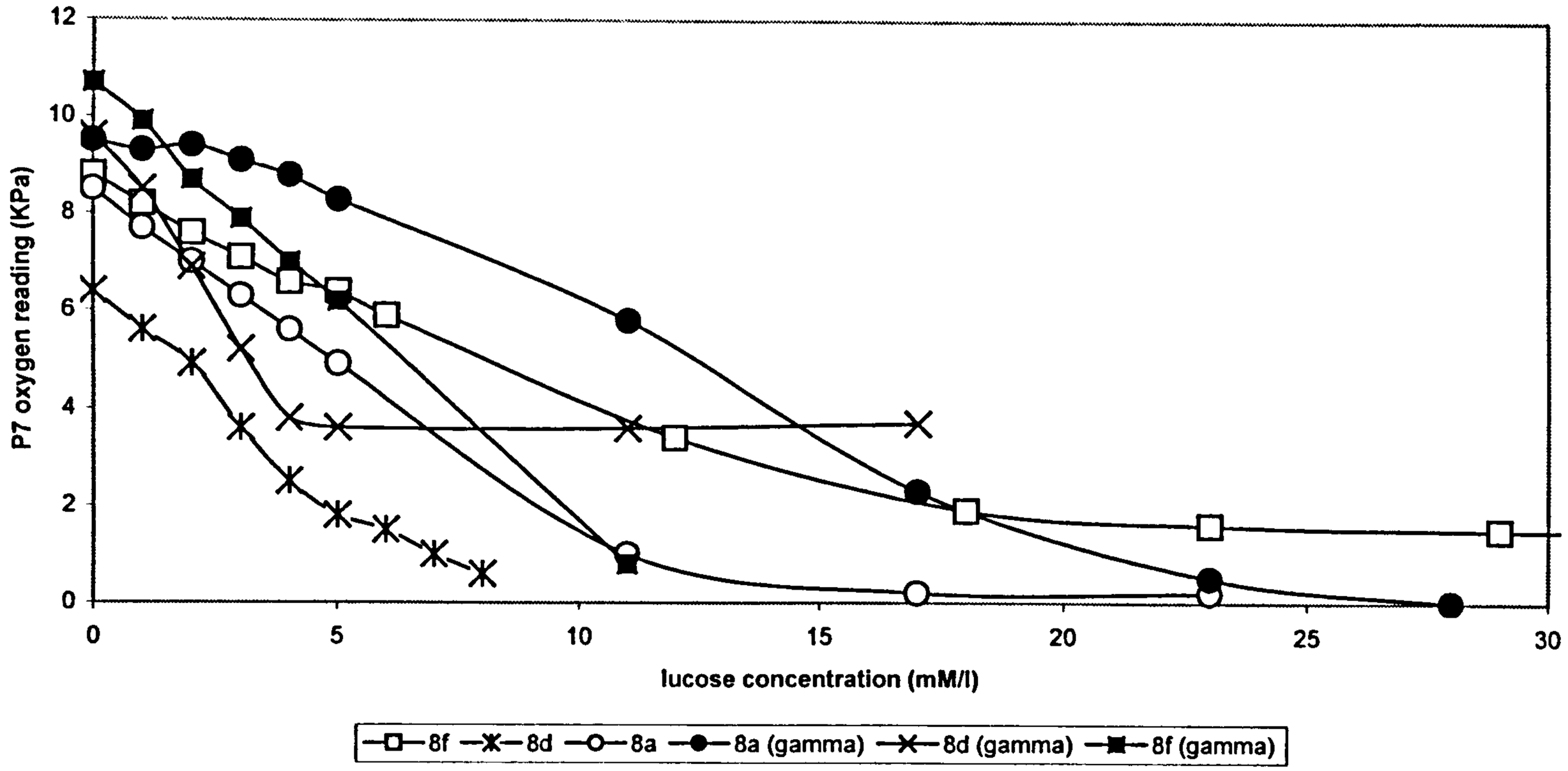

Figure 65. The response of the sensors following irradiation

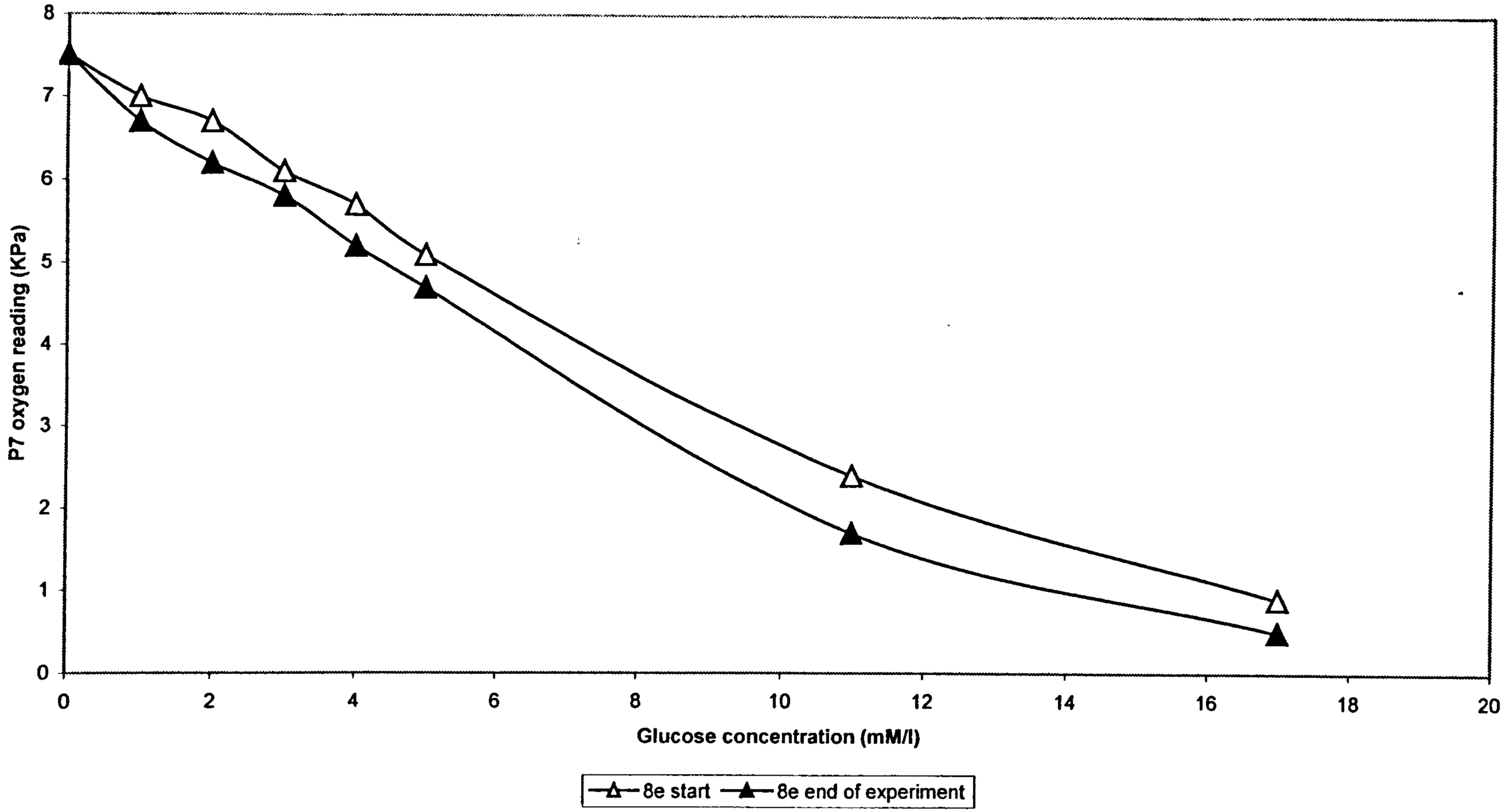

Figure 66. The performance of the control sensor at the start and end of the experiment

The sensors survived gamma sterilisation, although the process changes the performance of the sensors. The sensors are heated for five days above forty degrees (55°C), which also should destroy the GOD (section 2.2.5). However, immobilisation seems to have imparted thermal and radioactive stability on the enzyme, (section 2.3.5). Deactivation of large amounts of the enzyme, which would cause the sensor to operate in reaction-limited mode, is also possible, see Chapter 2. However, it is probably not the case as enzyme deactivation on that scale would probably destroy all of the GOD in the sensor, the chances of destroying just enough enzyme to leave the sensor partially operational are probably slim. The one surviving control showed good repeatability despite being stored for one month, indicating that the sensors have a good shelf life. However, due to the compromise of the watertight seal in the tonometer it is possible that the PBS in whole or part had leaked out of the P7 tonometer.

6.20 Gamma sterilisation of a dip coated PO2 sensor

Following the previous test of Sensor 10f, the sensor was rinsed, placed into the tonometer and posted to Diametrics medical to be sent for gamma sterilisation. The sensor was sterilised and returned one month later. In the previous experiments, the sensor was either sterilised dry, or in PBS, but with the watertight seals compromised to allow the sensors to be re-inserted into the tonometer without damage. This meant that the PBS solution may have leaked from the tonometer during transit.

In the previous experiment, the silicone watertight seal was removed from the tonometer to allow the sensor to be re-inserted. This meant that the solution inside the tonometer could possibly have escaped. So there is no guarantee that the sterilisation of the sensor was done wet.

To improve the experiment by ensuring that the PBS did not escape form the tonometer, the gas permeable vents were sealed with epoxy resin to prevent water loss through evaporation. The silicone washer, which was removed in the previous experiment, was cut in half to allow it to be re-fitted after the sensor was inserted into the tonometer. A piece of cotton was tied around it to allow the washer to be removed without damage to the sensor as shown in figure 67.

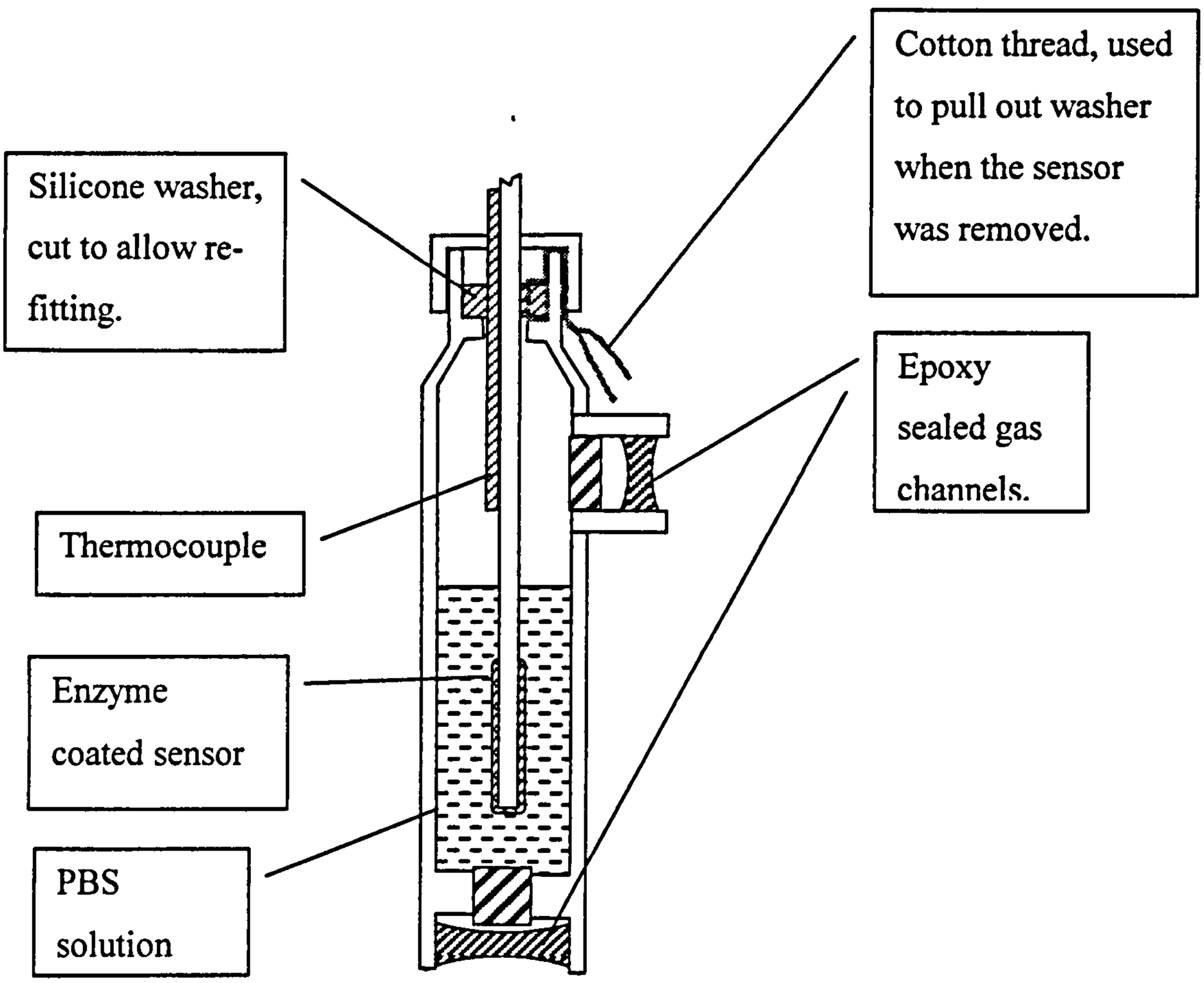

Figure 67. The modified P7 tonometer

6.20.1. Performance of the sensors after gamma sterilisation in PBS

After the return of the sensor, it was removed from the tonometer, manually calibrated and tested. The PBS remaining in the tonometer was removed using a hypodermic syringe and its volume measured at 3ml. This was a sufficient volume to keep the sensor wet during the sterilisation process. The results of the glucose calibration are shown in figure 68 and table 33.

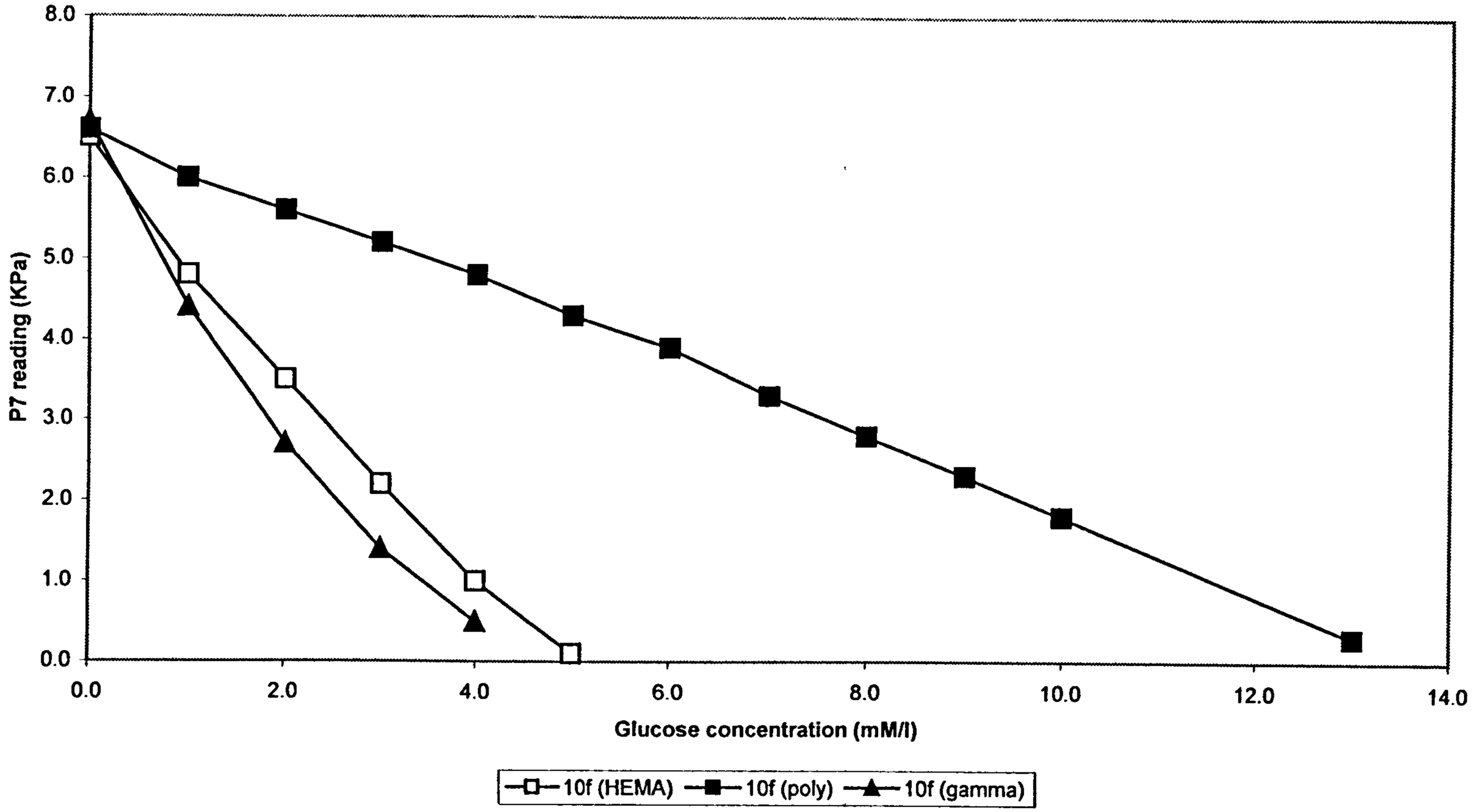

Figure 68. The response of Sensor 10f with a HEMA coat, a polyurethane coat and after gamma sterilisation

Sensor	10f (HEMA)	10f (poly)	10f (gamma)
Operational range (mM/l)	0 to 6	0 to 13	0 to 4
Linear range (mM/l)	0 to 5	0 to 13	0 to 3
Sensitivity (over linear range) (KPa/mM/l)	1.3	0.5	1.8
Approximate 90% Response time (linear range) (seconds)	100 to 200	100 to 200	NA

Table 33. The performance of sensor 10f before and after gamma exposure

The sensor has survived wet sterilisation with the reduction in range observed in previous sensors exposed to radiation. It was considered that the smaller volume of enzyme-layer might have caused the sensor to be more susceptible to the effects of irradiation than a larger one. As there was less enzyme in the sensor there is less spare enzyme, so any deactivation may quickly lead to the sensor working in reaction controlled mode. The effects observed could also have been caused by the destruction of the polyurethane.

6.21 Shelf life tests of dip coated PO2 sensors

To be of use as a practical glucose sensor, the sensor will have to be stored probably for extended periods in the order of three months. To investigate this testing, Sensor 10i was stored in refrigerated PBS for two months and then re-tested. Two further sensors, 10f and 10g, were stored for three months and then re-tested. The performance of the sensors before and after storage was then also compared. The performances of the three sensors before and after storage are shown in figure 69 and table 34.

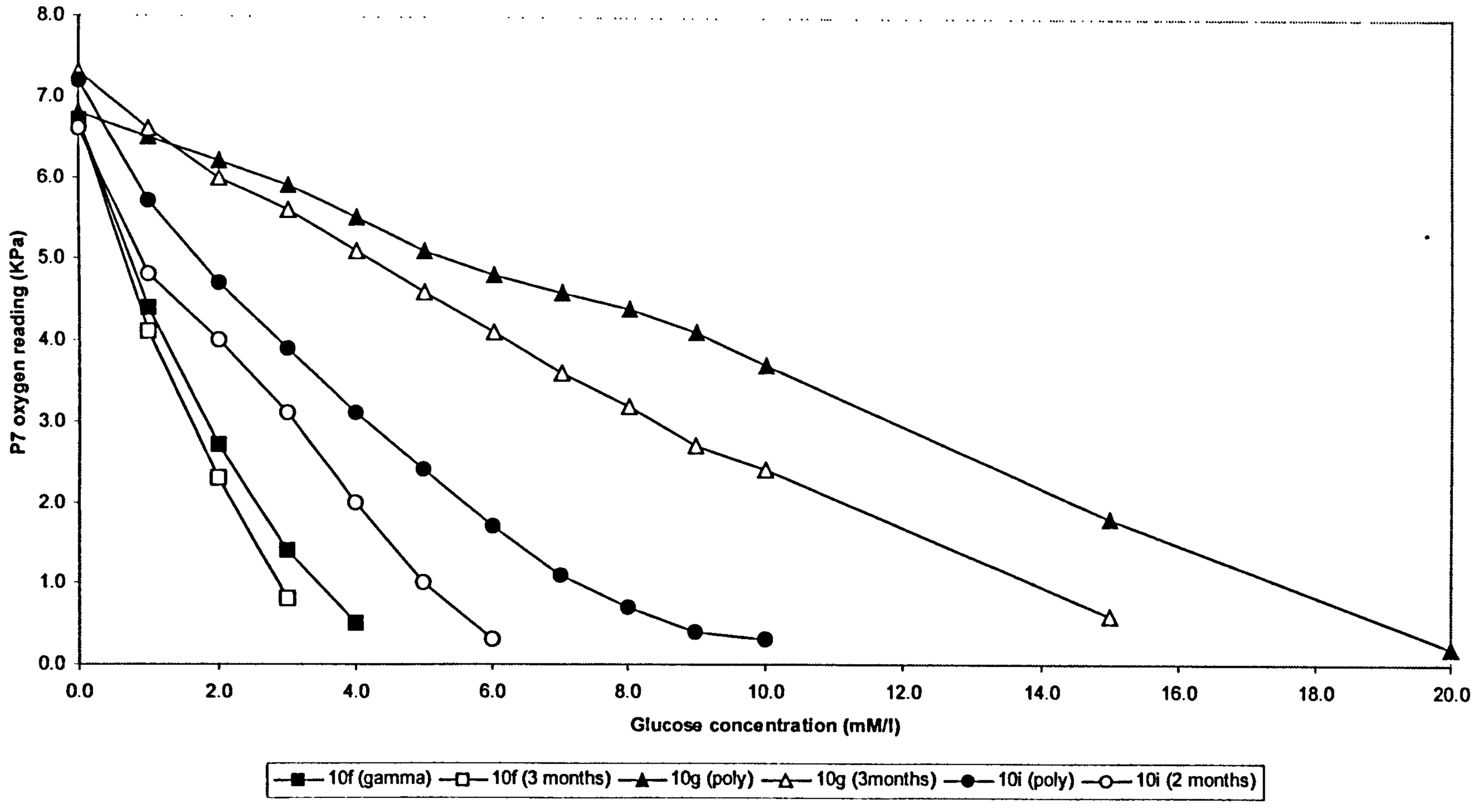

Figure 69. The performance of sensors 10i, 10f and 10g before and after storage

	Initial	3 months	Initial	3 months	Initial	2 months
Sensor	10f	10f	10g	10g	10i	10i
Operational range (mM/l)	0 to 4	0 to 3	0 to 20	0 to 15	0 to 10	. 0 to 6
Linear range (mM/l)	NA	0 to 3	0 to 20	0 to 15	0 to 7	0 to 6
Sensitivity (over linear range) (KPa/mM/l)	NA	2.0	0.3	0.5	1.0	1.1
Approximate 90% Response time (Average of 0 to 5 mM/l of max linear range) (seconds)	NA	100 to 200	400 to 500	200 to 300	100 to 200	100 to 200

Table 34. The performance parameters of sensors 10f, 10g and 10i before and after coating with polyurethane

The sensors performance had degraded in all three cases, although the range of the sensors had not degraded to the point where they could not be used as a potential glucose sensor. After storage, the 90% response times for the sensors decreases for sensors 10f and 10g but increased for sensor 10i. This is probably an illustration of the non-linear nature of the reaction taking place in membrane layers.

6.22 Effect of 24-hour operation on sensor performance

The sensors will have to operate from between 12 and 24 hours to provide nocturnal monitoring and to minimise the number of times the sensor is changed when in operation. To investigate the effect of 12 and 24 hour operation on the sensor performance characteristics, two sensors, 10g and 10i, were operated for 24 hours in 5mM/l of glucose.

After the conclusion of the previous experiments, two sensors, 10g and 10i were rinsed with distilled water and placed in PBS containing 5mM/l of glucose in 7.5% oxygen for a 24-hour period. At the end of the 24 hours the sensors were re-calibrated and re-tested. Their performance before and after the 24 hour run was then compared.

The performance of both sensors had changed after the 24-hour run as can be seen in figure 70 and table 35. Sensor 10g showed the greatest change, with its maximum range dropping form 15 to 11 mM/l, Sensor 10i actually shows an increase in range form 6 to 7 mM/l. The response time of sensors 10g and 10i, shown in table 35 has reduced.

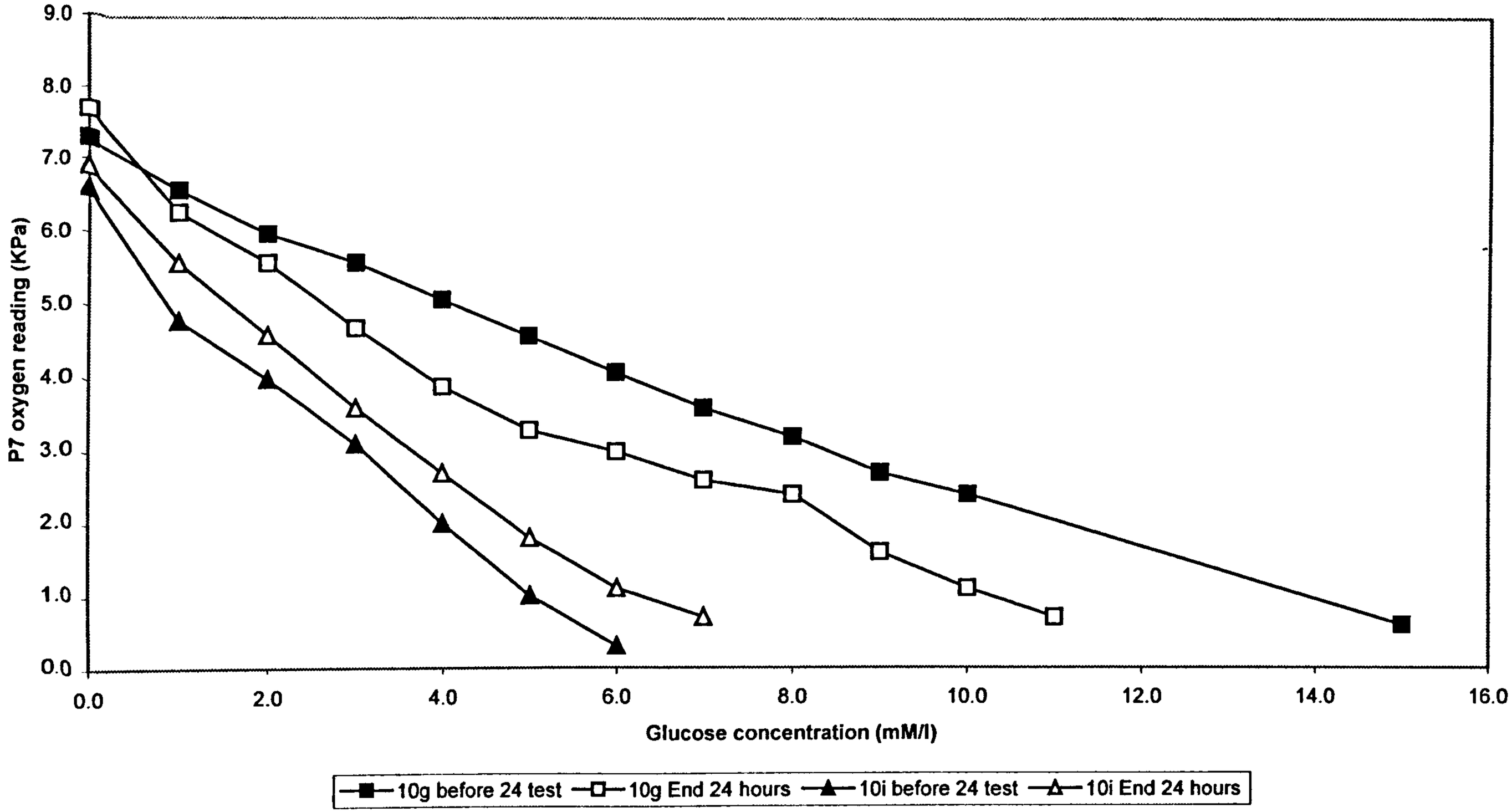

Figure 70. The response of the two sensors before and after 24-hour operation in 5mM/l

	Pre 24 hour run	Post 24 hour run	Pre 24 hour run	Post 24 hour run
Sensor	10g	10g	10i	10i
Operational range (mM/l)	0 to 15	0 to 11	0 to 6	0 to 7
Linear range (mM/l)	0 to 15	0 to 5	0 to 6	0 to 6
Sensitivity (over linear range) (KPa/mM/l)	0.5	0.9	1.1	1.0
Approximate 90% Response time (Average of 0 to 5 mM/l of max linear range) (seconds)	200 to 300	200 to 300	100 to 200	100 to 200

Table 35. The performance parameters of sensors 10g and 10i before and after 24 hour operation

The effects of the 24-hour run on the sensors are significant enough to necessitate a recalibration at least once during this period if this were an in vivo situation. The effect of 24-hour exposure to the glucose solution on the sensors is unclear. The changes cannot be attributed to calibration drift in the P7 sensor, as response times have changed with range. A calibration drift may change the range of the sensor by lowering or increasing the oxygen reading, but this would not affect the response time. Two other possible explanations are deactivation of the enzyme, pushing the sensor into a reaction-diffusion limited state, (Chapter 2) or some structural change in the membrane that is changing the mass transport resistance values. Either way, the error in measurement is sufficient to require recalibration at regular intervals of every six hours.

6.23 Summary of the sensor development and testing

6.23.1. The initial experiments on a standard P7 sensor

The initial glucose sensor (sensor 1) was made by dip coating the complete P7 sensor bundle in a GOD and HEMA mixture. This was then tested in a 15% oxygen tension at 37°C and pH 7.4. The sensor was found to have a range of 0 to 4mM/l with a 90% response time of <100 seconds. This range was extended using an outer coat of HEMA, which extended the range to 7 mM/l with no increase in response time. However, the sensor was found to have a range and sensitivity (1.1 to 0.4 KPa/mM/l) after 12 hours in a solution at 6mM/l. Catalase was added to the enzyme HEMA mixture in Sensor 2 to improve the design. Sensor 2, although performing well to increasing glucose concentrations, failed to show a response to decreasing glucose concentrations. Sensor 3 was made with a thinner outer HEMA coat than its predecessor and was shown to respond to decreasing glucose concentrations. A second oxygen sensor was used with Sensor 4 to provide a differential oxygen measurement. Initially this experiment indicated that GOD was leaving the HEMA layer and dissolving into solution. After rinsing with PBS solution this problem was resolved and the sensor was tested to up to 4 mM/l.

6.23.2. Coating of the enzyme HEMA mixture directly onto the P7 oxygen sensing fibre

A glucose sensor (Sensor 5) was then made by splitting open the P7 sensor bundle and coating the oxygen sensing fibre (PO2) directly. A riadially-symmetric sensor design was then made by enclosing the GOD, CAT and HEMA in a MPHF sleeve (Sensor 6). This sensor had a maximum range of 2 mM/l and was shown to respond to decreasing concentrations with T90 of <100 to increasing and decreasing concentrations. Sensors were then constructed using a different technique, which involved coating the PO2 sensors of the P7 sensor directly with HEMA, CAT and GOD. The coating technique produced a sensor (Sensor 7) with

an operational range of 6 mM/l and a 90% response time <100 seconds. A variation of this coating technique was used to produce Sensors 8a to 8g. This technique involved coating all four of the sensors in HEMA, GOD and CAT. This technique produced a wide variation in sensor performance with sensor ranges from 3 to 10mM/l.

6.23.3. The application of polyurethane for improved performance in low oxygen tensions

Two of these sensors (8a and 8g) were then improved by coating the sensors with polyurethane. The polyurethane coating increased the range of the sensors from 3 and 7mM/l to 21 and 17mM/l respectively. However, the signal produced by these sensors exhibited a large amount of noise in their signal. The sensors were also tested in both 7.5 and 15% oxygen tensions to investigate their performance in varying oxygen tensions. The profiles of the sensors were found to be similar in both oxygen tensions, suggesting an immunity to background oxygen variations. Following this experiment, all of the sensors were tested in 7.5% oxygen tensions as this better reflected the oxygen environment of the subcutaneous tissue.

6.23.4. An enzyme coating technique using an absorption method

The coating technique was then improved to allow a dip coating approach; this involved the removal of the pH and CO_2 sensors and the dip coating of only the PO2 sensor. Initially the sensors (9a) had a range of only 1mM/l. A new coating technique was tested which used an absorption coating technique where HEMA was applied to the surface of a PO2 sensor and then GOD and CAT absorbed into it from solution. This produced a sensor (Sensor 9b) with a range of 15 mM/l in 7.5% oxygen. The sensor was then coated in polyurethane but showed a spurious response following coating.

6.23.5. Improvement of the dip coating technique to optimise sensor performance

The dip coating technique was then optimised using a laser micrometer to measure the depth of the enzyme layer deposited. It was found that an enzyme layer of as thin as ≈60μm thick could be deposited using this new technique. This new optimised coating technique was then used to construct a sensor (9c) that had a range of up to 4mM/l. Sensor 9c and a second sensor (9d) constructed using the same method were then coated in polyurethane to extend their range. The polyurethane increased the range of the Sensor 9c from 4 to 24mM/l and sensor 9d from 7 to 24 mM/l, although the signal from the polyurethane coated sensors was noisy. Sensitivity for Sensor 9d changed from 1.8 to 0.3 KPa/mM/l after coating the response time, where it could be discerned, was <100 seconds for Sensor 9d before coating. Six sensors 10e to 10j were then created using the dip coating technique and the variation between sensors examined. Variations in performance were found, with sensing ranges from 10 to 20mM/l following coating with polyurethane.

6.23.6. Sterilisation of the sensors using gamma irradiation

Two sensors, 9c and 9d were then gamma sterilised while dry, both had an initial maximum range of 24mM/l. Following sterilisation with 25-40KGy gamma radiation the range of both sensors was reduced to 14 mM/l, although the performance profiles of the sensors were not identical. Sensors 8f, 8d, 8a and 10f were then gamma sterilised while in PBS solution, with similar results, the range of Sensor 10f for example, was reduced from 13 mM/l to 4 mM/l.

6.23.7. Investigations of the shelf life of the sensors

The effect of storage in refrigerated PBS for up to three months was then investigated using three sensors. The storage caused a decrease in range from 4 to

3mM/l (sensor 10f), 20 to 15mM/l (sensor 10g) and 10 to 6mM/l (sensor 10i). Response times were reduced in one case but unchanged in the second case, the third sensor's response was not linear so no response time was measured.

6.23.8. The effect of 24-hour operation on the sensors

Sensors 10g and 10i were finally tested over a 24-hour operation period in 5mM/l of glucose. It was found that the range of the sensors was reduced from 15 to 11mM/l for Sensor 10g and increased from 6 to 7mM/l for Sensor 10i. The response times for both sensors remained unchanged at between 200 to 300 seconds for Sensor 10g and 100 to 200 seconds for Sensor 10i.

7 Overall summary and conclusions

7.1 Introduction

In this chapter, the objectives of the research are briefly reviewed and the research carried out to fulfil these goals is summarised. The performance of the sensors produced is then evaluated and compared to the research goals. Limitations of both the sensors produced and the experimental method used to develop and test them is then discussed. The glucose sensor system produced is then compared with the general field of blood glucose sensors described in the literature. A comparison is then carried out between this sensor system and the most closely related fibre-optic sensors that have been developed by other groups. Finally, areas of further work on the research are considered and the contribution of the research to the field of blood glucose sensors is discussed.

7.2 Review of the goals of the research

The objective of this research was to develop a sensor capable of continuously and reliably monitoring blood glucose levels to improve the management of type I diabetes. Its development could help reduce or prevent both the long-term complications and hypoglycaemic episodes of insulin treated type I diabetes.

Rather than an investigation of the glucose sensing technology, the research was aimed at producing a practical glucose sensor that could possibly be put to clinical use as quickly as possible if the development proved successful. To this end the Paratrend 7 oxygen sensor was chosen as it was already in clinical use and therefore clinically safe and reliable. This sensor provided a solid core technology around which the glucose sensor could be developed without concerns about the reliability, safety or performance of the oxygen sensor.

As discussed in Chapter 1, for such a sensor to be of use it was decided that the sensor should fulfil various performance requirements. Briefly, these were a measurement range of 0 to 25 mM/l with a resolution of 1mM/l and an error no greater than 10% of the total signal (above 2.8mM/l). The 90% signal response time was required to be below 240 seconds and the sensor, if an implanted needle type, was to be no larger than 0.5 mm in diameter. As well as these requirements the sensor was to be sterilised, operate for between 12 and 24 hours and have a shelf life of the order of 3 months.

7.3 Summary of the research carried out

A commercial fibre optic oxygen sensor (Paratrend 7, Diametrics medical Ltd) was modified into a glucose measurement system capable of fulfilling all of the requirements stated above. From a crude prototype, the sensor design was developed into a ≈300μm diameter needle style fibre optic glucose sensor, which could withstand sterilisation by gamma radiation and still operate. The same design was shown to survive storage for up to three months followed by operation for 24-hours and still measure glucose concentrations well enough to detect hypoglycaemic episodes. The sensor design incorporated two active enzymes, glucose oxidase and catalase, a HEMA support matrix. HEMA and polyurethane diffusion controlling membranes were developed and incorporated into the sensor to increase the range and reduce sensitivity to background oxygen fluctuations. An experimental system capable of recreating physiological oxygen, temperature and pH conditions was constructed and used to test the sensors.

7.4 The performance of the glucose sensor produced by the research

The performance requirements of the sensors were described in detail at the start of the thesis, in this section these aims and what was achieved are compared.

7.4.1. The range and resolution of the sensors produced by the research

The first sensor performance goal to be considered will be the range of the sensor. A sensor with a range of up to 25 mM/l, see table 2, Chapter 2, was aimed for. With the crude dip coating techniques used in this research, there was an uncontrollable variation in the enzyme membrane dimensions and therefore the range of the sensors produced. Some sensors demonstrated high sensitivity but low maximum range, with one Sensor, 10a, having a maximum range of 1mM/l with a resolution down to ≈0.1 mM/l, others could measure glucose concentrations of up to 24 mM/l (Sensor 9d) with reduced sensitivity. This range is equal to or better than that observed with the electrochemical and fibre optic glucose sensors discussed in Chapter 2. However, most of those sensors were tested in atmospheric oxygen tensions, whereas in this research the sensors were tested in low oxygen tensions in order to replicate the subcutaneous environment. The other sensing techniques, such as NIRS and microdialysis, have also been shown to cover similar ranges to this sensor.

The range and sensitivity of this sensor design and all oxygen based GOD based designs are inextricably tied together. As described in Chapter 3, the glucose concentration is calculated from the decrease in oxygen tension, measured as the glucose concentration increases. The initial oxygen tension is the ambient of the environment of the sensor. In the case of this experimental work, the ambient oxygen tension of the sensor was at 7.5 KPa (for the later experiments). This means that the entire glucose range being covered must be effectively divided up into 7.5 KPa. This problem is further complicated by the fact that the Paratrend 7

performance specifications give a lower measurement limit of 2.7 kPa (table 6). Although in the experimental work it was observed that the sensor appeared to continue functioning below this tension, however, the validity of these values is uncertain. This leaves only the oxygen tension region form 2.7 to 7.5 kPa, a total of 4.8 kPa, to cover the entire glucose range. If we were to attempt to build a sensor that could cover the range 0 to 25 mM/l this would mean that the oxygen sensor would have a sensitivity of 4.8/25 or 0.192KPa/mM/l.

The next consideration in the resolution of the sensor is the error in the P7 oxygen measurement. Initially the in vivo performance characteristics of the sensor, table 7, Chapter 5, would seem the best indication of the error in a sensor operating in an in vivo environment. However, these values, in particular the precision of 13.2%, are calculated from the differences between the blood oxygen tension measured using the reference method and those reported by the P7. Differences in these measurements can be caused by many physiological factors; for example, placement of the sensor into the wall of the blood vessel as opposed to the centre of the vessel or coating of the sensor surface with biological material that would create a diffusion barrier to oxygen. It is unlikely that errors resulted from interference from other gasses as the sensor is unaffected by gasses found naturally occurring in the blood stream and its hydrophobic coating prevents analytes in solution from entering the sensor. In its application here, as a glucose sensor core, the P7 oxygen sensor is only being used to measure the oxygen tension in its immediate environment, in this case around ≈100-200μm, from its surface. This means that none of the physiological effects that probably played a role in the in vivo errors will be relevant and therefore the in vitro sensor test results, table 6 chapter 5, are the correct ones to apply to any calculations of accuracy. This will mean that the measurement error is now reduced to 5% from 13.2% (tables 6 and 7, chapter 5).

However, there is another consideration in calculating the error, as the proposed sensor was to use a second oxygen sensor as a reference to compensate for variations in environmental oxygen tensions. In the case of this reference oxygen

sensor, the in vivo results may be more relevant. The reference sensor is only being called upon to measure the oxygen tension, inside the MPHF coating, not the true environmental oxygen tension. So again, the in vitro measurements are probably more relevant.

The use of the reference sensor will also increase the possible error in the measurement. As there are now two sensors, an oxygen sensor with a possible error of 5% and the glucose sensor with a 5% error in its oxygen core measurement and then a further error caused by the response of its enzyme membrane.

This means that there is, in the worst-case scenario a possible error of a minimum of 10% of the true oxygen value in any single measurement. However if the sensors readings were averaged over time, say 30 seconds, with one measurement per second, this would allow 30 measurements to be averaged, and the error could then be reduced.

Considering a glucose sensor with a measurement error of 10% in the oxygen tension measurement, assuming a glucose sensor and oxygen reference sensor with a 5% error each (table 6, chapter 5). As the oxygen tension measured is inversely proportional to the glucose concentration the largest error will occur at the lowest glucose concentration. Therefore, at 0 mM/l of glucose, the oxygen tension measured at both the reference and the glucose sensor will be 7.5kPa. A 5% error in each sensor will give a oxygen tension range of 7.5 ± 0.4 kPa, the largest error that will be encountered. Assuming the worst-case scenario, this gives a total error in the oxygen tension measurement of at least 0.8 kPa.

So if a sensor was constructed to cover the full range from 0 to 25 mM/l the maximum error would be 0.8/0.192 = 4.2mM/l. This would obviously be a dangerous error. If however, two sensors were used, one to cover low glucose concentrations (0 to 10 mM/l) and the second to cover higher levels (10 to 25 mM/l). The lower range sensor (0 to 10 mM/l) would give a sensitivity of 4.8/10 =

0.48 kPa/mM/l. At the maximum error at 7.5 kPa i.e. 0 mM/l glucose concentration the error would be 0.8/0.48 = 1.7 mM/l. This is above the 1 mM/l error limit aimed for at the beginning of the thesis but is still small and will decrease with increasing glucose concentration. For example at 5 mM/l the error in the glucose sensor would be (7.5-(5x0.48))x0.05 = ±0.26 kPa and for the oxygen reference the error would be ±0.4 kPa. This gives a total maximum possible error of ±0.66 kPa which equates to ±1.4 mM/l. For the sensor covering the upper concentrations, the errors are less significant as the concentration of glucose is higher, i.e. they are a smaller percentage of the glucose concentration. For example, the sensor covering the range 10 to 15mM/l will have a sensitivity of 4.8/15 = ±0.32 kPa/mM/l. At 20 mM/l the error in the oxygen tension will be (7.5-(10x0.32))x0.05 = ±0.22 kPa, with a reference error of 0.4kPa this gives a total possible error of ±0.62 kPa which equates to ±1.3 mM/l which is only 6.5% of the glucose concentration measured.

Sensors that covered this range 0 to 10 mM/l between 7.5 and 2.7kPa were constructed; namely sensors 9d (after coating with polyurethane) and 8a (following gamma irradiation). Others sensors had a similar range but invaded the 2.7 to 0 kPa zone namely 8f (with polyurethane coat), 10i (with polyurethane coat), 10f (with polyurethane coat). Comparing this to the other fibre optic sensors, the multiple sensing sight sensor created by (Li and Walt 1995 ; Healey, Li et al. 1997) had an accuracy of 0.6mM/l but only covered the range of 0 to 2 mM/l and, like the other sensors, this sensor was tested in much higher concentrations of oxygen than this sensor. The electrochemical sensors have problems with interference from other blood constituents that have to be considered when their accuracy is calculated. Disregarding this however, these types of sensor have been shown to have resolutions equal or better than this sensor. The exudate and microdialysis sensors have also been shown to have similar or better resolution but are hampered by the delay in signal response. Although in some cases the NIRS has similar resolution the random interference they suffer makes them unreliable as a means to measure blood glucose

concentrations. The other techniques, such as PAS and kromoscopic analysis have insufficient data published to make comparisons.

Hysteresis in the sensor response is another potential source of measurement error. This was highlighted in the tests of sensor 7, section 6.7, where a glucose sensor was cycled through a glucose increase followed by a decrease and followed a hysteresis loop. Due to the complex nature of the reaction diffusion process at work in these sensors it is difficult to predict if hysteresis is likely to play a significant role in their behaviour. However, if it is present it could be a serious source of error, particularly following large changes in the blood glucose levels as the sensor would fail to return to a true value.

7.4.2. The response time of the sensors produced

Nearly all of the sensors produced demonstrated 90% response times well inside the 240-second limit. Some sensors showed response times in the order of below 100 seconds (9d). However, the majority operated in the 100 to 200 second range. The response time of the sensor is dependent on the dimensions and structure of the enzyme membrane through the diffusion resistance that the membrane puts up to glucose and oxygen. A membrane with a higher permeability should allow the membrane to equilibrate with its surroundings more quickly.

Some of the sensors were observed to reach their 90% response in below the 180 seconds limit of the P7 sensor, this was probably due to two reasons. Firstly, the values given for the performance of the Paratrend 7 are deliberately conservative for reasons of safety. Secondly, the removal of the MPHF coat and acrylimide filling would reduce the diffusion resistance to oxygen of the system, allowing it to respond to changes in the oxygen tension more quickly. The response times of the sensor presented here are superior to the exudates and microdialysis systems. Compared to the electrochemical and fibre optic sensors, similar response times are seen or in some cases are superior as in Rosenzweig and Kopelman 1996, whose sensor showed a response of 1.5 seconds due to its small size. The NIRS and PAS systems, in theory, can make measurements in a matter of seconds also depending on the equipment being used to collect the optical or acoustic signal.

7.4.3. Storage of the sensors and 24 hour operation

The requirements for the sensors to survive storage for 3 months were investigated using sensors 10f, 10g and 10i. All of these sensors showed a change in performance after storage. The reason for the changes in performance could have been due to enzyme diffusing out of the membrane into the storage solution. If this were the case, the loss of enzyme may have changed the operation of the

sensor into reaction controlled mode, or altered the diffusion resistance of the membrane to glucose and oxygen. The enzyme could also have been deactivated by some chemical process in the solution during storage, this would also possibly lead to the sensor moving to a reaction controlled mode of operation. Alternatively, the changes in performance could have been due to some long-term alterations in the structure of the HEMA or polyurethane membranes. This again would have led to alterations in the diffusion characteristics of the sensor and therefore its performance profile. There was no change in the response times of the sensors indicating that perhaps they are not operating in a reaction controlled mode where response time is dependent on glucose concentration, see Chapter 3.

If the sensors were operating in reaction controlled mode it would explain the changes in sensor operation in the following 24-hour operation test. However, this could also have been caused by deactivation of the GOD by hydrogen peroxide generated during the 24-hour operation.

The changes encountered during storage would have to be removed or reduced in a practical sensor. This could probably be achieved through a better immobilisation of the enzymes in the membrane using a longer soaking in glutaraldehyde or the use of a more efficient immobilisation technique. In addition, the enzyme loading of the membrane could be increased to allow more spare capacity in the system to handle enzyme loss or deactivation. From a safety point of view, the loss of enzyme into the body would not be acceptable as it would probably trigger an immune system response to the sensor, threatening both sensor operation and patient safety.

Compared to the other similar sensing technologies, i.e. electrochemical and fibre optic glucose sensors, this sensor's 24 hour operation was shorter than expected. Electrochemical sensors have been built which operated for several weeks in in vivo situations. Other fibre optic sensors have been shown to operate for several days before failing. This quickly reduced operational range of the sensor could be the result of insufficient loading of GOD into the membrane layer causing

deactivation of the enzyme which affected the sensors performance. Alternatively, the diffusion limiting membranes could have prevented the hydrogen peroxide from quickly leaving the sensor causing it to build up and deactivate the GOD despite the action of the CAT.

7.4.4. Sensor dimensions

Individual glucose sensors could be made with diameters from between 0.26 and 0.30 mm in diameter as was shown in section 6.12. However, the final glucose sensor will have to include a reference oxygen sensor and a temperature sensor enclosed in an MPHF sleeve. The combination of these sensors with the MPHF sleeve will probably be slightly larger than the 0.5 mm diameter aimed for at the beginning of the research. The size of the sensor could probably be further reduced through the use of a more precise enzyme membrane coating technique and a membrane with an increased mass transport resistance to glucose. The sensor size is comparable to its counterpart electrochemical and fibre optic sensors apart from (Rosenzweig and Kopelman 1996), which was only 100μm in diameter but was not constructed for in vivo operation.

7.4.5. Sterilisation of the sensors

The gamma sterilisation experiments proved an unexpected success with all of the sensors sterilised, either dry or in PBS surviving. It was expected that exposure to such radiation levels (20-40 KGy) and heating at 55°C for five days would destroy the enzymes in the sensors. However, although showing degradation in performances, which were probably due to structural changes in the HEMA and polyurethane matrices, the sensors did function. The cross linking of the GOD and CAT using glutaraldehyde probably played a role in helping the enzymes survive these conditions by allowing the enzyme to absorb the thermal energy and radiation without being denatured. The increased thermal stability has been described in the literature, see Chapter 3. The presence of catalase may have also

played a role in breaking down any hydrogen peroxide created by the process before it could damage the GOD in the enzyme layer (Bobbioni-Harsch, Rohner-Jeanrenaud et al. 1993; Woedtke, Julich et al. 2002).

7.5 Limitations of the experimental work

With only two P7 sensor base units, it was only possible to test one sensor and reference at a time. Although the basic principles of operation of the P7 oxygen sensor were available, as described in Chapter 5, details on the electronics and calculations carried out in the software were unavailable. This lead to the operation of the P7 oxygen sensor becoming slightly 'black box'. The dip coating technique used, although it proved effective enough to provide working sensors, was crude. This meant that the dimensions and therefore performance of the sensors could only be controlled to a very low tolerance. Because of this it was impossible to create identical sensors in order to compare their performance under various conditions. A working mathematical model of the sensor would possibly have been a useful tool during the research. However, with the crude dip coating technique used here, a model would have been of little use as it would not have been possible to control the membrane dimensions to match any values predicted as being ideal by such a model. Consequently, until a more precise coating technique is found a mathematical model would be of little use. In addition, the development of such a model was not a trivial endeavour and would probably constitute a research project of at least equal size to this thesis.

The measurement of the response times of the sensors was only an approximate measure, as the volumes of glucose being added to the solution were small (50µl) compared to the volume in the tonometer (50ml or 100ml). This meant that there was a random delay when the glucose solution mixed with the much larger volume of PBS solution in the tonometer. For the experiments where the glucose concentration was reduced, the change in glucose concentration was much faster than for increasing concentrations as large volumes of PBS, equal to the volume

previously in the tonometer, were added. This would lower the glucose concentration almost instantly and hence led to faster response times for the reducing glucose concentrations.

7.6 Comparison of the developed sensor with other glucose sensing technologies

The sensor described in this thesis is composed from several different technologies described in the literature; these are combined into a new glucose sensing approach. As with the other fibre optic glucose sensors, the interference problems of the electrochemical sensors are overcome by the florescence oxygen-measuring core (Moreno-Bondi, Wolfbies et al. 1990; Schaffar and Wolfbeis 1990; Li and Walt 1995; Healey, Li et al. 1997). The oxygen stoichiometric problem is attacked using polyurethane as with the electrochemical glucose sensor designs (Shichri, Yamasaki et al. 1982; Claremont, Sambrook et al. 1986; Shaw, Claremont et al. 1991). In addition, catalase is employed to also help redress oxygen limitation as well as to protect the GOD (Tse and Gough 1987; Wilson and Turner 1992). A major strength of this sensor design is the clinically proven oxygen sensing core technology of the P7. This tried and tested oxygen sensing base leaves only the GOD-CAT-HEMA technology to be developed and adapted. The use of this clinically proven sensor gave the produced glucose sensor an extremely stable and reliable core and was chosen so as to give the research the best chance of producing a working glucose sensor that could be developed for the treatment of diabetes.

7.7 Comparison of the developed sensor with other fibre-optic glucose sensors described in the published literature

In the published literature, the closest group of sensors to the sensor developed here are the fibre-optic glucose sensors described in Chapter 2, namely Moreno-Bondi, Wolfbies et al. 1990; Schaffar and Wolfbeis 1990; Li and Walt 1995; Healey, Li et al. 1997, which all used oxygen sensitive fluorescent dyes surrounded by GOD. Although these sensors did not employ CAT in their enzyme coatings, despite this the sensors constructed by Moreno-Bondi, Wolfbies et al. 1990 had a storage lifetime of 12 months when stored at 4°C. The sensor developed by Li and Walt 1995 showed similar performance to the sensors developed here although the lowest oxygen tensions tested were 10.1 KPa, so the sensor presented has been shown to operate in lower oxygen tensions. The sensor developed by Li and Walt 1995 also had a much smaller diameter than the sensor design presented in this thesis and measured oxygen as well as glucose. The multiple sensing sites, each covering a different range of glucose concentrations, would also allow the sensor to cover a wide range of glucose concentrations.

None of the other sensors cited in the literature use both glucose oxidase and catalase in their construction. Polyurethane outer membranes also do not appear to have been employed in the construction of any of the other fibre optic glucose sensors. The use of gamma radiation to sterilise a fibre-optic glucose sensor seems to be unique among fibre optic sensors although it has been used with electrochemical sensors (Bobbioni-Harsch, Rohner-Jeanrenaud et al. 1993; Woedtke, Julich et al. 2002).

7.8 Further work

The membrane coating technology should be developed and improved, possibly using a different technique to the dip coating methods described here. A technique needs to be developed where the membrane dimensions can be strictly controlled and hence the range and other parameters of the sensor dictated at will.

With a precision enzyme membrane coating technique the use of a mathematical model of the sensor may become viable. Such a model could be used to predict the performance of various sensor designs without the need for lengthy construction and experimental work. This would allow future work to be targeted towards designs that were most likely to provide the required performance parameters.

The lifetime of the sensors, in both storage and operation, needs to be improved; this could possibly be achieved through longer exposure to glutaraldehyde or some other means of improving enzyme immobilisation. Alternatively, greater amounts of enzyme could be loaded into the membrane layer.

To cover the full physiological range, a second sensor should be developed that can cover the upper range of glucose concentrations following gamma sterilisation. Combined with the sensors developed here, which cover the lower ranges, this would enable three sensors, an oxygen reference, the lower and upper range glucose sensors and a thermocouple, to be encapsulated in the MPHF sleeve in the same way as the current P7 multi-parameter sensor.

Following the development of the sensor to cover the upper range, the sensors should be put through the Diametrics manufacturing line to produce a sensor encapsulated in the MPHF sleeve. The performance of the sensor may be changed significantly by this and the enzyme-HEMA membrane changed appropriately.

Hysteresis in the sensors response should also be investigated in depth, both through mathematical models and experimental work. Appropriate membrane configurations could then be chosen to avoid this source of error in the measurement.

Finally, the sensor needs to be tested in vivo in subcutaneous tissue. The application of biocompatible and angiogenic membranes may also have to be used to overcome tissue response.

7.8.1. Contribution

A clinically proven commercial blood oxygen sensor (Paratrend 7) has been modified to detect glucose over the physiological concentration range and in vivo pH and temperature values. The sensor has been shown to operate in low oxygen tensions (7.5kPa) in order to potentially operate in the subcutaneous tissue where oxygen tensions of as low as this may be encountered. The range, sensitivity and response times of the sensor developed are sufficient to allow it to function as an hypoglycaemic alarm and as a means to adjust insulin. The sensor has also been shown to survive storage for three months and operation for 24 hours in physiological concentrations of glucose (5mM/l). The gamma ray sterilisation of the glucose sensors and its effect on performance investigated here has also not been previously reported. The use of catalase and GOD in a fibre optic glucose sensor has not been previously reported. In addition, the use of polyurethane as a glucose diffusion limiting membrane does not seem to have been applied to fibre optic glucose sensing systems before.

Appendix A

Software Developed to Interface Multiple P7 Monitors with a PC and Collect Data

Previously, the results were gathered in the form of printouts from the Paratrends. This was a time consuming process and did not allow the data to be saved or processed. A much more efficient method would be to download data from the P7 and to save this to the hard disk of a PC. It was also desirable to be able to insert markers in the data to indicate the time of addition of glucose or water to the tonometer during an experiment. To solve these problems, software was written which could interface a PC with two P7 via a serial port connection. This allowed data to be captured directly from the P7 and stored on the PC hard drive as digital data.

The software was written in Visual C++ using the Borland CBuilder package and a freeware serial port utility used was written by Giles Biddison (201 W, California 1407 Sunnyvale, CA 94086 USA). The software was designed to operate on a Windows 95 (Microsoft USA) system.

The software, 'DuelP7E.exe' collected data from two Paratrends simultaneously via two RS232 serial port connections and saved the data to two separate data files on a PC hard drive. The user could specify the file names and locations of the saved data. The program also allowed the user to insert markers in the saved data when glucose or water is added to a tonometer. The program had a graphical user interface as shown in figure A.1.

Figure A.1. The User interface for the DUELP7E software

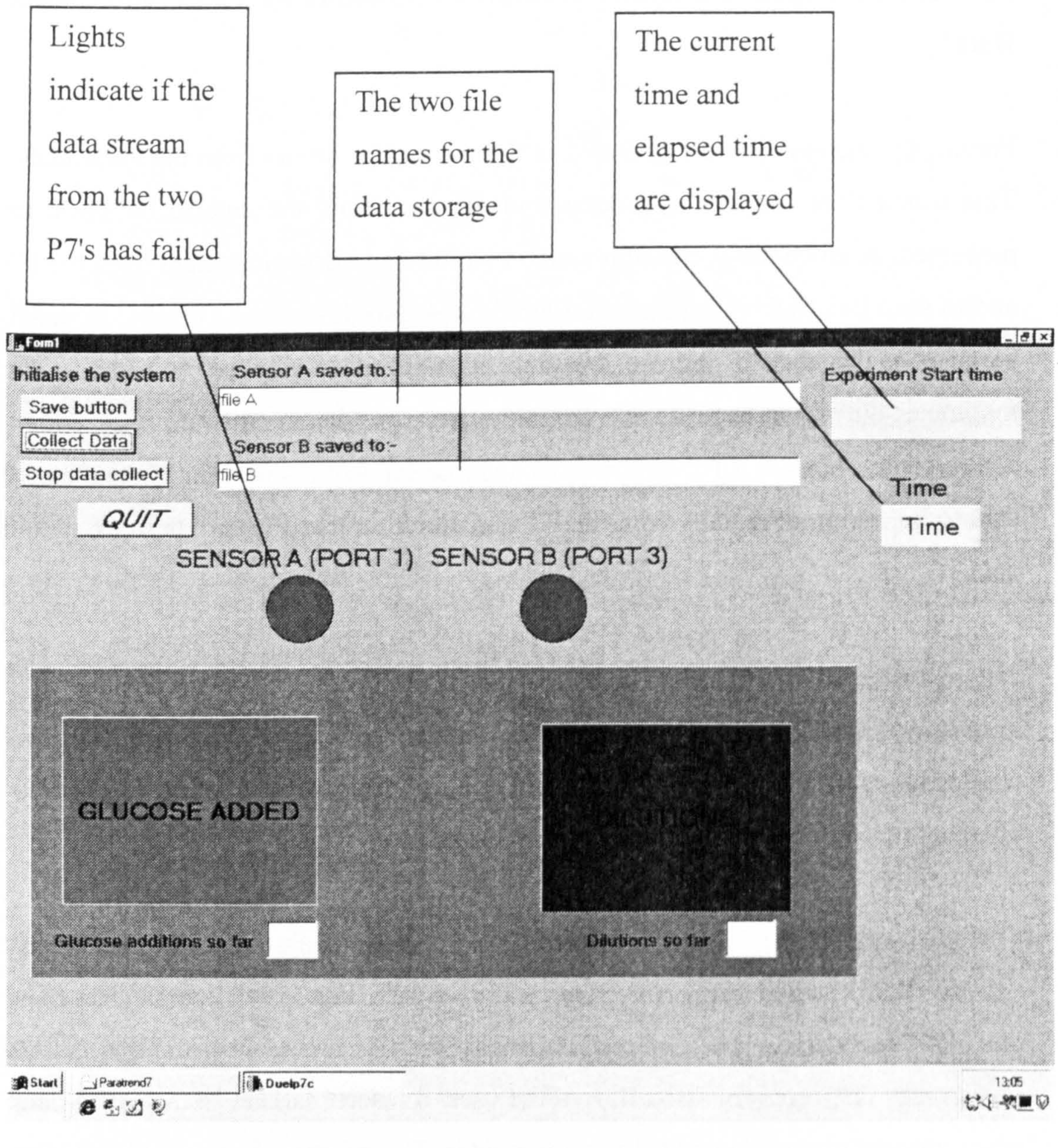

The locations and names of the saved files are displayed at the top of the screen. The program will not start data collection until file names have been specified. The data are stored as plain text files. The program is controlled using the four buttons to the top left of the screen. The start time of the experiment and the current time are displayed at the top right of the screen. The two red circles are

indicator lights, which flashed during data collection, to alert the user to any system failure (by their absence) during an experiment. The large green square labelled 'glucose added' and the blue square labelled 'dilutions' are buttons which, when clicked by the mouse cursor, will inset a marker in the data files. A safety feature is built into the button operation to prevent accidental double clicking of the buttons by the user. A running total of glucose or water events were displayed below these buttons. The 'stop data collect' and 'quit' buttons have built in fail safes which ask the user to confirm the command before it is carried out. The captured and stored data is shown in figure A.2

Figure A.2. An example of the data saved by the program.

```
T14:37:15
T14:37:161828456,"JUL 15, 1999","14:38:15",037150, 7.0,38.4,"ppp^"



T14:37:17
T14:37:181828458,"JUL 15, 1999","14:38:17",037150, 7.0,38.5,"pppY"



T14:37:19
ggggg

1828460,"JUL 15, 1999","14:38:19",037150, 7.0,38.5,"ppp^"



T14:37:20_
T14:37:21_1828462,"JUL 15, 1999","14:38:21",037150, 7.0,38.5,"pppc"
```

The format in which the data was captured from the P7 could not be altered. The data also arrived asynchronously from both the P7 sensors. The Borland software used could not suspend other Windows 95 program calls, meaning that the system was sometimes busy when data arrived at one of the serial ports. This caused

occasional overwriting of individual measurements by proceeding data strings. However, this happened infrequently and would only result in the loss of a few data points.

The text string at the top of figure A.2. is the standard output from the P7 serial port. The PO2 values are 7.0KPa and the temperature is 38.5 °C which are near the end of the string. The numbers beginning with 'T' are time values that are inserted into both files. This is the PC system time, and was inserted into both files when it was found that the clocks in the Paratrends could only be synchronised to within 1 minute of each other. This would lead to a time discrepancy in the measurements, so the PC system time was inserted into the files to be used as the time measurement in the data. A glucose or water event is shown by a 'ggggg' (shown in figure A.2). or 'wwwww' string inserted in the file for glucose or water respectively. The data can then be retrieved and processed using a spread sheet application.

Data sorting and formatting

Once the experiment was completed the data was sorted to a more usable format by a second program 'Duelsort.exe'. Duelsort.exe sorts through the data file, removing any corrupt data strings and creating a tab delineated file. An example of the file format is shown in figure A.3. below.

Figure A.3. The formatted data file

2204	7.4	0	0
2206	7.4	0	0
2209	7.4	0	0
2211	7.4	0	0
2212	7.3	1000	0
2214	7.3	0000	0
2216	7.1	0000	0
2218	7.0	0000	0

The time signal inserted in the raw data is used to create the time value in the left column. The next column is the PO2 value at that time the third column is the glucose signal which is represented as a 1000, and the fourth column is the dilution flag which is also represented by a 1000 value. Once sorted and formatted, the data is plotted and analysed using the EXCEL spreadsheet package, Microsoft Ltd USA.

Appendix B

Photographs of the Paratrend 7 system.

Figure B1. The Paratrend 7 senior system (foreground)

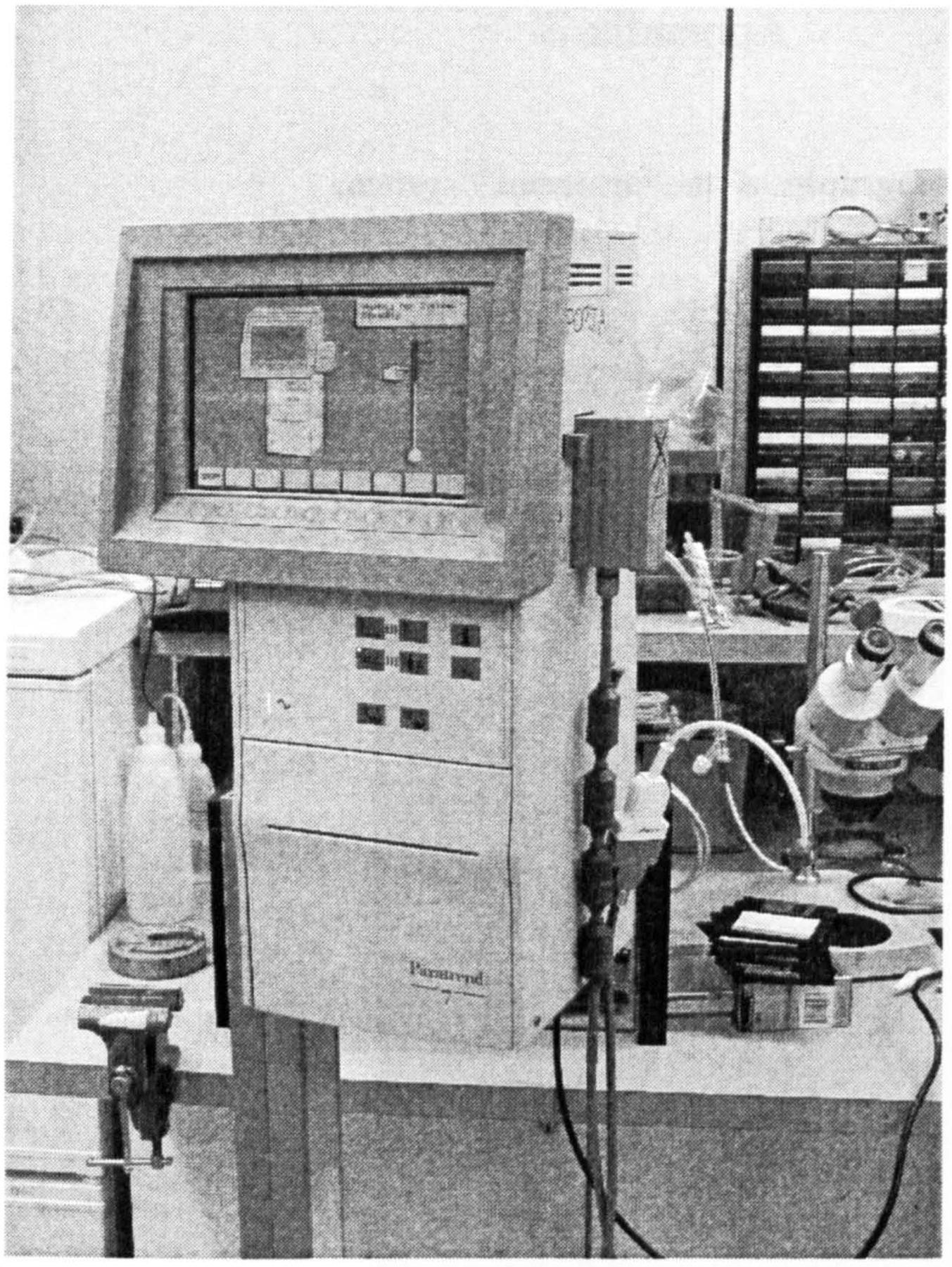

Figure B2. A close up of the P7 senior system.

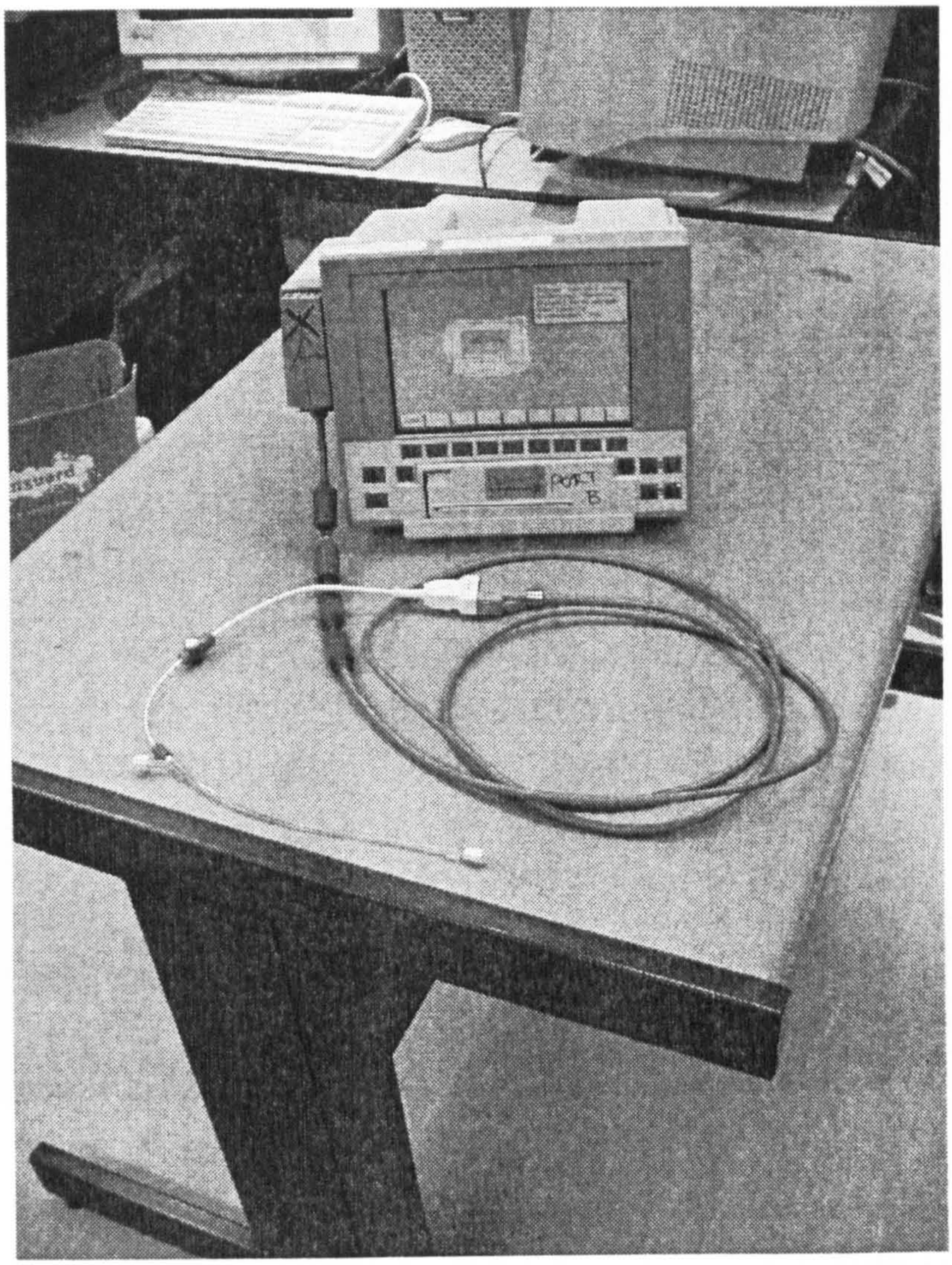

Figure B3. The P7 satellite system with oxygen sensor attached. The patient data module is shown labelled 'A'

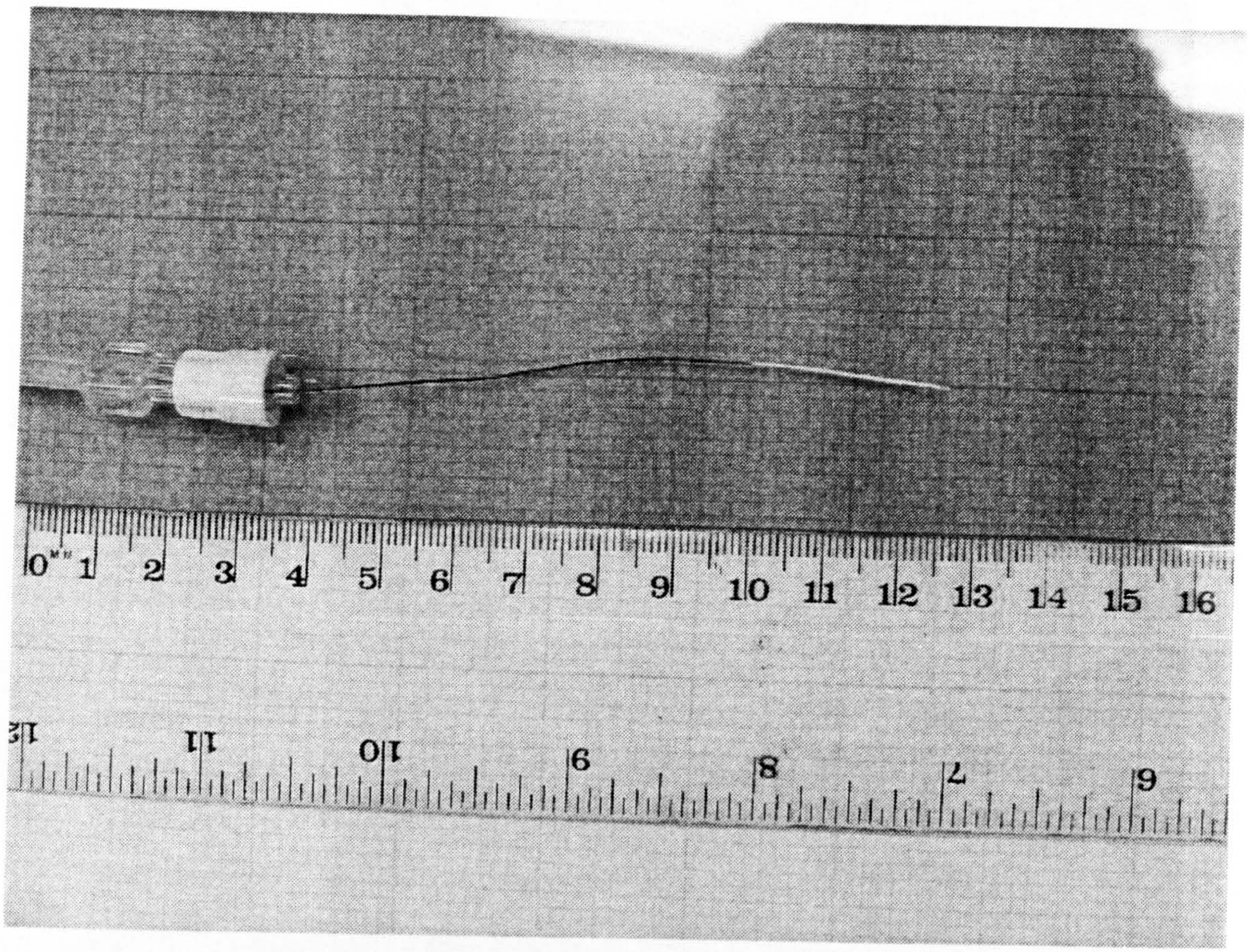

Figure B4. A close up of a standard P7 sensors tip, the white area is the MPHF sleeve encasing the three fibre optic sensors and the thermocouple. A scale in cm is shown at the bottom of the picture.

References

Amiel, S. A. (1998). Insulin injection treatment and its complications. Textbook of Diabetes. J. C. Pickup and G. Williams. London, Blackwell Science. **1**.

Arica, M. Y. and V. Hasirici (1993). "Bioreactor applications of glucose oxidase covalently bonded on pHEMA membranes." Biomaterials **14**(11): 803-809.

Armour, J. C., J. Y. Lucisano, B. D. McKean and D. A. Gough (1990). "Application of chronic intravascular blood glucose sensor in dogs." Diabetes **39**: 1519-1526.

Ashworth, D. C. and R. Narayanaswamy (1989). "Transducer mechanisms for optical biosensors. Part 2 Transducer design." Computer methods and progress in biomedicine **30**: 21-32.

Banting, F. G. and C. H. Best (1922). "The internal secretion of the pancreas." J Lab Clin Med **7**: 256-271.

Beach, R., F. Kuster and F. Moussy (1999). "Subminature implantable potentiostatand modified commercial telemetry device for remote glucose monitoring." IEEE transactions on instrumentation and measurment **48**(6): 1239-1245.

Bhandare, P., Y. Mendelson, R. A. Peura, G. Janatsch, J. D. kruse-Jarres, R. Marbach and H. M. Heise (1993). "Multivariate determination of glucose in whole blood using partial least-squares and artificial neural networks based on mid-infrared spectroscopy." Applied Spectroscopy **47**(8): 1214-1221.

Bhandare, P., Y. Mendleson, E. Stor and R. A. Peura (1994). "Comparison of multivariate calibration techniques for mid-IR absorption spectrometric determination of blood serum constituents." Applied Spectroscopy **48**(2): 271-273.

Bittner, A., H. M. Heise, T. Kochinsky and F. Gries (1997). "Evaluation of microdialysis and FT-IR ATR-spectroscopy for invivo blood glucose monitoring." Mikrochim Acta **14**: 827-828.

Blasi, R. A., S. fantini, M. A. Franceschini, M. ferrari and E. Gratton (1995). "Cerebral and muscle oxygen saturation measurement by frequency-domain near-infra-red spectrometer." Med. & Biol. Eng. & Comput. **33**: 228-230.

Bobbioni-Harsch, E., F. Rohner-Jeanrenaud, M. koudelka, N. d. Rooij and B. Jeanrenaud (1993). "Lifespan of a subcutaneous glucose sensors and their performances during dynamic glycaemia changes in rats." J Biomed Eng **15**: 457-463.

Bolinder, J., U. Ungerstedt and P. Arner (1992). "Microdialysis measurement of the absolute glucose concentration in subcutaneous adipose tissue allowing glucose monitoring in diabetic patients." Diabetologia **35**: 1177-1180.

Boulnois, J.-L. (1985). "Photophysical processes in recent medical laser developments: a review." Lasers in medical science **1**: 47-66.

Bourdillon, C., J. P. Bourgeois and D. Thomas (1980). "Covalent linkage of glucose oxidase on modified glassy Carbon Electrode. Kinetic Phenomena." American Chemical Society **102**: 4231-5.

Cameron, B., J. Baba and G. L. Cote (2001). "Measurement of the glucose transport time delay between the blood and aqueous humor of the eye for the eventual development of a noninvasive glucose sensor." Diabetes technology & Therapeutics **3**(2): 201-207.

Cheng, Z., E. Wang and X. Yang (2001). "Capacative detection of glucose using molecularly imprinted polymers." Biosensors and Bioelectronics **16**: 179-185.

Christison, G. and H. MacKenzie (1993). "Laser photoacoustic determination of physiological glucose concentrations in human whole blood." Medical and biological engineering and computing **31**: 284-290.

Chubdova, I., E. Vrbova, M. Kodicek, J. Janovcova and J. Kas (1996). "Fibre optic biosensor for the determination of D-glucose based on absorption changes of immobilised glucose oxidase." Analytica Chimica Acta **319**: 103-110.

Claremont, D. J. (1987). "Biosensors: Clinical requirements and scientific promise." Journal of medical and engineering & technology **11**(2): 51-56.

Claremont, D. J., I. E. Sambrook, C. Penton and J. C. Pickup (1986). "Subcutaneous implantation of a ferrocene-mediated glucose sensor in pigs." Diabetologica **29**: 817-821.

Cooper, C. E., C. E. Elwell, J. H. Meek, S. J. Matcher, J. S. Wyatt, M. Cope and D. T. Delpy (1996). "The noninvasive measurement of absolute cerebral deoxyhaemoglobin concentration and mean optical path length in the neonatal brain by second derivative near infrared spectroscopy." paediatric research **39**(no 1): 32-38.

Cope, M. and D. T. Delpy (1988). "System for Long-Term Measurement of Cerebral Blood and Tissue Oxygenation on Newborn-Infants by near-

Infrared Trans-Illumination." Medical & Biological Engineering & Computing **26**(3): 289-294.

Cote, G. L., M. D. Fox and R. B. Northrop (1992). "Noninvasive optical polarimetric glucose sensing using a true phase measurement technique." IEEE transaction on biomedical engineering **39**(7): 752-760.

Cronenberg, C., B. v. Groen, D. d. Beer and H. v. d. Heuvel (1991). "Oxygen-independent glucose microsensor based on glucose oxidase." Analytica Chimica Acta **242**: 275-278.

Cussler, E. L. (1988). Diffusion Mass Transfer in Fluid Sytems, Cambridge University Press.

Daley, J., J. Shearer, B. Mastrofrancesco and M. Caldwell (1990). "Glucose metabolism in injured tissue: A longitudinal study." Surgery(February): 187-192.

DCCT (1991). "Epidermology of severe hypoglycaemia in the diabetes control and complications trial." The American journal of medicine **90**: 450-459.

DCCT (1993). "The effect of intensive treatment of diabetes on the development and progression of long-term complications in insulin-dependent diabetes mellitus." The New England Journal of Medicine **329**: 977-86.

Diem, K. and C. Lenter, Eds. (1975). Scientific tables, Giegy Pharmaceuticals.

Entcheva, E. G. and L. K. Yotova (1994). "Analytical application of membranes with covalently bound glucose oxidase." Analytica Chimica Acta **299**: 171-177.

Fantini, S., M. A. Franceschini-Fantini, J. S. Maier, S. A. Walker, B. Barbieri and E. Gratton (1995). "Frequency-domain multichannel optical detector for noninvasive tissue spectroscopy and oximetry." Optical engineering **34**(1): 1/32-42.

Faris, F., M. Thorniley, Y. Wickramsinger, R. Houston, P. Rolfe, N. Livera and A. Spencer (1991). "Non-invasive in vivo near-infrared optical measurement of the penetration depth in the neonatal head." Clin. Phys. Physiol. Meas **12**(4): 353-358.

Fernquist-Forbes, E., B. Linde and R. Gunnarsson (1988). "Insulin Absorption and Subcutaneous Blood Flow in Normal Subjects During Insulin-Induced Hypoglycemia." Journal of Clinical Endocrinology and Metabolism **67**(3).

Ferrari, M., Q. Wei, L. Carraresi, R. D. Blasi and G. Zaccanti (1989). "Noninvasive determination of hemoglobin saturation in dogs by derivative near-infrared

spectroscopy." The American Physiology Society(Special comunications): H149-H1499.

Firbank, M., M. Hiraoka, M. Essenpries and D. T. Delpy (1993). "Measurement of the optical properties of the skull in the wavelength range 650-950nm." Physics in medicine and biology **38**(4): 503-510.

Fischer, U., R. Ertle, P. Abel, K. Rebrin, E. Brunstein, H. H. v. Dorsche and E. J. Freyse (1987). "Assesment of subcutaneous glucose concentration: validation of the wick technique as a reference for implanted electrochemical sensors in normal and diabetic dogs." Diabetelogia **30**: 940-945.

Fisher, U., K. Rebrin, T. Woedtke and P. Abel (1994). "Clinical usefulness of the glucose concentration in the subcutaneous tissue-properties and pitfalls of electrochemical biosensors." Horm metab **26**: 515-522.

French, A. P. and E. F. Taylor (1991). An introduction to quantum physics. London, Chapman & Hall.

Frier, B. M. (1997). Hypoglycaemia in diabetes mellitus. Textbook of Diabetes. J. C. Pickup and G. Williams. London, Blackwell Science. **I**.

Garg, S., R. Potts, N. Ackerman, S. Fermi, J. Tamada and H. Chase (1999). "Correlation of fingerstick blood glucose measurent with glucowatch biographer glucose results in young subjects with type 1 diabetes." Diabets Care **22**(10): 1708-1714.

Geotz, M., G. Cote, R. Erckens, W. March and M. Motamedi (1995/7). "Application of a multivariate technique to raman spectra for quantification of body chemicals." IEEE Transactions **42**(7): 728-731.

Gewehr, P. M. (1991). Development of an optical oxygen sensor for medical use based upon phosphorescence lifetime quenching and employing a polymer immobilized metalloporphyrin probe. Department of medical physics and bio-engineering. London, University College London.

Gewehr, P. M. and D. T. Delpy (1993). "Optical sensor based on phosphorescence lifetime quenching and employing a polymer immobilised metalloporohyrin probe." Medical and biol eng **31**: 2-10.

Gilligan, B. J., M. C. Schults, R. K. Rhodes and S. J. Updike (1994). "Evaluation of a subcutaneous glucose sensor out to 3 months in a dog model." Diabetes Care **17**(8).

Glaister, D. H. (1988). "Current and emerging technology in G-Loc detection: Noninvasive monitoring of cerebral microcirculation using near infrared." viation, space, and environmental medicine **january**: 23-28.

Gough, D. A., J. C. Armour, J. Y. Lucisano and B. D. Mckean (1986). "Short-term in vivo operation of a glucose sensor." Trans Am Soc Artif Intern Organs **XXXII**: 148-150.

Gough, D. A., J. K. Leypoldt and J. C. Armour (1982). "Progress toward a potentially implantable enzyme-based glucose sensor." Diabetes Care **5**(3): 190-198.

Gough, D. A., J. Y. Lucisano and P. H. S. Tse (1985). "Two-dimensional enzyme electrode sensor for glucose." Anal Chem **57**: 2351-2357.

Gray, H. (2000). Anatomy of the human body. Philadelphia, Lea & Febiger.

Green, A., A. K. Sjolie and O. Eshoj (1997). Insulin-dependent diabetes mellitus. Textbook of Diabetes. J. C. Pickup and G. Williams. London, Blackwell Science. **II**.

Guilbault, G. G. and G. Palleschi (1995). "Non-invasive biosensors in clinical analysis." Sensors & Bioelectronics **10**: 379-392.

Haaland, D. M., M. R. Robinson, G. W. Koepp, E. V. Thomas and R. P. Eaton (1992). "Reagentless near-infrared determination of glucose in whole blood using multivariate calibration." Applied Spectroscopy **46**(10): 1575-1578.

Hall, E. A. H. (1990). Biosensors. Melksham, Open University Press.

Hashiguchi, Y., M. Sakakida, K. Nishida, T. Uemura, K. Kaijiwara and M. Shichiri (1994). "Development of a miniturised gluicose monitoring system by combining a needle-type glucose sensor with microdialysis sampling method." Diabetes care **17**(5): 387-397.

Healey, B. G., L. Li and D. R. Walt (1997). "Multianalyte biosensors on optical imaging bundles." Biosensors & Bioelectronics **12**(6): 521-529.

Heinemann, L. (2000). Glucose sensors: current status and further developments. Proceddings 4th IFAC symposium
Modelling and Cotnrol in Biomedical Systems.

Heise, H. M. and R. Marbach (1994). "Effect of data pretreatment on noninvasive blood glucose measurement by diffuse reflectance NIR spectroscopy." SPIE **2089**: 114-115.

Heise, H. M., R. Marbach, T. Koschinsky and F. A. Gries (1992). "Multivariate determination of blood substrates in human plasma by FT-IR spectroscopy." Proceedings - 8th international conference on Fourier transform spectroscopy **1575**: 507-8.

Jagemann, K.-U., C. Fischbacher, K. Danzer, U. A. Muller and B. Mertes (1995). "Application of Near-Infrared Spectroscopy for Non-Invasive Determination of Blood/tissue Glucose Using Neural Networks." Zeitschrift fur Physikalische Cheme **191**: 179-190.

Jenkins, F. A. and H. E. White (1981). Fundamentals of Optics, McGraw-Hill.

Jobsis, F. F. (1977). "Noninvasive monitoring of cerebral and myocardial oxygen sufficiency and circulatory parameters." Science **198**: 1264-67.

Johnson, K. W., J. J. Mastrototaro, D. C. Howey, R. L. Brunelle, P. L. Burden-Brady, N. A. Bryan, C. C. Andrew, H. M. Rowe, D. J. Allen, B. W. Noffke, W. C. McMahan, R. J. Morff, D. Lipson and R. S. Nevin (1992). "In Vivo evaluation of an electroenzymatic glucose sensor implanted in subcutaneous tissue." Biosensors and Bioelectronics 7: 709-714.

Jones, D. B. and G. V. Gill (1997). Insulin-dependent diabetes mellitus: an overview. Textbook of Diabetes. J. C. Pickup and G. Williams. London, Blackwell Science. **I.**

Jones, D. B. and G. V. Gill (1997). Non-insulin-dependent diabetes mellitus: an overview. Textbook of Diabetes. J. C. Pickup and G. Williams. London, Blackwell Science. **I.**

Kayashima, S., T. Arai, M. Kikuchi, N. Sato, N. Nagata, O. Takatani, N. Ito, J. Kimura, T. Kuriyama and A. Kaneyoshi (1991). "New noninvasive transcutaneous approach to blood glucose monitoring: Successful glucose monitoring on human 75g OGTT with novel sampling chamber." IEEE Transactions on biomedical engineering **38**(8).

Kellener, R., R. Gobel, R. Goetz, B. Lendl and B. edl-mizaikoff (1995). "Recent progress on mid-ir sensing with optical fibers." SPIE **2508**: 212-223.

Kikuchi, M., S. Kayashima and N. Ito (1996). Transcutaneous Biochemical Substance Monitoring Based on Biosensors - Blood glucose and Lactate. IEEE Eng Med & Biol 18th Ann Int, Amsterdam.

Kohl, M., M. Cope, M. Essenpreis and D. Bocker (1994). "Influence of Glucose-Concentration on Light-Scattering in Tissue-Simulating Phantoms." Optics Letters **19**(24): 2170-2172.

Kohl, M., M. Essenpreis, D. Bocker and M. Cope (1995). Glucose induced changes in scattering and light transport in tissue simulating phantoms. Proc SPIE. San Jose: 2389.

Kolimbiris, H. (2000). Digital communications with satellite and fibre optrics applications, Prentice Hall.

Kost, J., S. Mitragotri, R. Gabbay, M. Pishko and R. Langer (2000). "Transdermal monitoring of glucose and other analytes using ultrasound." Nature Medicine **6**(3): 347-350.

Krentz, A. j. and M. Nattrass (1997). Acute metabolic complications of diabetes mellitus:diabetic ketoacidosis, hyperosmolar non-ketotic syndrome and lactic acidosis. Textbook of Diabetes. J. C. Pickup and G. Williams. London, Blackwell Science. **I**.

Kruszynska, Y. T. (1997). Normal metabolism: The physiology of fuel homeostatsis. Textbook of Diabetes. J. C. Pickup and G. Williams. London, Blackwell Science. **I**.

Kusano, H. (1989). "Glucose enzyme electrode with precutaneous interface which operates independently of dissolved oxygen." Clin Phys Physiol Meas **10**(1): 1-9.

Lakowickz, J. R. (1999). Principles of Fluorescence Spectroscopy. New York, Kluwer Academic/Plenum publishers.

Lehnniger, A. L. (1972). Biochemistry The molocular baisis of cell structure and function. New York, Worth Publishing Inc.

Lemke, K. (1988). "Mathematical simulation of an amperometric enzyme-substrate electrode with a PO2 basic sensor." Medical and biological Enginering and computing **26**: 523-532.

Lemke, K. and R. Lustermann (1991). "Electrocatalytic glucose sensor for subcutaneous application." bioelectrochemistry and Bioenergetics **26**: 43-61.

Leypoldt, J. K. (1981). Modeling of immobilised enzyme systems:Glucose oxidase studies. San Diego, University of California.

Leypoldt, J. K. and D. Gough (1984). "Model of a two-substrate enzyme electrode for glucose." Anal Chem **56**: 2896-2904.

Li, L. and D. R. Walt (1995). "Dual-analyte fiber-optic sensor for the simultaneous and continuous measurement of glucose and oxygen." Anal Chem **67**: 3746-3752.

Linde, B. (1997). The pharmacokinetics of insulin. Textbook of Diabetes. J. C. Pickup and G. Williams. London, Blackwell Science. **I**.

Lledias, F., P. Rangel and W. Hansberg (1998). "Oxidation of Catalase by singlet oxygen." The journal of biological chemistry **273**(17): 10630-10637.

MacKenzie, H. A., G. B. Christison, P. Hodgson and D. Blanc (1993). "A laser Photoacoustic sensor for analyte detection in aqueous systems." Sensors and actuators **B**(11): 213-220.

Maier, J. S., S. A. Walker, S. Fantini, M. A. Franceschini and E. Gratton (1994). "Possible correlation between blood glucose concentration and the reduced scattering coefficients of tissue in the near infrared." Optics letters **19**(24).

Mansouri, S. and J. S. Schultz (1984). "A minature optical glucose sensor based on affinity binding." Bio Technology: 855-890.

March, W. F., B. Rabinovitch, R. Adams, J. R. Wise and M. Melton (1982). "Ocular Glucose Sensor." Trans Am Soc Artif Intern Organs **XXVIII**: 232-235.

Martens, H. and T. Naes (1994). Multivariate Calibration, John Wiley & Sons Ltd.

Mathews, C. K. and K. E. v. Holde (1990). Biochemistry. Redwood City, The Benjamin/Cummings Publishing Company.

McEvoy, A., C. M. McDonagh and B. MacCraith (1996). "Dissolved oxygen sensor based on fluorescence quenching of oxygen-sensetive ruthenium complexes immobilised in Sol-Gekl-derived porous sillica coatings." Analyst **June**(121): 785-788.

McNamara, K. P., X. Li, A. D. Stull and Z. Rosenwig (1998). "Fibre-optic oxygen sensor based on the fluorescence quencing of tris(5-acrylamido, 1,10 phenanthroline) ruthenium chloride." Analytica Chimica Acta **361**: 73-83.

McNichols, R. J. and G. L. Cote (2000). "Optical glucose sensoing in biological fluids: an overview." Journal of biomedical optics **5**((1)): 5 -16.

Meadows, D. L. and J. S. Schultz (1993). "Design, Manufacture and characterization of an optical fiber glucose affinity sensor based on an homogeneous fluorescence energy transfer assay system." Analytica Chimica Acta **280**: 21-30.

Moatti-Sirat, D., F. Capron, V. Poitout, G. Reach, D. S. Bindra, Y. Zhang, G. S. Wilson and D. R. Thevenot (1992). "Towards continuous glucose monitoring: in vivo evaluation of a miniaturized glucose sensor implanted for several days in rat subcutaneous tissue." Diabetologia **35**: 224-230.

Moreno-Bondi, M. C., O. S. Wolfbies, M. J. P. Leiner and B. P. H. Scaffer (1990). "Oxygen optrode for use in a fiber-optic glucose biosensor." Anal. Chem. **60**: 2377-2380.

Moussey, F., D. J. Harrison, D. W. Obrian and R. V. Rajotte (1993). "Performance of a sucutaneously implanted needle-type glucose sensor employing a novel trilayer coating." Anal. Chem **65**: 2072-2077.

Neykov, A. and T. Georgiev (1998). "Mathematical modelling of amperometric biosensor systems with non-linear enzynme kinetics." Chem Biochem Eng **Q 12**: 73-79.

Noda, M., N. Taniguichi, M. Kimura, A. Kinoshita, F. Kubo, N. Kuzuya and Y. Kanazawa (1994). "Completely Noninvasive measurement of human blood glucose in vivo using near infrared waves." Proc Int Congress SER Exerpia Med **1057**: 255-9.

Olsson, B., H. Lundback and G. Johansson (1986). "Theory and application of diffusion-limited amperometric enzyme electrode detection in flow injection analysis of glucose." Anal Chem **58**: 1046-1052.

Pan, Q., S.-y. Qui, Shu-yi-Zhang and S.-m. Zhu (1988). "Application of Photoacoustic Spectroscopy to Human Blood." Springer series in optical sciences(58): 542-545.

Patterson, D. (1996). Artificial Neural Networks Theory and Application, Prentice Hall.

Pickup, J. C. (1997). Diabetic control and its measurement. Textbook of Diabetes. J. C. Pickup and G. Williams. London, Blackwell Science. **I.**

Pickup, J. C. (1998). Alternative forms of insulin delivery. Textbook of DIabetes. J. C. Pickup and G. Williams. London, Blackwell Science. **1.**

Pickup, J. C., G. W. Shaw and D. J. Claremont (1989). "In vivo molecular sensing in Diabetes Mellitus: an implantable glucose sensor with direct electron transfer." Diabetologia **32**: 213-217.

Pickup, J. C. and G. Williams, Eds. (1997). Textbook of Diabetes. London, Blackwell science.

Quan, K. M., G. B. Cristison, H. A. MacKenzie and P. Hodgson (1993). "Glucose determination by a pulsed photoacoustic technique: an experimental study using a gelatin-based tissue phantom." Phys. Med. Biol. **38**: 1911-1922.

Rabinovitch, B., W. F. March and R. L. Adams (1982). "Noninvasive glucose monitoring of the aqueous humour of the eye: Part I. Measurement of very small optical rotations." Diabetes care **5**(3): 254-258.

Rao, G., R. H. Guy, P. Glikfeld, W. R. LaCourse, L. Leung, J. Tamada, R. O. Potts and N. Azimi (1995). "Reverse Iontophoresis: Noninvasive Glucose

Monitoring in Vivo in Humans." Phamaceutical Research **12**(12): 1869-1873.

Rasimas, J. P., K. A. Berglund and G. J. Blanchard (1996). "A molecular lock-and-key approach to detecting solution phase self-assembly.
A fluorescence and absorption study of ceramic acid in aqueous glucose solutions." J Phys Chem **100**: 7220-7229.

Rhemrev-Boom, R. M., R. G. Tiessen, A. A. Jonker, K. Venema, P. Vadgama and J. Korf (2002). "A lightweight measuring device for the continuous in vivo monitoring of glucose by means of ultraslow microdialysis in combination with a miniaturised flow-through biosensor." Clinica Chimica Acta **316**: 1-10.

Rinken, T. and T. Tenno (2001). "Dynamic model of amperometric biosensors. Characterisation of glucose biosensor output." Biosensors and Bioelectronics **16**: 53-59.

Robinson, M. R., R. P. Eaton, d. M. Haaland, G. W. Koepp, E. V. Thomas, B. R. Stallard and P. L. Robinson (1992). "Noninvasive glucose monitoring in diabetic patients: A preliminary Evaluation." Clinical chemistry **38**: 1618-1622.

Rosenzweig, Z. and R. Kopelman (1996). "Analaytical properties and sensor size effects of a micrometer-sized optical fiber glucose biosensor." Anal. Chem. **68**: 1408-1413.

Scchulmeister, T. (1990). "Mathematical modeling of the dynamic behavour of amperometric enzyme electrodes." Selective Electrode Reviews **12**(2): 203-261.

Schaffar, B. P. H. and O. S. Wolfbeis (1990). "A fast responding fibre optic glucose biosensor based on an oxygen optrode." Biosensors & Bioelectronics **5**: 137-148.

Schmidt, F. J., W. J. Slutter and M. S. A. J (1993). "Glucose concentration in subcutaneous extracellular space." Diabetes care **16**(5).

Schmidtke, D. W., A. C. Freeland, A. Heller and R. T. Bonnecaze (1998). "Measurement and modelling of the transient difference between blood and subcutaneous glucose concentrations in the rat after injection of insulin." Proc. Natl. Acad. Sci. **95**: 294-299.

Schulmeister, T. and D. Pfeiffer (1993). "Mathematical modelling of amperometric enzyme electrodes with perforated membranes." Biosensors and bioelectronics **8**: 75-79.

Schultz, J. S., S. Mansouri and I. J. Goldstein (1982). "Affinity sensor: A new technique for developing implantable sensors for glucose and other metabolites." Diabetes Care **5**(3): 245-253.

Service, F. J., P. C. O'brien, S. D. Wise, S. Ness and S. M. LeBlanc (1997). "Dermal interstitial glucose as an indicator of ambient glycemia." Diabetes Care **20**(9).

Shahriari, M. R., J. Y. Ding, J. Tong and G. S. Jr (1993). "Sol-Gel coating based fiber optic O2/DO sensor." Proc SPIE **2068**: 224-240.

Sharma, A. and S. G. Sculman (1999). Introduction to fluorescence spectroscopy, John - Wiley & Sons Inc.

Shaw, G. W., D. J. Claremont and J. C. Pickup (1991). "In vitro testing of a simply constructed, highly stable glucose sensor suitable for implantation in diabetic patients." Biosensors & Bioelectronics **6**: 401-406.

Shichri, M., Y. Yamasaki, R. Kawamori, N. Hakui and H. Abe (1982). "Wearable artificial endocrine pancreas needle-type glucose sensor." The Lancet **20**: 1129-1131.

Singer, E., G. L. Duveneck, M. Ehrat and H. M. Widmer (1994). "Fiber optic sensor for oxygen determination in liquids." Sensors and Actuators **A**: 41-42.

Skoog, D. A. and J. J. Leary (1992). Principles of Instrumental Analysis.

Sodickson, L. A. and M. J. Block (1994). "Kromoscopic Analysis: A possible alternative to spectroscopic analysis for noninvasive measurement of analytes in vivo." Clin Chem **40**(9): 1838-1844.

Spanner, G. and R. Niebner (1996). "New concept for the noninvasive determination of physiological glucose concentrations using modulated laser diodes." Fresenius J Anal Chem **354**: 306-310.

Sternberg, F., C. Meyerhoff, F. Mennel, F. Bischof and E. Pfiefer (1995). "Subcutaneous glucose concentration in humans." Diabetes care **18**(9): 1266-1269.

Sternberg, F., C. Meyerhoff, F. J. Mennel, H. Mayer, F. Bischof and E. F. Pfeiffer (1996). "Does fall in tissue glucose precede fall in blood glucose?" Diabetologia **39**: 609-612.

Tamada, J. A., N. J. V. Bohannon and R. O. Potts (1995). "Measurement of glucose in diabetic subjects using noninvasive transdermal extraction." Nature Medicine **1**(11): 1198-1201.

Tolosa, L., H. Malak, G. Raob and J. R. Lakowicz (1997). "Optical assay for glucose based on the luminescence decay time of the long wavelength dye Cy5." Sensors and Actuators **B45**: 93-99.

Troupe, C., I. Drummond, C. Graham, J. Grice, P. John, J. Wilson, M. Jubber and N. Morrison (1998). "Diamond-based glucose sensors." Diamiond and related materials **7**: 575-580.

Tse, P. H. S. and D. A. Gough (1987). "Time-Dependent Inactivation of Immobilized Glucose oxidase and Catalase." Biosensors and Bioelectronics **XXIX**: 705-713.

Turo, N. J. (1991). Modern molecular photochemistry. Mill Valley California, University science books.

Updike, S., M. Shults, B. Gilligan and R. Rhodes (2000). "A Subcutaneous Glucose Sensor With Improved Longevity, Dynamic Range, and Stability of Calibration." Diabetes Care **23**(2): 208-214.

Velho, G., P. Froguel and G. Reach (1989). "Determination of peritoneal glucose kinetics in rats: implications for the peritoneal implantation of closed-loop insulin delivery systems." Diabetologia **32**: 331-336.

Ward, W. K., L. B. Jansen, E. Anderson, G. Reach, J.-C. Klien and G. S. Wilson (2002). "A new amperometric glucose microsensor: in vitro and short-term in vivo evaluation." Biosensors and Bioelectronics **17**: 181-189.

WHO, W. H. Organization, D. o. N. D. Surveillance and Geneva (1999). Definition, Diagnosis and Classification of Diabetes Mellitus and its Complications: Part 1: Diagnosis and Classification of Diabetes Mellitus. Geneva, World Health Organization.

Williams, G. and J. C. Pickup (1997). Problems with metabolic control in insulin dependent diabetes mellitus. Textbook of Diabetes. J. C. Pickup and G. Williams. London, Blackwell Science. **I**.

Wilson, G. S., Y. Zhang, G. Reach, D. Moatti-Sirat, V. Poitout, D. R. Thevenot, F. Lemonnier and J.-C. Klein (1992). "Progress toward the Development of an Implantable Sensor for Glucose." Clin Chem **38/9**: 1613-1617.

Wilson, R. and A. P. F. Turner (1992). "Glucose Oxidase: An Ideal Enzyme." Biosensors and Bioelectronics **7**: 165-185.

Woedtke, T. v., W. D. Julich, V. Hartmann, M. Sieber and P. U. Abel (2002). "Sterilization of enzyme glucose sensors: problems and concepts." Biosensors and Bioelectronics **17**: 373-382.

Yang, H., T. D. Chung, Y. T. Kim, C. A. Choi, C. H. Jun and H. C. Kim (2002). "Glucose sensor using a microfabricated electrode and electropolymerized bilayer films." Biosensors and Bioelectronics **17**: 251-259.

Yang, Q. L., P. Atanasov and E. Wilkins (1997). "A novel amperometric transducer design for needle-type implantable biosensor applications." Electroanalysis **9**(16): 1252-1256.

Zhang, Y. and G. S. Wilson (1993). "In vitro and in vivo evaluation of oxygen effects on a glucose oxidase based implantable glucose sensor." Analytica Chimica Acta **281**: 513-520.